iScience

CellPress
OPEN ACCESS

Article

Tungstate-Catalyzed Biomimetic Oxidative Halogenation of (Hetero)Arene under Mild Condition

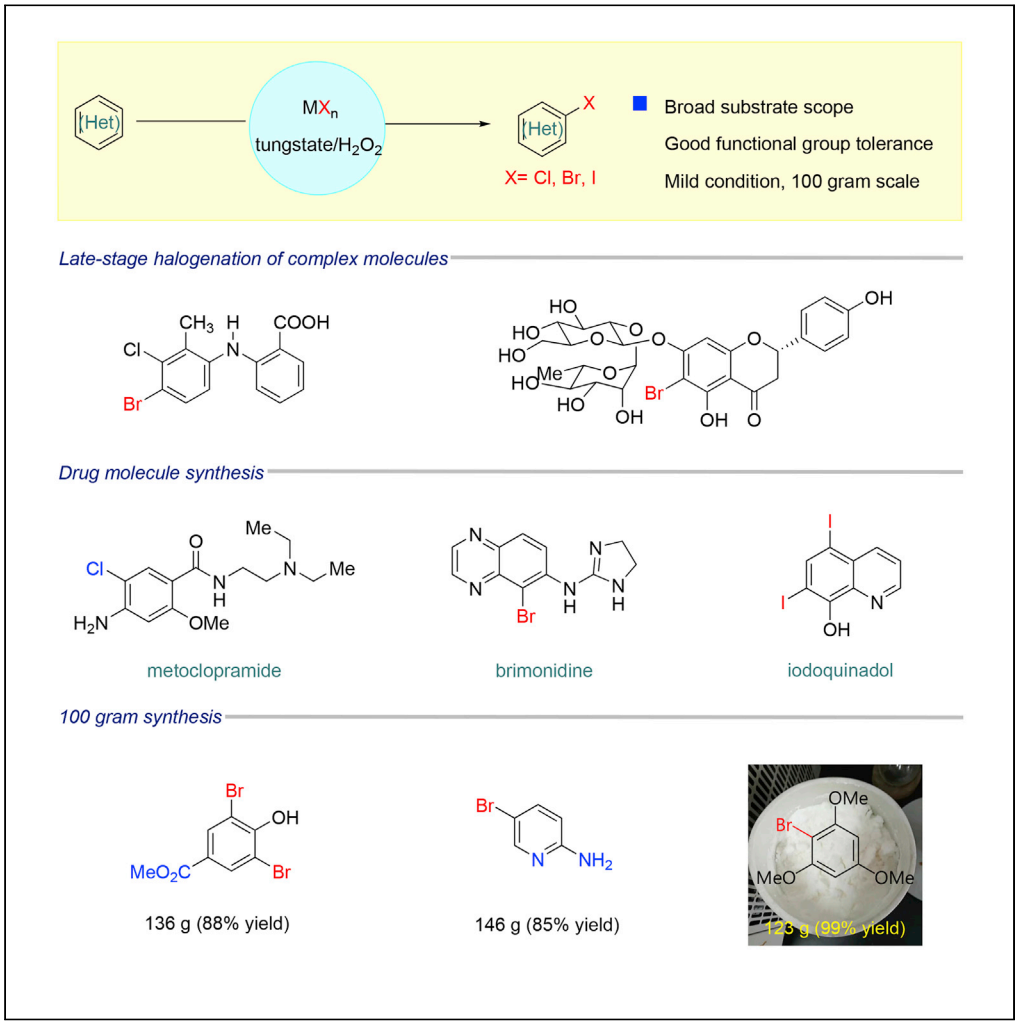

Zhuang Ma, Helin Lu, Ke Liao, Zhilong Chen

czldreamer@hotmail.com, pmchenzl@hust.edu.cn

HIGHLIGHTS

Tungstate-catalyzed halogenation of (hetero) arenes under mild condition

Robust in 100-g-scale synthesis; good functional group tolerance

Late-stage halogenation of complex molecules; good application in drug synthesis

Ma et al., iScience 23, 101072 May 22, 2020
https://doi.org/10.1016/j.isci.2020.101072

iScience

CellPress
OPEN ACCESS

Article

Tungstate-Catalyzed Biomimetic Oxidative Halogenation of (Hetero)Arene under Mild Condition

Zhuang Ma,[1] Helin Lu,[1] Ke Liao,[1] and Zhilong Chen[1,2,*]

SUMMARY

Aryl halide (Br, Cl, I) is among the most important compounds in pharmaceutical industry, material science, and agrochemistry, broadly utilized in diverse transformations. Tremendous approaches have been established to prepare this scaffold; however, many of them suffer from atom economy, harsh condition, inability to be scaled up, or cost-unfriendly reagents and catalysts. Inspired by vanadium haloperoxidases herein we presented a biomimetic approach for halogenation (Br, Cl, I) of (hetero)arene catalyzed by tungstate under mild pH in a cost-efficient and environment- and operation-friendly manner. Broad substrates, diverse functional group tolerance, and good chemo- and regioselectivities were observed, even in late-stage halogenation of complex molecules. Moreover, this approach can be scaled up to over 100 g without time-consuming and costly column purification. Several drugs and key precursors for drugs bearing aryl halides (Br, Cl, I) have been conveniently prepared based on our approach.

INTRODUCTION

(Hetero)aryl halides (Br, Cl, I) are embodied in many biologically important molecules, like natural products, drugs, and drug leads (Hernandes et al., 2010). In organic molecules, replacing a proton by a halide can significantly improve their properties, including solubility, polarity, melting point, stability, binding affinity, selectivity to biological targets, and metabolism. Recently, halogen bonding emerges as a useful tool in both catalyst and drug design (Wilcken et al., 2013). For example, chloride is normally used as bioisostere of methyl and hydroxyl groups, whereas bromide is frequently used as bioisostere of isopropyl and trifluoromethyl groups. The isotopes of iodide, like ^{123}I and ^{131}I, are widely used in medical setting for imaging, such as iopanoic acid. Meanwhile, as one of the most useful building blocks in organic synthesis, (hetero)aryl halides are broadly utilized in countless transformations like cross-couplings (e.g., Suzuki coupling, Buchwald-Hartwig coupling, Ullman coupling) (Johansson et al., 2012) (Figure 1A).

Conventional approach to introduce halides (Br, Cl, I) on (hetero)arenes heavily relies on electrophilic halogenation with various of reagents, like chlorine, bromine, iodine, NCS, NBS, ^{t}BuOCl, and Palau'chlor[4] (Rodriguez et al., 2014). Such electrophilic halogenation process, unavoidably, generates another part of molecule as waste, like HBr and succinimide from bromine and NBS, respectively. Besides, they also suffer from being erosive, explosive, or toxic. The Sandmeyer reaction (Kumar et al., 2012) is another commonly used approach to prepare (hetero)aryl halides. However, multiple steps, lots of chemical wastes, and harsh reaction conditions are necessary. Oxidative halogenation serves as an important alternative (Podgoršek et al., 2009), like transition metal (TM)-catalyzed C-H bond functionalization (Petrone et al., 2016), photo-/electrocatalysis (Br, Cl) (Hering et al., 2016; Yuan et al., 2019; Liang et al., 2019), and HX (X = Br, Cl)/oxidant (Fosu et al., 2019; Srivastava et al., 1996; Ross, and Burrows, 1987; Ben-Daniel et al., 2003). Albeit significant progress has been achieved, there is still large room to improve. For example, the TM-catalyzed oxidative halogenations normally require noble catalysts, directing groups, harsh conditions, or costly oxidants. Some frequently encountered functional groups cannot be tolerated in electrocatalysis, such as alkyl carboxylic acids (Kolbe electrolysis). Acid-sensitive groups (e.g., alkene, *tert*-butylcarbamate, alcohol, and basic *N*-atoms) and primary/secondary alcohols (Srivastava et al., 1996) cannot survive well in HX/oxidant as well. The large-scale synthesis (>100g) is also quite challenging for these methods, due to cost-unfriendly reagents, harsh conditions, or difficulties in purification. Halogenation in nature, on the other hand, can be achieved in high selectivity even with complex molecules under mild conditions via utilizing nucleophilic halides by enzymes, like metalloenzymes and flavoenzymes (Latham et al., 2018; Butler and Sandy, 2009; Gkotsi et al., 2018; Vailancourt et al., 2006). However, its industrial application still needs

[1]School of Pharmacy, Tongji Medical School, Huazhong University of Science and Technology (HUST), 13# Hang Kong Road, Qiaokou District, Wuhan, Hubei 430030, P. R. China

[2]Lead Contact

*Correspondence: czldreamer@hotmail.com, pmchenzl@hust.edu.cn

https://doi.org/10.1016/j.isci.2020.101072

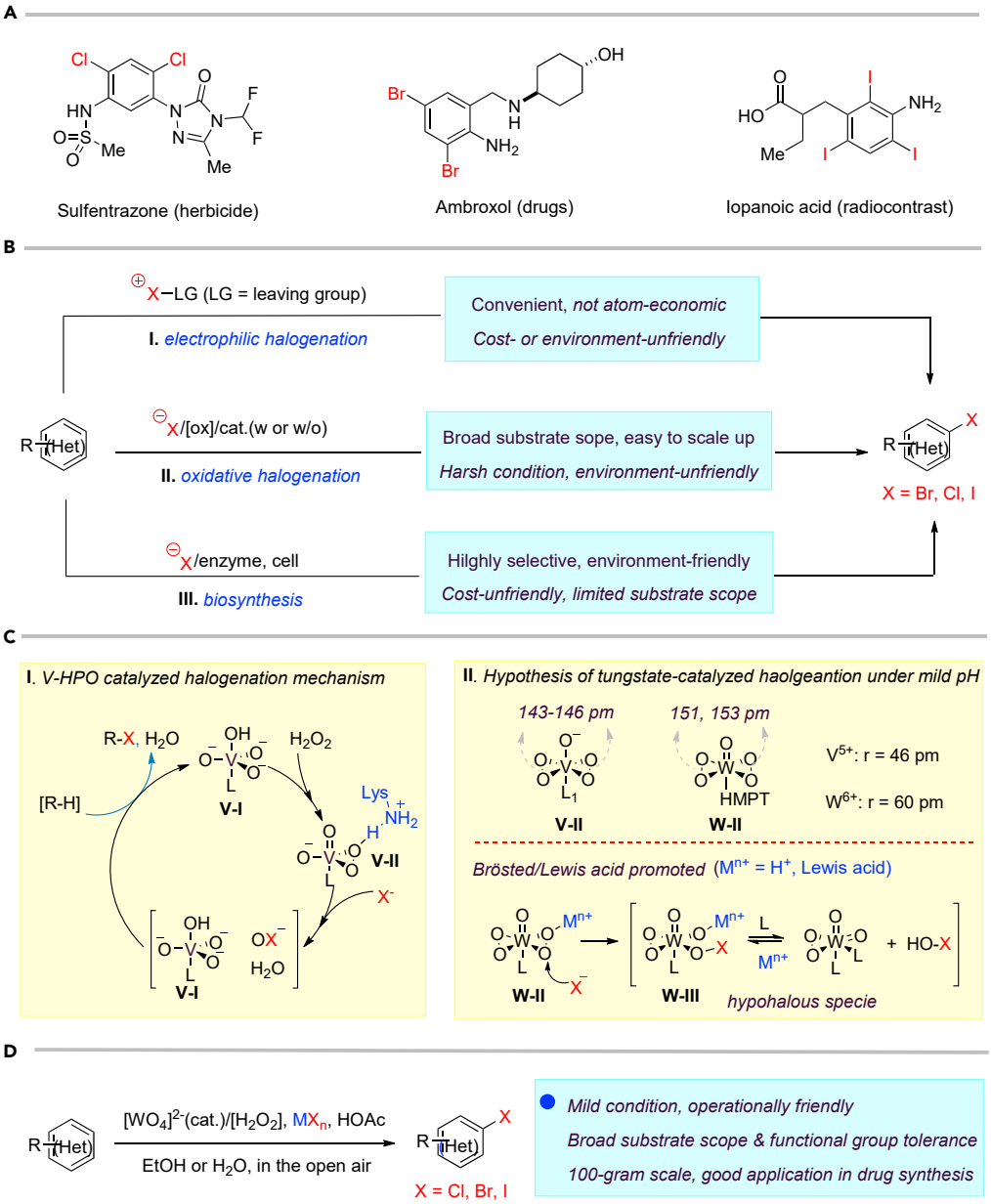

Figure 1. Previous Approach for Halogenation (Br, Cl, I) and Our Strategy

(A) Typical examples of biologically important (hetero)aryl halides.

(B–D) (B) Previous reported approaches for halogenation developed in laboratories. (C) The reaction mechanism of vanadium haloperoxidases (V-HPO) and comparison of V-η^2-peroxy and W-η^2-peroxy intermediates. (D) Biomimetic halogenation catalyzed by tungstate. HMPT, hexamethylphos-phor triamide.

improvements in several aspects due to limited substrate scopes, high requirements of condition to maintain enzyme activity (solvent, temperature, pH, and so on), and inconvenient isolation process in large-scale synthesis (Figure 1B).

The biomimetic halogenation provides a possible access to such ideal halogenation. Inspired by vanadium haloperoxidases (V-HPO) (Latham et al., 2018; Winter and Moore, 2009), vanadium-catalyzed biomimetic halogenation (de la Rosa et al., 1992) has attracted lots of attention. According to the mechanism, a V-η^2-peroxy intermediate (**V-II**) was formed first in the presence of H_2O_2 and then opened by halide assisted by H-bonding from proximate lysine, yielding an electrophilic hypohalite (OX^-, HOX or V-OX, X = Br, Cl, I)

captured by (hetero)arenes (Winter and Moore, 2009) (Figure 1C, I). However, vanadium is difficult for industrial production as critical hazard by Europea Union regulation (Assem and Levy, 2009). Theoretically, any transition metal can also fulfill such biomimetic halogenations if only they can form such η^2-peroxy intermediates. Thus, many researches have focused on searching for other TM catalysts for this biomimetic halogenation (Herget et al., 2018). However, low pH condition was normally required to maintain the activity of catalysts, and many acid-sensitive functional groups cannot be tolerated. Actually, development of biomimetic halogenation under mild pH is a long-time challenge. Among them, tungsten (W) (Beinker et al., 1998; Sels et al., 1999; Badetti et al., 2015) has attracted great interest. Given that W-η^2-peroxy intermediate has more charged metal ion-bearing larger-radii (W^{6+}, 60 pm versus V^{5+} 46 pm) and longer O-O bonds than those of V-η^2-peroxy intermediate (151, 153 pm for W, 143–146 nm for V) (Reynlds and Butler, 1996; Amato et al., 1986; Mimoun et al., 1983; Drew and Einstein, 1972; Stomberg, 1986; Djordjevic et al., 1985; Begin et al., 1975), it is supposed to be a better peroxy electrophile as observed in oxidation of (thiolato)-cobalt (III) complexes (Ghiron and Thompson, 1988). Meanwhile, the electrophilicity of W-η^2-peroxy, we believe, can be further enhanced by Brønsted or Lewis acid (Kikushima et al., 2010), promoting the formation of hypohalous species (**W-III**, HOX) (Roy and Bhar, 2010). From this perspective, biomimetic W-catalyzed halogenation under mild pH could be possible (Figure 1C, II). Herein, we present such a tungstate-catalyzed, biomimetic oxidative halogenation (Br, Cl, I) of (hetero)arene in a scalable (>100 g), inexpensive, environment- and operation-friendly manner, along with broad substrate scope, diverse functional group tolerance, and good chemo- and regioselectivity (Figure 1D).

RESULTS AND DISCUSSION

Condition Optimization for Tungstate-Catalyzed Oxidative Bromination of (Hetero)Arene

Initially, aniline **1-1** was selected as model substrate for our hypothesis. After lots of efforts in condition screening, ultimately the desired product **2-1** can be obtained in good yield in the presence of 5 mol % sodium tungstate, 1.1 equivalents of NaBr, and 6.0 equivalents of H_2O_2 (30% aq.) in EtOH assisted by adding 1.1 equivalents of HOAc (Table 1, entry 1). The reaction still moved on but at a much slower rate without adding HOAc (Table 1, entry 2). Only trace amount of the product can be detected by thin-layer chromatography without catalyst in background reaction (Table 1, entry 3). Polyoxotungstate also worked well in this reaction, with a little bit lower yield (Table 1, entry 4 and 5). Other bromides, like LiBr and KBr, afforded the product **2-1** as well in eroded efficiency (Table 1, entry 6 and 7). Sodium perborate failed to afford any product (Table 1, entry 8). Other protonic solvents, like MeOH, also worked smoothly (Table 1, entry 9). Notably, the reaction went on well even in H_2O, although both starting material and product were not well dissolved (Table 1, entry 10). Decreasing the loading of either catalyst or H_2O_2 evidently reduced the reaction efficiency (Table 1, entry 11-12). Only trace *ortho*-bromination (**2-1B**), dibromination (**2-1C**), and nitroso products (**2-1D**) were observed in all condition screenings. In addition, no azo or azoxy products were observed (Ke et al., 2019), demonstrating good chemo- and regioselectivity of this transformation (Tables 1, see also S1 and S2 and Figure S6).

Substrate Scope of Tungstate-Catalyzed Oxidative Bromination

With the optimized reaction condition at hand, the substrate scope for bromination was investigated as summarized in Table 2. Overall, anilines, phenols, other electronically rich (hetero)arenes, and carbonyl compounds can all afford the bromination products smoothly in moderate to excellent yield. Diverse functional groups were well tolerated, including ester (**2-1**, **2-3**, **2-11**, **2-16**, **2-20**), amide (**2-2**, **2-12**), hydroxy (**2-7** to **2-12**), nitrone (**2-4**, **2-10**), halogens (**2-7**, **2-22**), morpholine (**2-6**), methoxy (**2-13**, **2-14**), carboxylic acid (**2-9**), and ketone (**2-15**). Good to excellent chemo- and regioselectivity were observed as well. The *para*-product was favored over *ortho*-product (e.g., **2-1**, **2-2,** and **2-6**). The unprotected amine groups in anilines remained untouched, even though the azoxy formation could dominate the reaction (Ke et al., 2019). Unlike the dimerization and dearomatization frequently encountered under similar conditions (Dewar and Nakaya, 1968), the oxidative bromination of phenol still worked smoothly in this reaction. Adding 2.2 equiv NaBr and HOAc, the dibromination products can be easily prepared as well (**2-10**, **2-11**, **2-12**) (Figure 2B). Interestingly, only monobromination of 1,3,5-trimethoxy benzene (**2-14**) was observed without any dibromination product and 1,3-dicarbonyl compounds afforded the α-bromination product.

As it is well known, the Lewis basicity of nitrogen (N) could hamper the reaction by coordinating to transition metals as observed in halogenation catalyzed by Pd, Cu, Rh, and Ru (Petrone et al., 2016, Wan et al., 2006). In addition, heteroarenes bearing strong basic nitrogen (e.g., pyridine, isoquinoline, and quinolone) can form salts with HOAc, leading to a decrease in their nucleophilicity and enhancement of the pH value in

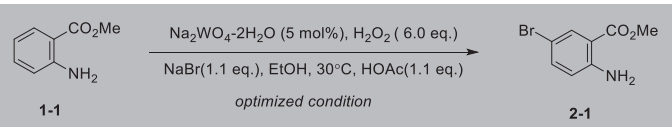

Entry	Vary from Optimized Condition	Yield[a]	Major By-products
1	None	78%–83%	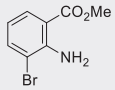 2-1B
2	Without HOAc	<50% conversion for 3 days	
3	Without Na_2WO_4-$2H_2O$	Trace[b]	
4	$H_3O_{40}PW_{12}$-xH_2O instead of Na_2WO_4-$2H_2O$	64%[c]	
5	$(NH_4)_{10}(H_2W_{12}O_{42})$-$xH_2O$ instead of Na_2WO_4-$2H_2O$	77%[c]	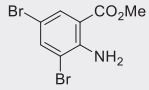 2-1C
6	LiBr instead of NaBr	66%[d]	
7	KBr instead of NaBr	75%[d]	
8	SPB instead of H_2O_2	N.R	
9	MeOH instead of EtOH	67%	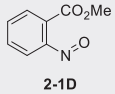 2-1D
10	H_2O instead of EtOH	67%	
11	Na_2WO_4-$2H_2O$, 1 mol % instead of 5 mol %	67%	
12	2.0 equiv H_2O_2 instead of 6.0 equiv	57%	

Table 1. Condition Optimization

N.R, no reaction

[a]All the reactions were conducted in 1.0-mmol scale (**1-1**) for 12 h, isolated yield.

[b]2.0 equivalents of HOAc was utilized.

[c]1.5 equivalents NaBr and 2.0 equiv. HOAc were utilized.

[d]1.5 equivalents of NaBr and 2.0 equivalents of HOAc were utilized, and the reactions were conducted at 50°C

the reaction. Surprisingly, the bromination of *N*-containing heteroarenes still proceeded smoothly in our reaction, including indole (**2-16**), indole analogs (**2-17**, **2-18**, **2-19**), pyrroles (**2-20**, see also Figure S7), carbazone (**2-21**), imidazo[1,2-a]pyridine (**2-22**), pyridine (**2-23**), isoquinoline (**2-24**, see also Figure S8), and quinoline (**2-25**). Actually, the reactions were conducted in neutral condition to some extent for those basic heteroarenes. Of note, no *N*-oxide products were observed in all tested heteroarenes, indicating excellent chemoselectivity in this reaction.

Late-stage bromination of complex molecules, like drug leads and bioactive natural products, is highly appealing, facilitating quick structure-activity relationship studies given the diverse transformations based on aryl bromides. It is reasonable to hypothesize that the selective late-stage bromination of complex molecules can be achieved, considering the good functional group tolerance as observed in previous studies. However, it can be challenging to obtain good chemo- and regioselectivities for substrates bearing multiple reaction sites with slightly different chemical surroundings. Nonetheless, the late-stage bromination of complex molecules was proved to be successful in our reaction. For instance, the slight difference of multiple reactive positions in olfenamic acid (**2-26**) and sulfapyridine (**2-27**) could be distinguished, affording the single monobromination products in high yield. Tyrosine (**2-28**), indole-2-one (**2-29**), and estrone (**2-30**, see also Figure S9) also yielded the monobromination products in good chemo- and regioselectivity. It is worth pointing out that the acid-sensitive *tert*-butylcarbamate group was well tolerated in our reaction, demonstrating that our approach has better functional group tolerance than that of reported HX/oxidant system. Notably, saccharide scaffolds are maintained untouched, as shown in cytidine (**2-31**, see also Figure S10) and naringin (**2–32**, see also Figure S11), albeit many oxidant transformations could occur with such

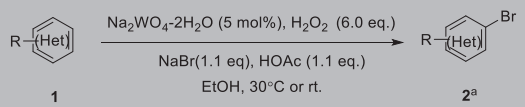

- *Broad substrate scope & good functional group tolerance*
- *Late stage functionalization of complex molecules*
- *Environmentally & operationally friendly*

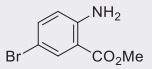	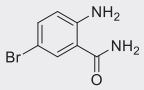	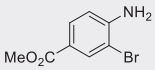	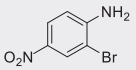	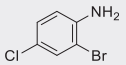
2-1, 91% (*p: o: d* = 21:1:1)	**2-2**, 52%	**2-3**, 85% (89%[b] in H_2O)	**2-4**, 75% (90% brsm)	**2-5**, 69%[c]
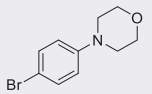	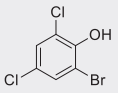	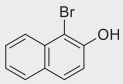	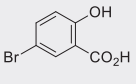	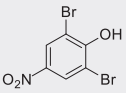
2-6, 57%	**2-7**, 65% (76%[b] in H_2O)	**2-8**, 54%	**2-9**, 70%	**2-10**, 93%[d]
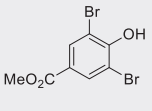	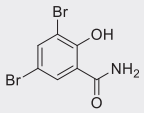	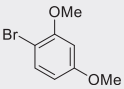	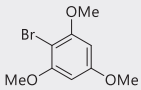	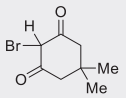
2-11, 86%[d]	**2-12**, 83%[d]	**2-13**, 86%	**2-14**, 98% (92%[b] in H_2O)	**2-15**, 62% yield
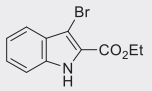				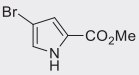
2-16, 81%	**2-17**, 74%	**2-18**, 73%	**2-19**, 72%	**2-20** 52% (*m: d* = 5:1)
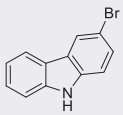	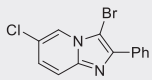	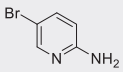	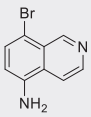	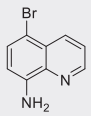
2-21, 38% (79% brsm)	**2-22**, 92%	**2-23**, 79%	**2-24**, 61% (*m: d* = 2:1)	**2-25**, 33%
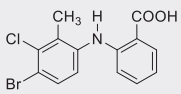	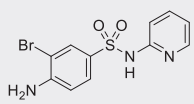	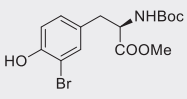	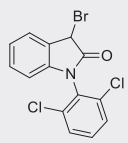	
2-26, 97% (tolfenamic acid)	**2-27**, 74% (sulfapyridine)	**2-28**, 34% (98% brsm) (derived from tyrosine)	**2-29**, 31% (45% brsm) (indole-2-one)	
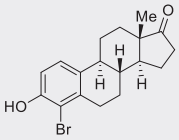	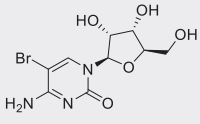	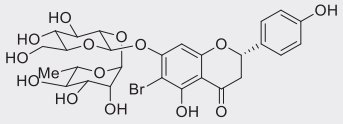		
2-30, 48% (56% brsm, m: d = 11:1) (estrone)	**2-31**, 83% (by HNMR) (cytidine)	**2-32**, 75% (by NMR, 2:1 rr) (naringin)		

Table 2. Substrate Scope of Tungstate-Catalyzed Oxidative Bromination of (Hetero)Arene

p, *para*-bromination product; *o*, *ortho*-bromination product; *m*, mono-bromination; *d*, dibromination product; rr, regioselective ration; brsm, based on recovered starting material.

Unless noted, all the reactions were conducted in 1.0-mmol scale (**1**) with Na_2WO_4-$2H_2O$ (5 mol %), NaBr (1.1 equivalents), H_2O_2 (30 % aq., 6.0 equivalents.), HOAc (1.1 equiv.) in EtOH (5.0 mL) at 30°C isolated yield (see also Figure S1).

[b]The reactions were conducted in H_2O with Na_2WO_4-$2H_2O$ (2.5 mol %), NaBr (1.1 equivalent), H_2O_2 (30 % aq., 1.1 equivalent) and HOAc (1.1 equivalent) (see also Figure S2).

[c]5.0-mmol scale.

[d]2.2 mmol NaBr (2.2 equivalents) and HOAc (2.2 equivalents) were utilized.

multiple unprotected hydroxyl groups. Water is the ideal reaction solvent, from the perspective of cost and environmental concerns. Delightfully, our reaction worked in water as well (see also Table S3), giving comparable results as those in EtOH (**2-2**, **2-3**, **2-7**, **2-14**).

Substrate Scope of Tungstate-Catalyzed Oxidative Chlorination and Iodination

The oxidative chlorination and iodination were also investigated as summarized in Table 3. Noticing that the redox potential of chloride is higher than that of bromide, oxidative chlorination was more challenging. Indeed, unlike the fact that the bromination worked smoothly with NaBr and KBr, no chlorination product was observed in the presence of NaCl or KCl. After tedious efforts in condition optimization, ultimately it was found that $BaCl_2$ could afford the chlorination products in best yield with model substrate **1-1** (see also Tables S4 and S5). Aniline, phenol, other electronically rich (hetero)arenes, and carbonyl compounds all worked well. Good functional group tolerance was observed as well, including ester (**2-33**, see also Figure S12; **2-40**), free aniline (**2-33**, **2-34**), morpholine (**2-35**, see also Figure S13), halide (**2-36**, **2-42**), alkoxyl (**2-37**), carboxylic acid (**2-38**), and ketone (**2-39**). Compared with bromination, chlorination generally required longer reaction time and higher reaction temperature. Although iodide is easier to be oxidized than bromide, such biomimetic oxidative iodination of (hetero)arenes is scarcely reported (Sels et al., 2005). Moreover, the aryl iodide product can potentially be further oxidized into hyperiodide species (Banik et al., 2016), leading to undesired by-products. To our delight, such overoxidation was not observed in this reaction (Emmanuvel et al., 2006). Selected substrates were investigated, and all afforded the products in moderate to excellent yield, including aniline (**2-43**, **2-45**), phenol (**2-44**), and heteroarene (**2-46**, **2-47**). It should be pointed out that the background of iodination worked as well without catalyst. However, the catalyst acceleration was also evident as observed in some substrates, and longer reaction time is required without catalyst (**2-45**, **2-47**).

100-g-Scale Preparation of (Hetero)Aryl Bormide

The reaction can be scaled up to over 100 g without any erosion of efficiency, including aniline (Table 4, **2-1** and **2-3**), phenol (Table 4, **2-11**), and other electronically rich (hetero)arene (Table 4, **2-14** and **2-23**). Of note, the reaction can be conducted in beakers in the open air, and the products precipitated upon completion during gram-scale reaction, obtained in high purity only by filtration and washing (see also Figure S5). These results suggested the good potential of our reaction in industrial preparation of (hetero)aryl halide.

Synthetic Application in Drugs and Key Precursors for Drugs

Many drugs and drug leads contain aryl halide (Br, Cl, I) motifs, thus we would like to explore the utility of our approach in their preparation. The quinoline halides were embodied in several antibiotic drugs and bioactive compounds, like chlorquinaldol, iodoquinadol, cloxiquine, clioquinol, and broxyquinoline. Although they were reported to be good ligands for tungsten (Archer and Bonds, 1967), the oxidative halogenation of 8-hydoxyquinolines was achieved successfully. Clioquinol (**2-48**), iodoquinadol (**2-49**), broxyquinoline (**2-50**), and precursor for broxaldine (**2-51**) were all obtained in moderate to good yield. Of note, all these reactions were conducted in multiple gram scale without silica gel column purification, typically like the precursor for broxalide (**2-51**) (Swain et al., 1986) (Figure 2A). The key intermediate for brimonidine (**2-52**) (Jeon et al., 1995), a medicine to treat ocular hypertension, rosacea, and open-angle glaucoma, was conveniently prepared (Figure 2B). As dopamine antagonists are used as antiemetic drugs, both bromopride and metoclopramide bear an aryl halide motif derived from salicylic acid (Kato et al., 1991), which were conveniently prepared from methyl 4-amino-2-methoxybenzoate according to our approach (**2-53** and **2-54**) (Figure 2C). Benzbromaron is a broadly utilized drug to treat gout. However, the dibromination of its precursor, compound **1-43**, with bromine, only afford 35% yield of benzbromarone along with the monobromination impurities (Wempe et al., 2011). By contrast, pure benzbromarone (**2-55**)

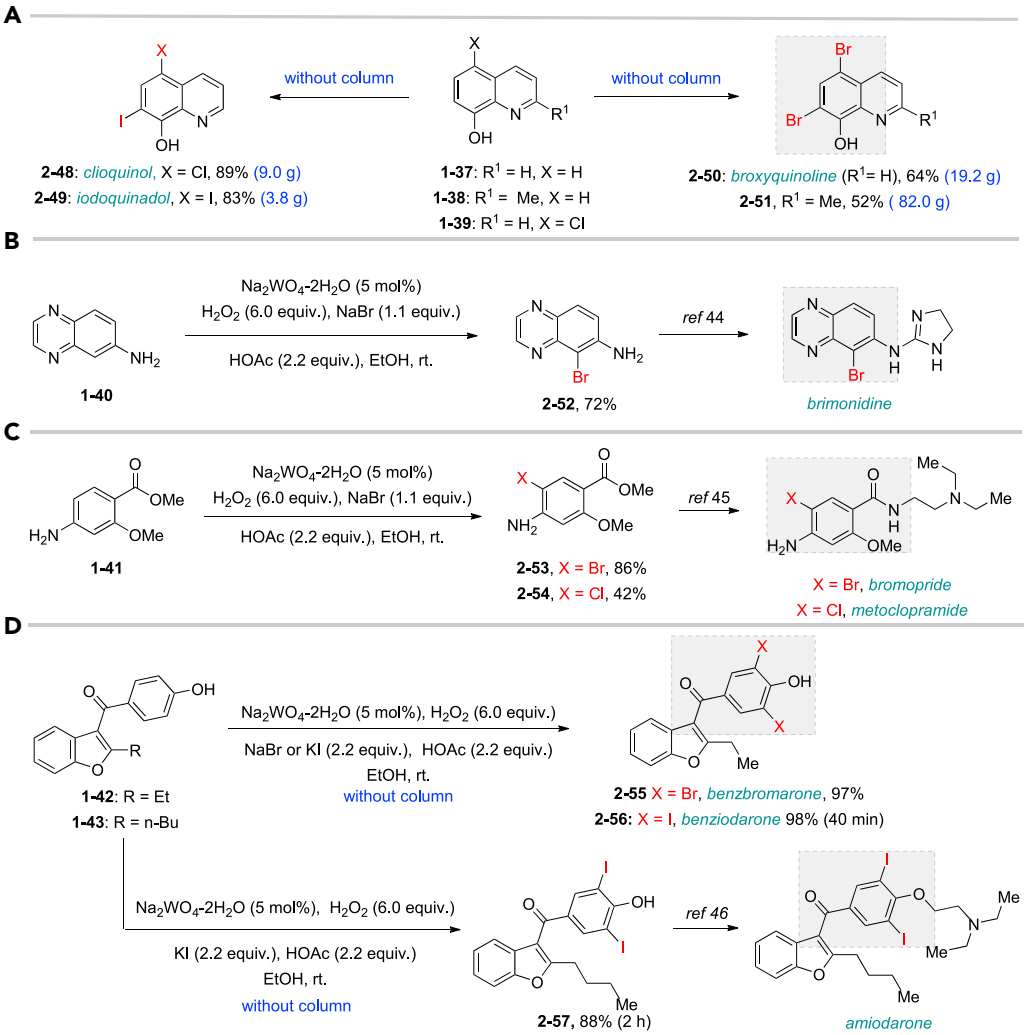

Figure 2. Application in Synthesis of Selected Drugs and Key Precursors

(A) Synthesis of quinoline drugs or key precursors, including clioquinol, iodoquinado, broxyquinoline, and precursor for broxaldine.

(B) Synthesis of key precursor for brimonidine, a drug to treat ocular hypertension, rosacea, and open-angle glaucoma.

(C) Synthesis of key precursor bromopride and metoclopramide, antiemetic drugs.

(D) Synthesis for benzofuran drugs: benzbromaron, benziodarone, and amiodarone.

was obtained in excellent yield under mild condition even without column purification by utilizing our approach. Benziodarone (**2–56**), a vasodilator, was obtained in excellent yield as well. Compared with the poor yield and chemoselectivity by utilizing NaClO/KI/NaOH (Snead et al., 2008) the iodination of compound **1-50** worked quite well in our reaction, giving the key precursor for amiodarone (**2-57**), a drug to treat arrhythmias (Figure 2D).

Mechanism Study

To figure out whether the bromine radical is involved in this reaction, substrate **1-45** was selected as a probe. If the bromine radical existed as reaction intermediate, product **2-59** should be observed. However, only product **2-58** was isolated in moderate yield, excluding that the bromination went through radical reaction pathway (Figures 3A and see also S14). HOAc was used only in 1.1 equivalents as reagent in this reaction, rather than solvent, to stabilize the Br^+ species. We suppose the HOAc played dual key roles in this halogenation (Maheswari et al., 2006): (1) neutralizing the hydroxyl anion from H_2O_2 and (2) providing H-bonding to the key W-η^2-peroxy intermediate **W-II**. For chlorination, the chloride salts (MCl_n) also played key dual role: (1) providing chloride and (2) being a Lewis acid to the W-η^2-peroxy intermediate (**W-II**) similar to V-catalyzed bromination (Kikushima et al.,

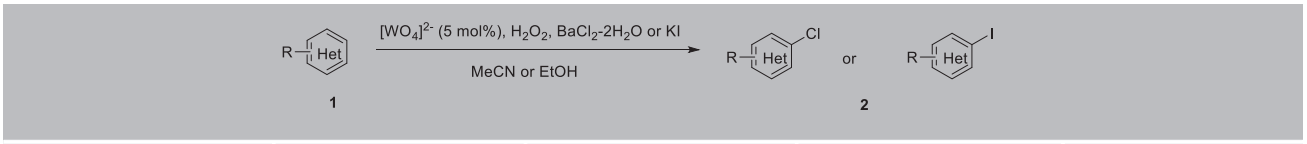

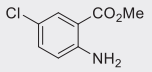	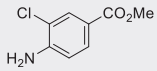	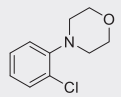	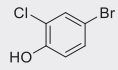	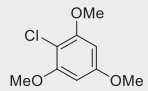
2-33[a], 81% (p: *o* = 2.2: 1)	**2-34**[a], 49% (64% brsm)	**2-35**[a], 58% (p: *o* = 1: 3.5)	**2-36**[a], 82%[bb]	**2-37**[a], 51% (74% brsm)
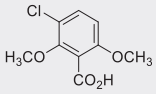	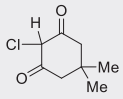	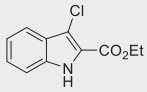		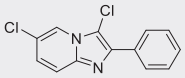
2-38[a], 44% (56% brsm)	**2-39**[a], 43%	**2-40**[a], 70% (91% brsm)	**2-41**[a], 56% (62% brsm)	**2-42**[a], 35% (78% brsm)
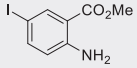	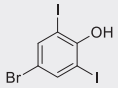	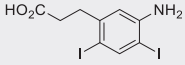		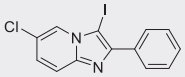
2-43[c], 39% (48% brsm)	**2-44**[c,d,e], 97%[d] (13 h) (93%[e], w/o. cat.,17 h)	**2-45**[c,d], 65%[d] (40 min) (66%e, w/o. cat., 6 h)	**2-46**[c], 89% (15 min) (96%[e], w/o. cat., 15 min)	**2-47**[c], 97% (20 min) (99%[e], w/o. cat., 1 h)

Table 3. Substrate Scope of Tungstate-Catalyzed Oxidative Chlorination and Iodination

brsm, based on recovered starting material; p, *para*-chlorination product; *o*, *ortho*-chlorination product.

[a]Unless noted, the chlorination reactions were carried out in 1.0-mmol scale (**1**) in MeCN (5.0 mL) at 50°C with Na_2WO_4-$2H_2O$ (5 mol %), H_2O_2 (30% aq. 4.0 equiv.), $BaCl_2 \cdot 2H_2O$ (1.2 equiv), and HOAc (1.0 equiv) (see also Figure S3).

[c]The iodination reaction was conducted in 1.0-mmol scale (**1**) in EtOH at room temperature (20–25°C) with Na_2WO_4-$2H_2O$ (5 mol %), H_2O_2 (30% aq. 6.0 equiv), KI (1.1 equiv), and HOAc (1.1 equiv) (see also Figure S4).

[b]Trifluoro acetic acid was used instead of HOAc.

[d]2.2 equivalents of KI and HOAc were used.

[e]No catalyst was added as control experiments.

2010). Both the HOAc and metal ion (M^{n+}) can increase the electrophilicity of W-η^2-peroxy intermediate **W-II** by H-bonding or Lewis acid-base interaction (Figure 3B). From this perspective, weakening such H-boding effect will decrease the reaction efficiency. Indeed, the reaction proceeded much slower without HOAc or in aprotic solvent, such as THF (Figure 3C, see also Table S2). On the other side, the strength of the Lewis acidity of metal cations can control the chlorination as well, in consist with evidently different reactionefficiency when utilizing different chloride salts. For example, no chlorination product was detected in the presence of LiCl, NaCl, and KCl; however, dichlorination product **2-34C** was isolated as major product in the presence of $CaCl_2$ or $SrCl_2$ even reducing their loading. By contrast, monochlorination products (**2-34**, **2-34B**) were obtained as major

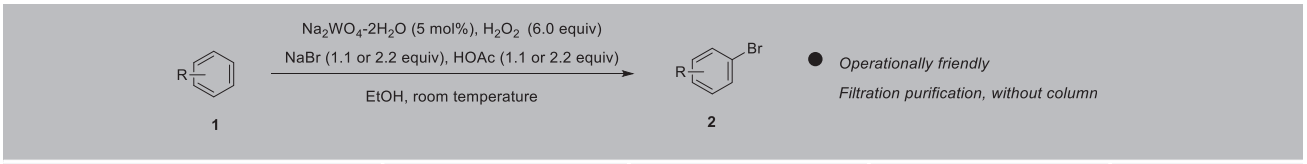

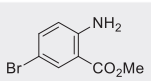	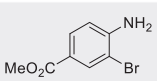	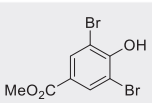	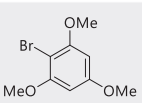	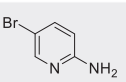
2-1, 93%, 221g (p: *o*: *d* = 20: 3: 3)	**2-3**, 94%, 107 g	**2-11**, 88%,136 g	**2-14**, 99%, 123 g	**2-23**, 85%, 146 g

Table 4. 100-g-Scale Bromination

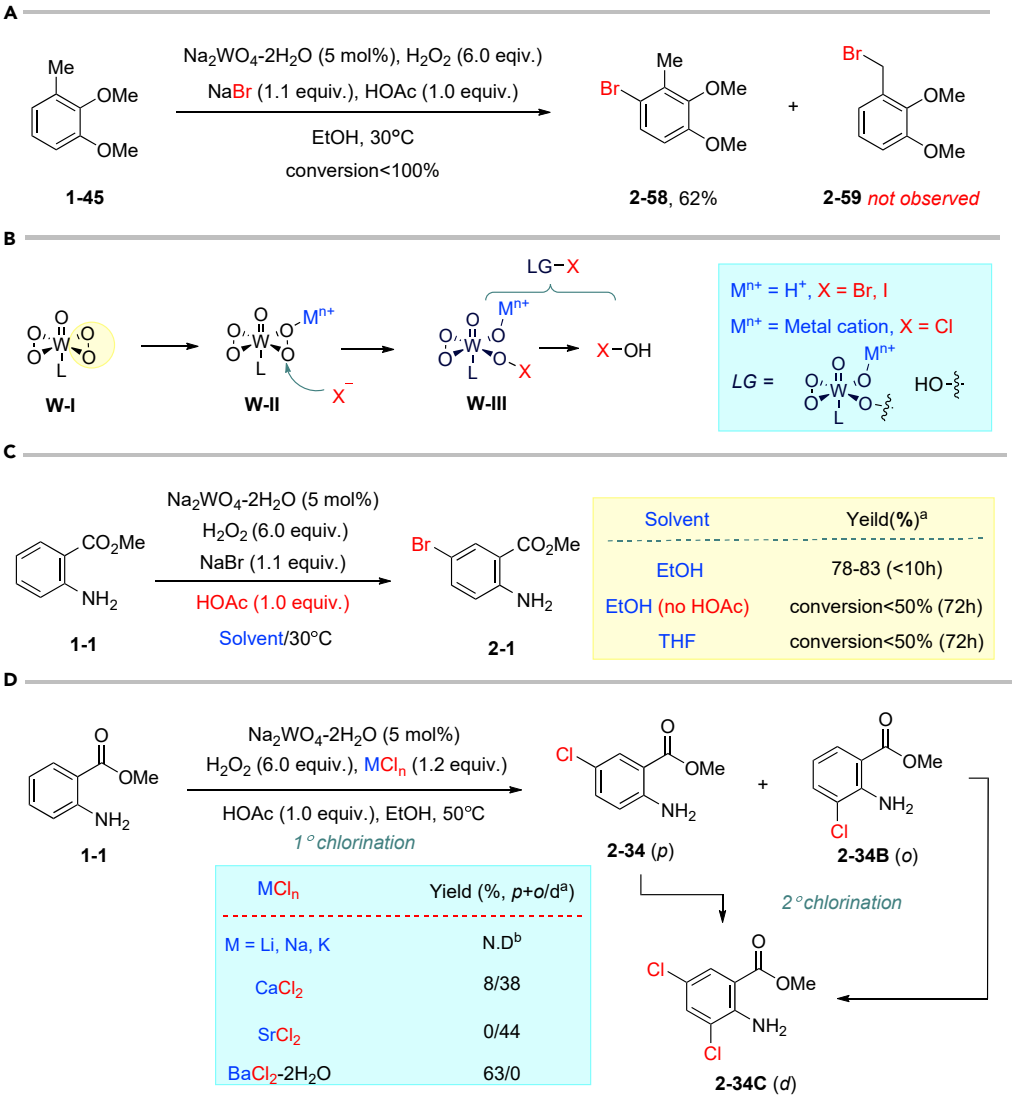

Figure 3. Hypothesis of Mechanism of Bromination/Iodination and Control Experiments

(A) Radical trapping experiment.

(B) Hypothesis of H-bonding effect with Brønsted acid.

(C) Control experiments to probe the importance of H-bonding.

(D) Effects of metal ion in chloride salts in chlorination.

products with $BaCl_2$ even extending reaction time. In addition, the major hypohalous species in chlorination should be **W-III** rather than HOCl; otherwise, the chloride salts should not have significant impact on products' distribution on monochlorination and dichlorination (Figure 3D, see also Table S4).

Proposed Reaction Mechanism

Other polyoxotungstate catalyst intermediates might also be involved (Corsini and Subramanian, 1978), like dinuclear peroxotungstate **W-VI** (Kamata et al., 2007), thus we used **W-IV** as a model to illustrate the reaction mechanism given that the reaction center is the peroxyl moiety. Based on all the control experiments, we proposed the reaction mechanism as following. Initially, the tungstate **W-V** would form W-η^2-peroxy intermediate **W-V** and then **W-I** in the presence of H_2O_2 and HOAc. The peroxy moiety in **W-I** was opened by halide (Roy and Bhar, 2010) in the assistance of Brønsted acid (bromination, iodination) or Lewis acid (chlorination) to yield hypohalous species **W-III** or HOX, which was trapped by (hetero)arene

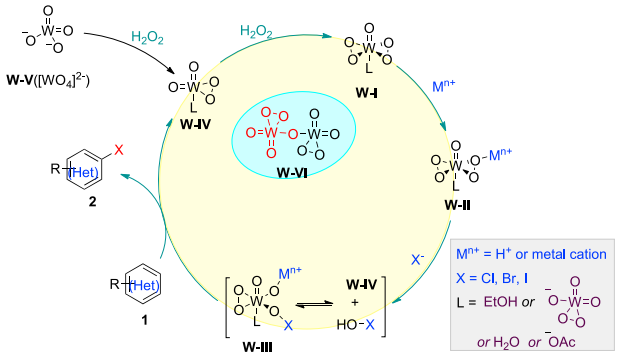

Figure 4. Proposed Reaction Mechanism

via electrophilic halogenation to afford the desired products. The HOAc and EtOH can also serve as a ligand to tungstate catalyst (Figure 4).

In summary, we have developed a tungstate-catalyzed, biomimetic, cost-efficient, environment- and operation-friendly approach for halogenation (Br, I, Cl) of (hetero)arene under mild pH. Broad substrate scope, diverse functional group tolerance, and late-stage bromination of bioactive complex molecule were achieved in this reaction. Besides, water can be utilized as solvent and >100-g scale reaction was conveniently accessed without column purification. Furthermore, several drugs and key precursors for drugs have been conveniently prepared. Primary mechanism studies suggested that Brønsted or Lewis acid can accelerate the reaction and control the products' distribution.

Limitations of the Study

Our reaction provides a green and robust access to (hetero)aryl halides and works well for most tested substrates. However, limitation still exists. For example, the chlorination normally takes longer reaction time and has lower efficiency than bromination and iodination. Some too electronically rich substrates like indole involve other undesired oxidative transformations along with halogenation. In addition, more than 1 equivalent of H_2O_2 is required for the completion of this reaction under current optimized conditions. Further improvement to enhance the reaction efficiency with broader substrate scope is under investigation in our laboratory.

METHODS

All methods can be found in the accompanying Transparent Methods supplemental file.

DATA AND CODE AVAILABILITY

Procedure for experiments and characterization data for products are available in Supplemental Information.(Figure S15-S149) Any other data are available from the corresponding author upon reasonable request.

SUPPLEMENTAL INFORMATION

Supplemental Information can be found online at https://doi.org/10.1016/j.isci.2020.101072.

ACKNOWLEDGMENTS

Financial support was provided by the National Natural Science Foundation of China (21602011) and the talent recruitment fund of Huazhong University of Science and Technology (HUST). The authors also would like to thank the Analytical and Testing Center in HUST for assistance in NMR and HRMS data collection.

AUTHOR CONTRIBUTIONS

Z.C. conceived and directed the project; Z.C., Z.M., H.L., and K.L. designed the experiments; Z.M. and K.L. performed the condition optimization for bromination/chlorination; Z.M. performed the condition optimization of iodination; H.L. performed the reactions in water; Z.M. performed the substrates scope investigation; Z.C. and Z.M. collected and analyzed the data; Z.C. prepared the manuscript.

DECLARATION OF INTERESTS

The authors declare no conflicts of interest.

Received: January 31, 2020
Revised: March 13, 2020
Accepted: April 14, 2020
Published: May 22, 2020

REFERENCES

Amato, G., Arcoria, A., Ballistreri, F.P., Tomaselli, G.A., Bortolini, O., Conte, V., Di Furia, F., Modena, G., and Valle, G. (1986). Oxidations with peroxotungsten complexes: rates and mechanism of stoichiometric olefin epoxidations. J. Mol. Catal. *37*, 165–175.

Archer, R.D., and Bonds, W.D., Jr. (1967). A completely cheated spin-paired eight-coordinate tungsten(IV) complex. J. Am. Chem. Soc. *89*, 2236–2237.

Assem, F.L., and Levy, L.S. (2009). A review of current toxicological concerns on vanadium pentoxide and other vanadium compounds: gaps in knowledge and directions for future research. J. Toxicol. Environ. Health B Crit. Rev. *12*, 289.

Badetti, E., Romano, F., Marchiò, L., Taşkesenlioğlu, S., Daştan, A., Zonta, C., and Licini, G. (2015). Effective bromo and chloro peroxidation catalyzed by tungsten(VI) amino triphenolate complexes. Dalton. Trans. *45*, 14603.

Banik, S.M., Medley, J.W., and Jacobsen, E.N. (2016). Catalytic, asymmetric difluorination of alkenes to generate difluoromethylated stereocenters. Science *353*, 51–54.

Begin, D., Einstein, F.W.B., and Field, J. (1975). Asymmetrically coordinated diperoxo compound. Crystal structure of tripotassium oxodiperoxooxalatovanadate(V) monohydrate. Inorg. Chem. *14*, 1785–1790.

Beinker, P., Hanson, J.R., Meindl, N., and Medina, I.C.R. (1998). Oxidative iodination of aromatic amides using sodium perborate or hydrogen peroxide with sodium tungstate. J. Chem. Res. *1998*, 204–205.

Ben-Daniel, R., De Visser, S.P., Shaik, S., and Neumann, R. (2003). Electrophilic aromatic chlorination and haloperoxidation of chloride catalyzed by polyfluorinated alcohols: a new manifestation of template catalysis. J. Am. Chem. Soc. *125*, 12116–12117.

Butler, A., and Sandy, M. (2009). Mechanistic considerations of halogenating enzymes. Nature *460*, 848–854.

Corsini, A., and Subramanian, K.S. (1978). Studies on the tungstate solution in acid medium. J. Inorg. Nucl. Chem. *40*, 1777–1779.

Dewar, M.J.S., and Nakaya, T. (1968). Oxidaive coupling of phenols. J. Am. Chem. Soc. *90*, 7134–7135.

Djordjevic, C., Craig, S.A., and Sinn, E. (1985). A polymeric peroxo heteroligand vanadate(V). Synthesis, spectra, and structure of MI [$VO(O_2)(C_4H_5O_4N)$]. Inorg. Chem. *24*, 1281–1283.

Drew, R.E., and Einstein, F.W.B. (1972). Crystal structure of ammonium oxodiperoxoamminevanadate(V). Inorg. Chem. *11*, 1079–1083.

Emmanuvel, L., Shukla, R.K., Sudalai, A., Gurunath, S., and Sivaram, S. (2006). $NaIO_4$/KI/NaCl: a new reagent system for iodination of activated aromatics through in situ generation of iodine monochloride. Tetra. Lett. *47*, 4793–4796.

Fosu, S.C., Hambira, C.M., Chen, A.D., Fuchs, J.R., and Nagib, N.D. (2019). Site-selective C–H functionalization of (hetero)arenes via transient, non-symmetric iodanes. Chem *5*, 417–428.

Ghiron, A.F., and Thompson, R.C. (1988). Kinetic study of the oxygen-transfer reactions from the oxo diperoxo complexes of molybdenum (VI) and tungsten(VI) to (thiolato)- and (sulfenato) cobalt (III) complexes. Inorg. Chem. *26*, 4766–4771.

Gkotsi, D.S., Dhaliwal, J., McLachlan, M.M., Mulholand, K.R., and Goss, R.J.M. (2018). Halogenases: powerful tools for biocatalysis (mechanisms application and scope). Curr. Open Chem. Biol. *43*, 119–126.

Herget, K., Freichs, H., Pfitzner, F., Tahir, M.N., and Tremel, W. (2018). Functional enzyme mimics for oxidative halogenation reactions that combat biofilm formation. Adv. Mater. *30*, 1707073.

Hering, T., Mühldorf, B., Wolf, R., and König, B. (2016). Halogenase-inspired oxidative chlorination using flavin photocatalysis. Angew. Chem. Int. Ed. *55*, 5342–5345.

Hernandes, Z.M., Cavalcanti, S.M.T., Moreira, D.R.M., Azevedo, , Jr., and Lima, W.F.D. (2010). Halogen atoms in the modern medicinal chemistry: hints for the drug design. Curr. Drug Targets *11*, 303–314.

Jeon, Y.T., Luo, C., Forray, C., Vaysse, P.J.J., Branchek, T.A., and Gluchowski, C. (1995). Pharmacological evaluation of UK-14,304 analogs at cloned human α adrenergic receptors. Bio. Med. Chem. Lett. *5*, 2255–2258.

Johansson, S.C., Kitching, M.O.T.J., and Colacot, S.V. (2012). Palladium-catalyzed cross-coupling: a historical contextual perspective to the 2010 Nobel Prize. Angew. Chem. Int. Ed. *51*, 5062–5085.

Kamata, K., Kuzuya, S., Uehara, K., Yamaguchi, S., and Mizuno, N. (2007). μ-η^1: η^1-peroxo-bridged dinuclear peroxotungstate catalytically active for epoxidation of olefins. Inorg. Chem. *46*, 3768–3773.

Kato, S., Morie, T., Kon, T., Yoshida, N., Karasawa, T., and Matsumoto, J. (1991). Novel benzamides as selective and potent gastrokinetic agents. 2. Synthesis and structure-activity relationships of 4-amino-5-chloro-2-ethoxy-N-[[4-(4-fluorobenzyl)-2-morpholinyl]methyl]benzamide citrate (AS-4370) and related compounds. J. Med. Chem. *34*, 616–624.

Ke, L., Zhu, G., Qian, H., Xiang, G., Chen, Q., and Chen, Z. (2019). Catalytic selective oxidative coupling of secondary *N*-alkylanilines: an approach to azoxyarene. Org. Lett. *21*, 4008–4013.

Kikushima, K., Moriuchi, T., and Hirao, T. (2010). Vanadium-catalyzed oxidative bromination promoted by brønsted acid or Lewis acid. Tetrahedron *66*, 6906–6911.

Kumar, L., Mahajan, T., and Agarwal, D.D. (2012). Aqueous bromination method for the synthesis of industrially important intermediates catalyzed by micellar solution of sodium dodecyl sulfate (SDS). Ind. Eng. Chem. Res. *51*, 2227–2234.

Latham, J., Brandenburger, E., Shepherd, S.A., Menon, B.R.K., and Micklefield, J. (2018). Development of halogenase enzymes for use in synthesis. Chem. Rev. *118*, 232–236.

Liang, Y., Lin, F., Adeli, Y., Jin, R., and Jiao, N. (2019). Efficient electrocatalysis for the preparation of (hetero)aryl chlorides and vinyl chloride with 1,2-dichloroethane. Angew. Chem. Int. Ed. *58*, 4566–4570.

Maheswari, P.U., Tang, X., Hage, R., Gamez, P., and Reedijk, J. (2006). The role of carboxylic acids on a Na_2WO_4/H_2WO_4-based biphasic homogeneous alkene epoxidation, using H_2O_2 as oxidant. J. Mol. Cat. A *258*, 295–301.

Mimoun, H., Saussine, L., Daire, E., Postel, M., Fischer, J., and Weiss, R. (1983). Vanadium(V) peroxy complexes. New versatile biomimetic reagents for epoxidation of olefins and hydroxylation of alkanes and aromatic hydrocarbons. J. Am. Chem. Soc. *105*, 3101–3110.

Petrone, D.A., Ye, J., and Lautens, M. (2016). Modern transition-metal-catalyzed carbon–halogen bond formation. Chem. Rev. *116*, 8003–8104.

Podgoršek, A., Zupan, M., and Iskra, J. (2009). Oxidative halogenation with "green" oxidants: oxygen and hydrogen peroxide. Angew. Chem. Int. Ed. *48*, 8424–8450.

Reynlds, M.S., and Butler, A. (1996). Oxygen-17 NMR, electronic and vibrational spectroscopy of transition metal peroxo complexes: correlation with reactivity. Inorg. Chem. *35*, 2378–2383.

Rodriguez, R.A., Pan, C.-M., Yabe, Y., Kawamata, Y., Eastgate, M.D., and Baran, P.S. (2014).

Palaúchlor: a practical and reactive chlorinating reagent. J. Am. Chem. Soc. *136*, 6908–6911.

de la Rosa, R.I., Clague, M.J., and Butler, A. (1992). A functional mimic of vanadium bromoperoxidase. J. Am. Chem. Soc. *114*, 760–761.

Ross, S.A., and Burrows, C.J. (1987). Bromination of pyrimidines using bromide and monoperoxysulfate: a competition study between cytidine, uridine and thymidine. Tetra. Lett. *38*, 2805–2808.

Roy, S., and Bhar, S. (2010). Sodium tungstate-catalyzed "On-water" synthesis of β-arylvinyl bromides. Green. Chem. Lett. Rev. *3*, 341–347.

Sels, B., Levecque, P., Brosius, R., De Vos, D., Jacobs, P., Gammon, D.W., and Kinfe, H.H. (2005). A new catalytic route for the oxidative halogenation of cyclic enol ethers using tungstate exchanged on takovite. Adv. Synth. Catal. *347*, 93–104.

Sels, B., Vos, D.D., Buntinx, M., Pierard, F., Mesmaeker, K.-D., and Jacobs, P. (1999). Layered double hydroxides exchanged with tungstate as biomimetic catalysts for mild oxidative bromination. Nature *400*, 855–857.

Snead, A.N., Miyakawa, M., Tan, E.S., and Scanlan, T.S. (2008). Trace amine-associated receptor 1 (TAAR1) is activated by amiodarone metabolites. Bio. Med. Chem. Lett. *18*, 5920–5922.

Srivastava, S.K., Chauhan, P.M.S., and Bhaduri, A.P. (1996). Novel site-specific one-step bromination of substituted benzene. Chem. Commun. (Camb.) *23*, 2679–2680.

Stomberg, R. (1986). The crystal structures of potassium bis(oxalato)oxoperoxovanadate(V) hemihydrate, $K_3[VO(O_2)(C_2O_4)_2].{}^1/_2H_2O$, and potassium bis(oxalato)dioxovanadate(V) trihydrate, $K_3[VO_2(C_2O_4)_2].3H_2O$. Acta Chem. Scand. *A40*, 168–176.

Swain, R., Bapna, J.S., Das, A.K., Chandrasekar, S., Swaminathan, R.P., Bosco, B., Veliath, S., and Thombre, D.P. (1986). A study on the neurotoxicity of broxyquinoline and brobenzoxaldine combination in therapeutic doses, Human. Toxicol *5*, 35–41.

Vailancourt, F.H., Yeh, E., Vosburg, D.A., Garneau-Tsodikova, S., and Walsh, C.T. (2006). Nature's inventory of halogenation catalysts: oxidative strategies predominate. Chem. Rev. *106*, 3364–3378.

Wan, X., Ma, Z., Li, B., Zhang, K., Cao, S., Zhang, S., and Shi, Z. (2006). Highly selective C-H functionalization/halogenation of acetanilide. J. Am. Chem. Soc. *128*, 7416–7417.

Wempe, M.F., Jutabha, P., Quade, B., Iwen, T.J., Frick, M.M., Ross, I.R., Rice, P.J., Anzai, N., and Endou, H. (2011). Developing potent human uric acid transporter 1 (hURAT1) inhibitors. J. Med. Chem. *54*, 2701–2713.

Wilcken, R., Zimmermann, M.O., Lange, A., Joerger, A.C., and Boeckler, F.M. (2013). Principles and applications of halogen Bonding in medicinal chemistry and chemical biology. J. Med. Chem. *56*, 1363–1388.

Winter, J.M., and Moore, B.S. (2009). Exploring the chemistry and biology of vanadium-dependent haloperoxidases. J. Bio. Chem. *284*, 18577–18581.

Yuan, Y., Yao, A., Zheng, Y., Gao, M., Zhou, Z., Qiao, J., Hu, J., Ye, B., Zhao, J., Wen, H., and Lei, A. (2019). Electrochemical oxidative clean halogenation using HX/NaX with hydrogen evolution. iScience *12*, 293–303.

iScience, Volume *23*

Supplemental Information

Tungstate-Catalyzed Biomimetic Oxidative Halogenation of (Hetero)Arene under Mild Condition

Zhuang Ma, Helin Lu, Ke Liao, and Zhilong Chen

Transparent Methods

I. General Information

Glassware and stir bars were dried in an oven at 70 °C for at least 12h and then cooled in a desiccator cabinet over Drierite prior to use. Optimization and substrate screen were performed in 20 mL vials. All other reactions were performed in round-bottom flasks sealed with rubber septa. Plastic syringes or pipets were used to transfer liquid reagents. Reactions were stirred magnetically using Teflon-coated, magnetic stir bars. Analytical thin-layer chromatography (TLC) was performed using glass plates pre-coated with 0.25 mm of 230–400 mesh silica gel impregnated with a fluorescent indicator (254 nm and 320 nm). TLC plates were visualized by exposure to ultraviolet light and/or exposure to $KMnO_4$ stain as well as phosphomolybdic acid (PMA) and cerium molybdate stain. Organic solutions were concentrated under reduced pressure using a rotary evaporator. Flash-column chromatography was performed on silica gel (60 Å, standard grade).

Materials and Instrumentation. Nuclear magnetic resonance spectra were recorded at ambient temperature (unless otherwise stated) on Bruke 400 MHz spectrometers. All values for proton chemical shifts are reported in parts per million (δ) and are referenced to the residual protium in $CDCl_3$ (δ 7.26), CD_3OD (δ 3.31) and DMSO-D_6 (δ 2.50). All values for carbon chemical shifts are reported in parts per million (δ) and are referenced to the carbon resonances in $CDCl_3$ (δ 77.0), CD_3OD (49.00) and DMSO-D_6 (39.52). NMR data are represented as follows: chemical shift, multiplicity (s = singlet, d = doublet, t = triplet, q = quartet, quin = quintet, m = multiple, br = broad), coupling constant (Hz), and integration. Infrared spectroscopic data is reported in wavenumbers (cm^{-1}). High-resolution mass spectra were obtained using a liquid chromatography-electrospray ionization and Time-of-flight mass spectrometer.

All the starting materials, including (hetero)arenes, carbonyl compounds, catalysts, oxidants, metal halide and solvents were commercially available. All the reaction solvents were not anhydrous.

II. General procedure for oxidative halogenation

General procedure A for oxidative bromination of (hetero)arene or activated carbonyl compounds. To the mixture of (hetero)arene or carbonyl compounds (**1**, 1.0 mmol, 1.0 equivalent), Na_2WO_4-$2H_2O$ (16 mg, 0.05 mmol, 5 mol %) and NaBr (112 mg, 1.1 mmol, 1.1 equivalent) was added 5.0 mL EtOH. After compound **1** was dissolved in EtOH, HOAc (66 mg, 66 μL, 1.1 mmol, 1.1 equivalent) followed by adding H_2O_2 (30% aq., 0.6 mL, 6.0 mmol, 6.0 equivalent). The reaction was conducted at 30℃ until compound **1** was all consumed (for some substrates the reactions were stopped with conversion less than 100% due to low reaction rate). Next around 100 mL EtOAc was added to dilute the reaction solution. The reaction mixture was then washed by H_2O (20 mL), $NaHCO_3$ (aq., 20 mL), brine (20 mL), and dried with Na_2SO_4. The desired product **2** was isolated after filtration, concentration, and flash chromatography. The dibromination reaction was conducted with 2.2 equivalent of NaBr and HOAc (**Figure S1**).

Figure S1. Oxidative bromination of (hetero)arenes and carbonyl compounds, related to Table 2

General procedure B for oxidative bromination of (hetero)arene in water. The reactions were conducted in the similar manner as **General Procedure A**: Na_2WO_4-$2H_2O$ (2.5 mol%), NaBr (1.1 equivalent), H_2O_2 (30% aq., 1.1 equivalent) and HOAc (1.1 equivalent) in 5.0 mL H_2O (**Figure S2**).

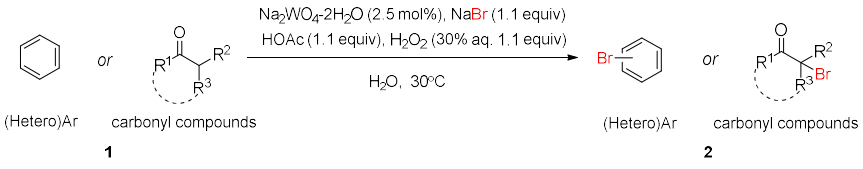

Figure S2. Oxidaive bromination of (hetero)arene in water, related to Table 2

General procedure C for oxidative chlorination of (hetero)arene and carbonyl compounds. To the mixture of (hetero)arene or carbonyl compounds (**1**, 1.0 mmol, 1.0 equivalent), K_2WO_4 (16 mg, 0.05 mmol, 5 mol %) and

$BaCl_2 \cdot 2H_2O$ (293 mg, 1.2 mmol, 1.2 equivalent) was added 5.0 mL MeCN. After compound **1** was dissolved in MeCN, HOAc (66 mg, 60 μL, 1.0 mmol, 1.0 equivalent) followed by adding H_2O_2 (30% aq., 0.4 mL, 4.0 mmol, 4.0 equivalent). The reaction was conducted at 50℃ until compound **1** was all consumed (for some substrates the reactions were stopped with conversion less than 100% due to low reaction rate). Next EtOAc (100 mL) was added to dilute the reaction solution, followed by being washed with H_2O (20 mL), $NaHCO_3$ (aq., 20 mL), brine (20 mL), and dried by Na_2SO_4. The chlorination product **2** were isolated after filtration, concentration and flash chromatography (**Figure S3**).

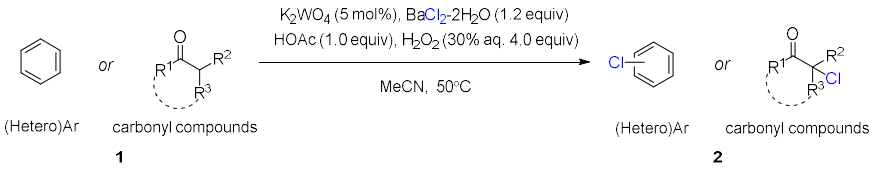

Figure S3. Oxidative chlorination of (hetero)arenes and carbonyl compounds, related Table 3

General procedure D for oxidative iodination of (hetero)arene. The reactions were conducted in the same manner as **General Procedure A** by employing KI at room temperature. The diiodination reaction was conducted with 2.2 equivalent of KI and HOAc (**Figure S4**).

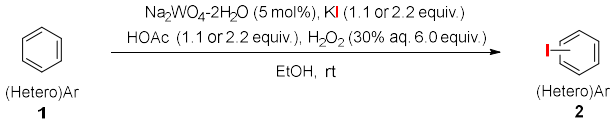

Figure S4. Oxidative iodination of (hetero)arenes, related Table 3

General procedure E 100-gram scale reaction. The reactions were conducted in the similar fashion as **General Procedure A**. The starting material (hetero)arene, $Na_2WO_4 \cdot 2H_2O$, NaBr and HOAc was dissolved in minimum amount of EtOH/H_2O, followed by adding H_2O_2 slowly at room temperature. Upon completion, the desired product **2** participated as solid due to lower solubility. Thus, the pure product was obtained simply by filtration, washed with H_2O and EtOH, and dried in *vacuum* (**Figure S5**).

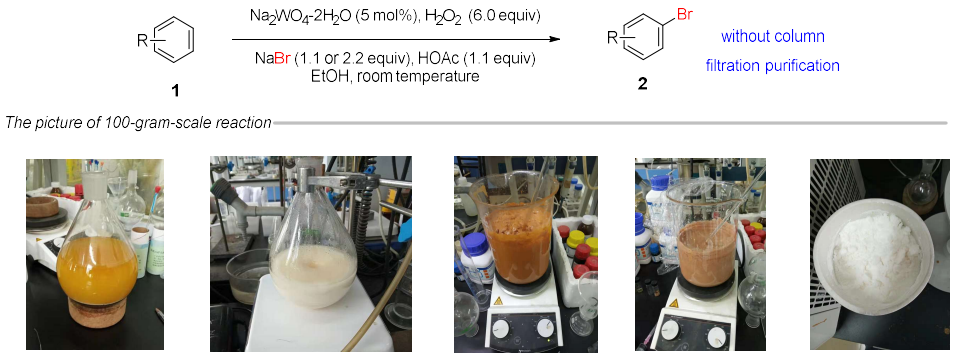

Figure S5. 100 g scale reactions, related to Table 4

III. Condition optimization

Table S1. Condition optimization for tungstate-catalyzed oxidative bromination 1, relate Table 1

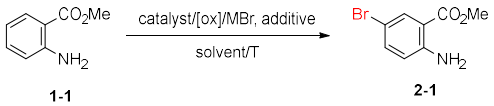

1-1 2-1

Entry	Catalyst (mol%)	[ox] (eq.)	MBr (eq.)	additive (eq.)	solvent	T/°C	yeild(%)[a]
MBr source screeing							
1	Na_2WO_4-$2H_2O$ (5)	H_2O_2 (6.0)	LiBr (1.0)	HOAc (1.0)	EtOH	50	62
2	Na_2WO_4-$2H_2O$ (5)	H_2O_2 (6.0)	LiBr (1.5)	HOAc (2.0)	EtOH	50	66
3	Na_2WO_4-$2H_2O$ (5)	H_2O_2 (6.0)	KBr (1.5)	HOAc (2.0)	EtOH	50	75
4	Na_2WO_4-$2H_2O$ (5)	H_2O_2 (6.0)	NaBr (1.5)	HOAc (2.0)	EtOH	50	84
5	Na_2WO_4-$2H_2O$ (5)	H_2O_2 (6.0)	NaBr (1.1)	HOAc (1.5)	EtOH	50	79
6	Na_2WO_4-$2H_2O$ (5)	H_2O_2 (6.0)	NaBr (1.1)	HOAc (1.5)	EtOH	30	78
7	Na_2WO_4-$2H_2O$ (5)	H_2O_2 (6.0)	NaBr (1.1)	HOAc (1.1)	EtOH	30	77-83
Catalyst screening							
8	$(NH_4)_{10}(H_2W_{12}O_{42})$-$xH_2O$ (5)	H_2O_2 (6.0)	NaBr (1.5)	HOAc (2.0)	EtOH	30	77
9	$H_3O_{40}PW_{12}$•xH_2O (5)	H_2O_2 (6.0)	NaBr (1.5)	HOAc (2.0)	EtOH	30	64
10	K_2WO_4 (5)	H_2O_2 (6.0)	NaBr (1.5)	HOAc (2.0)	EtOH	30	74
11	$CaWO_4$ (5)	H_2O_2 (6.0)	NaBr (1.5)	HOAc (2.0)	EtOH	30	71
12	Na_2WO_4-$2H_2O$ (1)	H_2O_2 (6.0)	NaBr (1.1)	HOAc (1.1)	EtOH	30	67
13	--	H_2O_2 (6.0)	NaBr (1.5)	HOAc (2.0)	EtOH	30	trace
Oxidant screening							
14	Na_2WO_4-$2H_2O$ (5)	^{t}BuOOH (6.0)	NaBr (1.5)	HOAc (2.0)	EtOH	30	N.R
15	Na_2WO_4-$2H_2O$ (5)	SPB (6.0)	NaBr (1.5)	HOAc (2.0)	EtOH	30	N.R
16	Na_2WO_4-$2H_2O$ (5)	--	NaBr (1.5)	HOAc (2.0)	EtOH	30	N.R
17	Na_2WO_4-$2H_2O$ (5)	H_2O_2 (4.0)	NaBr (1.5)	HOAc (2.0)	EtOH	30	conversion<50%
18	Na_2WO_4-$2H_2O$ (5)	H_2O_2 (2.0)	NaBr (1.1)	HOAc (1.1)	EtOH	30	57

a: all the reaction was conducted in 1.0 mmol scale (**1-1**), stirring for 12h, isolated yield

Table S2. Condition optimization for tungstate-catalyzed oxidative bromination 2, relate Table 1 and Figure 3

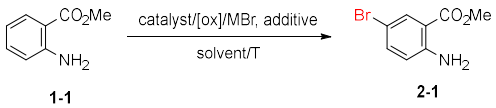

1-1 **2-1**

Entry	Catalyst (mol%)	[ox] (eq.)	MBr (eq.)	additive (eq.)	solvent	T/°C	yeild(%)[a]
Solvent screening							
1	Na_2WO_4-$2H_2O$ (5)	H_2O_2 (6.0)	*NaBr (1.1)*	HOAc (1.0)	EtOH	30	*78-83*
2	Na_2WO_4-$2H_2O$ (5)	H_2O_2 (6.0)	*NaBr (1.1)*	HOAc (2.0)	MeOH	30	67
3	Na_2WO_4-$2H_2O$ (5)	H_2O_2 (6.0)	*NaBr (1.1)*	HOAc (2.0)	iPrOH	30	85
4	Na_2WO_4-$2H_2O$ (5)	H_2O_2 (6.0)	*NaBr (1.1)*	HOAc (2.0)	THF	30	conversion<50%
5	Na_2WO_4-$2H_2O$ (5)	H_2O_2 (6.0)	NaBr (1.1)	HOAc (1.5)	MeCN	30	conversion<50%
6	*Na_2WO_4-$2H_2O$ (5)*	*H_2O_2 (6.0)*	*NaBr (1.1)*	*HOAc (1.5)*	*EtOAc*	30	conversion<50%
7	Na_2WO_4-$2H_2O$ (5)	H_2O_2 (6.0)	NaBr (1.1)	HOAc (1.1)	Toluene	30	N.R
8	Na_2WO_4-$2H_2O$ (5)	H_2O_2 (6.0)	NaBr (1.1)	HOAc (1.1)	DCM	30	N.R
9	Na_2WO_4-$2H_2O$ (5)	H_2O_2 (6.0)	NaBr (1.1)	HOAc (1.1)	DMF	30	N.R

a: all the reactions were conducted in 1.0 mmol scale (**1-1**), 12h, isolated yield; N.R = No reaction

Table S3. Condition optimization for tungstate-catalyzed oxidative bromination in water, relate Table 1 and 2

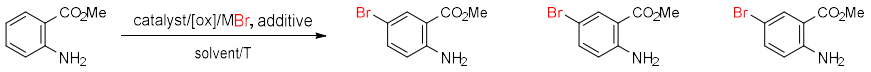

1-1 **2-1** **2-1B** **2-1C**

entry	Catalyst (mol%)	[ox] (equiv.)	MBr (equiv.)	Additive (equiv.)	solvent	T/°C	time	**2-1:2-1B:2-1C** [a]
1	$NaWO_4$-$2H_2O$ (5.0)	H_2O_2 (6)	NaBr (1.2)	HOAc (1.1)	H_2O	30	24	12:1.5:1
2	$NaWO_4$-$2H_2O$ (2.5)	H_2O_2 (6)	NaBr (1.2)	HOAc (1.1)	H_2O	30	24	>20:1:1
3	$NaWO_4$-$2H_2O$ (1.0)	H_2O_2 (6)	NaBr (1.2)	HOAc (1.1)	H_2O	30	18	10:1:0
4	$NaWO_4$-$2H_2O$ (2.5)	H_2O_2 (3)	NaBr (1.2)	HOAc (1.1)	H_2O	30	18	10:1:0
5	$NaWO_4$-$2H_2O$ (2.5)	H_2O_2 (1.5)	NaBr (1.2)	HOAc (1.1)	H_2O	30	16.5	>98:1:1
6	$NaWO_4$-$2H_2O$ (2.5)	H_2O_2 (1.1)	NaBr (1.2)	HOAc (1.1)	H_2O	30	21.5	10.0:1
Control experiment								
7	--	H_2O_2 (1.1)	NaBr (1.1)	HOAc (1.1)	H_2O	30	16	trace
8	$NaWO_4$-$2H_2O$ (5)	H_2O_2 (1.1)	NaBr (1.1)	--	H_2O	30	16	conversion<10%
9	--	H_2O_2 (1.1)	NaBr (1.1)	--	H_2O	30	16	N.R

a: all the reactions were run in 1.0 mmol scale (**1-1**), the ration between **2-1**, **2-1B** and **2-1C** was determined by H-NMR of crude products without purfication, and the conversion = 100%; N.R = No Reaction

Although this reaction work well in water, however, only limited substrates can be solved in H_2O. Therefore, currently the reaction in EtOH is still favored.

Table S4. Condition optimization for tungstate-catalyzed oxidative chlorination, related to Table 3 and Figure 3

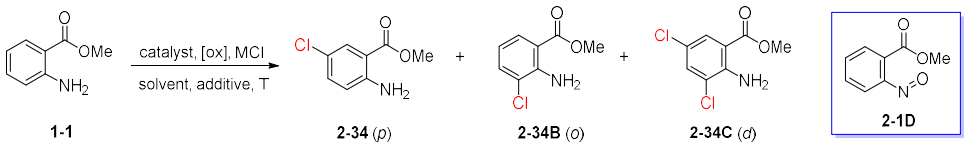

1-1 **2-34** (*p*) **2-34B** (*o*) **2-34C** (*d*) **2-1D**

entry[a]	MCl (eq.)	cat (mol%)	solvent	additive (eq.)	[ox] (eq.)	T(°C)	time (h)	yield (%*p*/*o*/*d*[b])
Chloride source screening								
1	NaCl (1.2)	Na_2WO_4 (5)	EtOH	AcOH (1.0)	H_2O_2 (6.0)	50	34	N.D[c]
2	KCl (1.2)	Na_2WO_4 (5)	EtOH	AcOH (1.0)	H_2O_2 (6.0)	50	22	N.D[c]
3	LiCl (1.2)	Na_2WO_4 (5)	EtOH	AcOH (1.0)	H_2O_2 (6.0)	50	22	N.D[c]
4	NH_4Cl(1.2)	Na_2WO_4 (5)	EtOH	AcOH(1.0)	H_2O_2 (6.0)	50	11	N.D[c]
5	$CaCl_2$(1.2)	Na_2WO_4 (5)	EtOH	AcOH (1.0)	H_2O_2 (6.0)	50	5.5	8/0/38
6	$BaCl_2$-$2H_2O$ (1.2)	Na_2WO_4 (5)	EtOH	AcOH (1.0)	H_2O_2 (6.0)	50	8.5	63(*p*+*o*)/0
7	$CdCl_2$(1.2)	Na_2WO_4 (5)	EtOH	AcOH (1.0)	H_2O_2 (6.0)	50	21.5	N.D[c]
8	$SrCl_2$(1.2)	Na_2WO_4 (5)	EtOH	AcOH (1.0)	H_2O_2 (6.0)	50	9.5	0//0/44
9	$ScCl_3$(1.2)	Na_2WO_4 (5)	EtOH	AcOH (1.0)	H_2O_2 (6.0)	50	9.5	0/0/43
10	$ZrCl_4$(1.2)	Na_2WO_4 (5)	EtOH	AcOH (1.0)	H_2O_2 (6.0)	50	8.5	0/0/17

a: all the reactions were conducted in 1.0 mmol scale (**1-1**); b: isolated yield after silica gel column; c: trace or no desired product, the nitroso byproduct **2-1D** was isolated as major product; N.D = not determined

Table S5. Condition optimization for tungstate-catalyzed oxidative chlorination 2, related to Table 3 and Figure 3

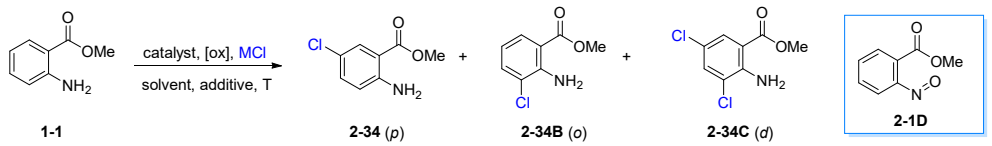

1-1 **2-34** (*p*) **2-34B** (*o*) **2-34C** (*d*)

entry[a]	MCl (eq.)	cat (mol%)	solvent	additive (eq.)	[ox] (eq.)	T(°C)	time (h)	yield (%, *p*/*o*/*d*[b])
Solvent screening								
6	$BaCl_2$-$2H_2O$ (1.2)	Na_2WO_4-$2H_2O$ (5)	EtOH	AcOH (1.0)	H_2O_2 (6.0)	50	8.5	63 (*p*+*o*)/0
11	$BaCl_2$-$2H_2O$ (1.2)	Na_2WO_4-$2H_2O$ (5)	^{i}PrOH	AcOH (1.0)	H_2O_2 (6.0)	50	85.5	N.D[c]
12	$BaCl_2$-$2H_2O$ (1.2)	Na_2WO_4-$2H_2O$ (5)	MeOH	AcOH (1.0)	H_2O_2 (6.0)	50	63	N.D[c]
13	$BaCl_2$-$2H_2O$ (1.2)	Na_2WO_4-$2H_2O$ (5)	CH_3CN	AcOH (1.0)	H_2O_2 (6.0)	50	65.5	57/22/0
14	$BaCl_2$-$2H_2O$ (1.2)	Na_2WO_4-$2H_2O$ (5)	EtOAc	AcOH (1.0)	H_2O_2 (6.0)	50	97	N.D[c]
15	$BaCl_2$-$2H_2O$ (1.2)	Na_2WO_4-$2H_2O$ (5)	THF	AcOH (1.0)	H_2O_2 (6.0)	50	97	N.D[c]
16	$BaCl_2$-$2H_2O$ (1.2)	Na_2WO_4-$2H_2O$ (5)	H_2O	AcOH (1.0)	H_2O_2 (6.0)	50	16.5	trace
17	$BaCl_2$-$2H_2O$ (1.2)	Na_2WO_4-$2H_2O$ (5)	toluene	AcOH (1.0)	H_2O_2 (6.0)	50	47	N.D[c]
18	$BaCl_2$-$2H_2O$ (1.2)	Na_2WO_4-$2H_2O$ (5)	TFE	AcOH (1.0)	H_2O_2 (6.0)	50	40	N.D[c]
19	$BaCl_2$-$2H_2O$ (1.2)	$(NH_4)_{10}[H_2W_{12}O_{42}]$ (5)	EtOH	AcOH (1.0)	H_2O_2 (6.0)	50	27	24/20/0
20	$BaCl_2$-$2H_2O$ (1.2)	$H_3O_{40}PW_{12}$ (5)	EtOH	AcOH (1.0)	H_2O_2 (6.0)	50	22.5	3/20/0
21	$BaCl_2$-$2H_2O$ (1.2)	K_2WO_4 (5)	CH_3CN	AcOH (1.0)	H_2O_2 (6.0)	50	11	57/23/0
22	$BaCl_2$-$2H_2O$ (1.2)	$CaWO_4$ (5)	CH_3CN	AcOH (1.0)	H_2O_2 (6.0)	50	57.5	N.D[c]
Additive screening								
23	$BaCl_2$-$2H_2O$ (1.2)	Na_2WO_4-$2H_2O$ (5)	EtOH	CCl_3COOH (1.0)	H_2O_2 (6.0)	50	23	N.D[c]
24	$BaCl_2$-$2H_2O$ (1.2)	Na_2WO_4-$2H_2O$ (5)	EtOH	CF_3COOH(1.0)	H_2O_2 (6.0)	50	23	0/0/12
25	$BaCl_2$-$2H_2O$ (1.2)	Na_2WO_4-$2H_2O$ (5)	EtOH	Benzoic acid (1.0)	H_2O_2 (6.0)	50	35	32/8/0
26	$BaCl_2$-$2H_2O$ (1.2)	Na_2WO_4-$2H_2O$ (5)	EtOH	Crylic acid (1.0)	H_2O_2 (6.0)	50	35	18/9/0
Oxidant screening and control experiments								
27	$BaCl_2$-$2H_2O$ (1.2)	K_2WO_4 (5)	CH_3CN	AcOH (1.0)	H_2O_2 (4.0)	50	11	56/26/0
28	$BaCl_2$-$2H_2O$ (1.2)	K_2WO_4 (5)	CH_3CN	AcOH (1.0)	H_2O_2 (3.0)	50	47	44/33/0
29	$BaCl_2$-$2H_2O$ (1.2)	Na_2WO_4 (5)	EtOH	AcOH (1.0)	SPB (3.0)	50	59	N.D[c]
30	$BaCl_2$-$2H_2O$ (1.2)	K_2WO_4(5)	CH_3CN	AcOH(1.0)	H_2O_2(2.0)	50	110.5	60/20/0
31	$BaCl_2$-$2H_2O$ (1.2)	K_2WO_4(5)	CH_3CN	AcOH (1.0)	H_2O_2 (1.0)	50	153.5	conversion low
32	$BaCl_2$-$2H_2O$ (1.2)	K_2WO_4(2.5)	CH_3CN	AcOH (1.0)	H_2O_2 (4.0)	50	142	conversion low
33	$BaCl_2$-$2H_2O$ (1.2)	K_2WO_4 (5)	CH_3CN	AcOH (1.0)	H_2O_2 (4.0)	RT	84	conversion low
34	$BaCl_2$-$2H_2O$ (1.2)	none	CH_3CN	AcOH (1.0)	H_2O_2 (4.0)	50	11.5	N.R
35	$BaCl_2$-$2H_2O$ (1.2)	K_2WO_4(5)	CH_3CN	AcOH (1.0)	none	50	11.5	N.R

a. all the reactions were conducted in 1.0 mmol scale (**1-1**); b: isolated yield; c: major product is 2-1D; N.D = not determined; N.R = No reaction; TFE = trifluroethanol; SPB = sodium perborat.

V. Byproducts detection

For some substrates, the chemo- or regioselectivivties are not good, and more than one products were isolated as shown in following. The most frequently encountered byproducts in this reaction come from dibromination. But for some free anilines, the formation of nitroso or azoxy might also be involved.

During the condition optimization, the major byproduct **2-1D** was observed during condition optimization along with the isomer of bromination product (**2-1B**, methyl 2-amino-3-bromobenzoate) and dibromination product **2-1C**. Product **2-1B** and **2-1C** were very close to each other on TLC plate and difficult for isolation (**Figure S6**).

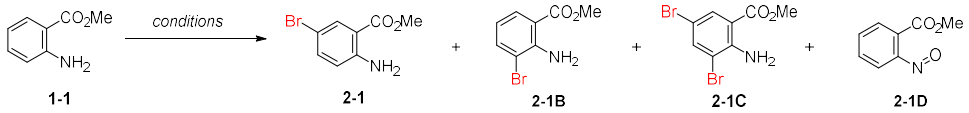

Figure S6. Byproducts formation during condition optimization, related to Table 1

The bromination of methyl 1*H*-pyrrole-2-carboxylate proceeded according to according to **General Procedure A** for 24h, affording two products (**2-20** and **2-20B**) (**Figure S7**).

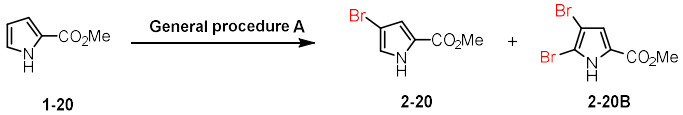

Figure S7. Bromination of 1*H*-pyrrole-2-carboxylate, related to Table 2

The bromination of isoquinolin-5-amine proceeded according to according to **General Procedure A** for 24 h, and two products (**2-24** and **2-24B**) were isolated (**Figure S8**).

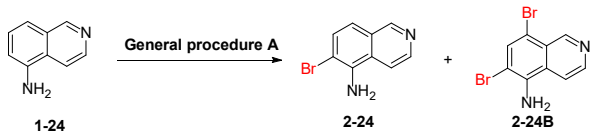

Figure S8. Bromination of isoquinolin-5-amine, related to Table 2

The bromination of estrone proceeded according to according to **General Procedure A** for 6 days, affording products **2-28** (153 mg, 44% yield) and **2-28B** (16 mg, 4% yield), and estrone was recycled 37.2 mg (14% yield) (**Figure S9**).

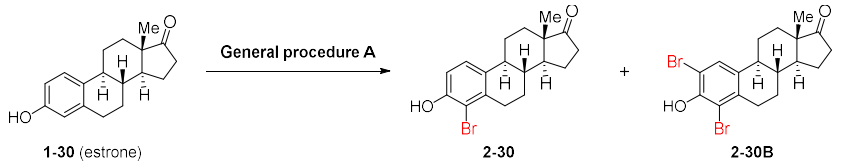

Figure S9. Bromination of estrone, related to Table 2

The bromination of cytarabine was conducted according to **General Procedure A** in water for 5.5h. Given that cytarabine and its bromination product **2-31** were well dissolved in water, the yield was determined by H-NMR of crude product after simply removing all the reaction solvent as a white liquid (396 mg) (**Figure S10**).

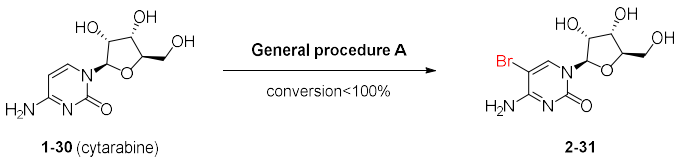

Figure S10. Bromination of cytarabine, related to Table 2

The oxidative bromination of naringin proceeded according to **General Procedure A** in 1.0 mmol scale. The crude mixture of products was obtained after the reaction went on for 35h as white solid. Both naringin and the bromination products (**2-32** and **2-32B**) were well dissolved in water due to the disaccharide chain, thus the conversion and yield was determined by H-NMR of this crude mixture (**Figure S11**).

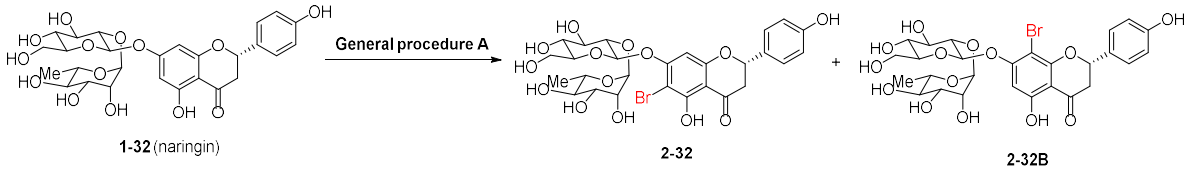

Figure S11. Bromination of cytarabine, related Table 2

The chlorination of methyl 2-aminobenzoate proceeded according to according to **General Procedure C** for 11h, affording products **2-34** and **2-34B** (**Figure S12**).

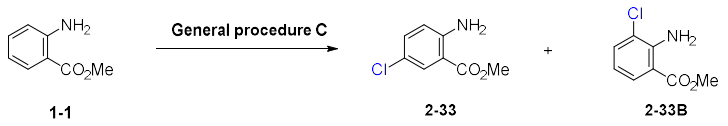

Figure S12. Chlorination of methyl 2-aminobenzoate, related to Table 3

The chlorination of methyl 4-phenylmorpholine was conducted according to **General Procedure C** for 16.5h, affording products **2-35** and **2-35B** (**Figure S13**).

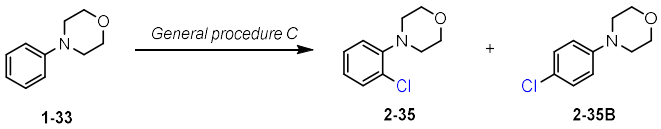

Figure S13. Chlorination of 4-phenylmorpholine, related to Table 3

VI. Mechanism study

In order to dig out more details of the reaction mechanism, compound 1, 2-dimethoxy-3-methylbenzene (**1-45**) was probed in bromiantion reactions. Product **2-61** was isolated in moderate yield, while **2-62** was not observed, thus excluding the existence of bromine radical intermediate during the reaction (**Figure S14, Figure 3a**).

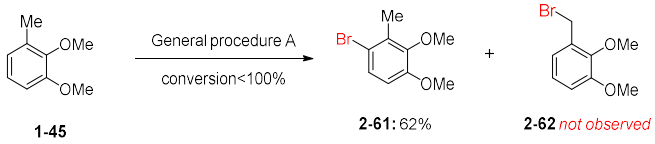

Figure S14. Primary mechanism study, related Figure 3

VII. NMR Spectrums of intermediates and products

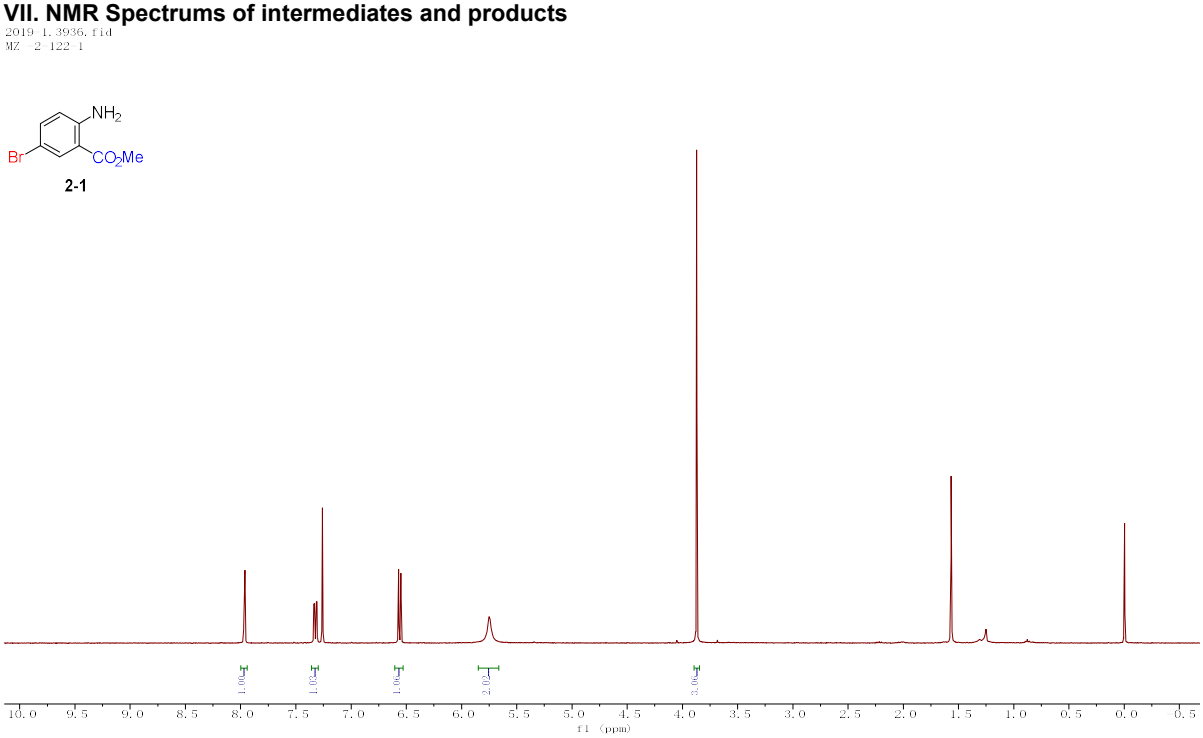

Figure S15. ^{1}H NMR of product **2-1**, related Table 2

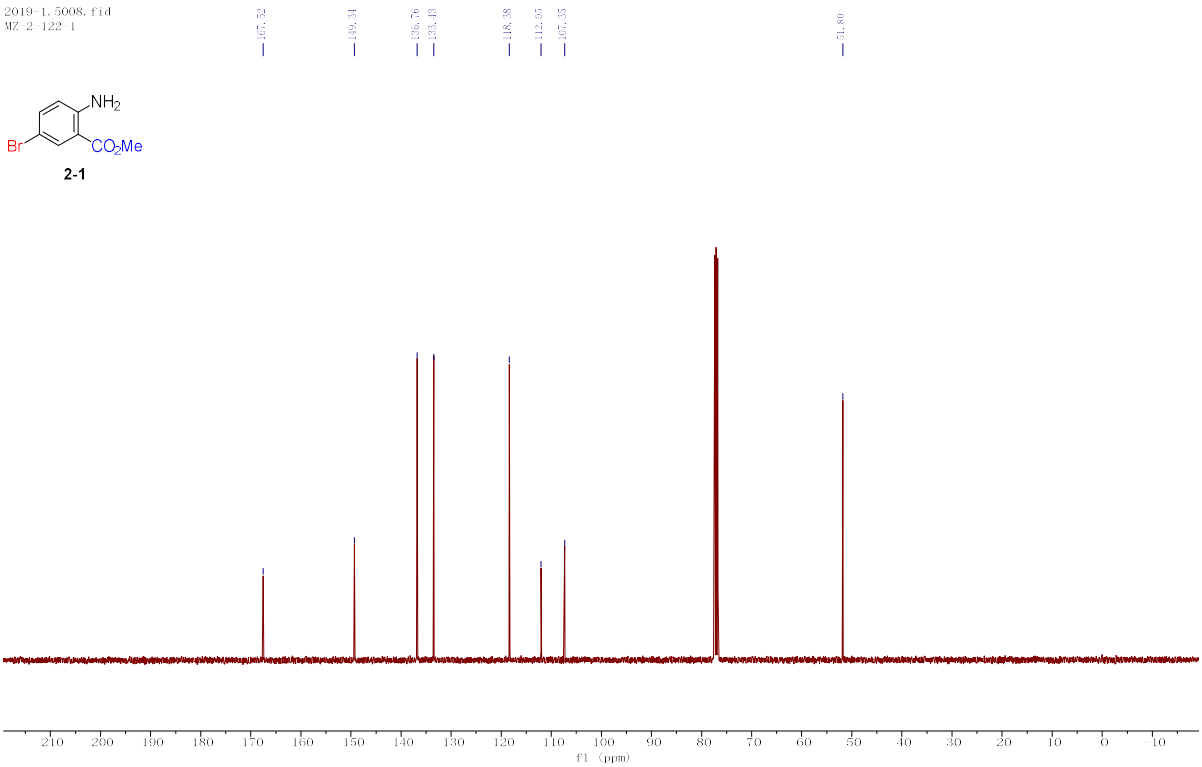

Figure S16. ^{13}C NMR of product **2-1**, related Table 2

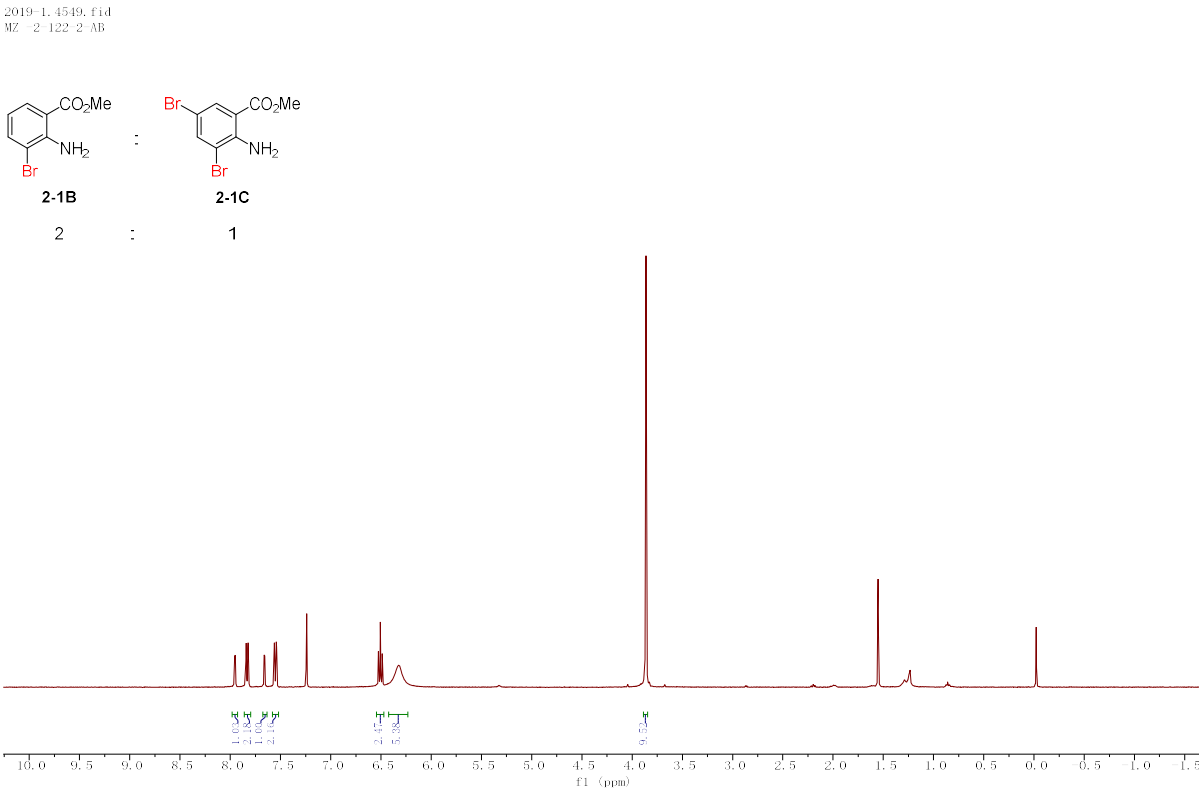

Figure S17. ^{1}H-NMR of products **2-1B** and **2-1C**, related Table 1

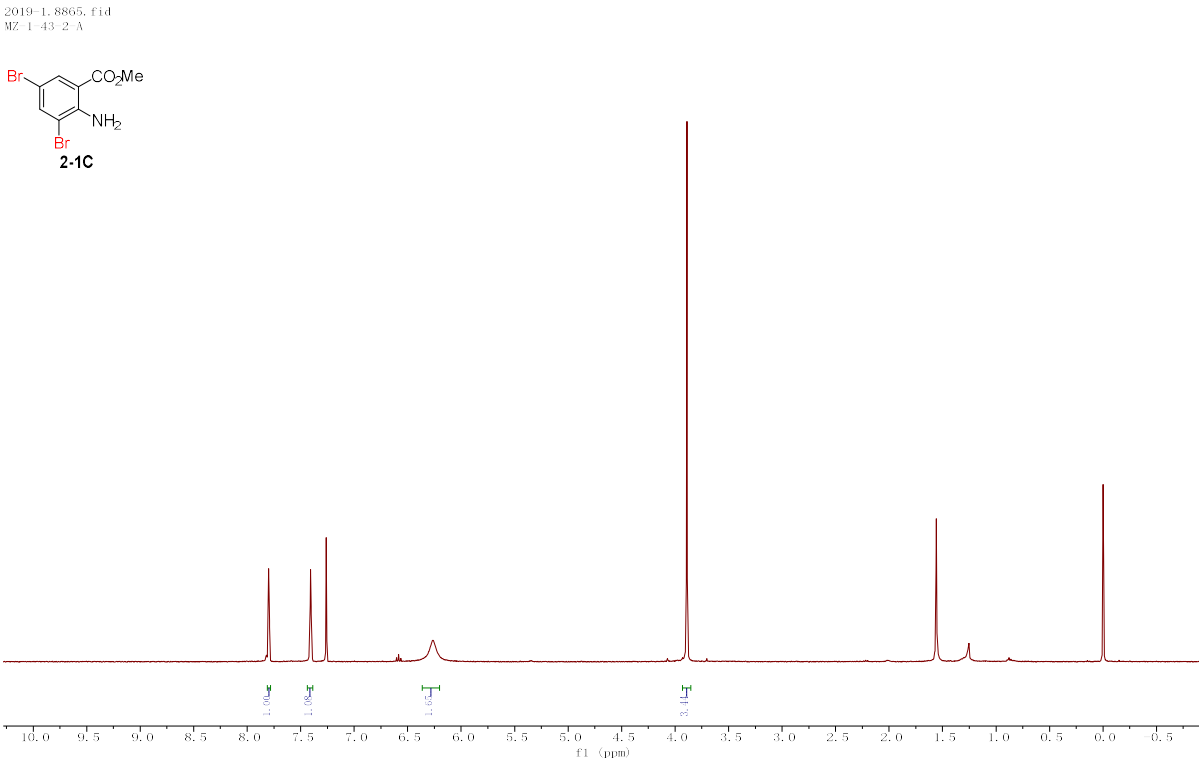

Figure S18. ^{1}H NMR of product **2-1C**, related Table 1

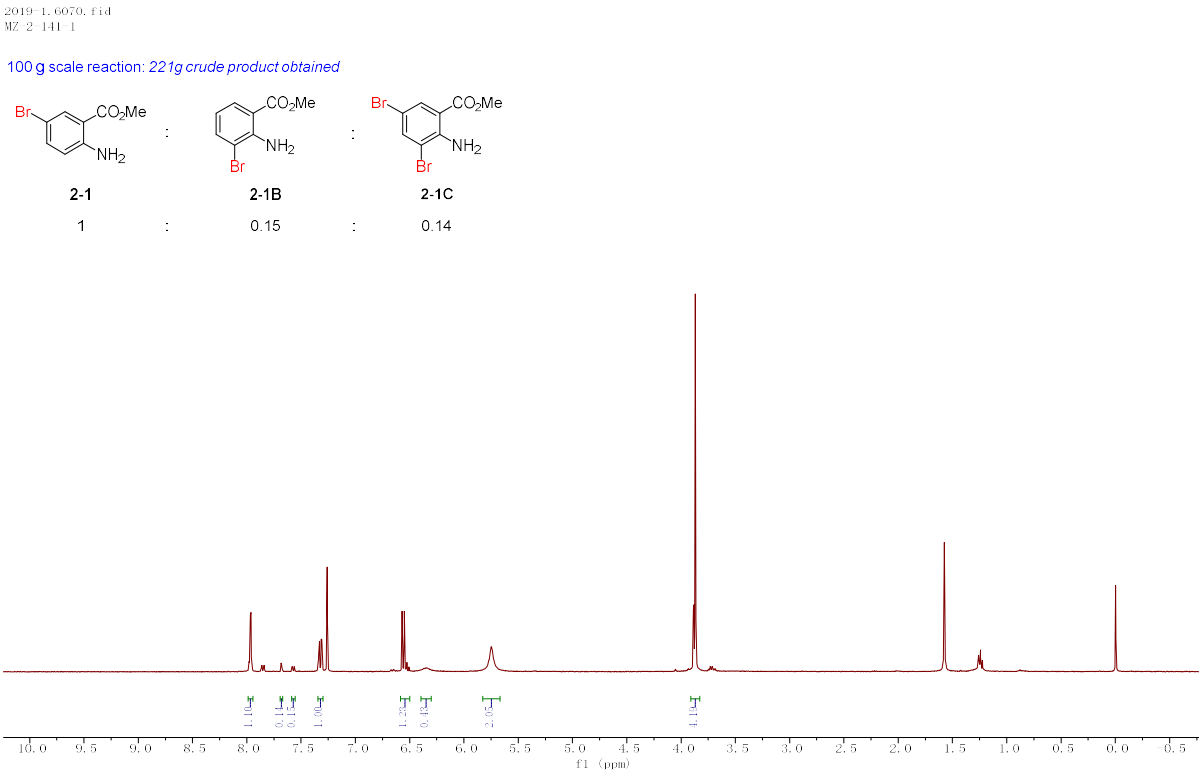

Figure S19. ^{1}H NMR of crude product **2-1** in 100 g scale, related Table 2

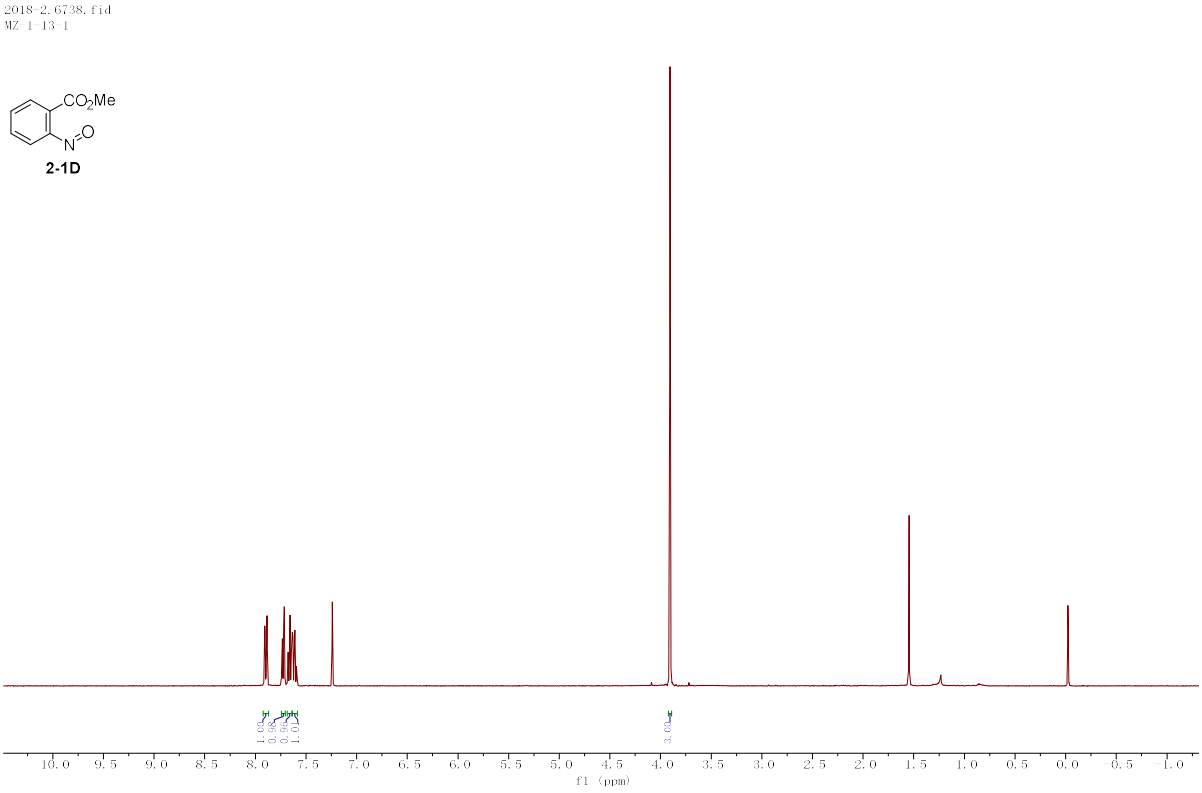

Figure S20. ^{1}H NMR of product **2-1D**, related Table 1

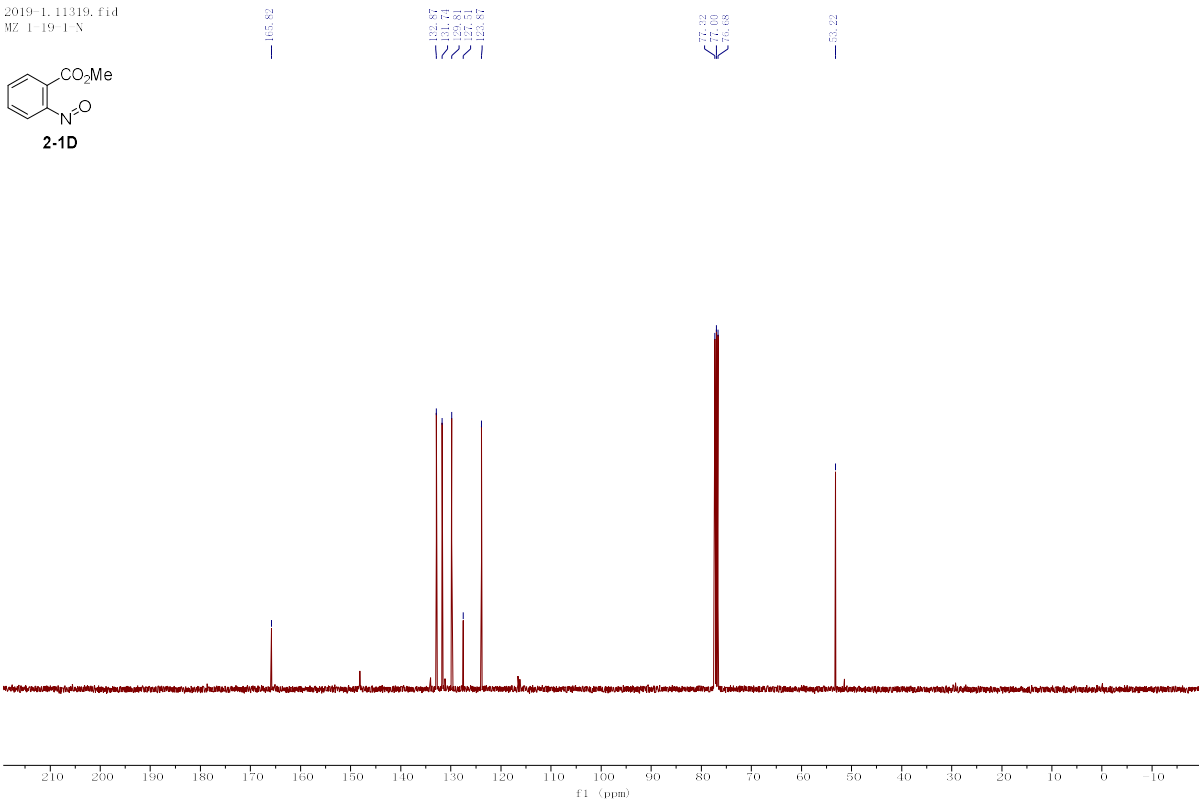

Figure S21. ^{13}C NMR of product **2-1D**, related Table 1

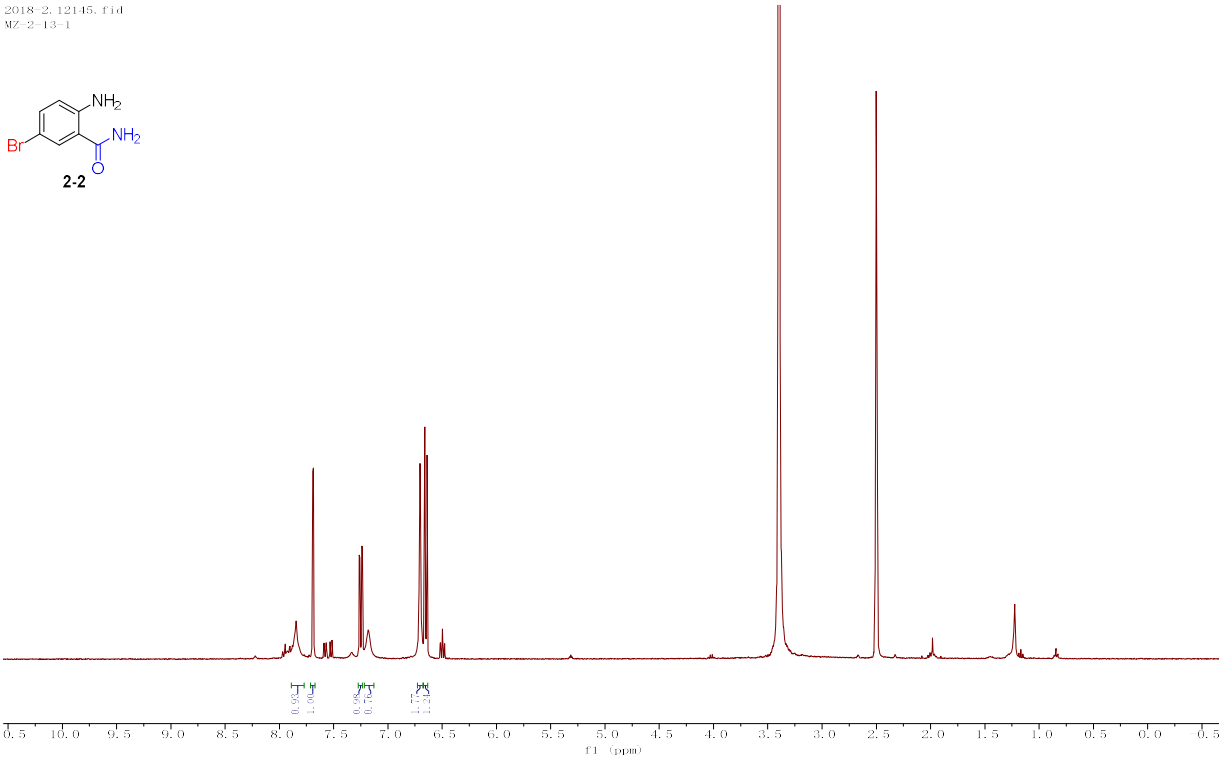

Figure S22. ^{1}H NMR of product **2-2**, related Table 2

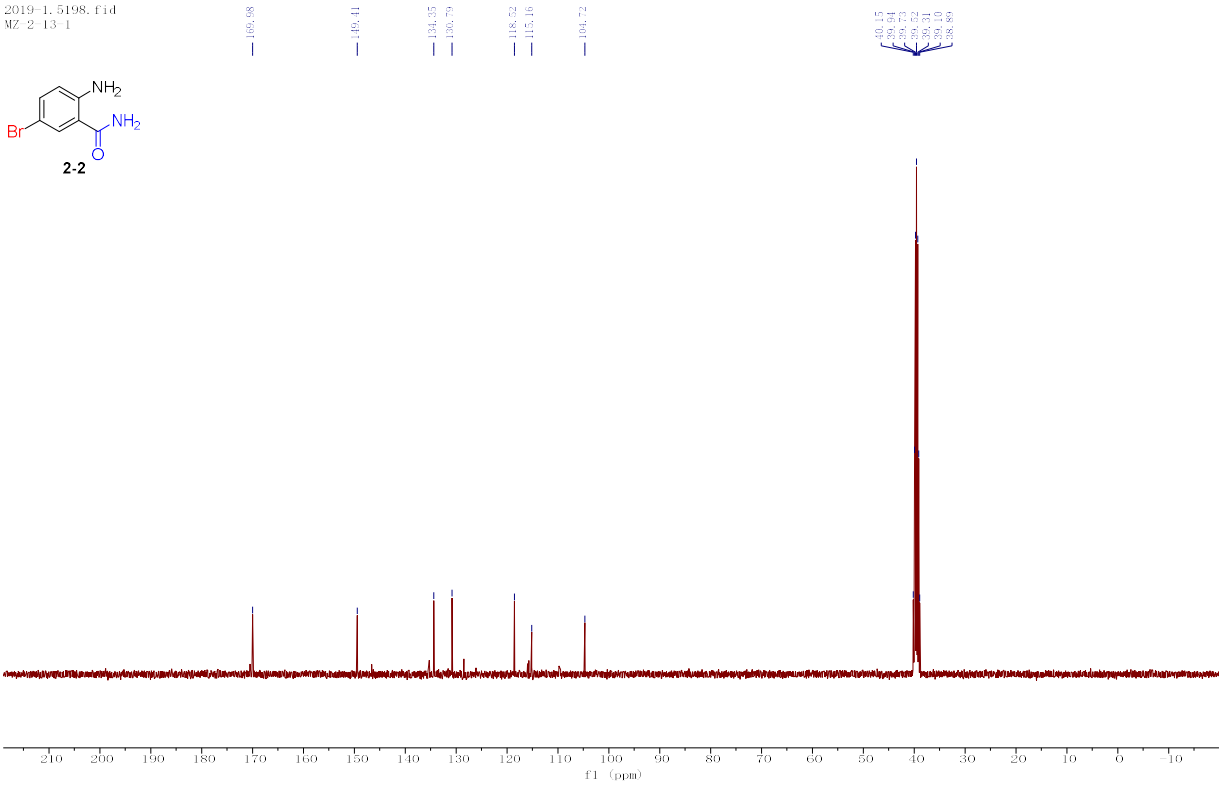

Figure S23. ^{13}C NMR of product **2-2**, related Table 2

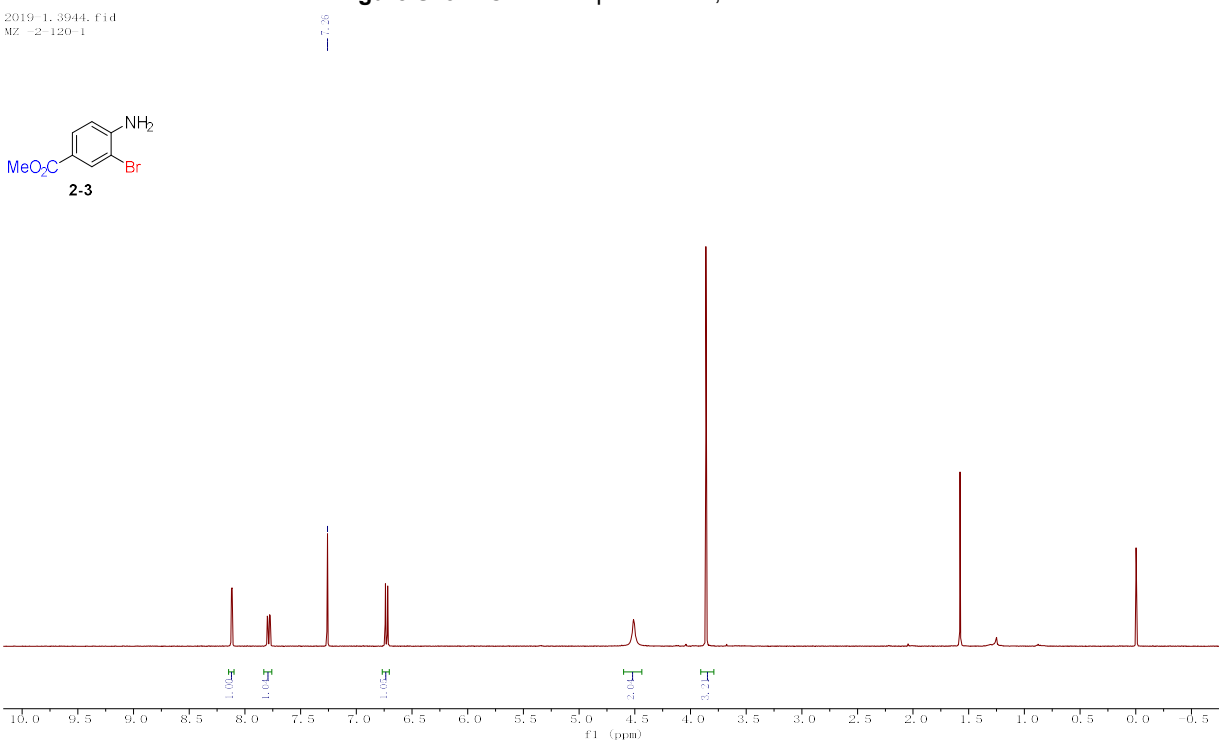

Figure S24. ^{1}H NMR of product **2-3**, related Table 2

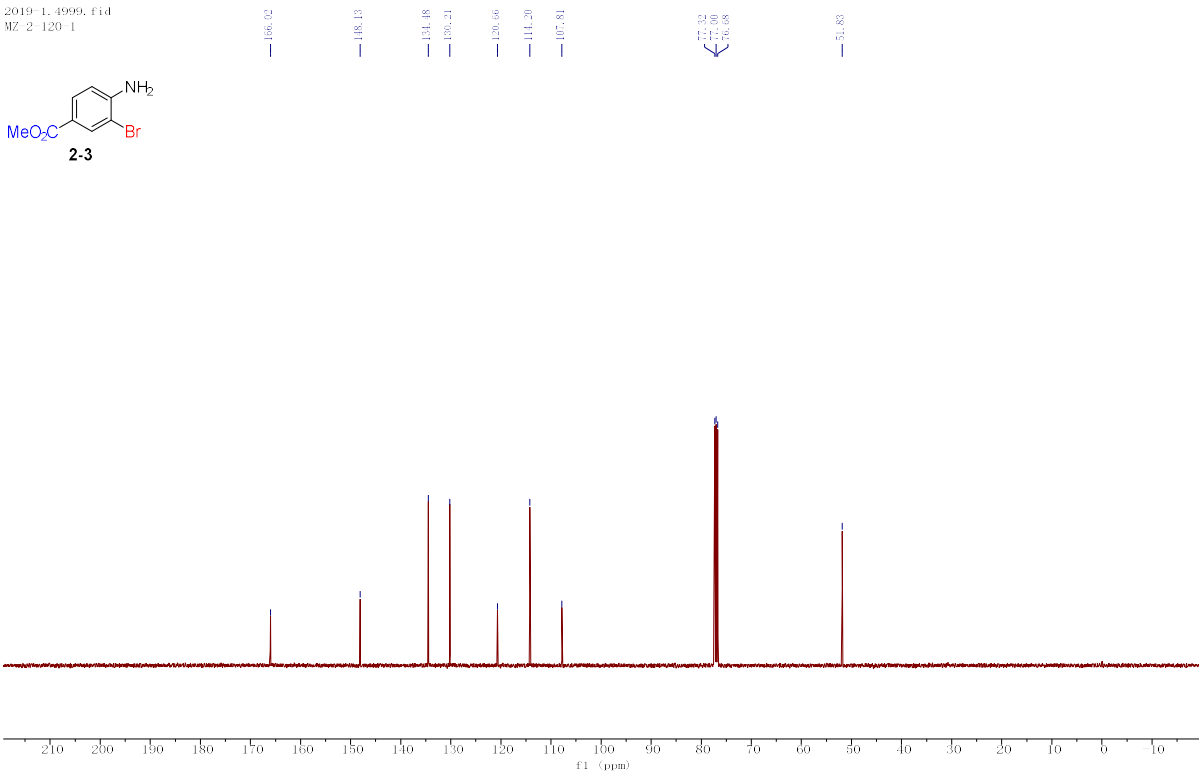

Figure S25. ^{13}C NMR of product **2-3**, related Table 2

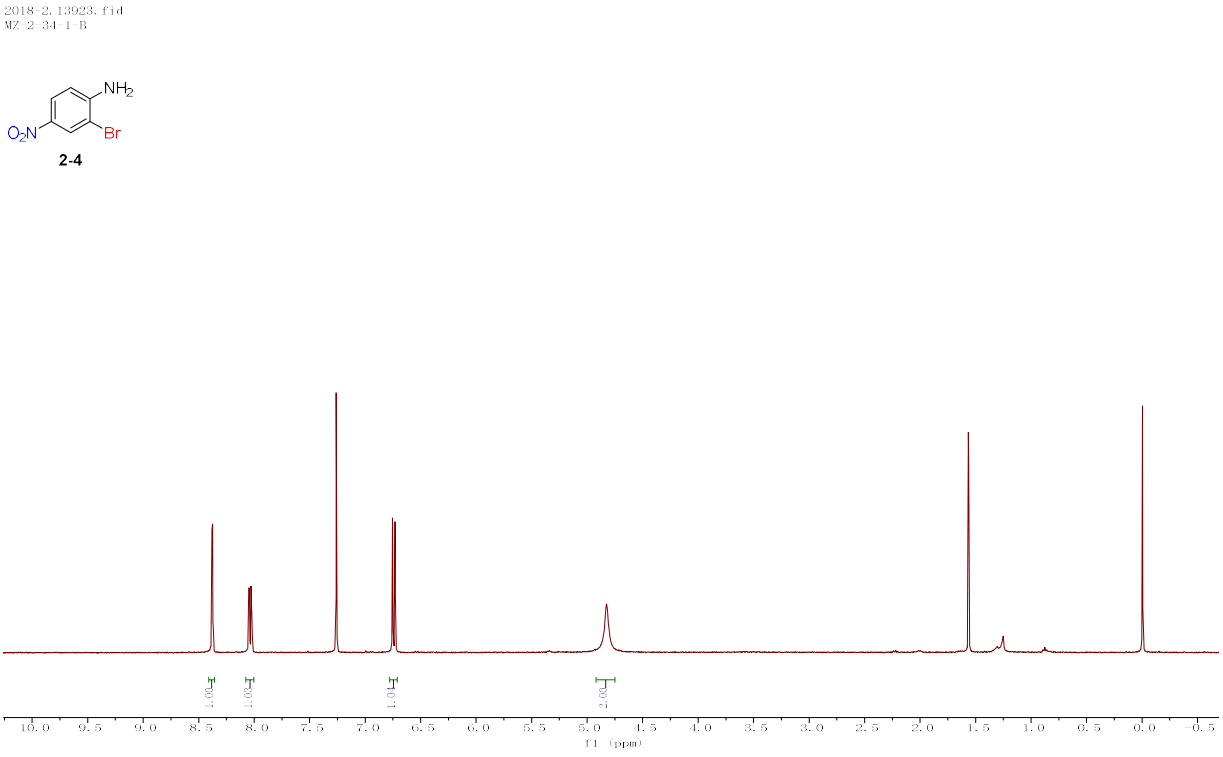

Figure S26. ^{1}H NMR of product **2-4**, related Table 2

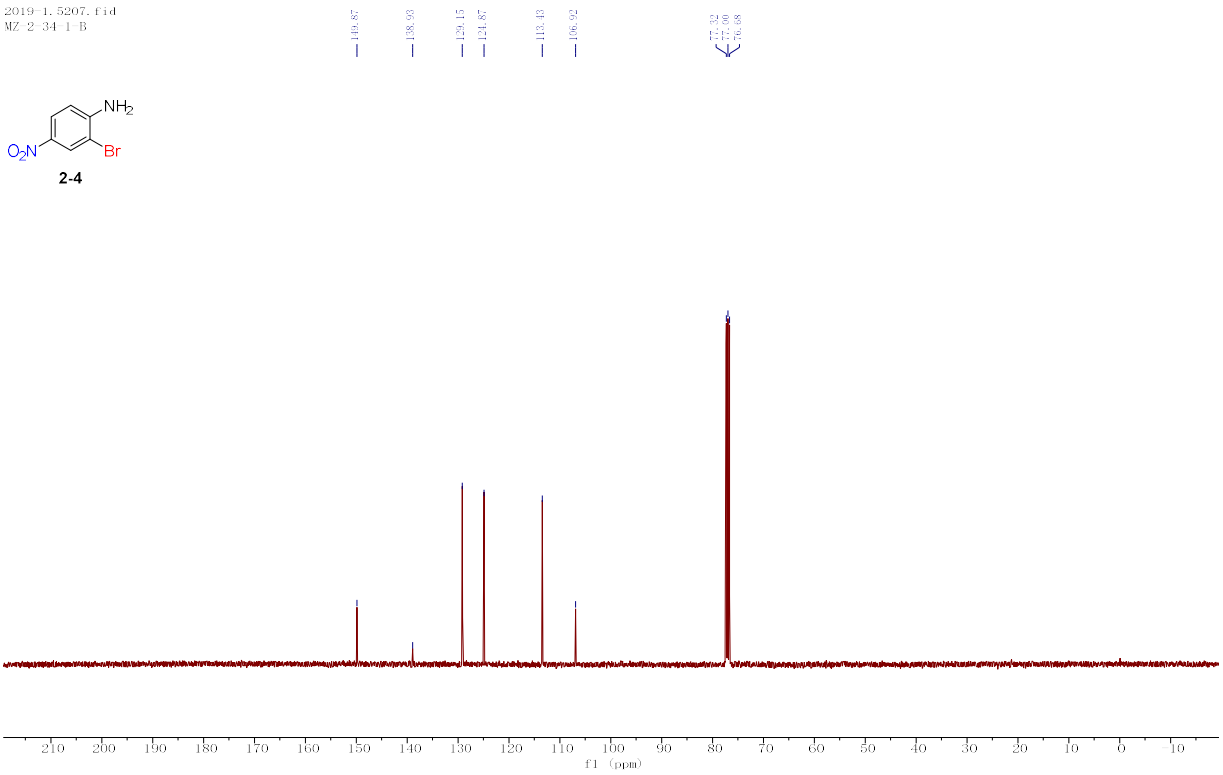

Figure S27. ^{13}C NMR of product **2-4**, related Table 2

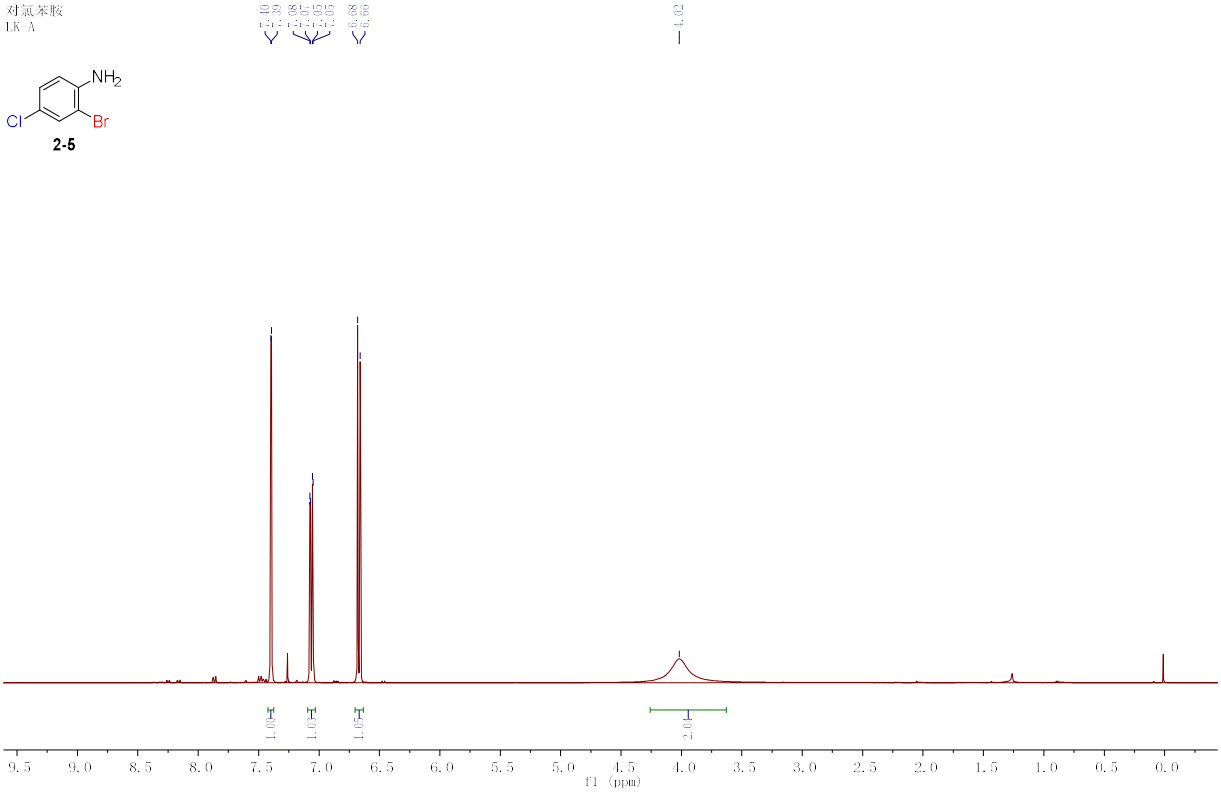

Figure S28. ^{1}H NMR of product **2-5**, related Table 2

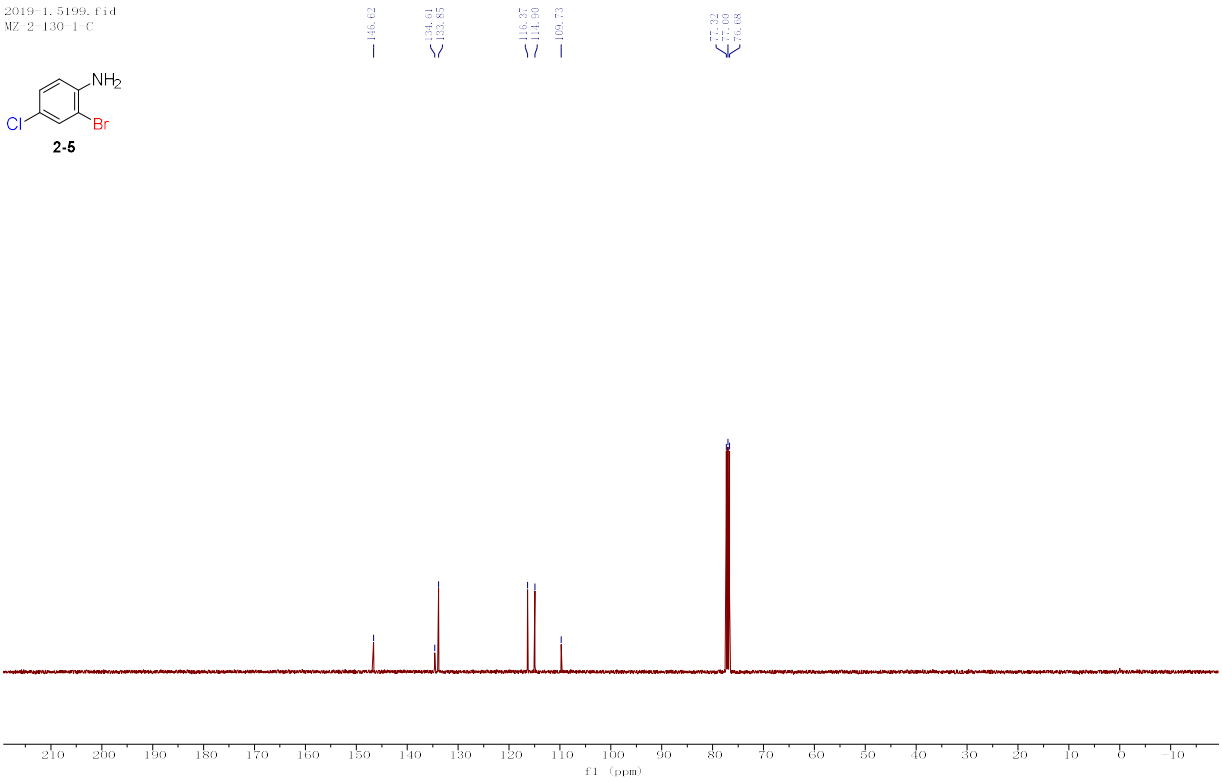

Figure S29. ^{13}C NMR of product **2-5**, related Table 2

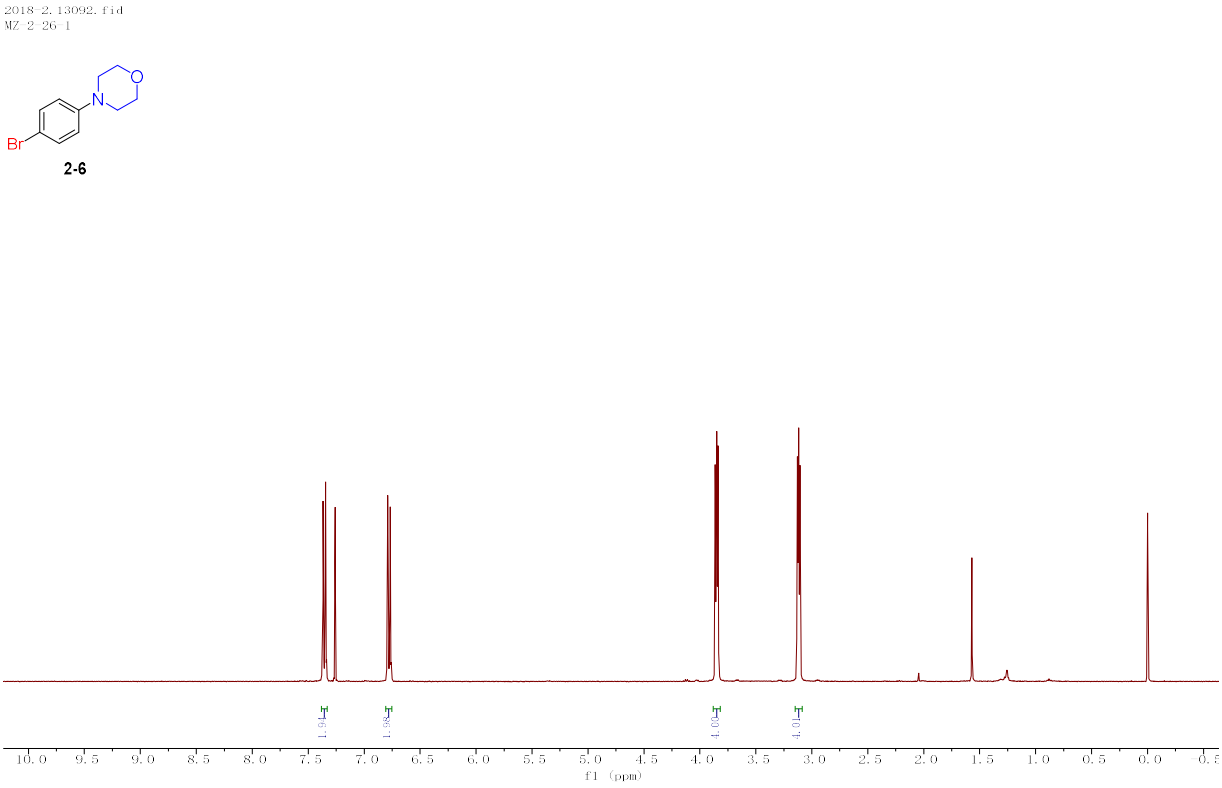

Figure S30. ^{1}H NMR of product **2-6**, related Table 2

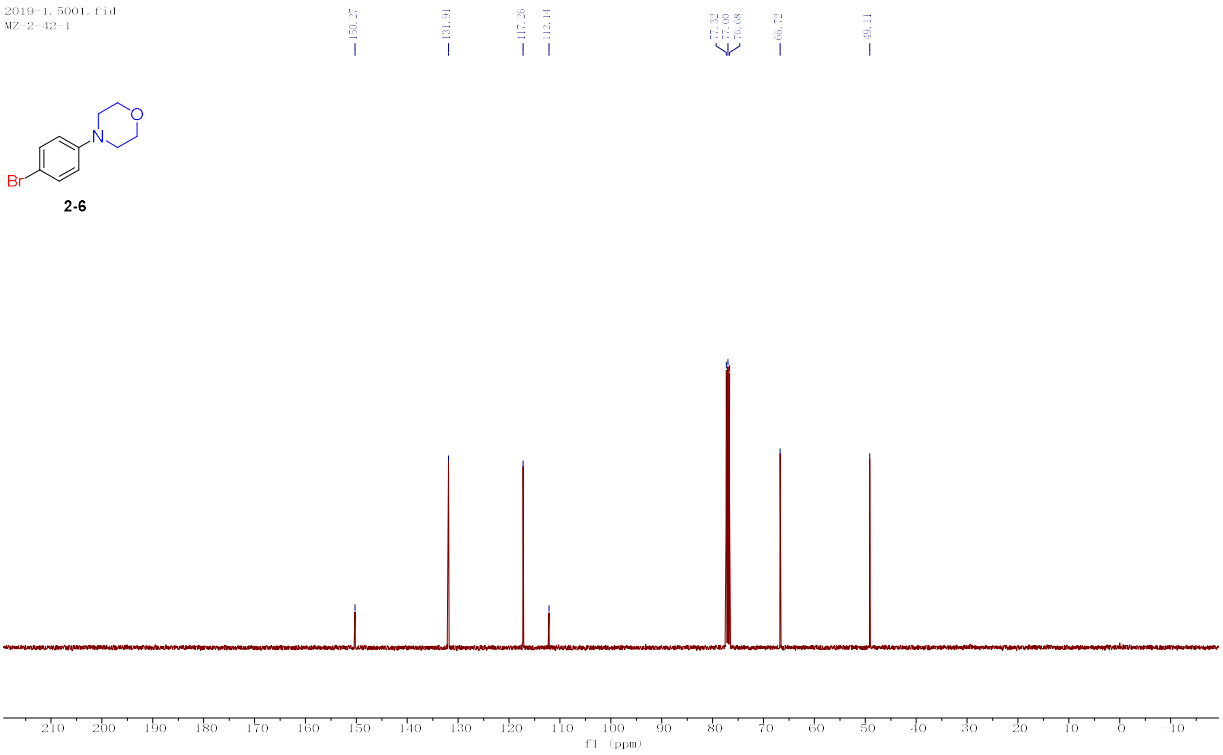

Figure S31. ^{13}C NMR of product **2-6**, related Table 2

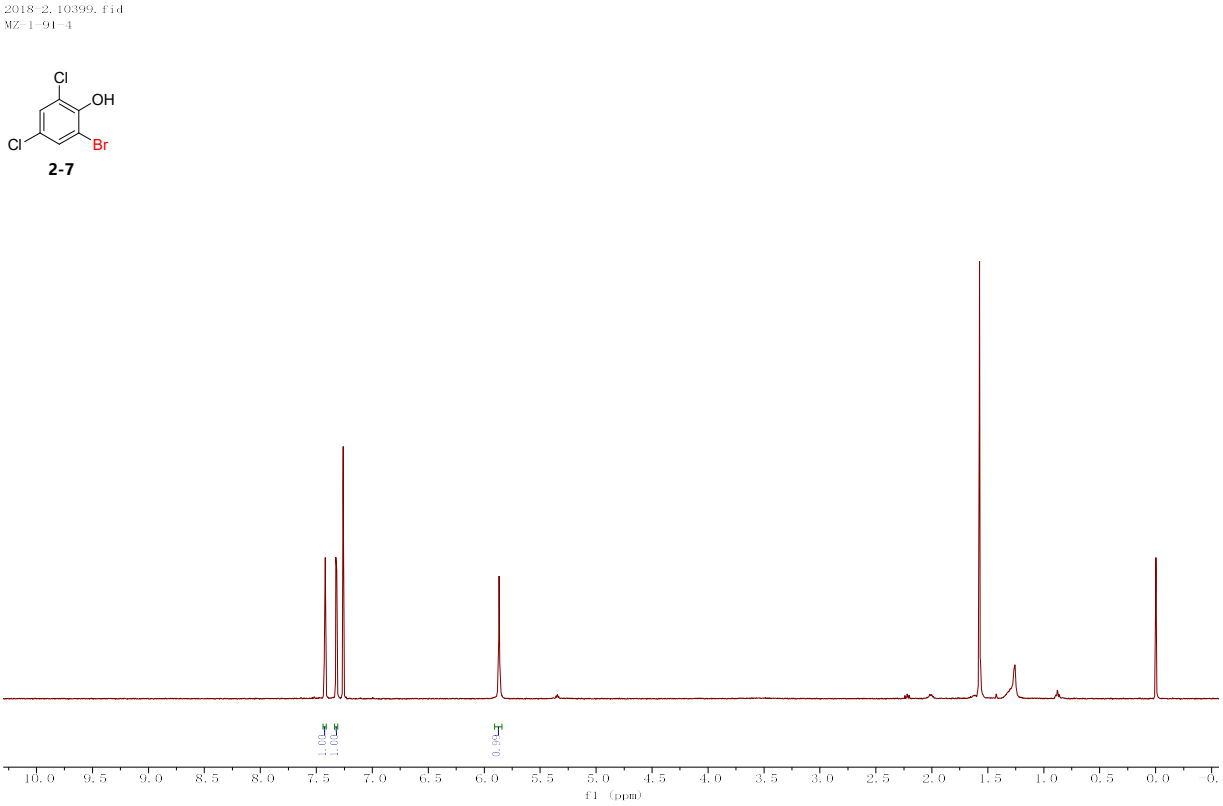

Figure S32. ^{1}H NMR of product **2-7**, related Table 2

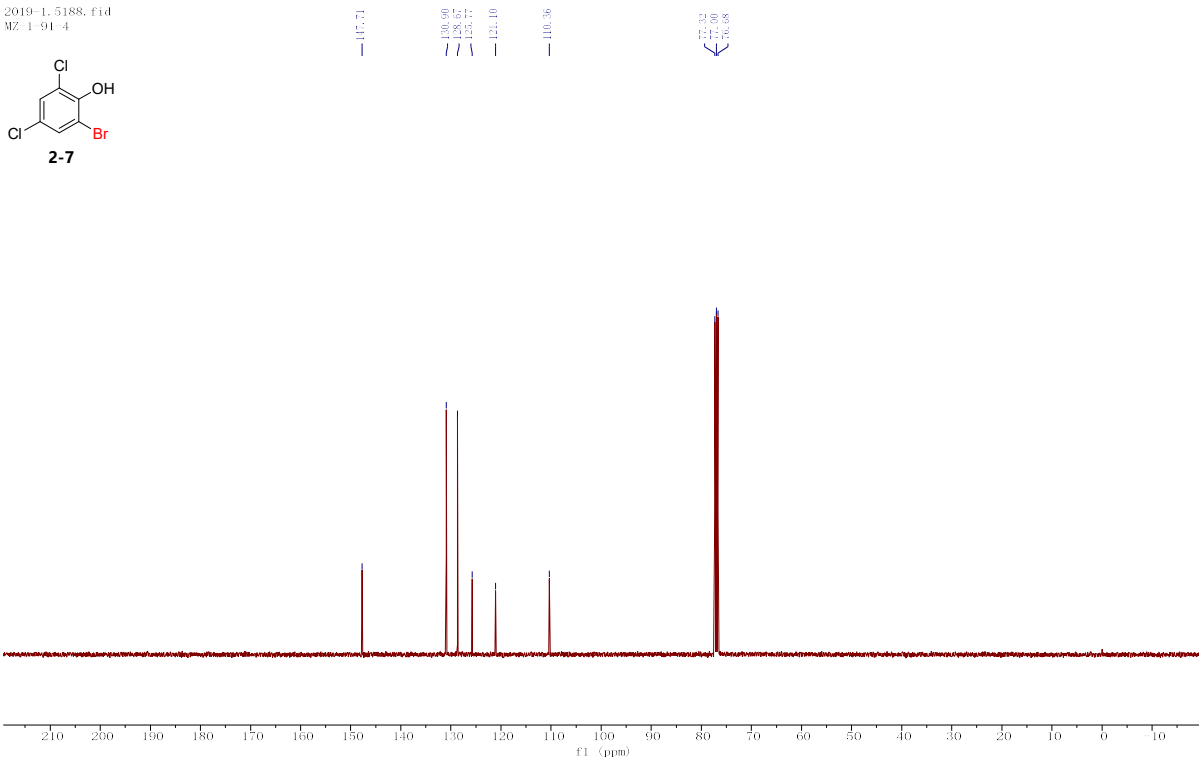

Figure S33. ^{13}C NMR of product **2-7**, related Table 2

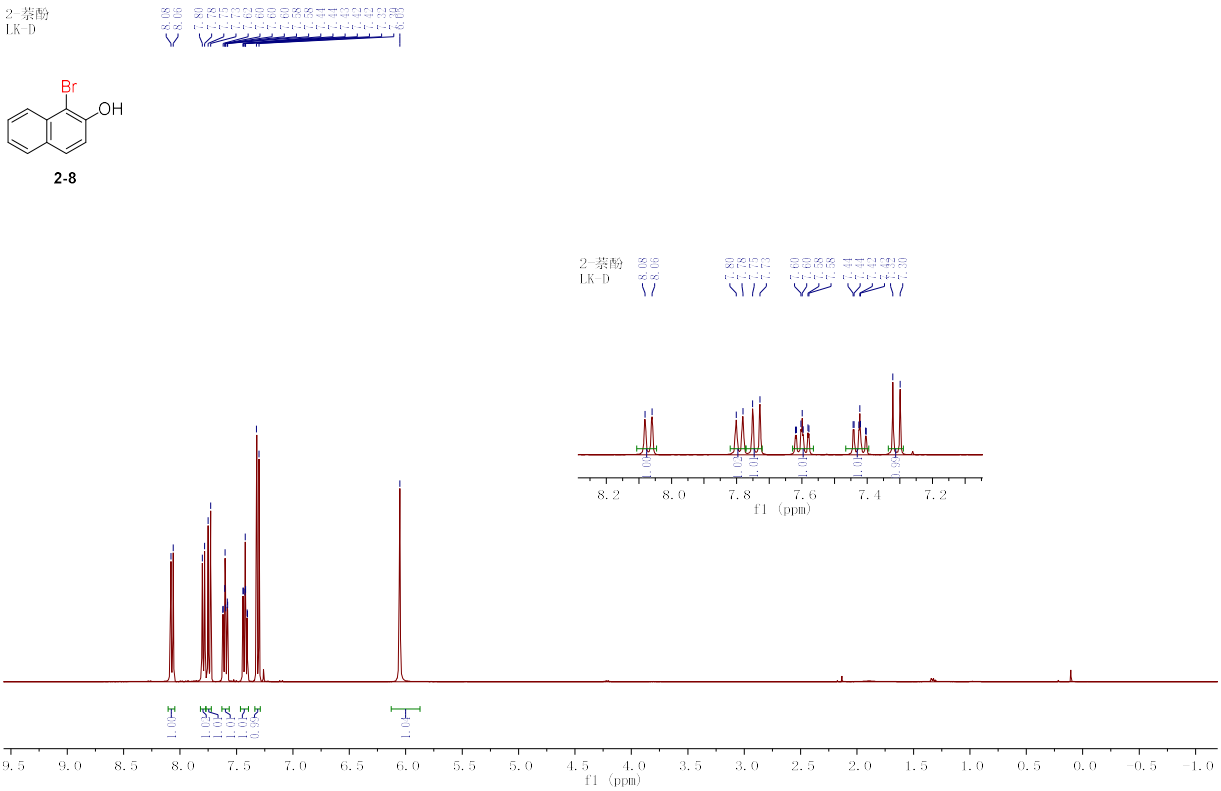

Figure S34. ^{1}H NMR of product **2-8**, related Table 2

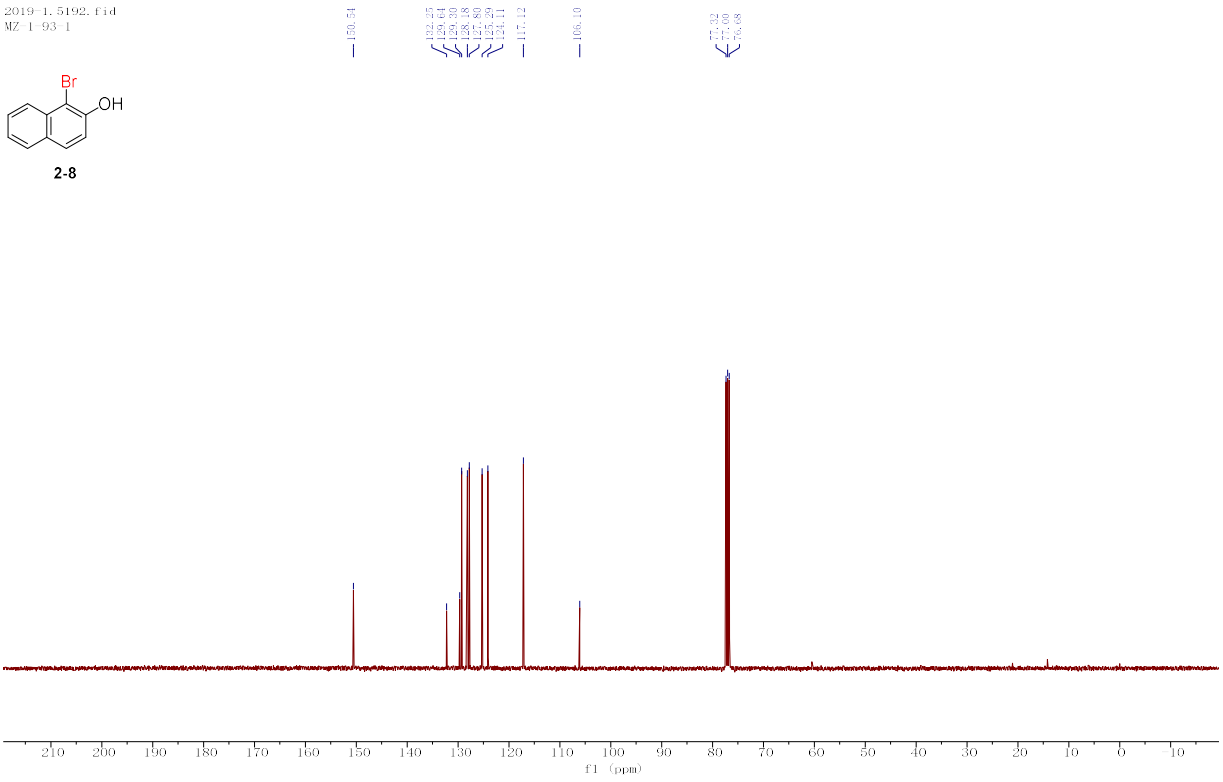

Figure S35. ^{13}C NMR of product **2-8**, related Table 2

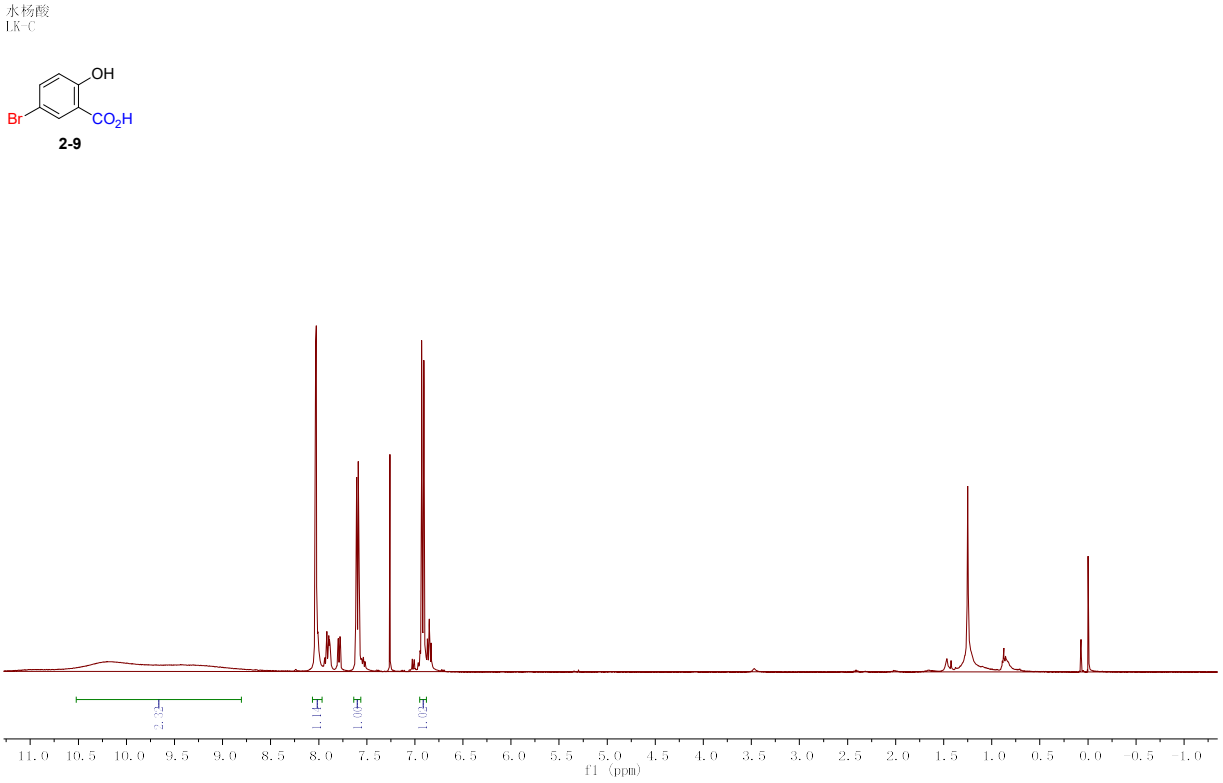

Figure S36. ^{1}H NMR of product **2-9**, related Table 2

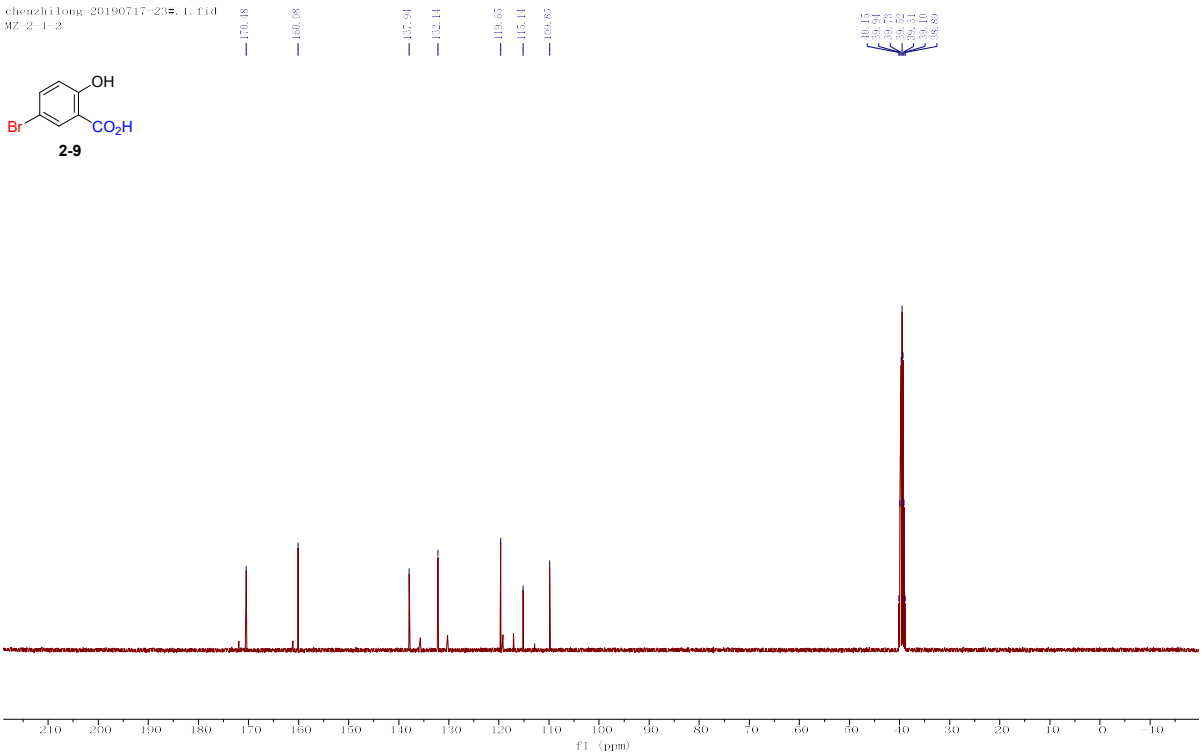

Figure S37. ^{13}C NMR of product **2-9**, related Table 2

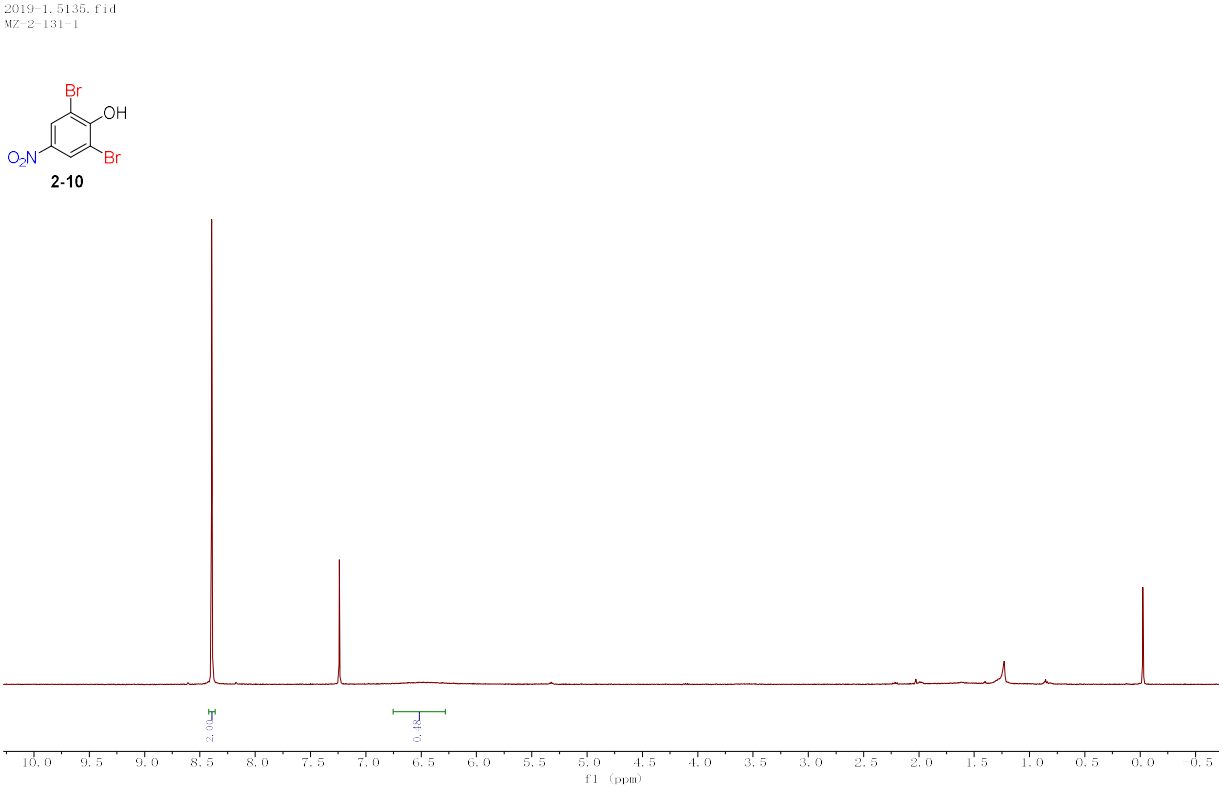

Figure S38. ^{1}H NMR of product **2-10**, related Table 2

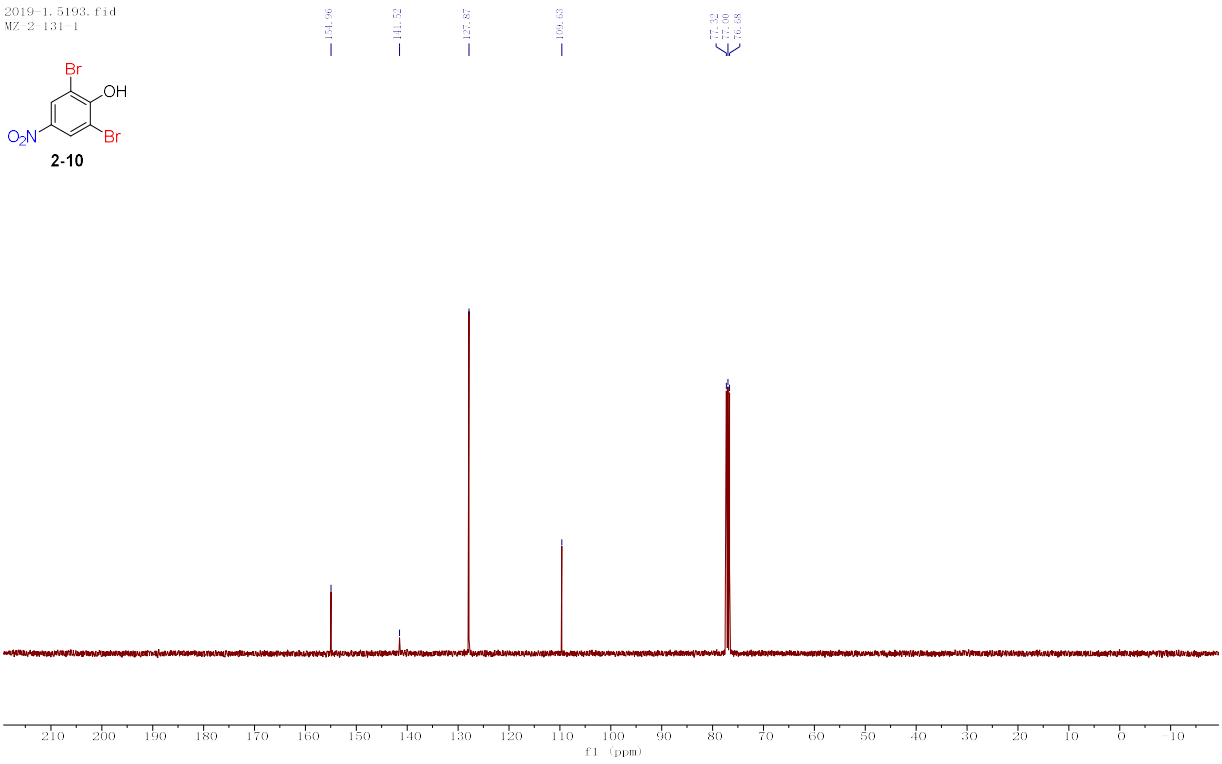

Figure S39. ^{13}C NMR of product **2-10**, related Table 2

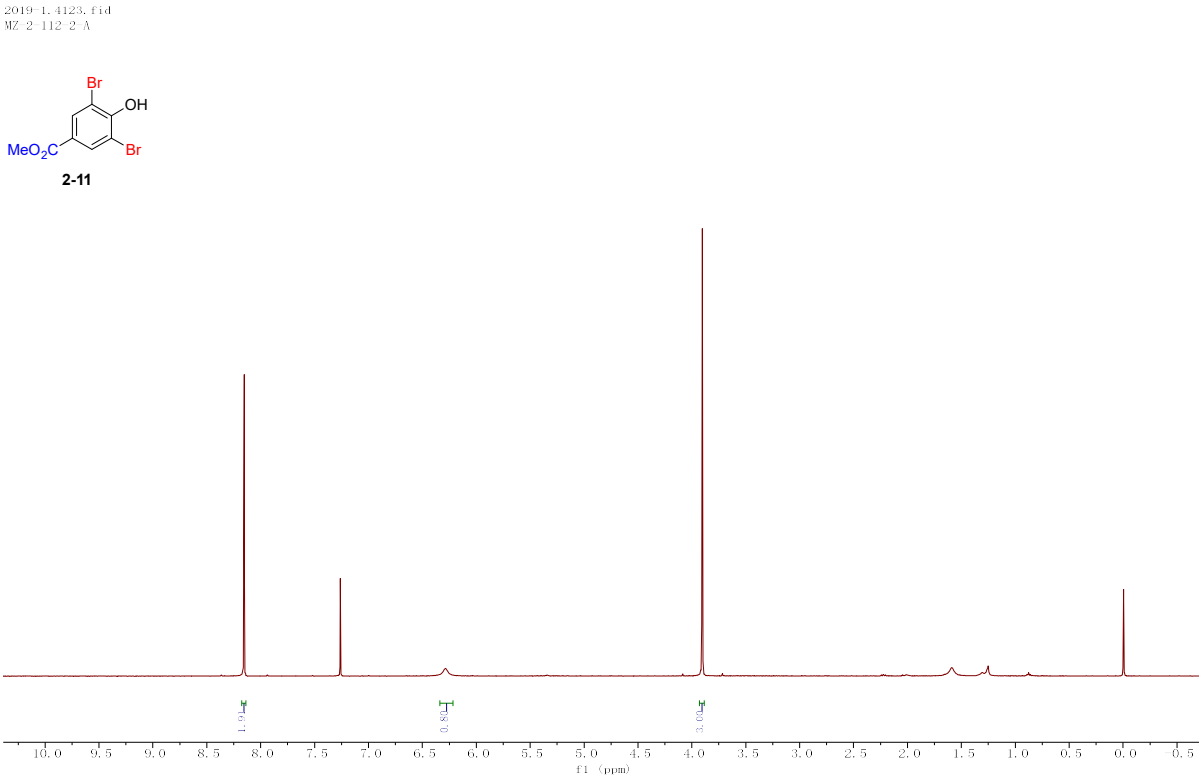

Figure S40. ^{1}H NMR of product **2-11**, related Table 2

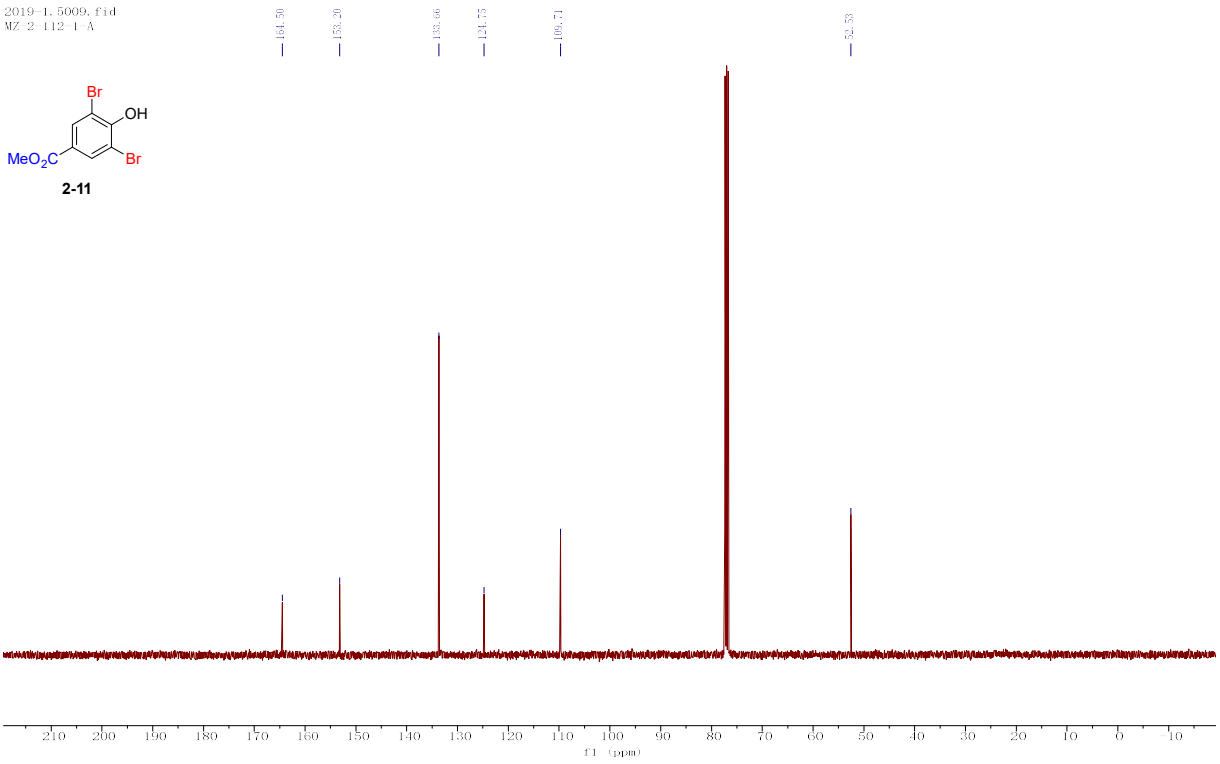

Figure S41. ^{13}C NMR of product **2-11**, related Table 2

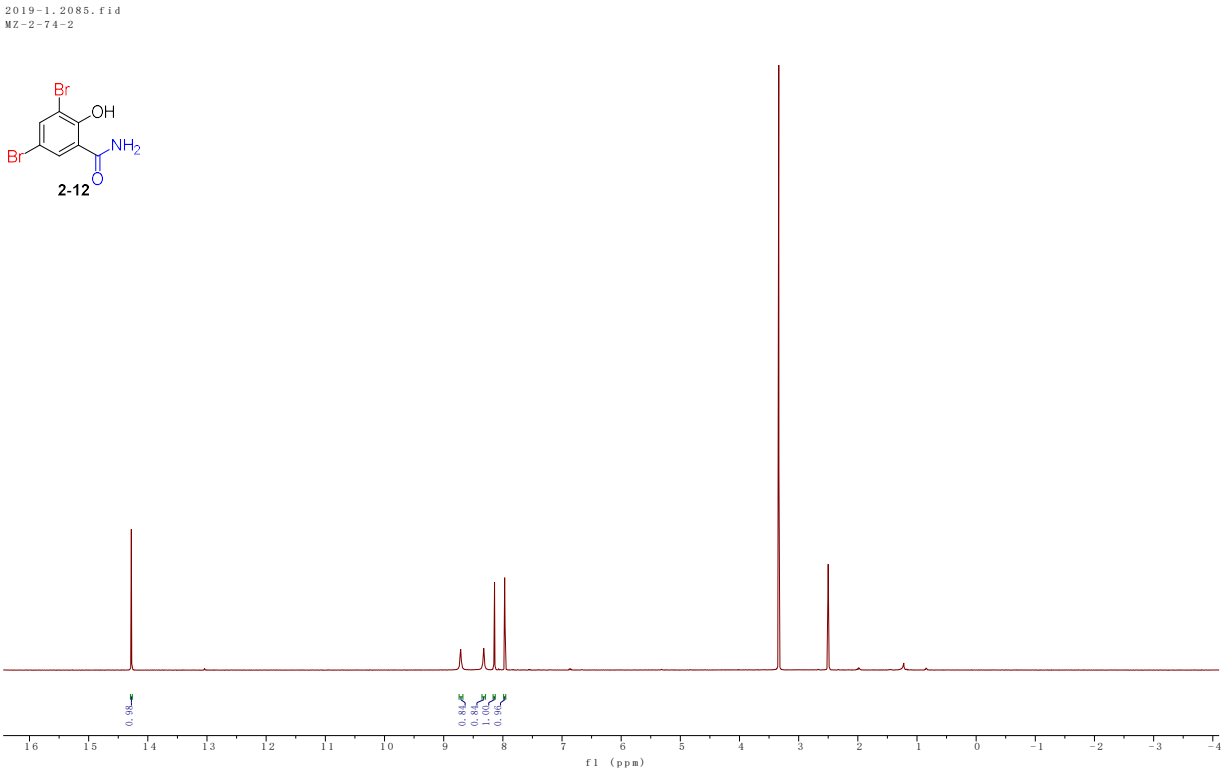

Figure S42. ^{1}H NMR of product **2-12**, related Table 2

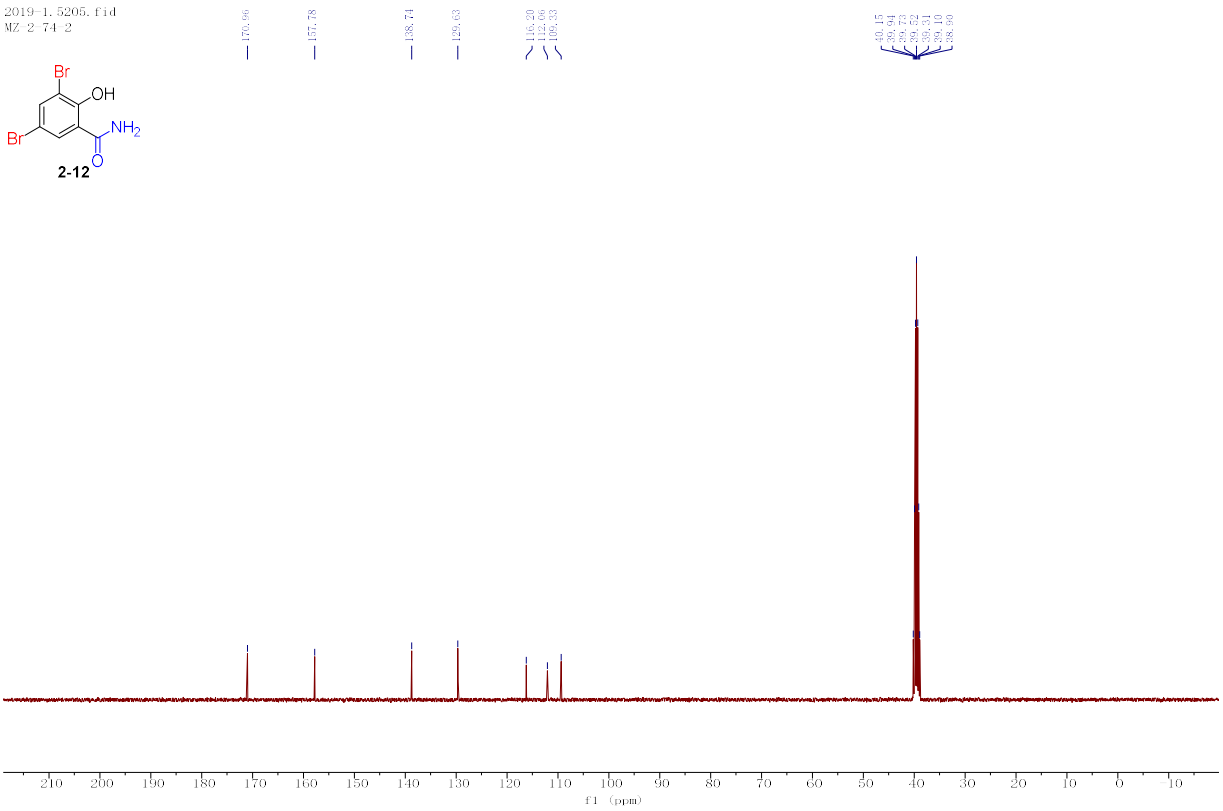

Figure S43. ^{13}C NMR of product **2-12**, related Table 2

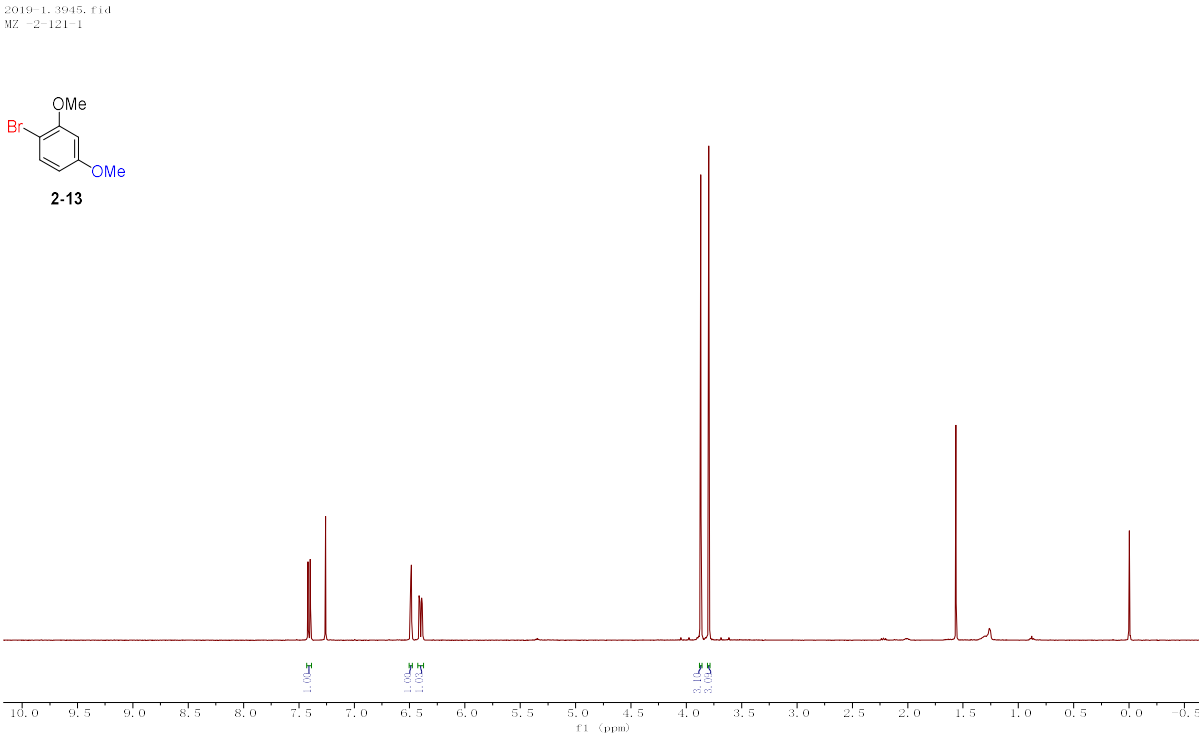

Figure S44. ^{1}H NMR of product **2-13**, related Table 2

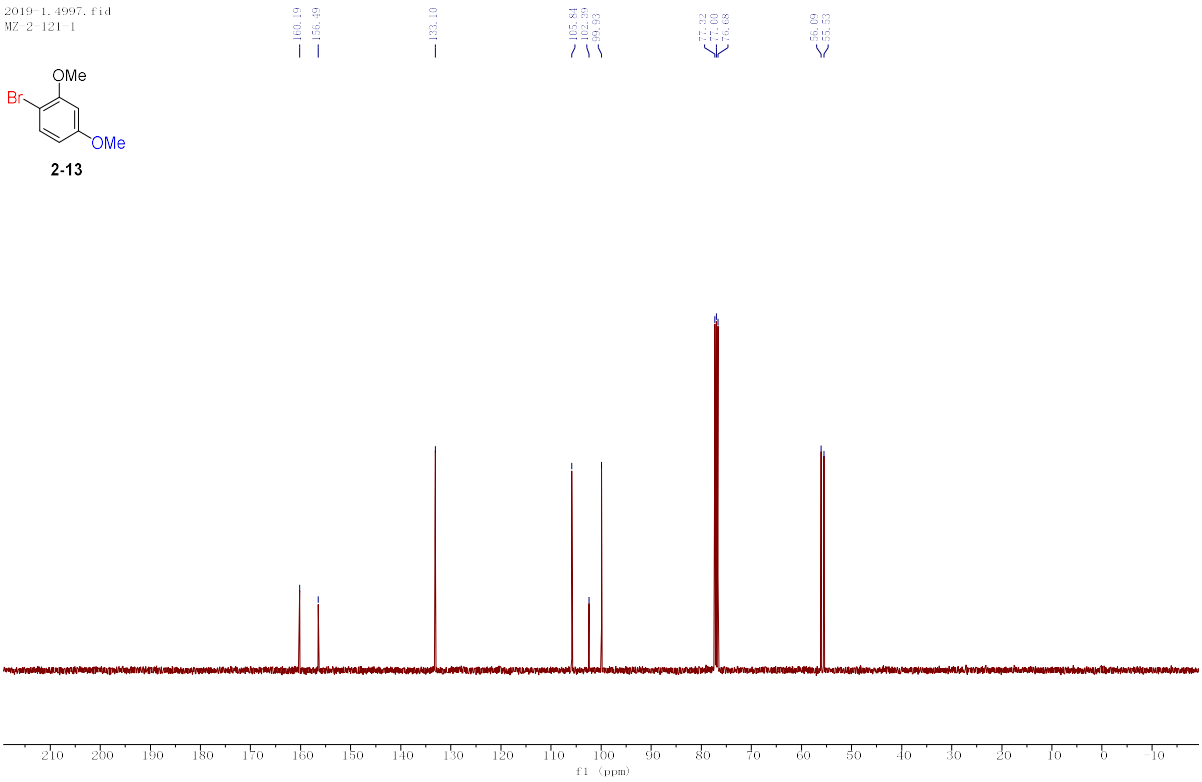

Figure S45. ^{13}C NMR of product **2-13**, related Table 2

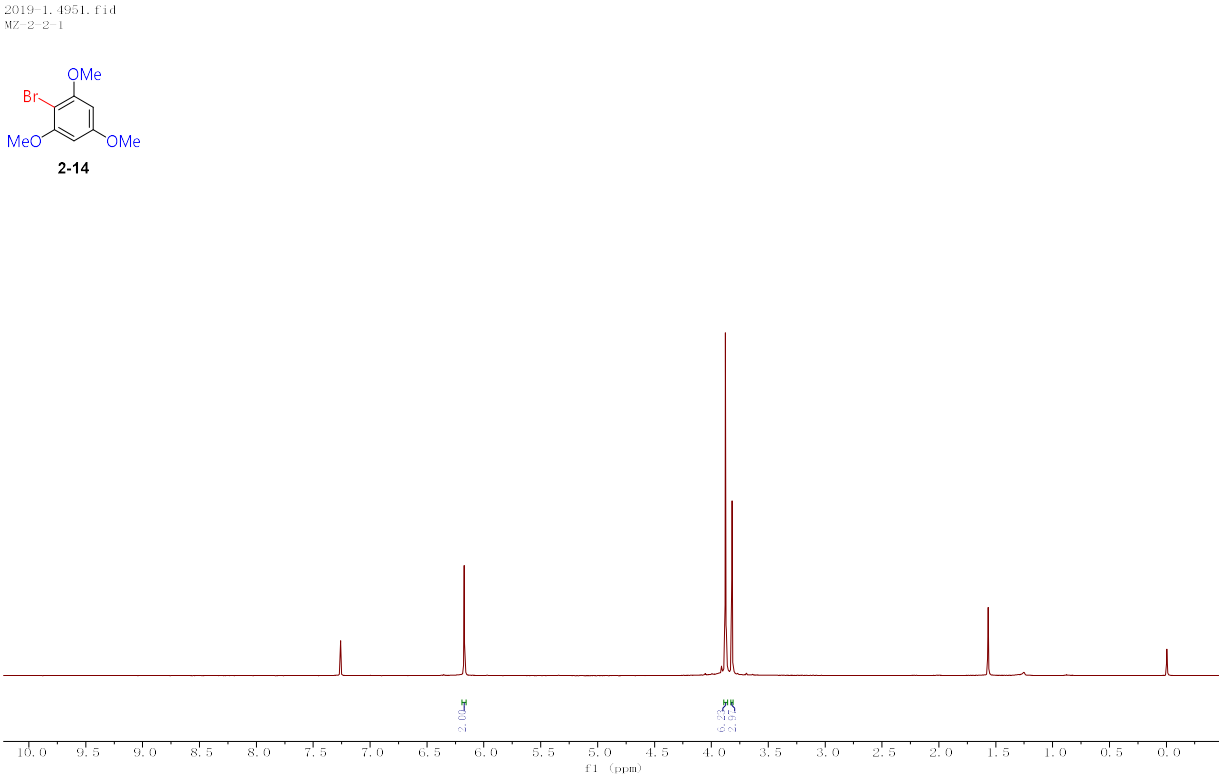

Figure S46. ^{1}H NMR of product **2-14**, related Table 2

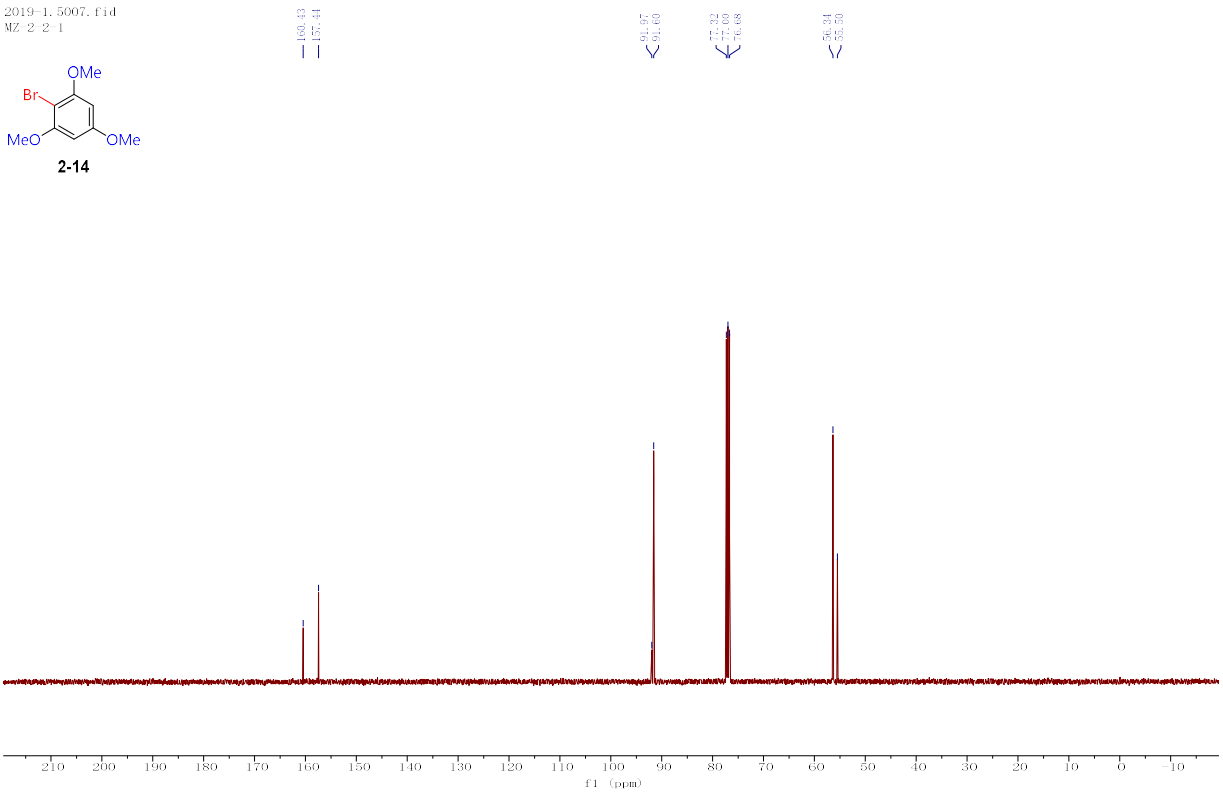

Figure S47. ^{13}C NMR of product **2-14**, related Table 2

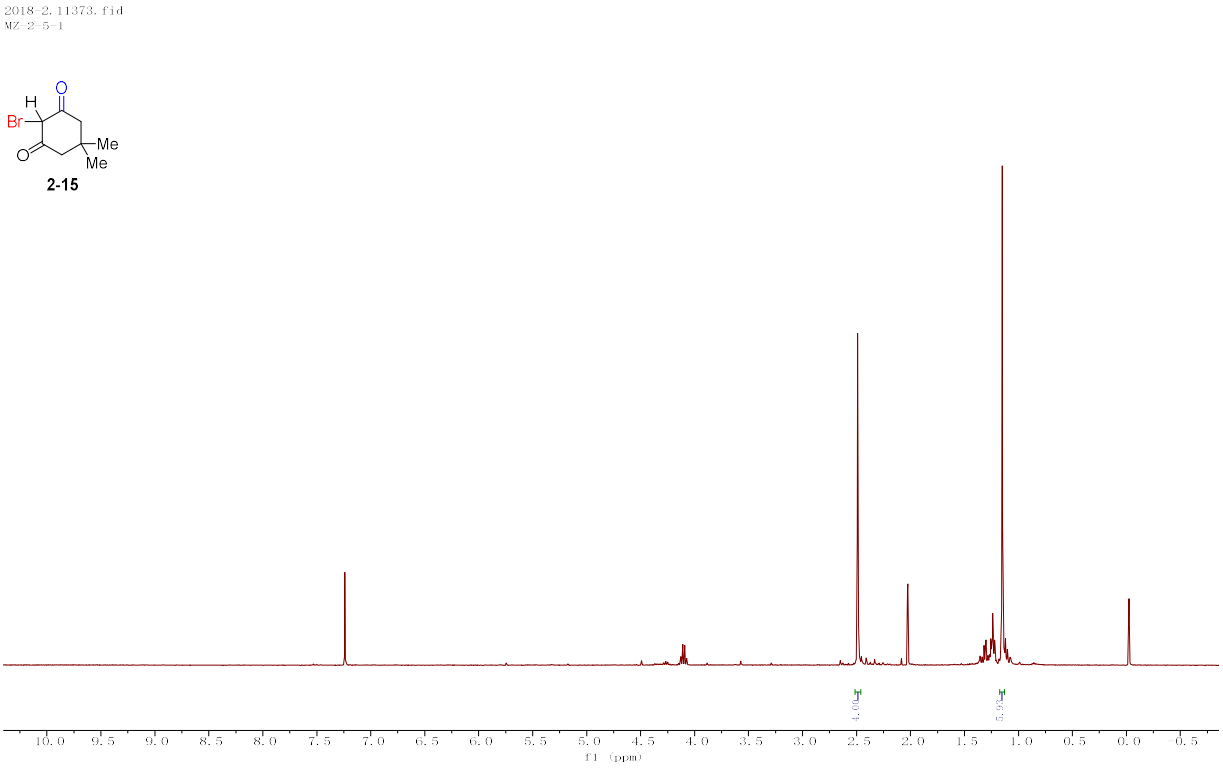

Figure S48. ^{1}H NMR of product **2-15**, related Table 2

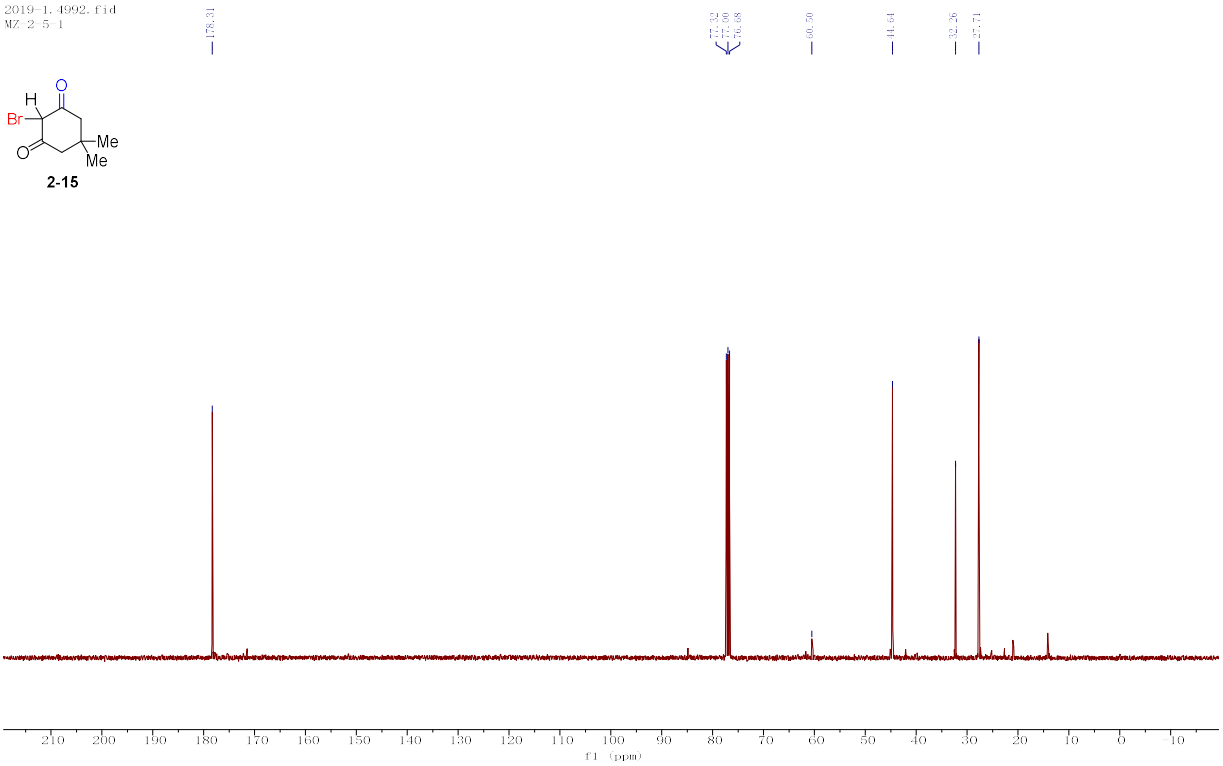

Figure S49. ^{13}C NMR of product **2-15**, related Table 2

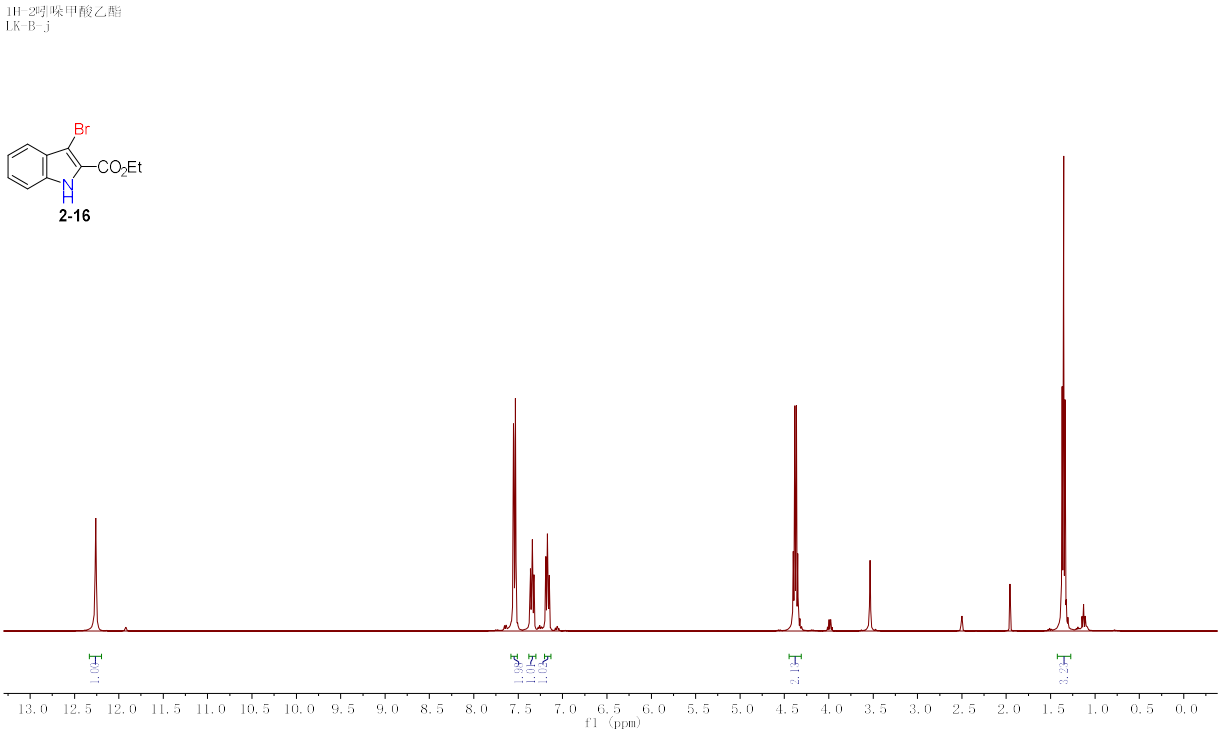

Figure S50. ^{1}H NMR of product **2-16**, related Table 2

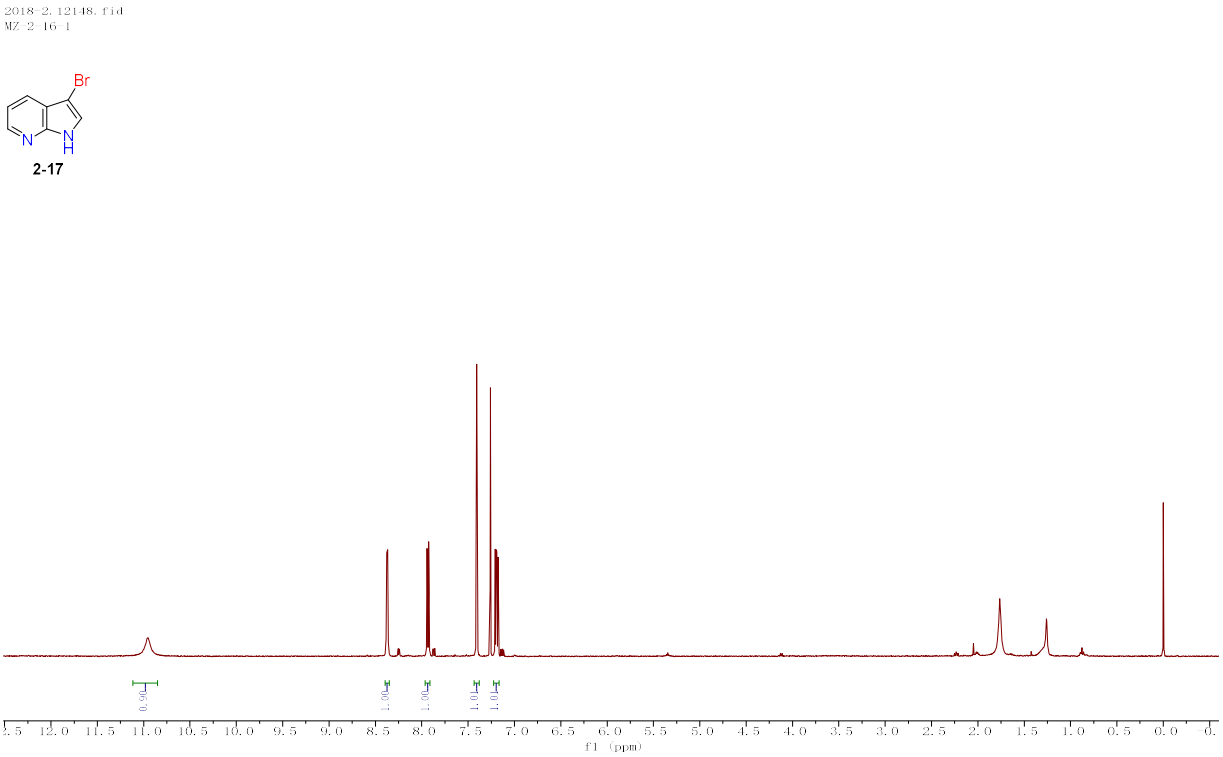

Figure S51. ^{1}H NMR of product **2-17**, related Table 2

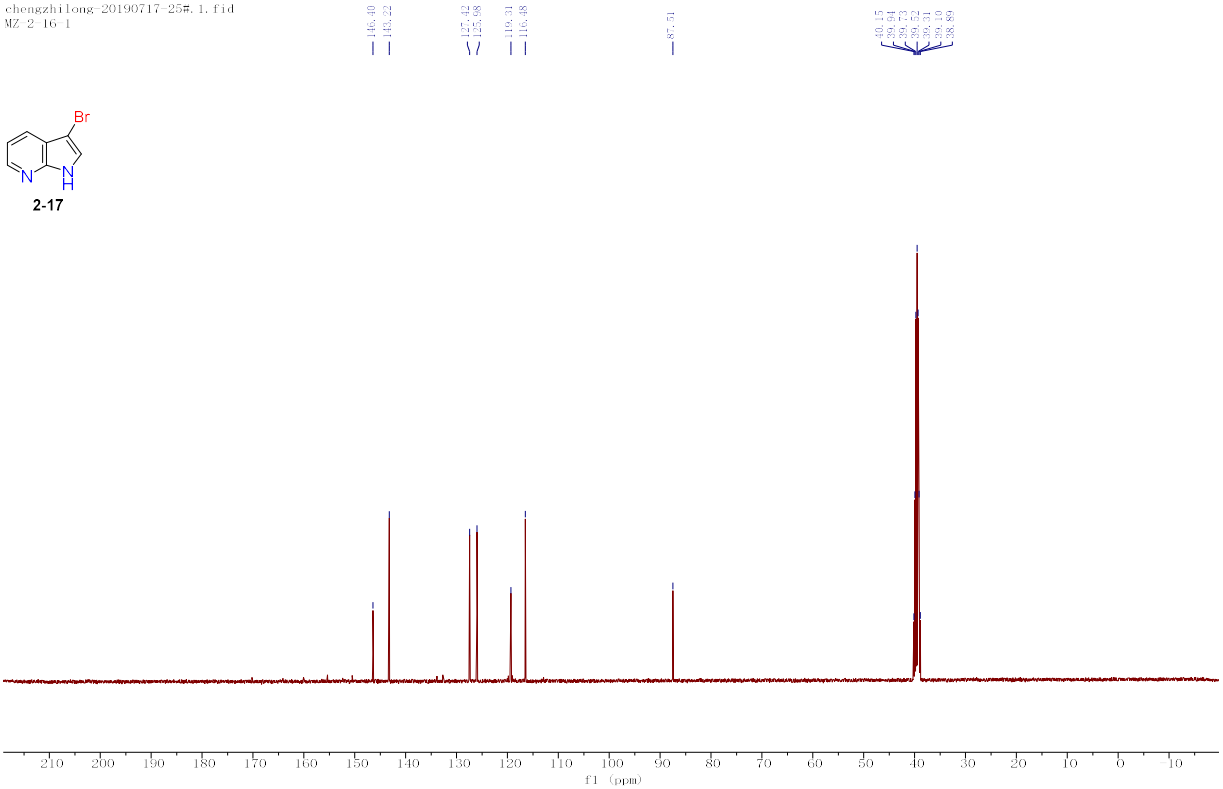

Figure S52. ^{13}C NMR of product **2-17**, related Table 2

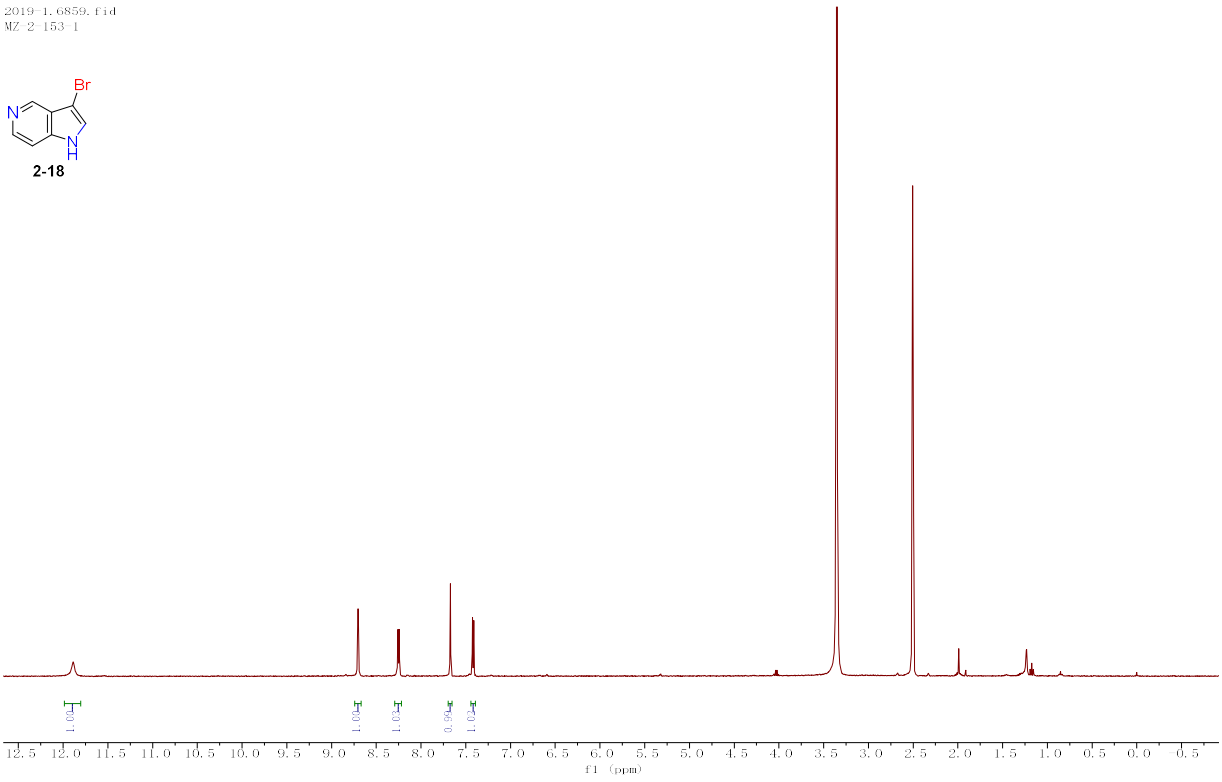

Figure S53. ^{1}H NMR of product **2-18**, related Table 2

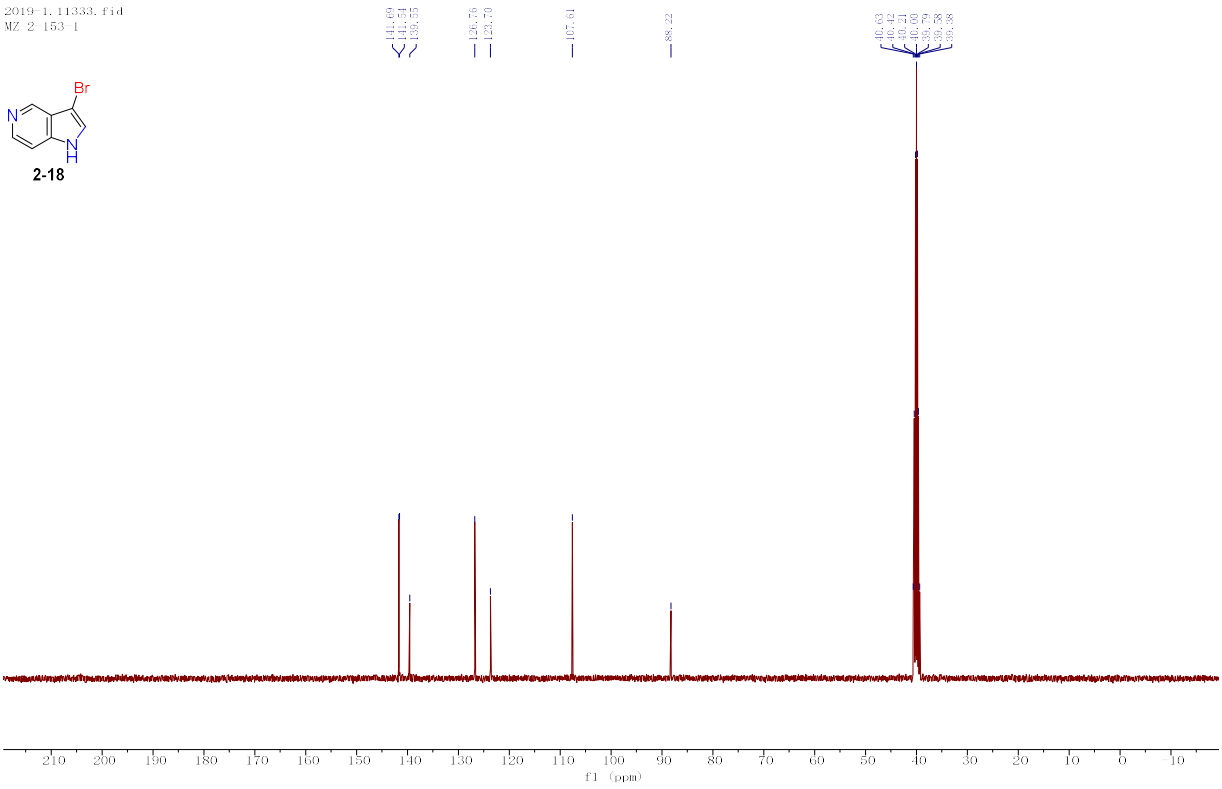

Figure S54. ^{13}C NMR of product **2-18**, related Table 2

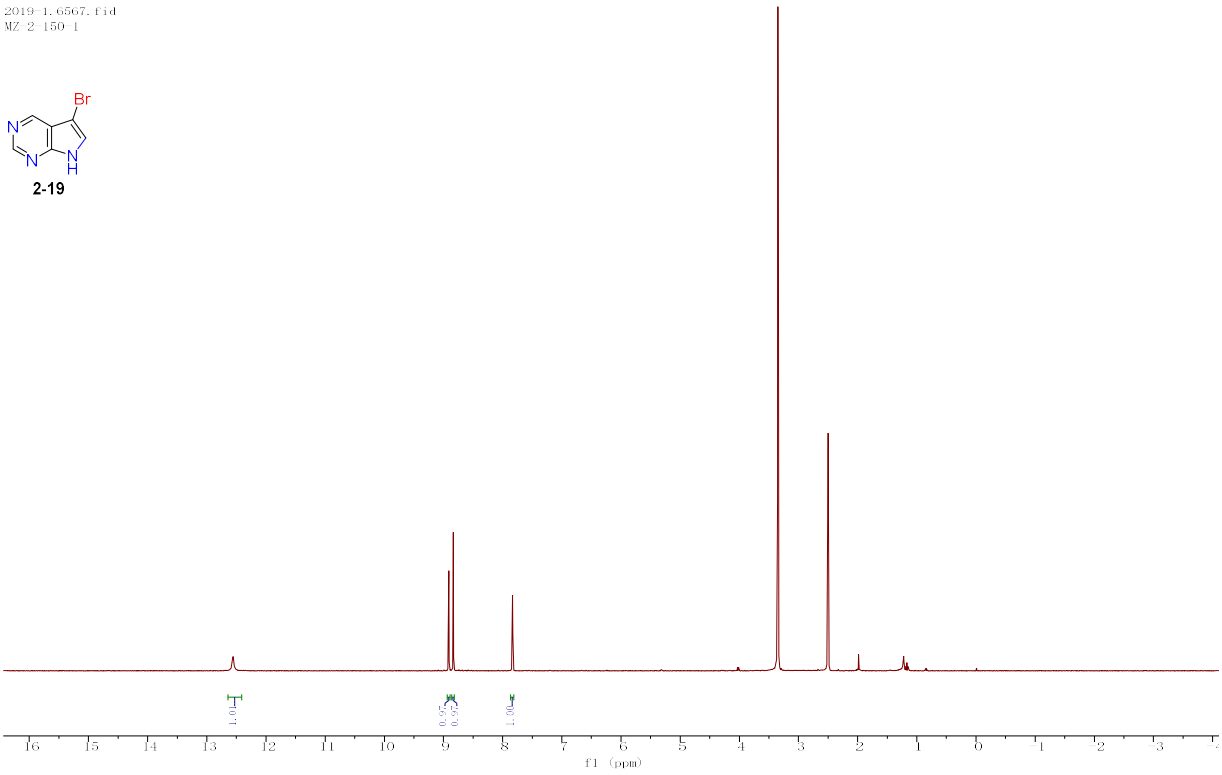

Figure S55. ^{1}H NMR of product **2-19**, related Table 2

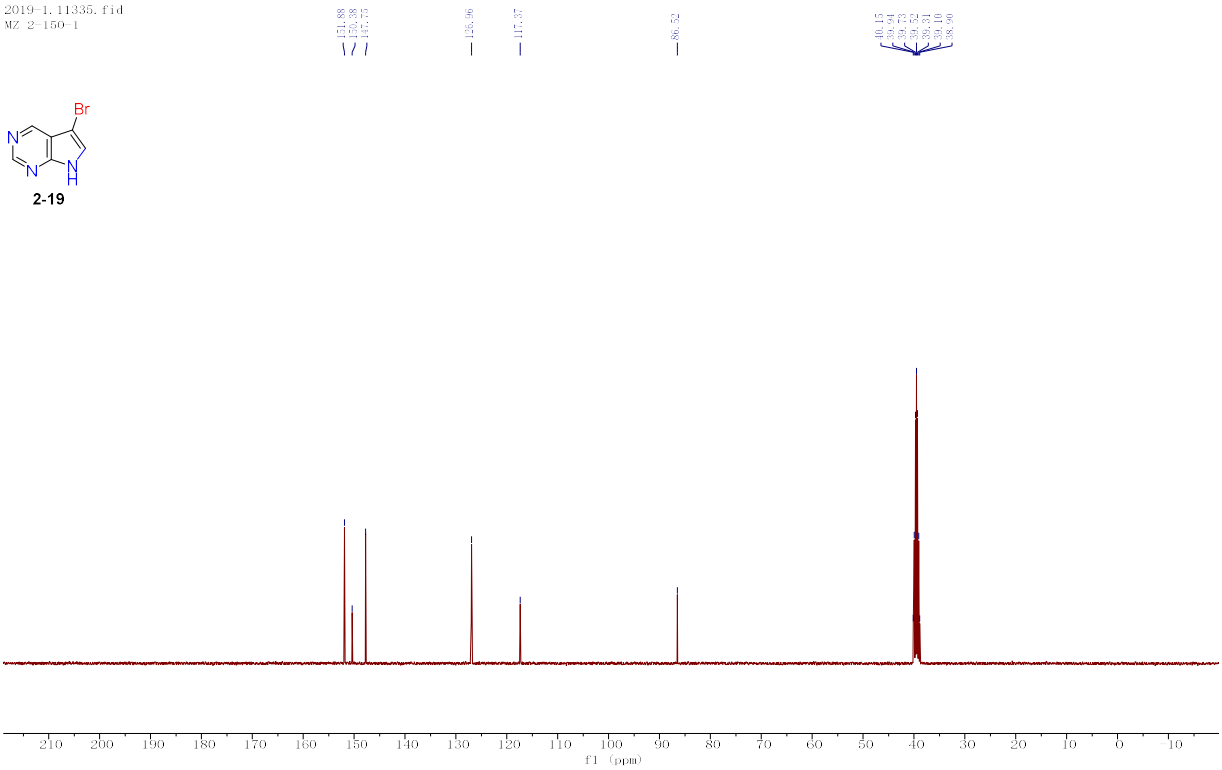

Figure S56. ^{1}H NMR of product **2-19**, related Table 2

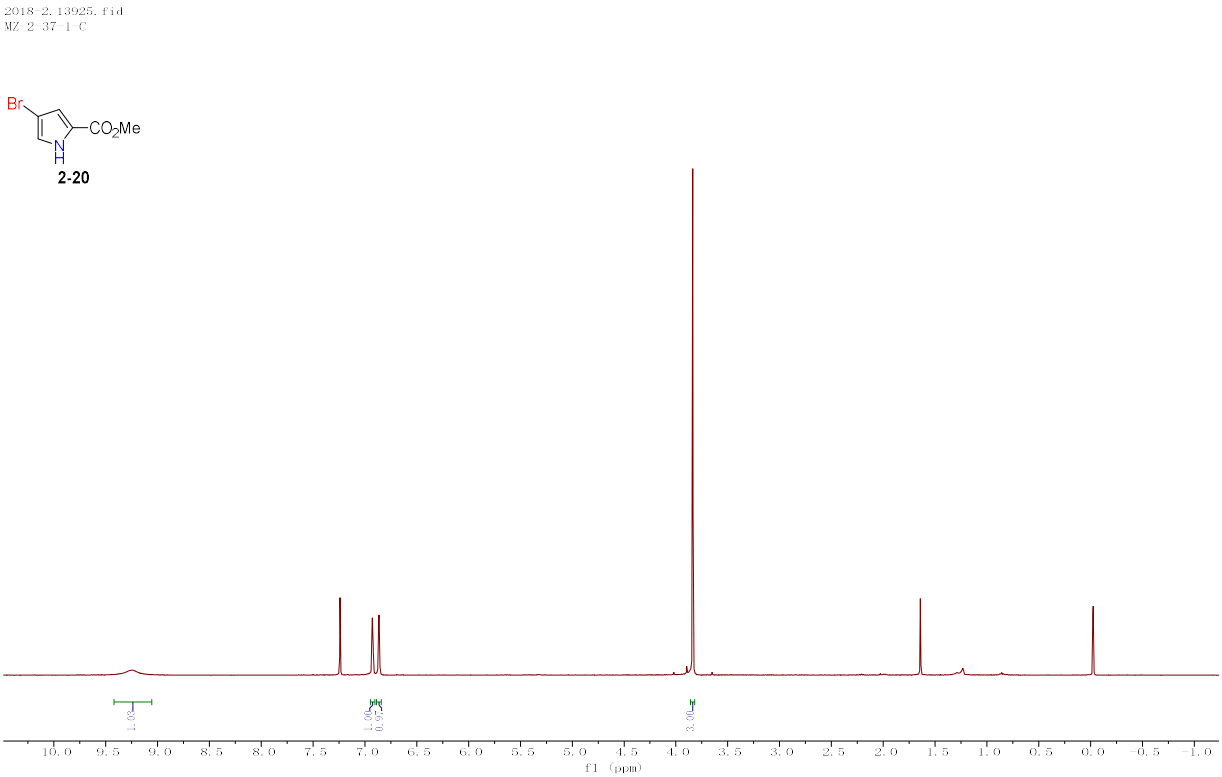

Figure S57. ^{1}H NMR of product **2-20**, related Table 2

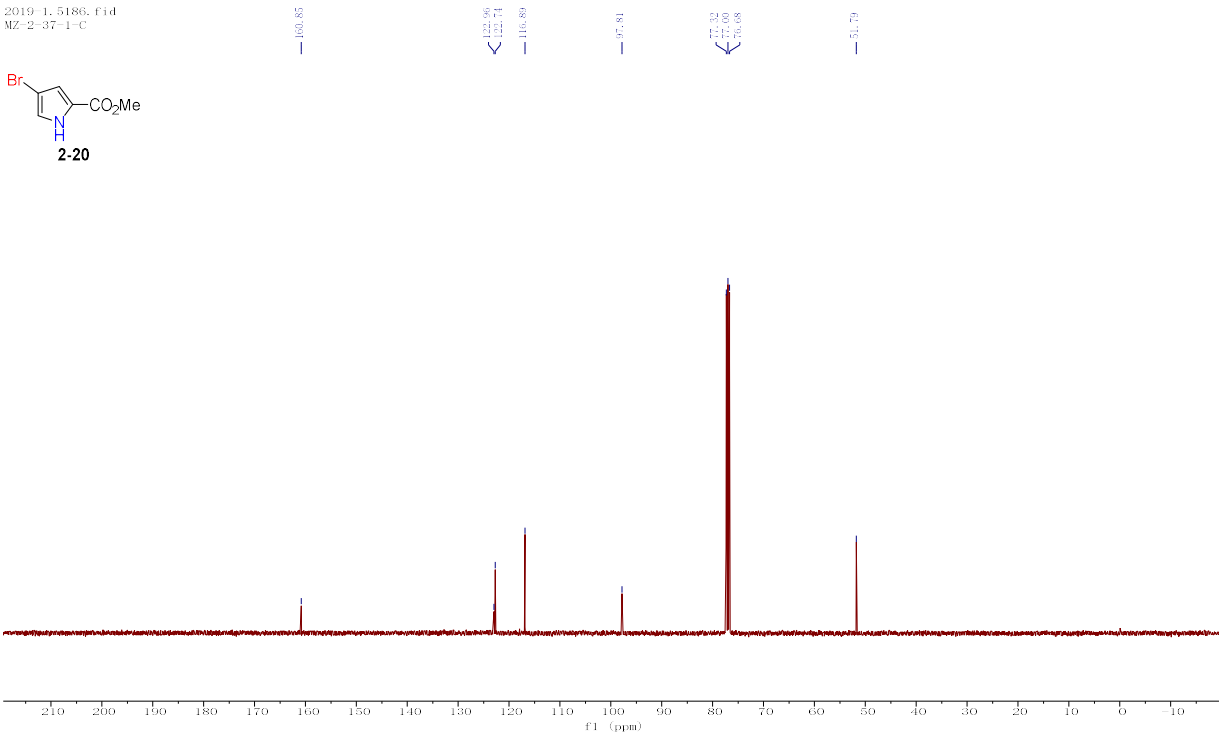

Figure S58. ^{13}C NMR of product **2-20**, related Table 2

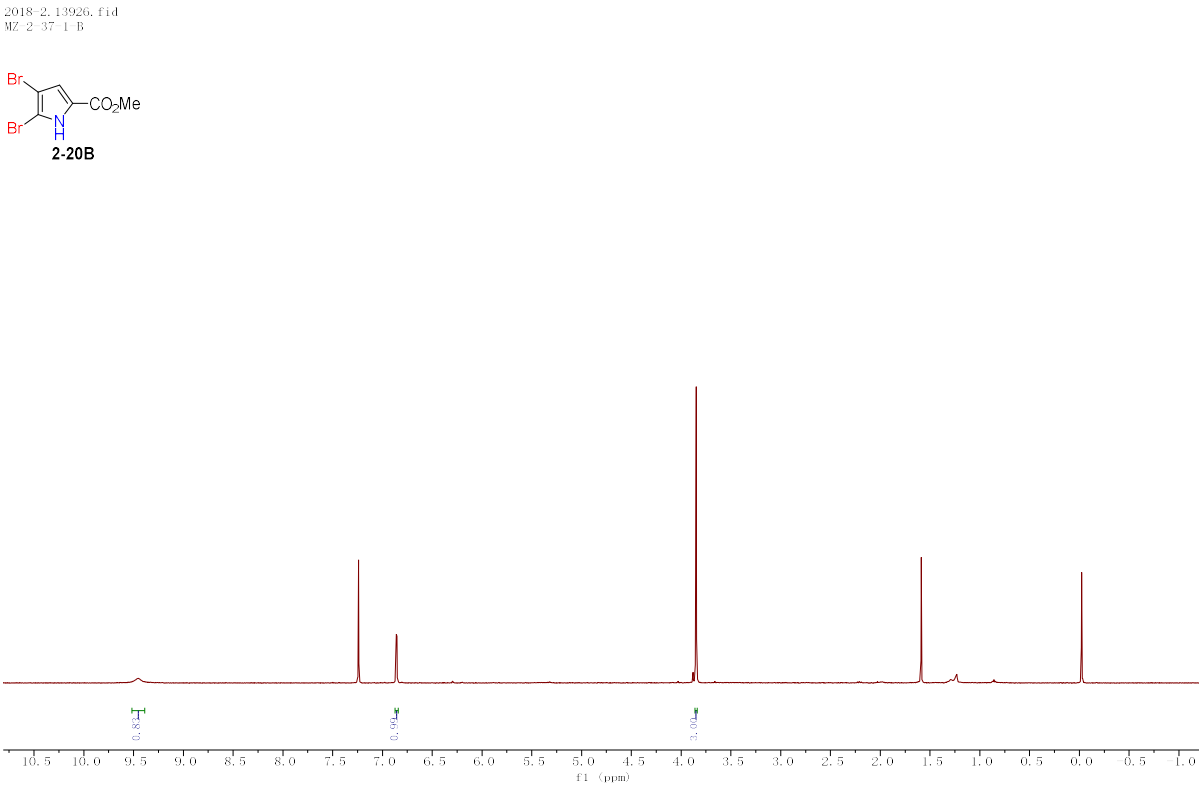

Figure S59. ^{1}H NMR of product **2-20B**, related Table 2

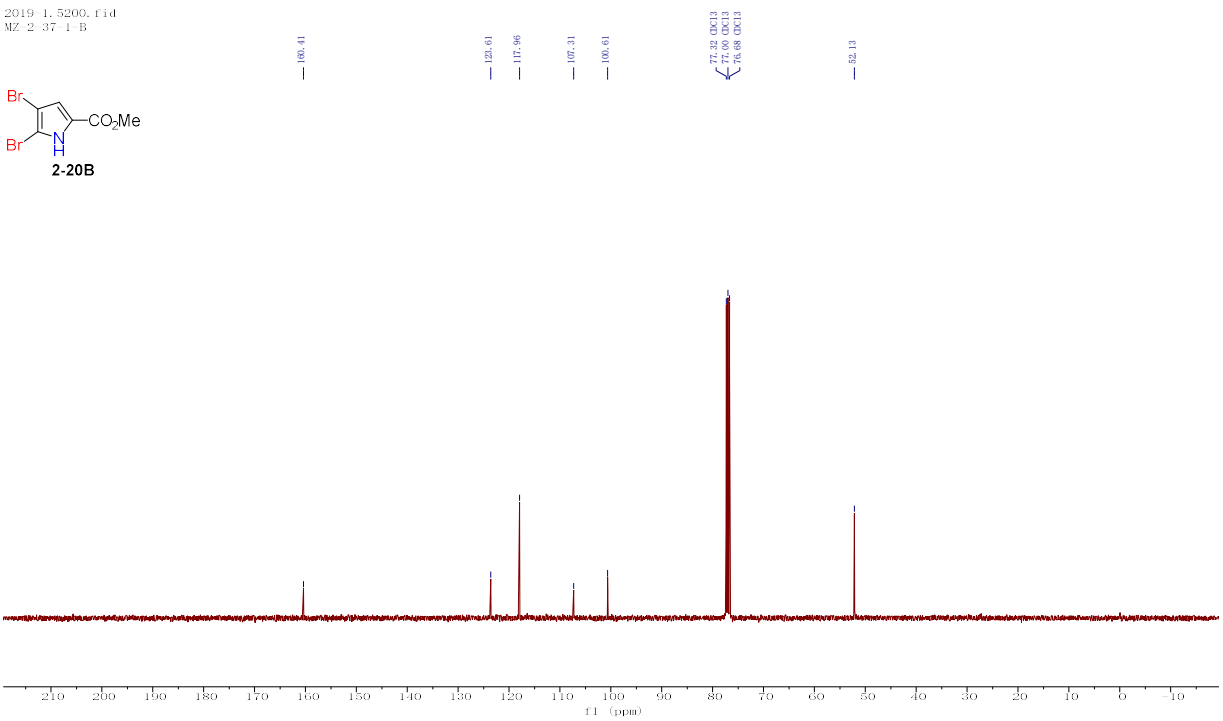

Figure S60. ^{13}C NMR of product **2-20B**, related Table 2

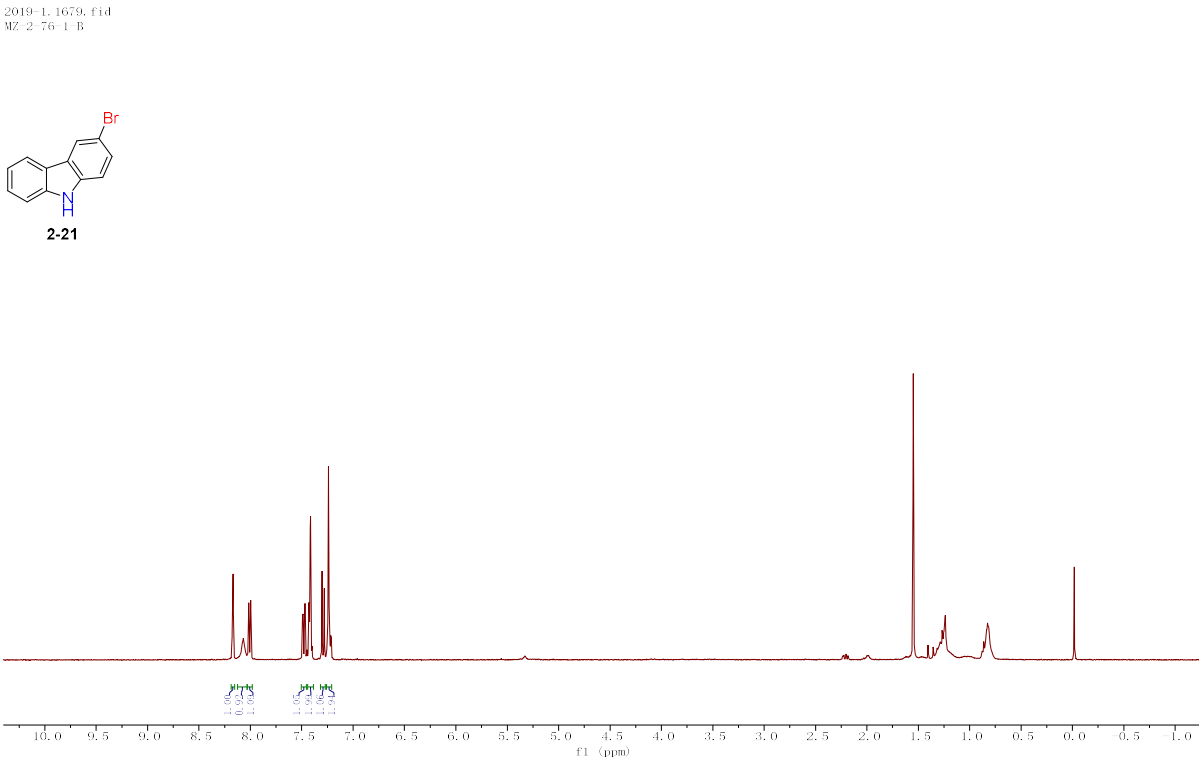

Figure S61. ^{1}H NMR of product **2-21**, related Table 2

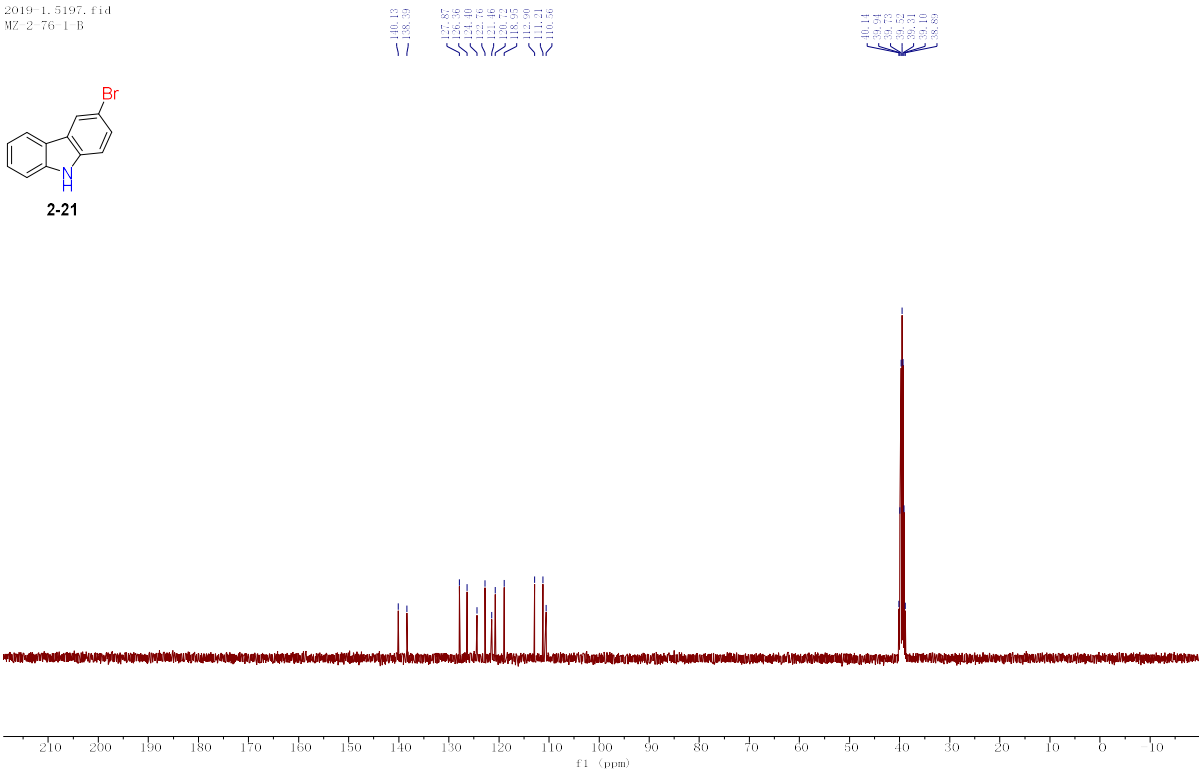

Figure S62. ^{13}C NMR of product **2-21**, related Table 2

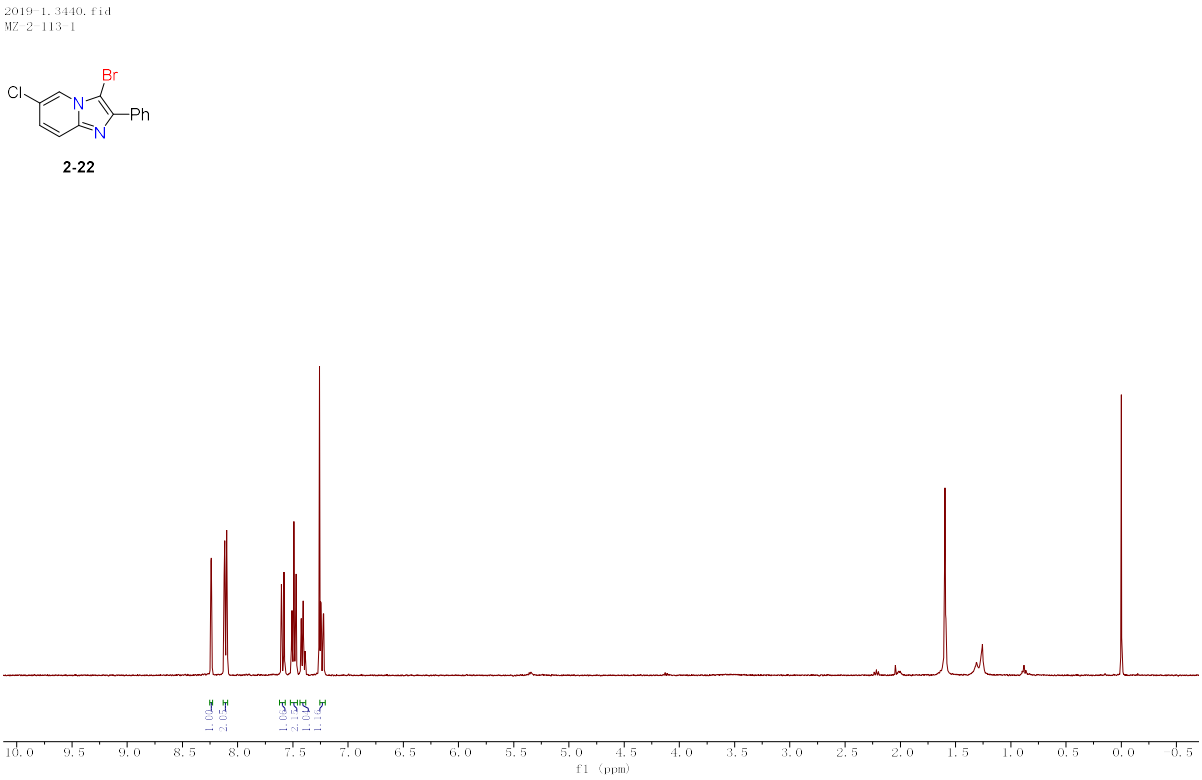

Figure S63. ^{1}H NMR of product **2-22**, related Table 2

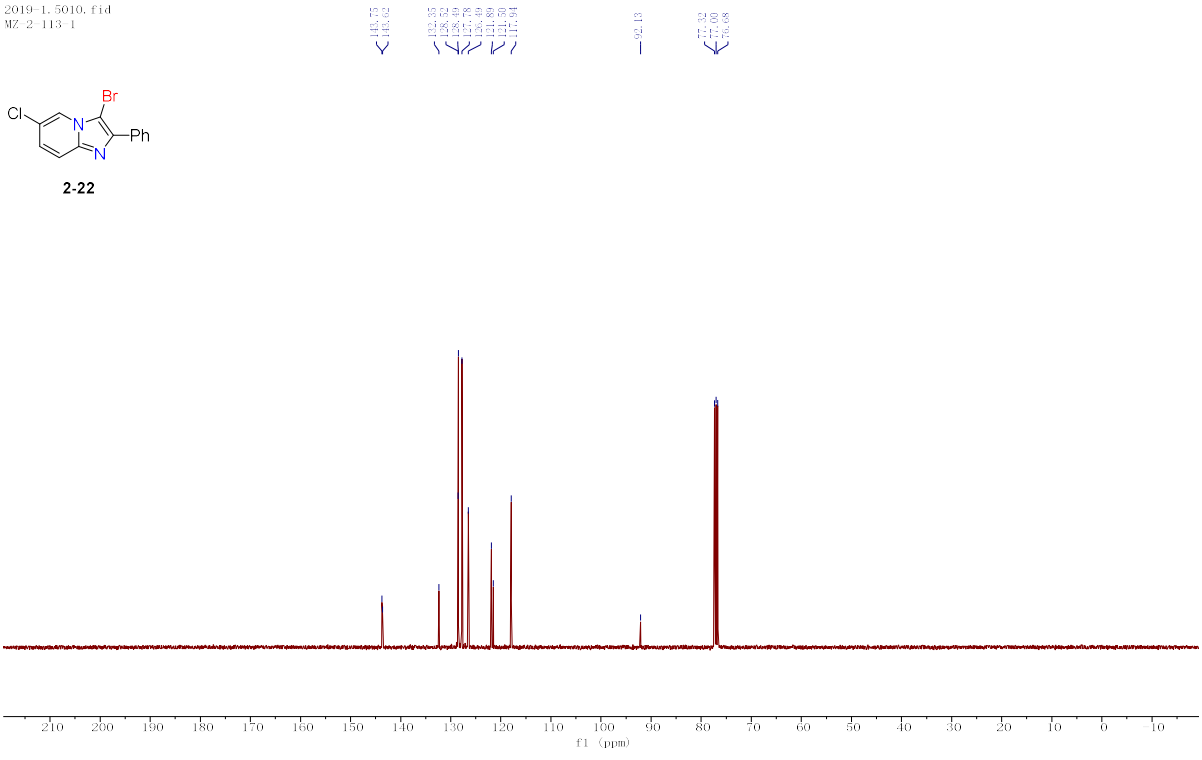

Figure S64. ^{13}C NMR of product **2-22**, related Table 2

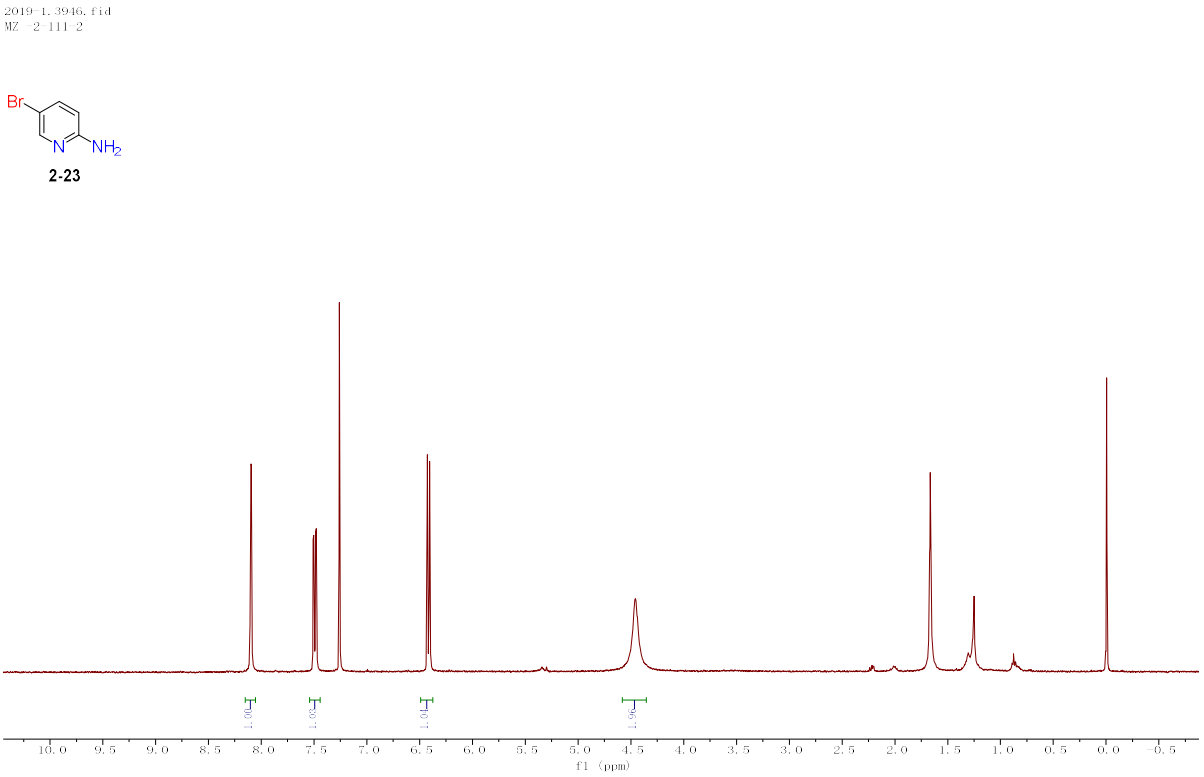

Figure S65. ^{1}H NMR of product **2-23**, related Table 2

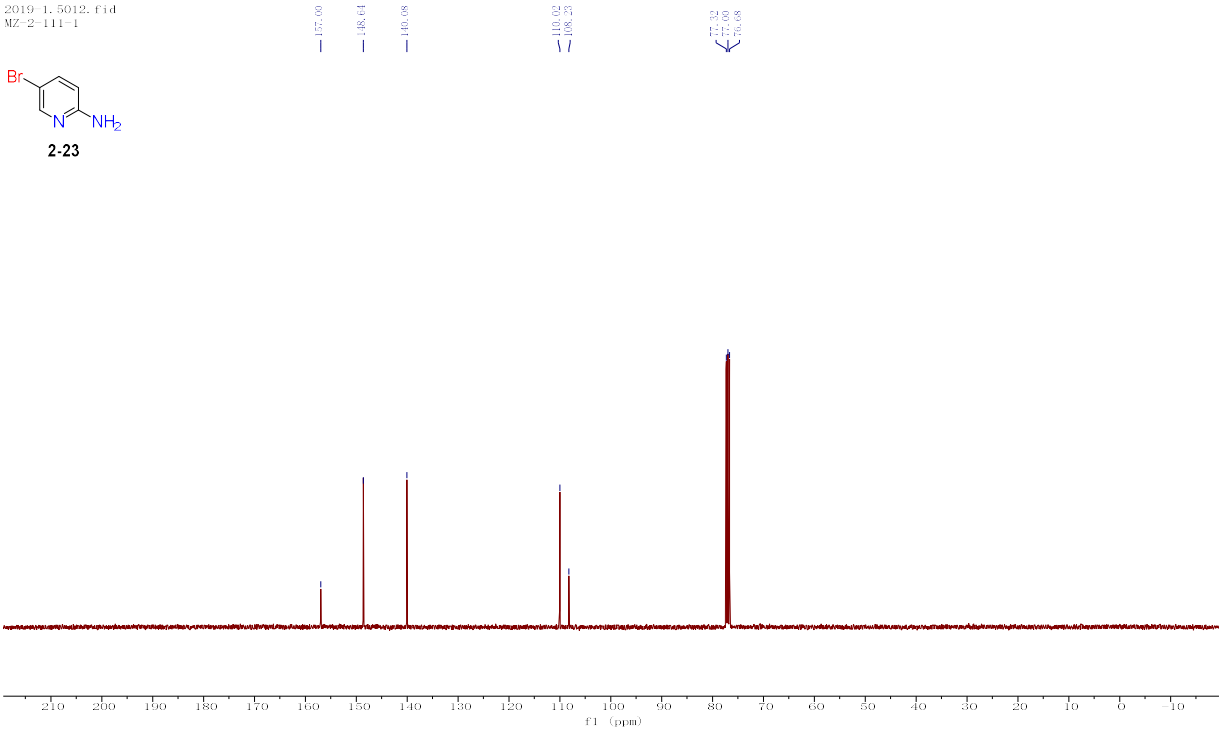

Figure S66. ^{13}C NMR of product **2-23**, related Table 2

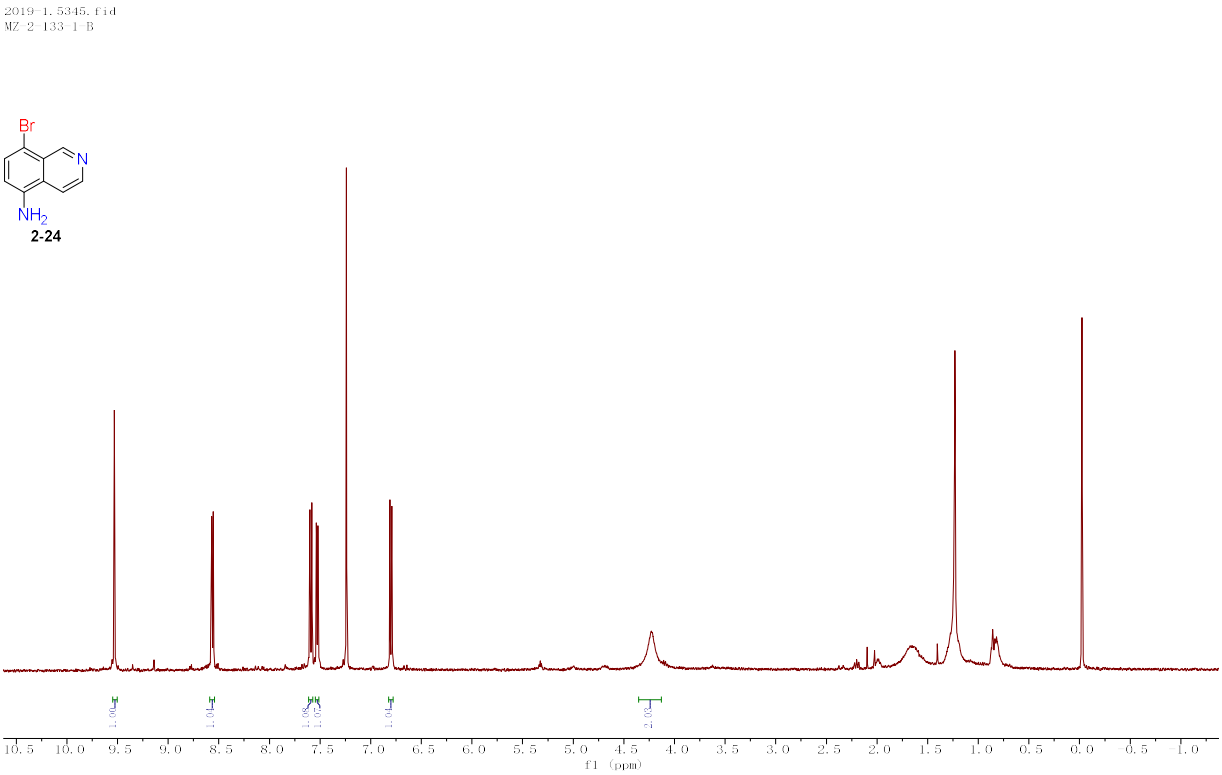

Figure S67. ^{1}H NMR of product **2-24**, related Table 2

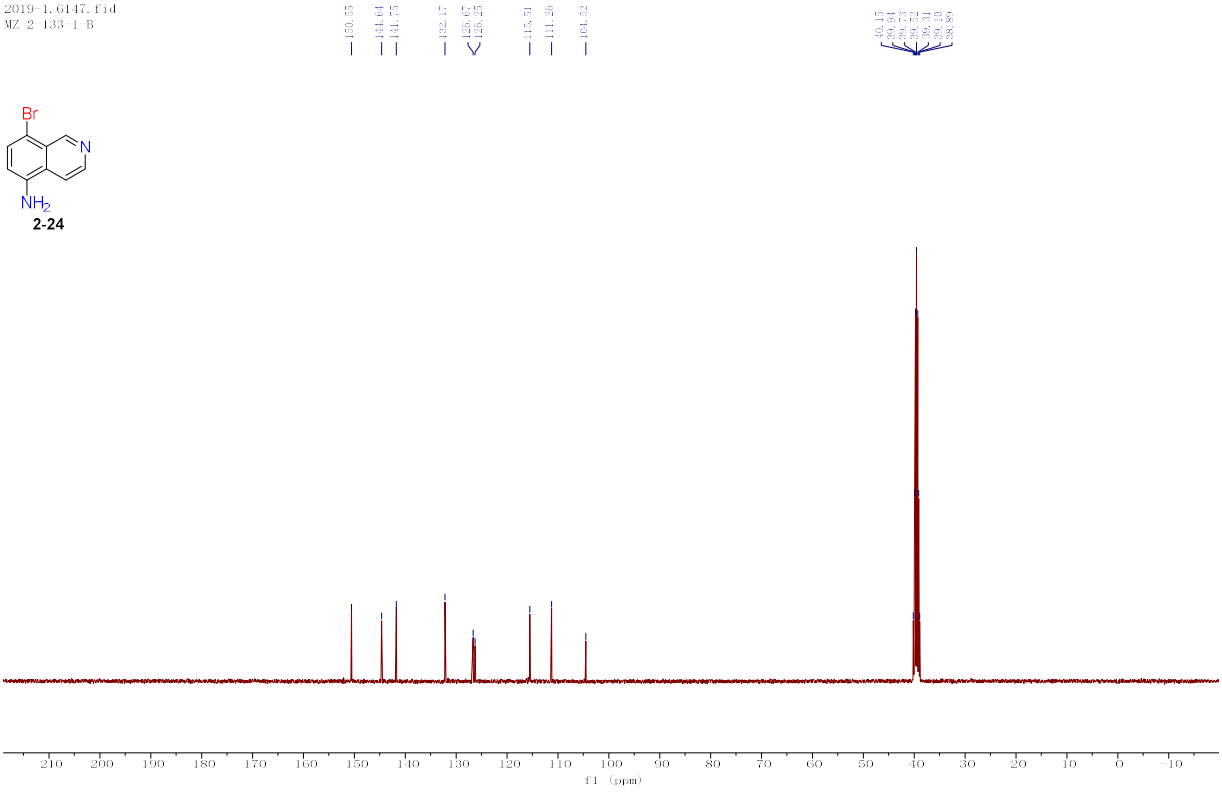

Figure S68. ^{13}C NMR of product **2-23**, related Table 2

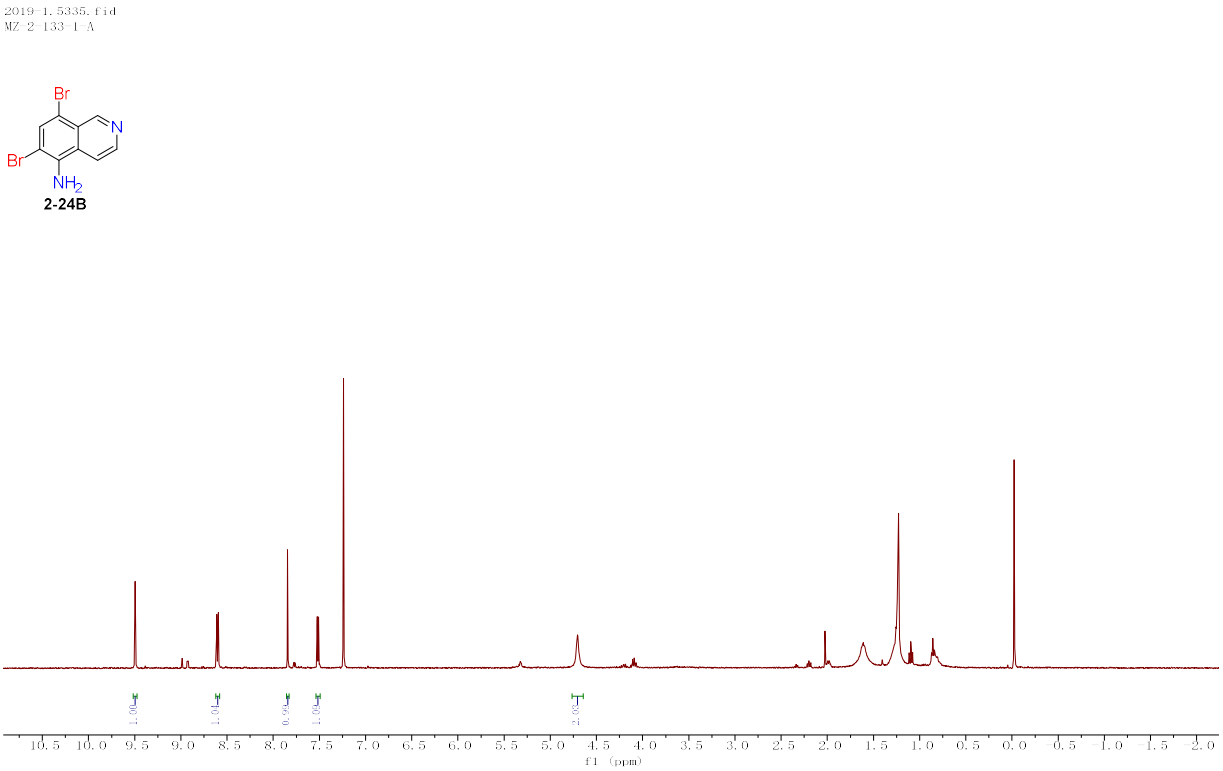

Figure S69. ^{1}H NMR of product **2-24B**, related Table 2

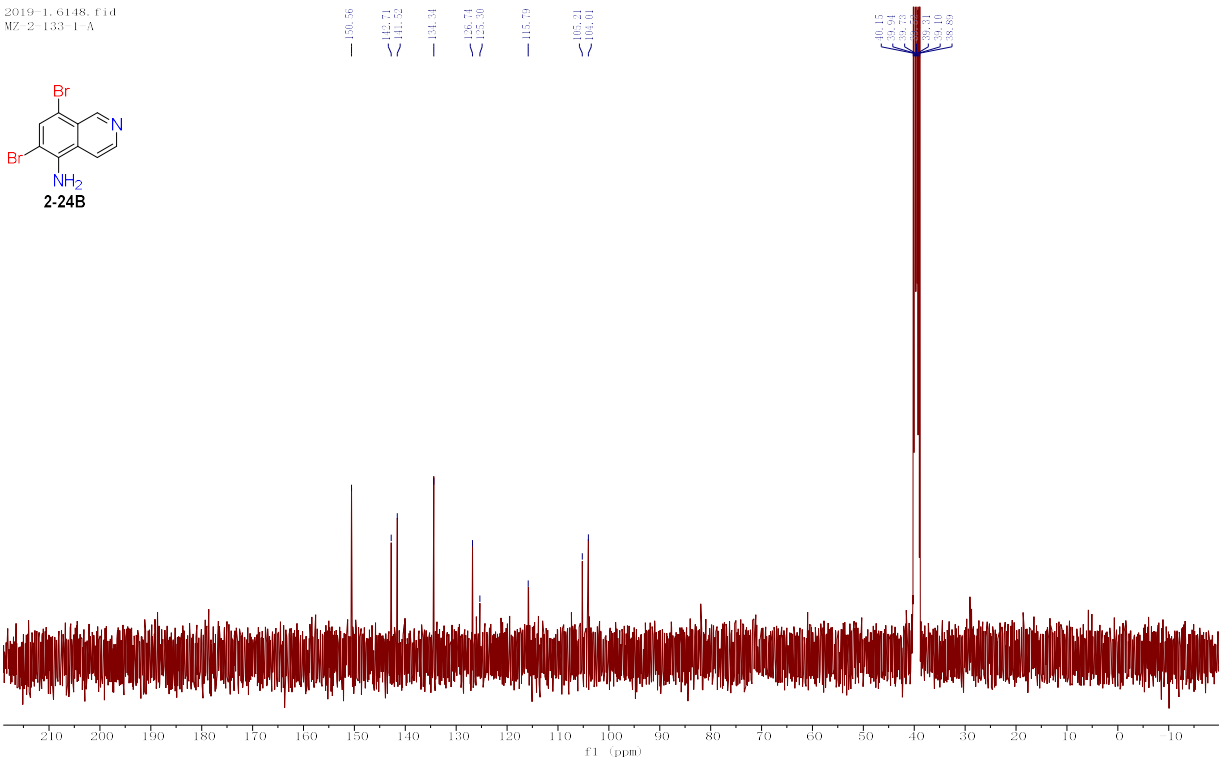

Figure S70. ^{13}C NMR of product **2-24B**, related Table 2

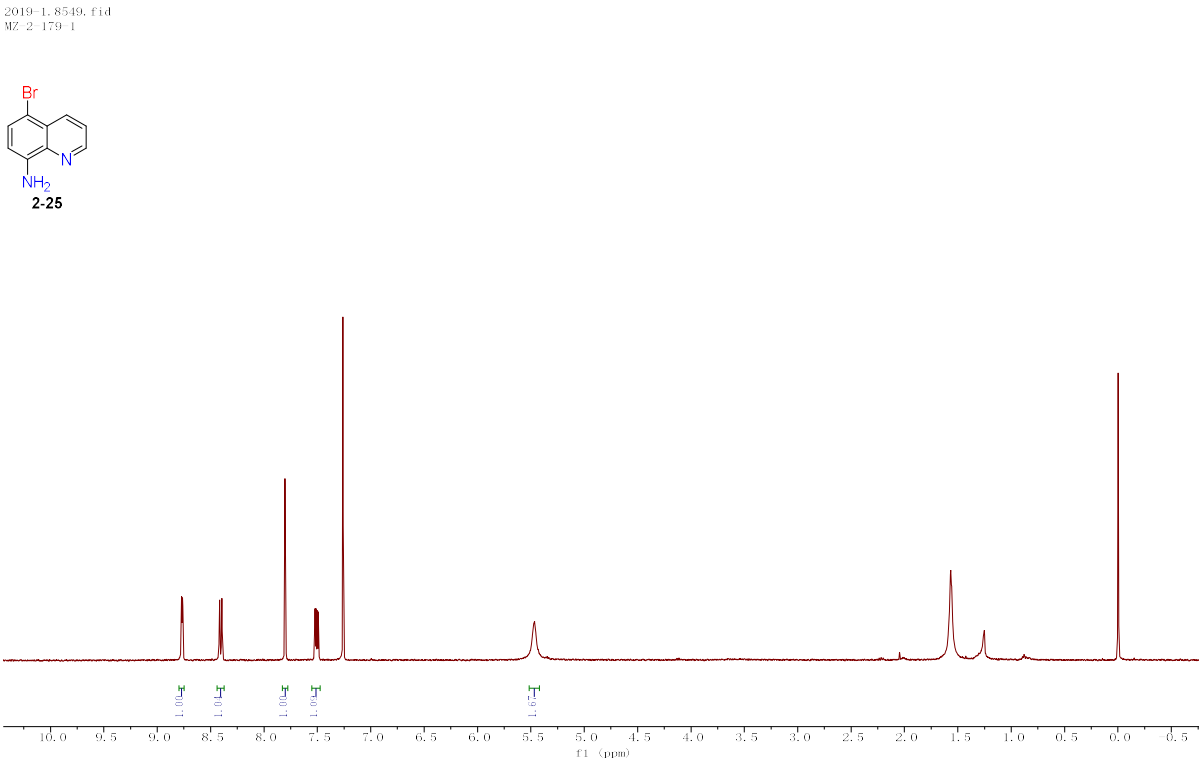

Figure S71. ^{1}H NMR of product **2-25**, related Table 2

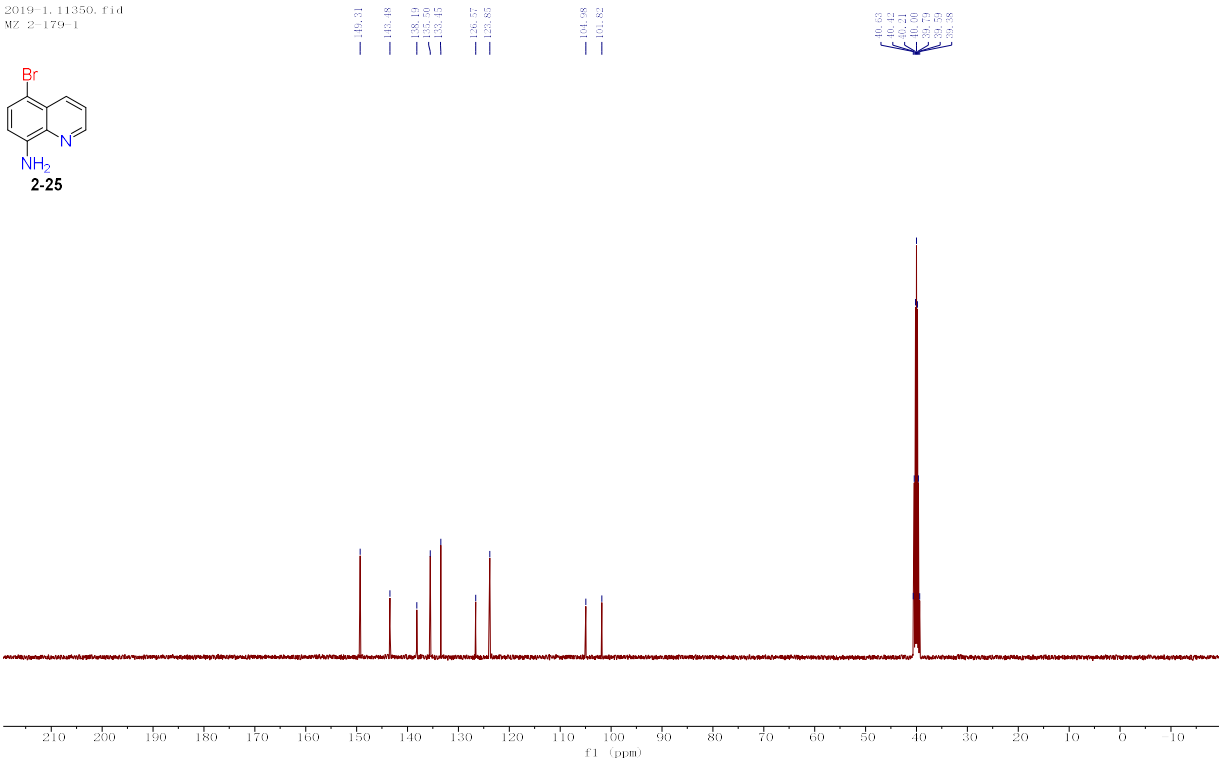

Figure S72. ^{13}C NMR of product **2-25**, related Table 2

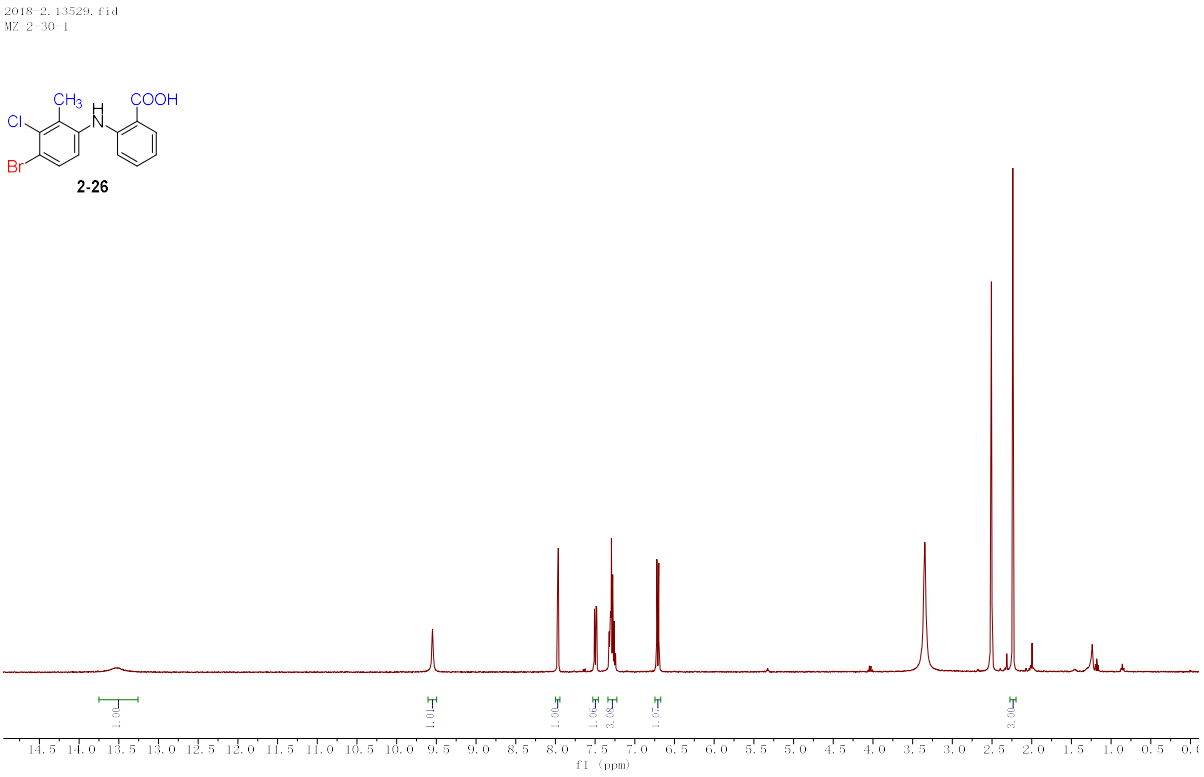

Figure S73. ^{1}H NMR of product **2-26**, related Table 2

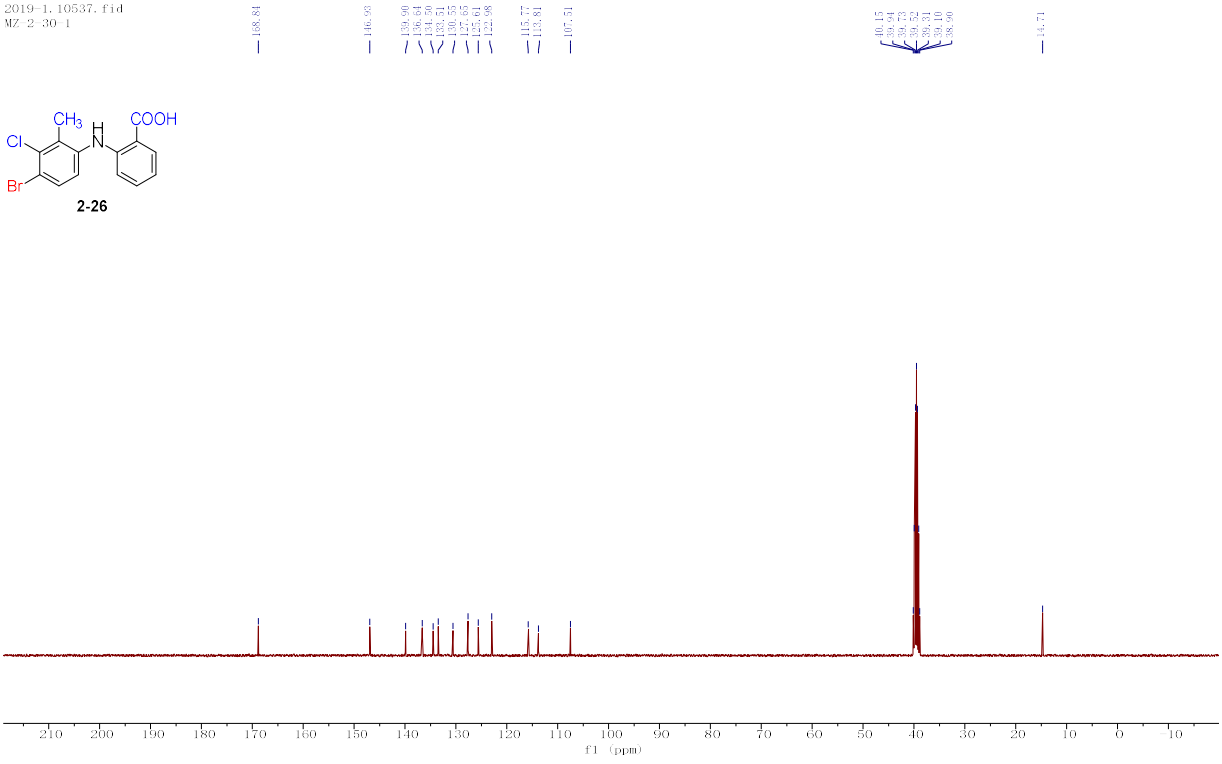

Figure S74. ^{13}C NMR of product **2-26**, related Table 2

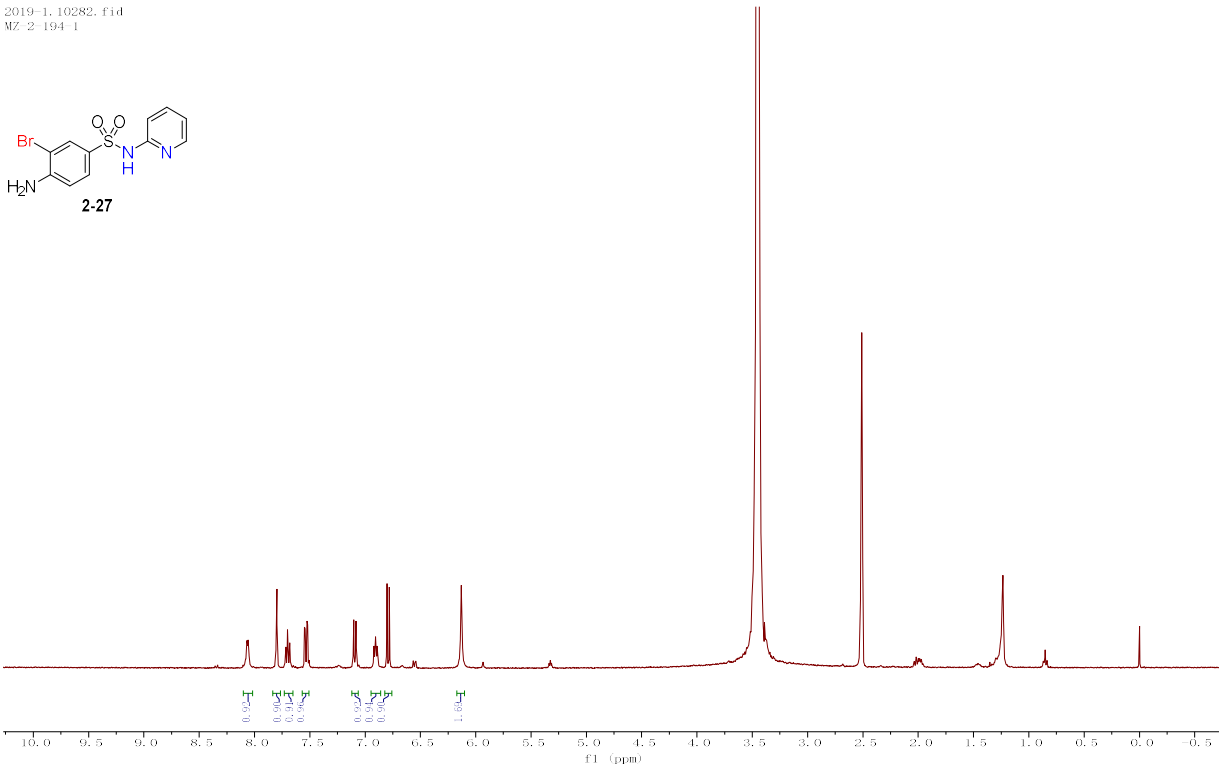

Figure S75. ^{1}H NMR of product **2-27**, related Table 2

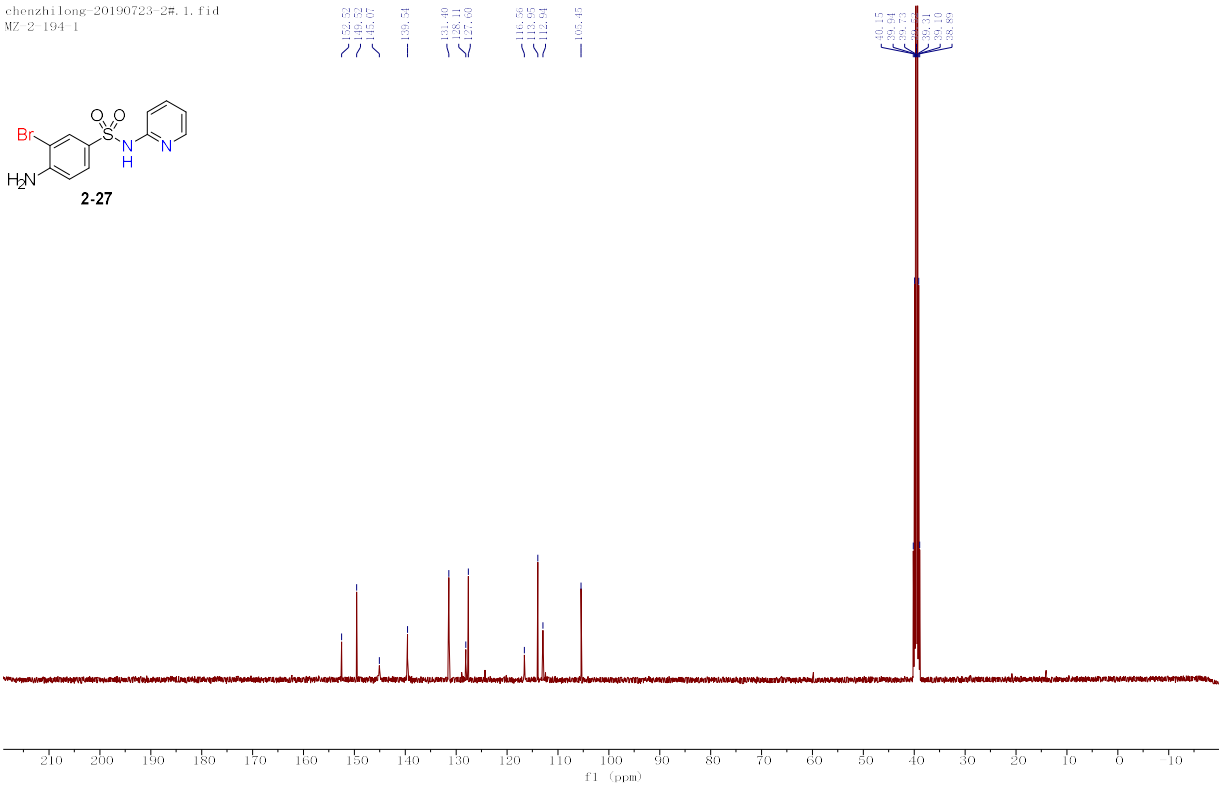

Figure S76. ^{13}C NMR of product **2-27**, related Table 2

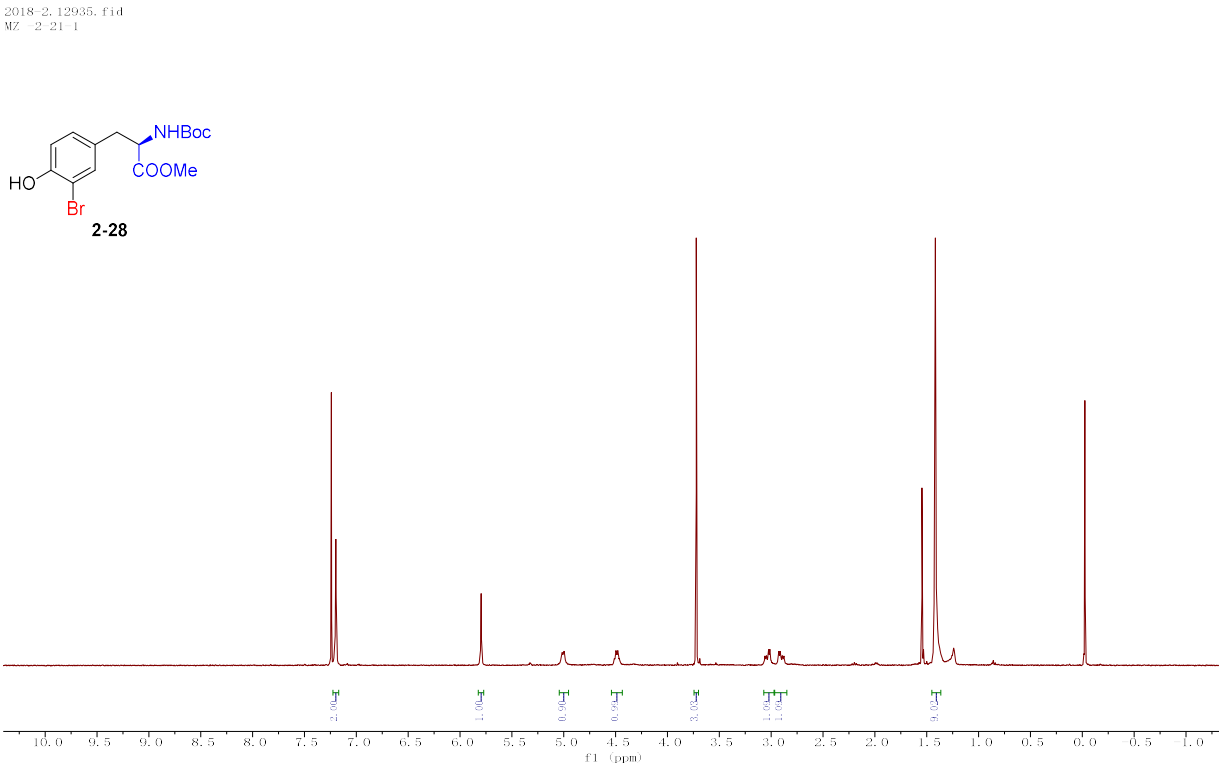

Figure S77. ^{1}H NMR of product **2-28**, related Table 2

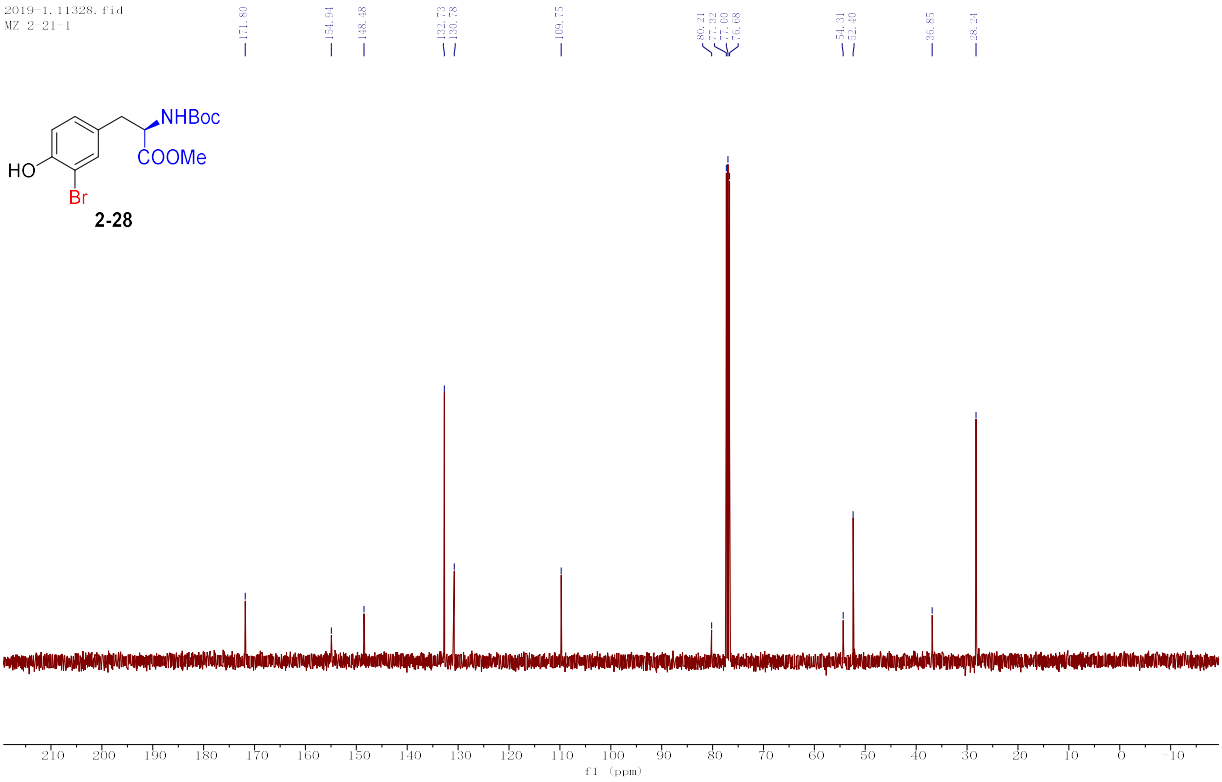

Figure S78. ^{13}C NMR of product **2-28**, related Table 2

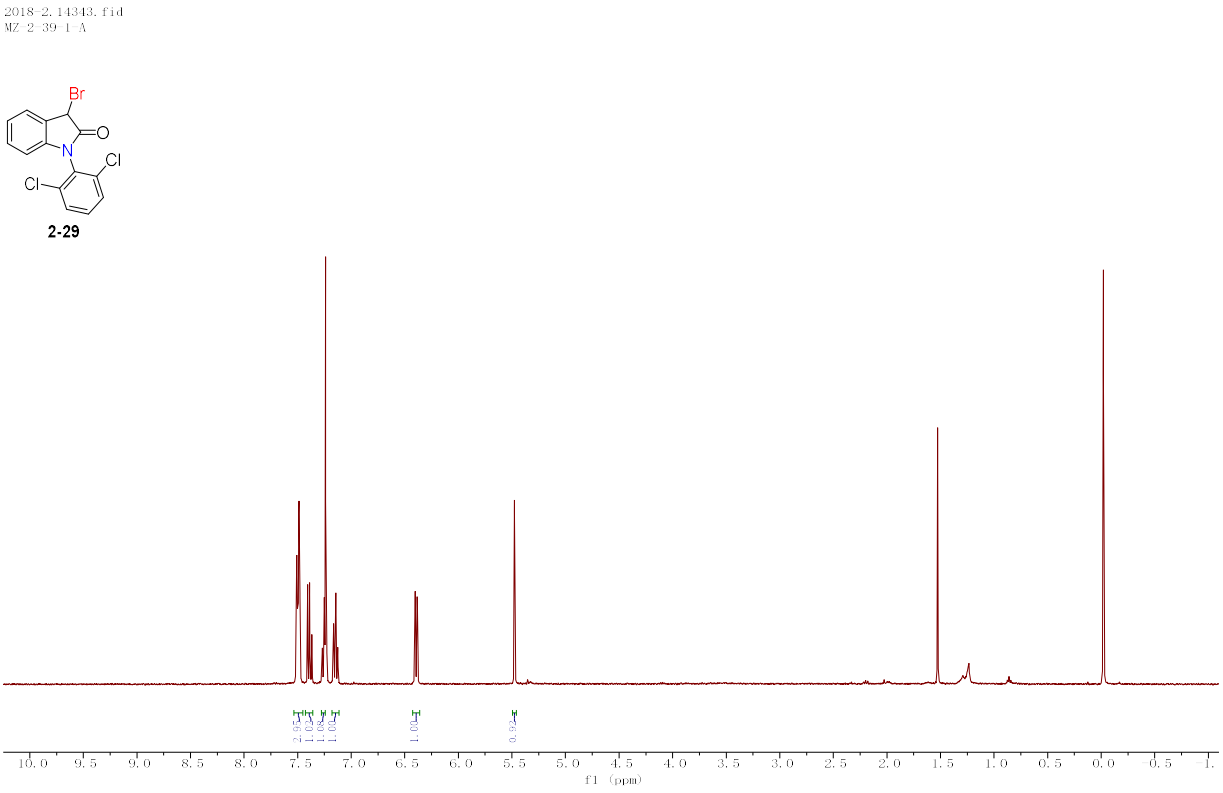

Figure S79. ^{1}H NMR of product **2-29**, related Table 2

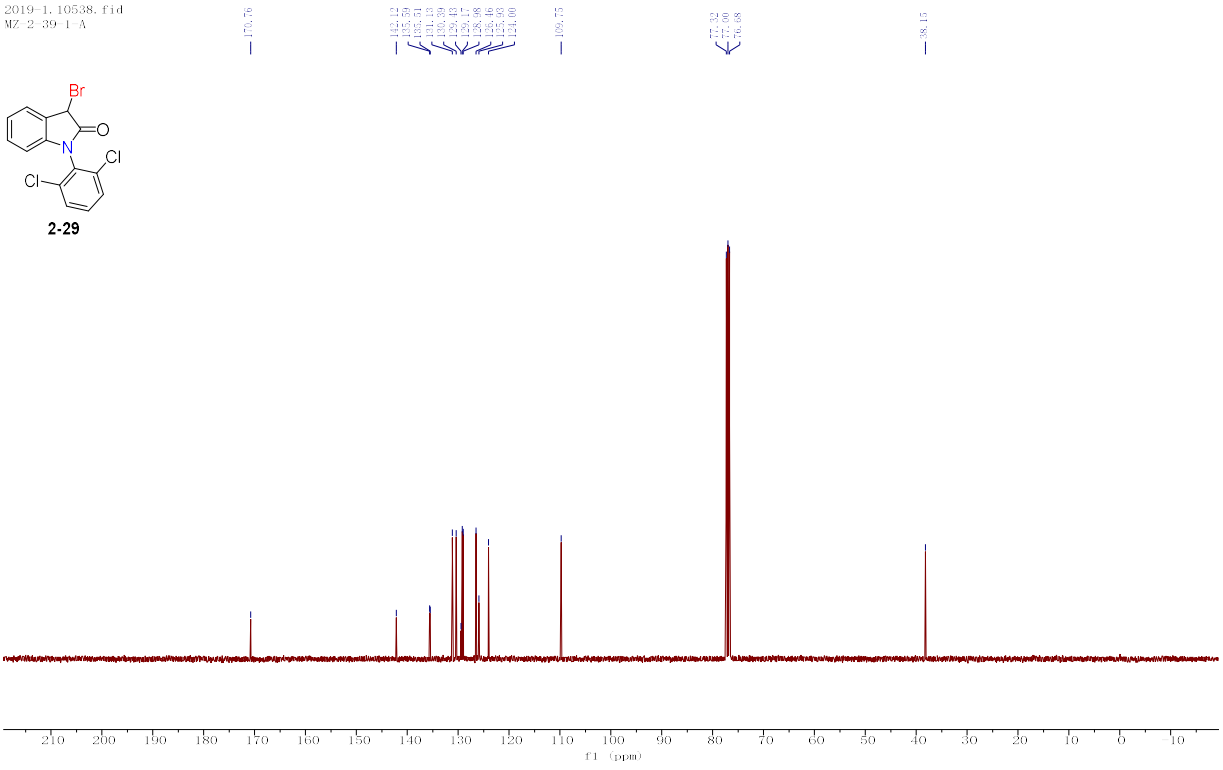

Figure S80. ^{13}C NMR of product **2-29**, related Table 2

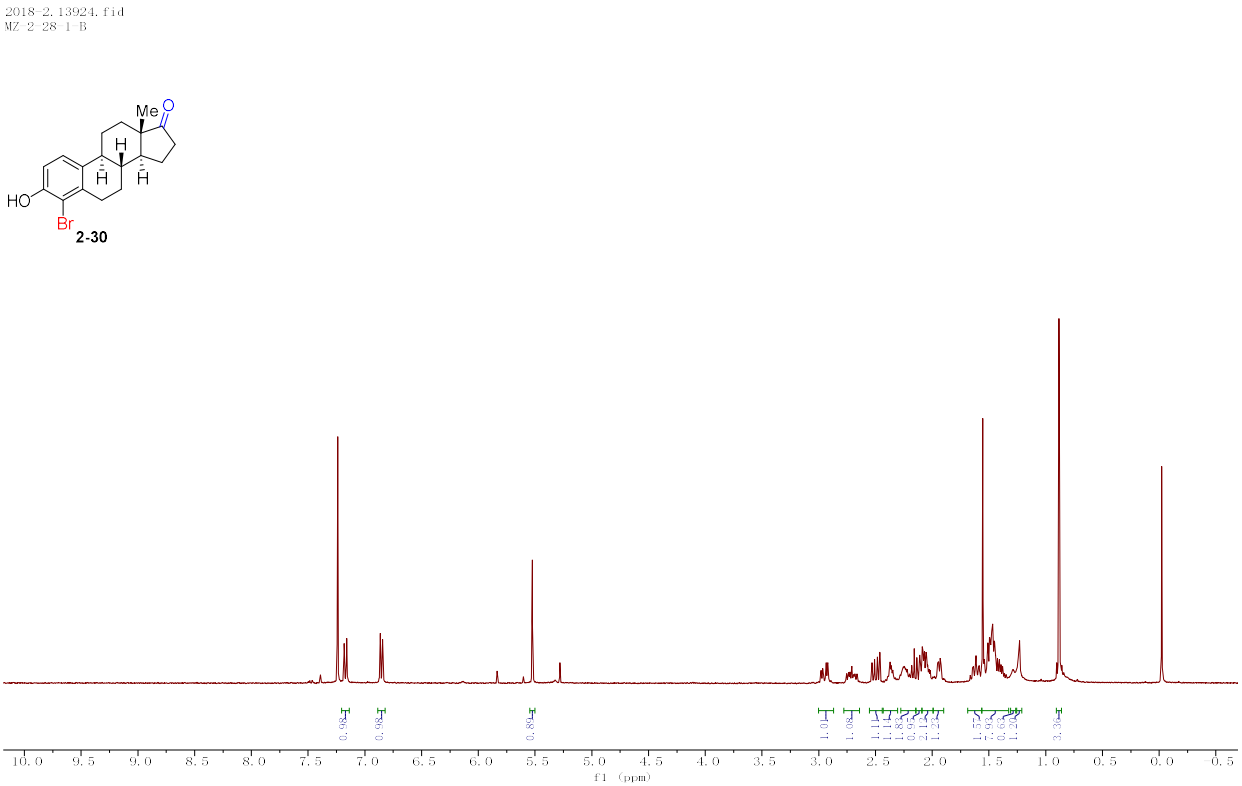

Figure S81. ^{1}H NMR of product **2-30**, related Table 2

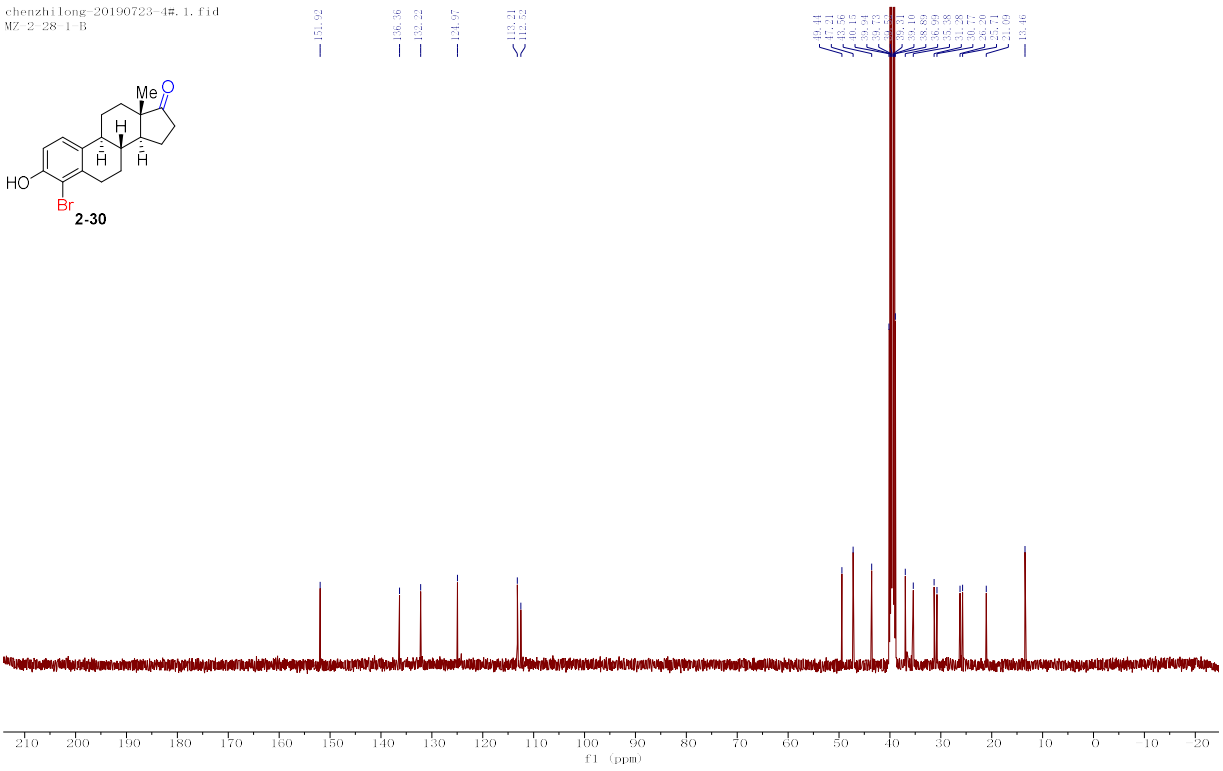

Figure S82. ^{13}C NMR of product **2-30**, related Table 2

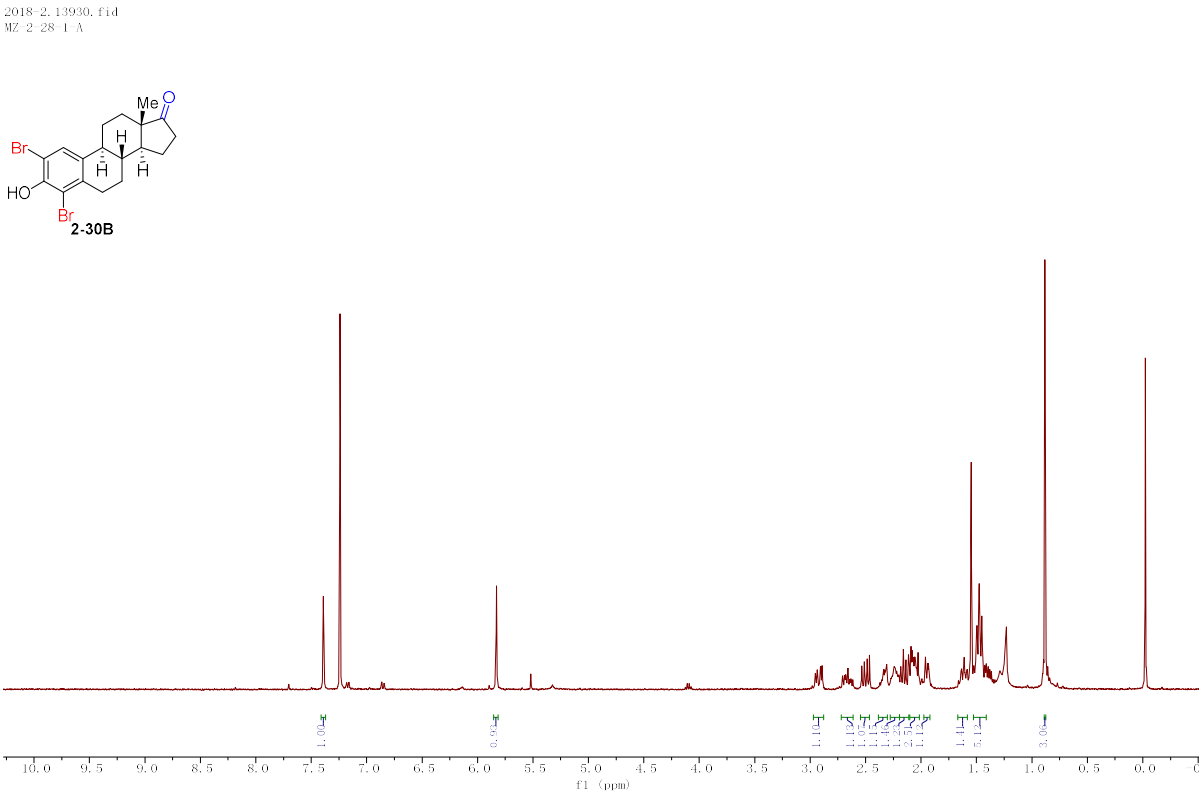

Figure S83. ^{1}H NMR of product **2-30B**, related Table 2

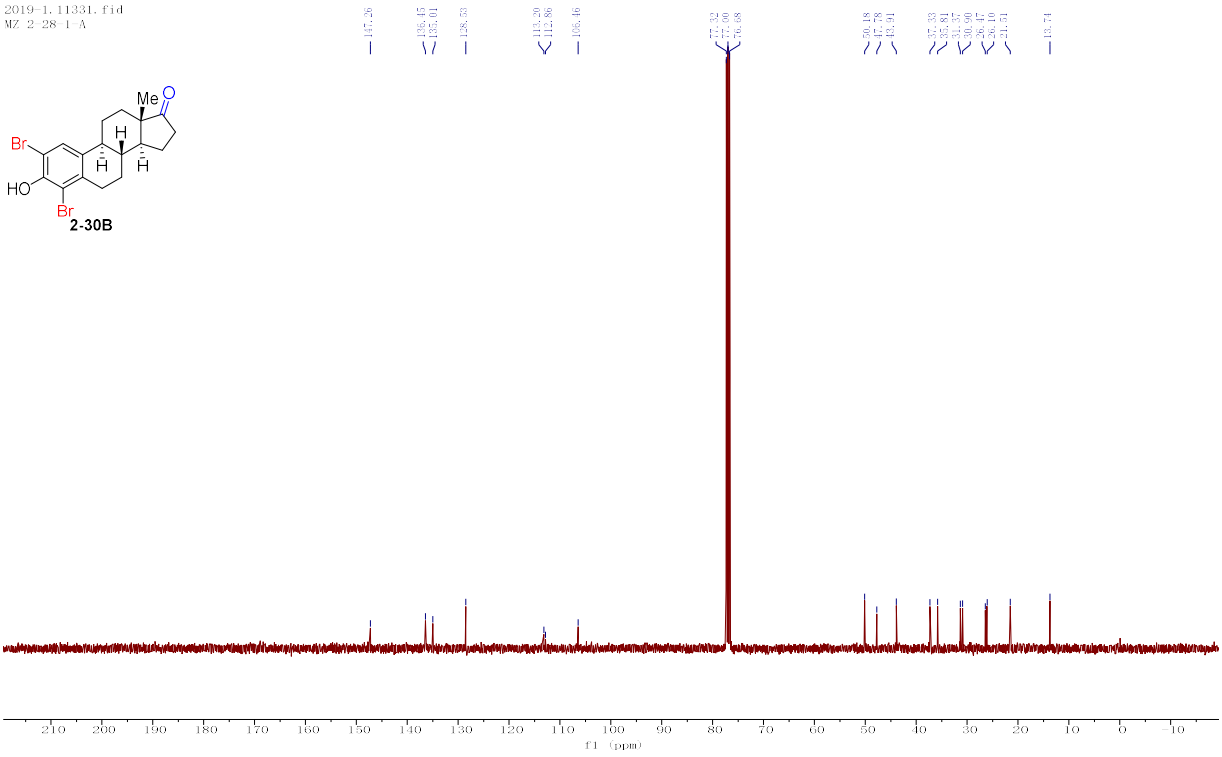

Figure S84. ^{13}C NMR of product **2-30**, related Table 2

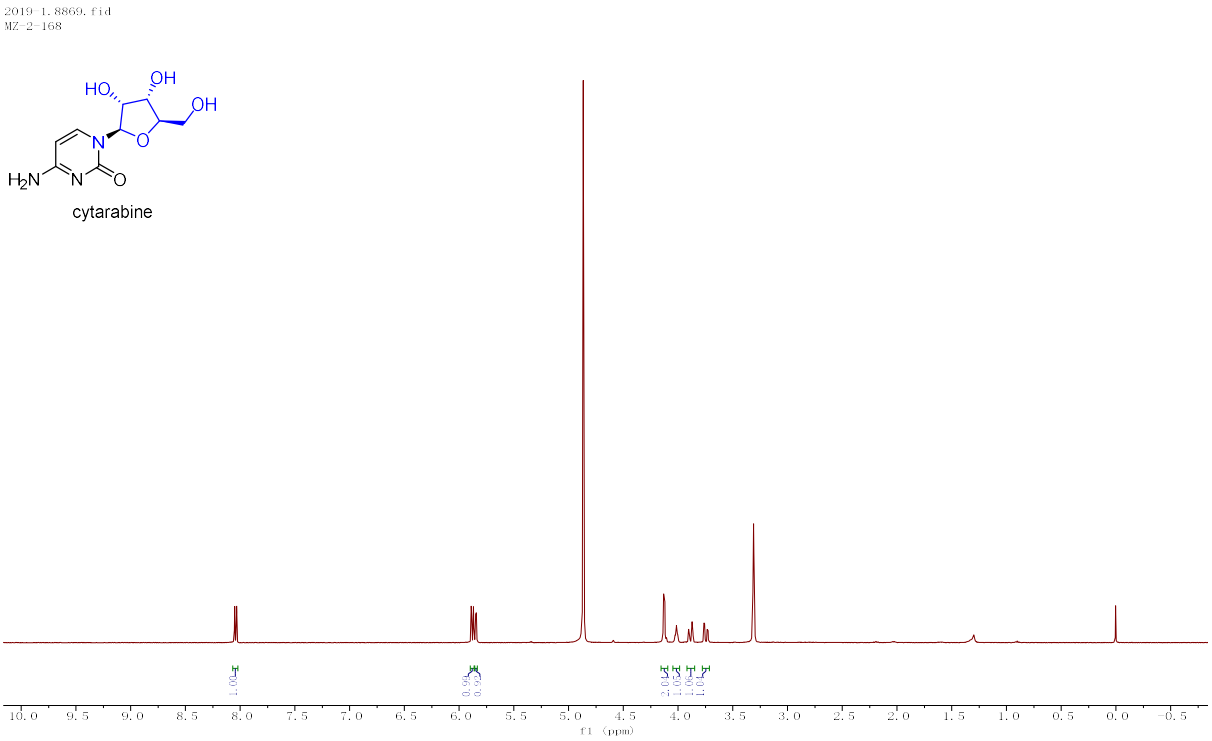

Figure S85. ^{1}H NMR of product cytarabine, related Table 2

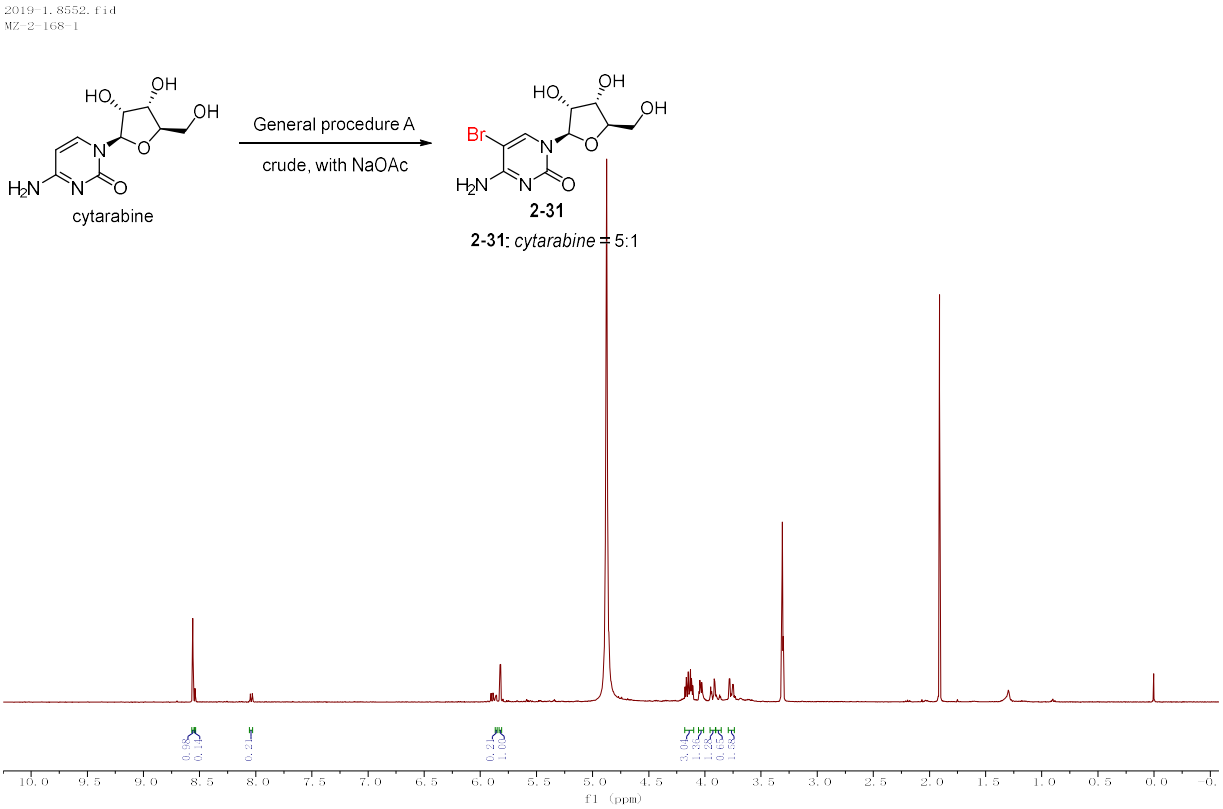

Figure S86. ^{1}H NMR of crude product from bromination of cytarabine, related Table 2

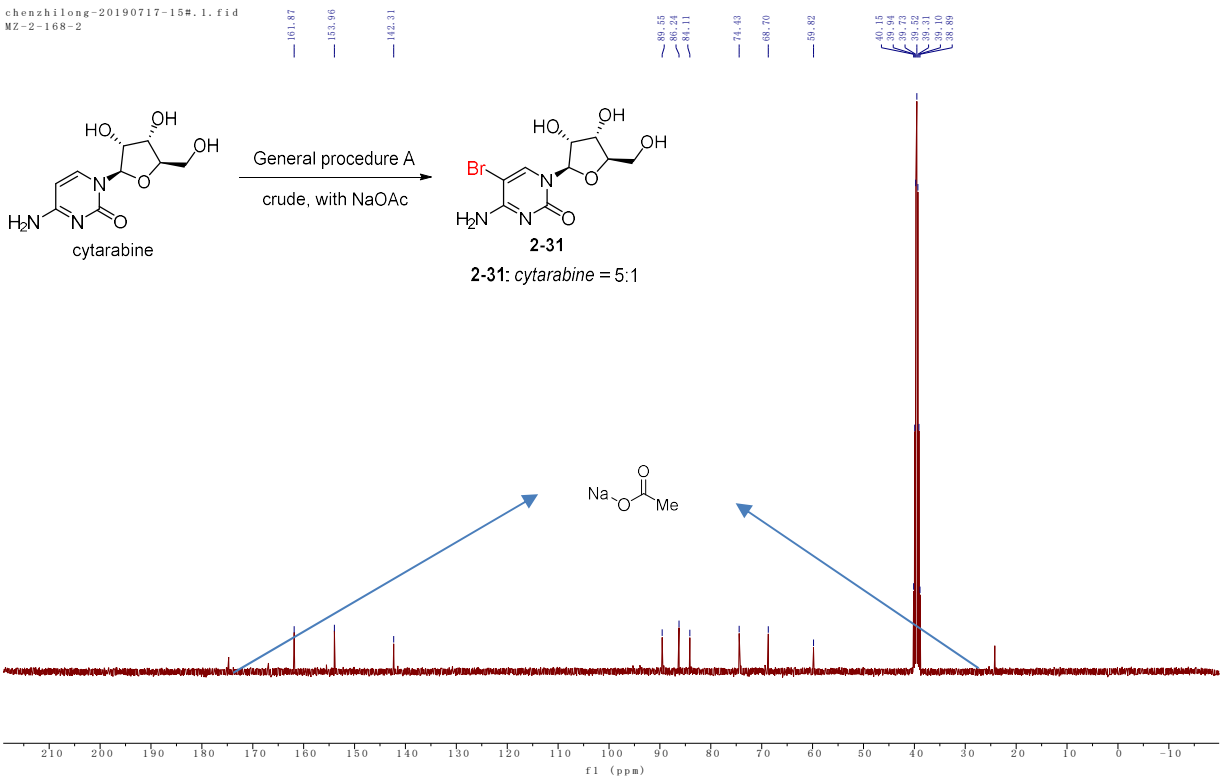

Figure S87. ^{13}C NMR of crude product from bromination of cytarabine, related Table 2

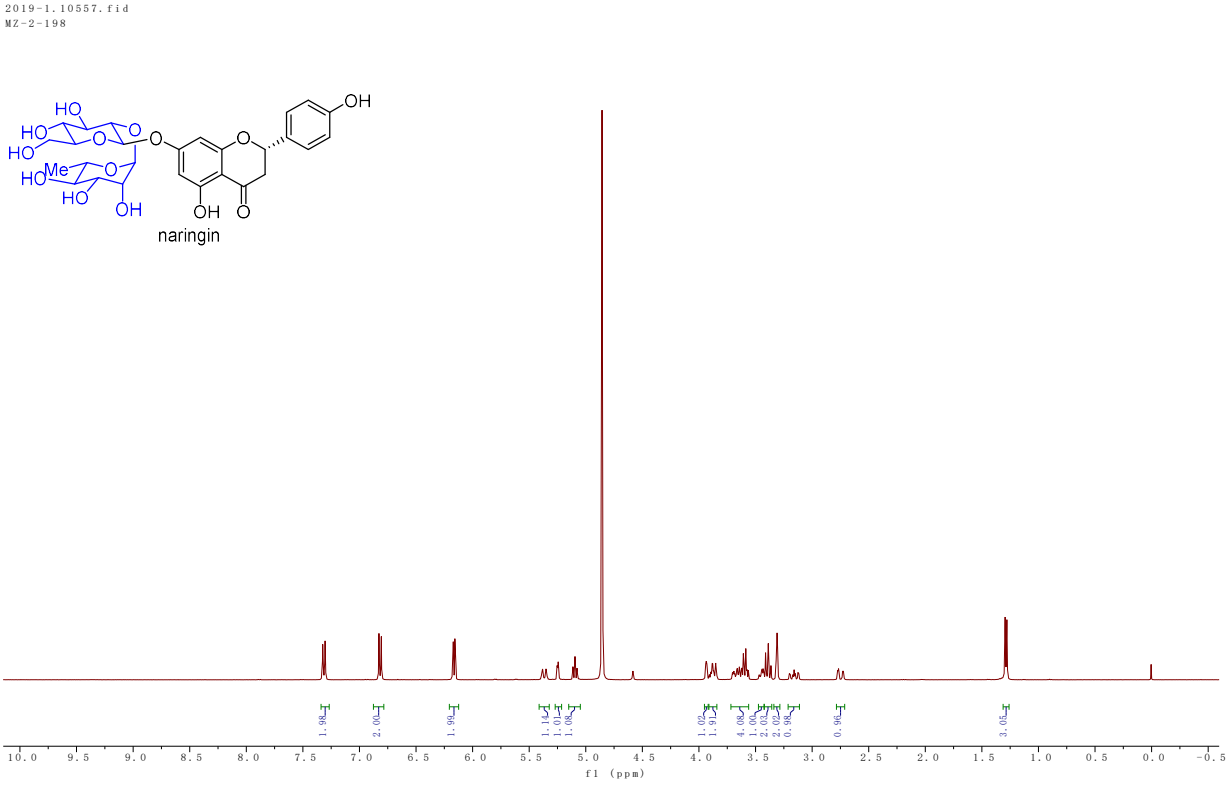

Figure S88. ^{1}H NMR of product naringin, related Table 2

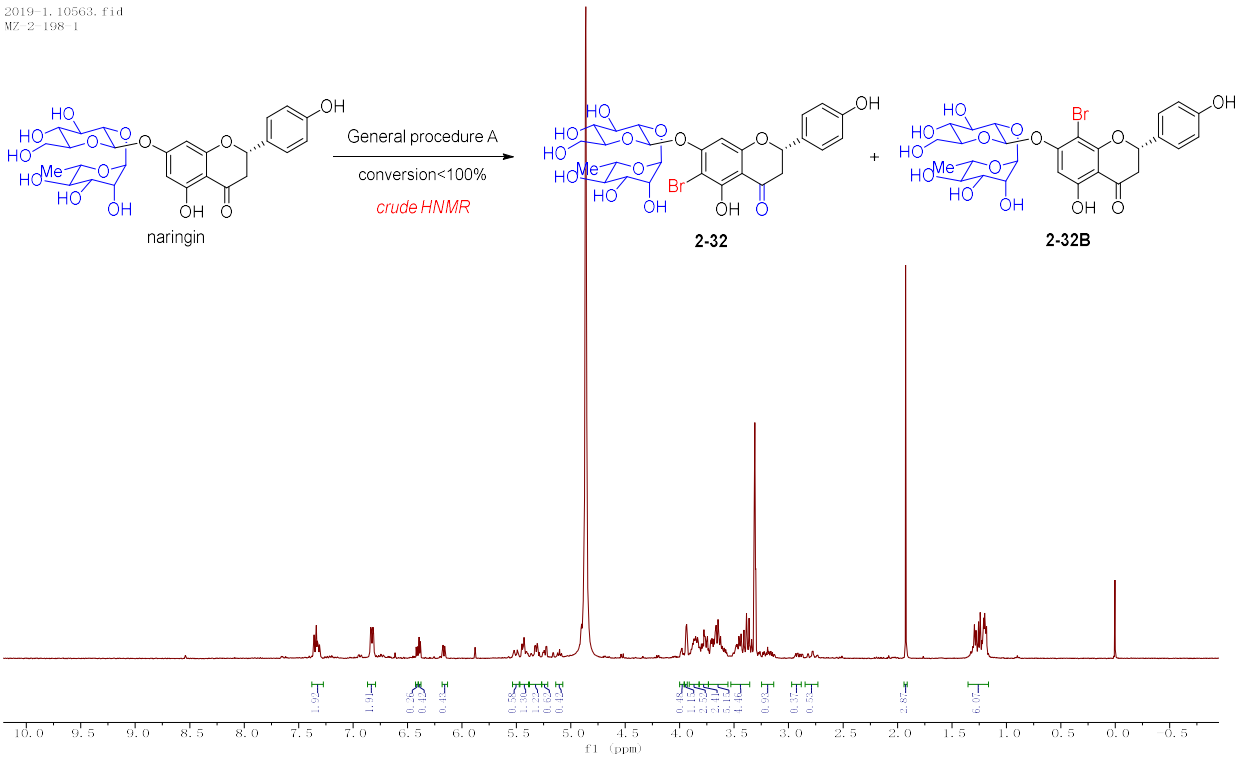

Figure S89. ^{1}H NMR of crude products from bromination of naringin, related Table 2

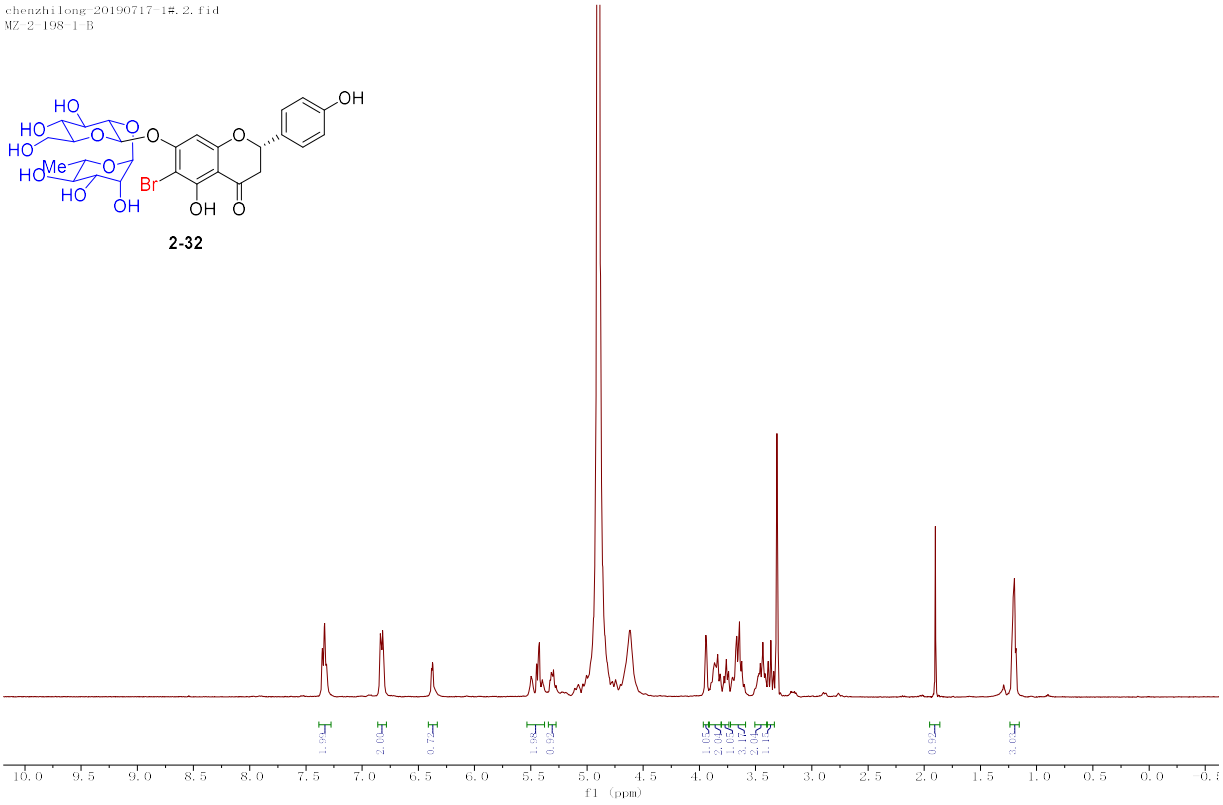

Figure S90. ^{1}H NMR of crude product **2-32**, related Table 2

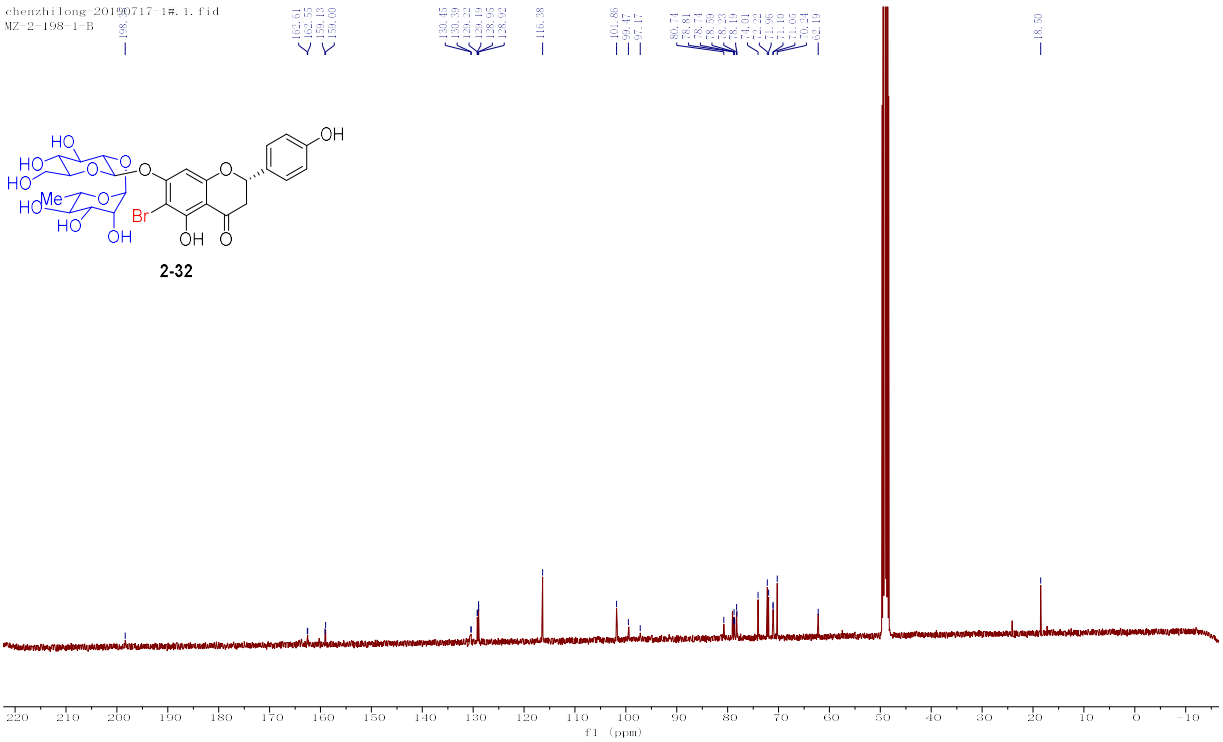

Figure S91. ^{13}C NMR of crude product **2-32**, related Table 2

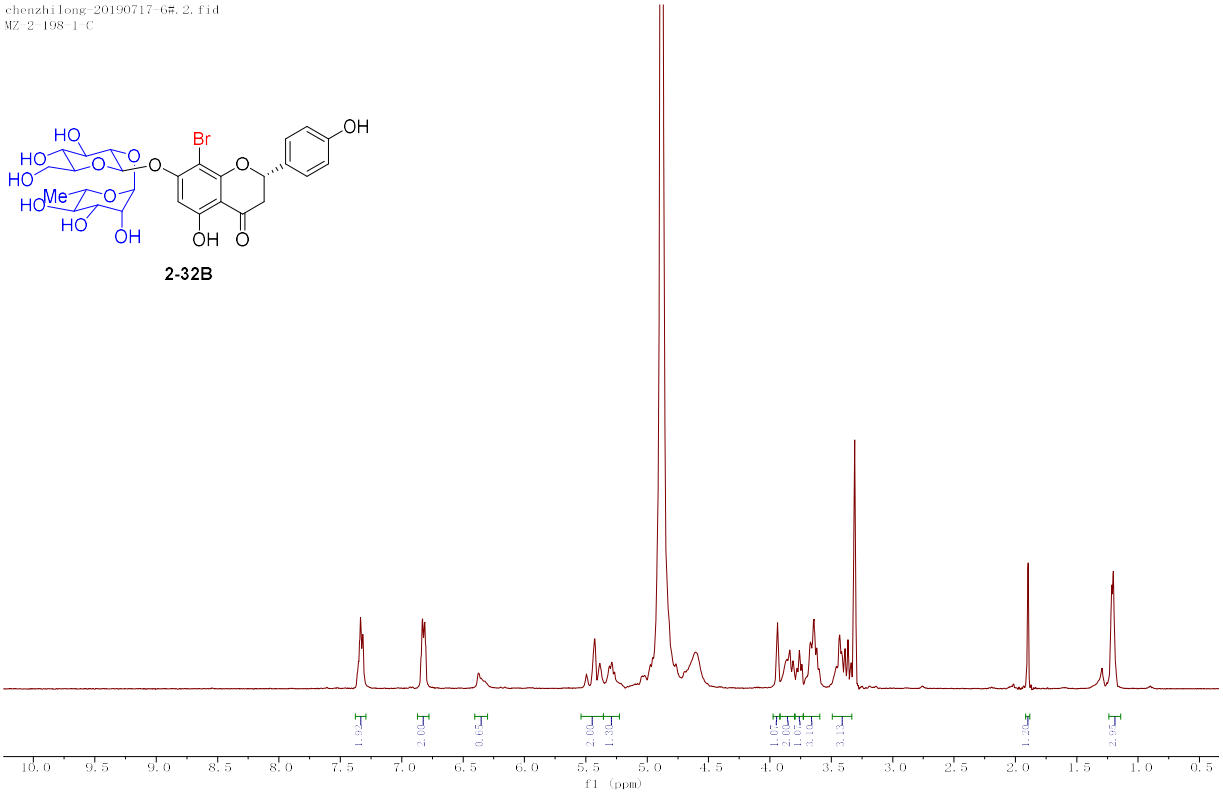

Figure S91. ^{1}H NMR of crude product **2-32B**, related Table 2

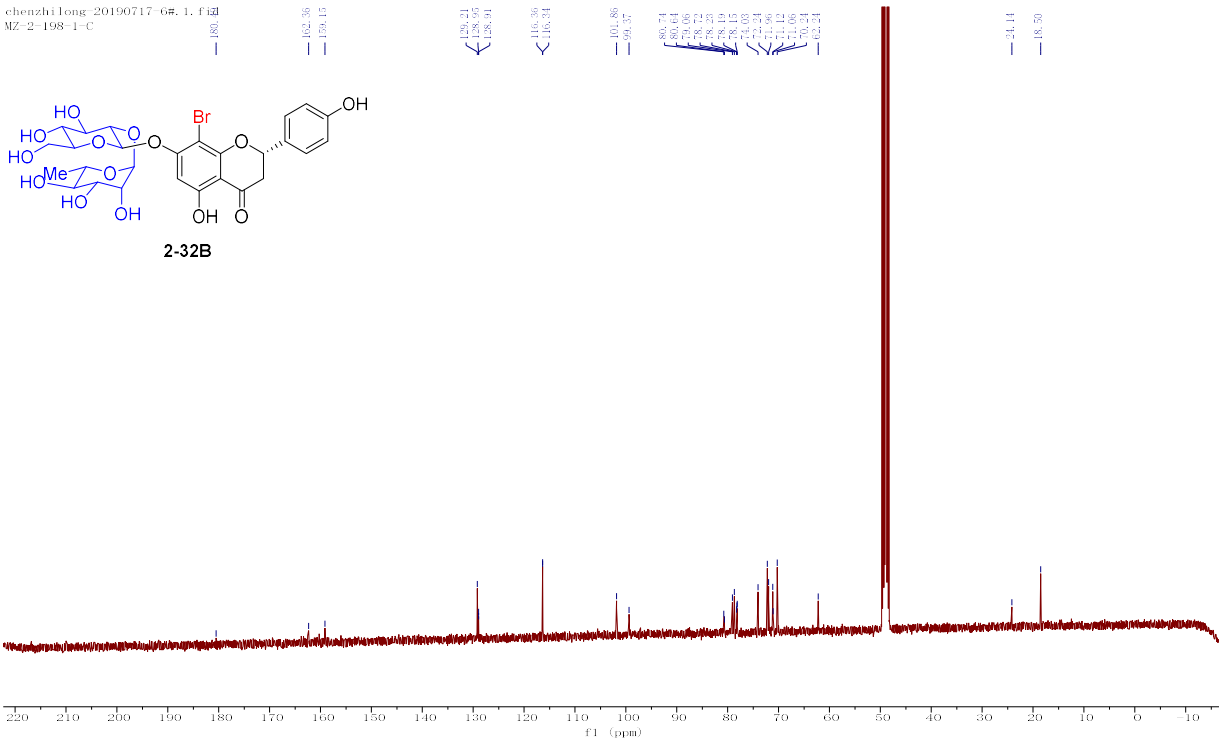

Figure S93. ^{13}C NMR of crude product **2-32B**, related Table 2

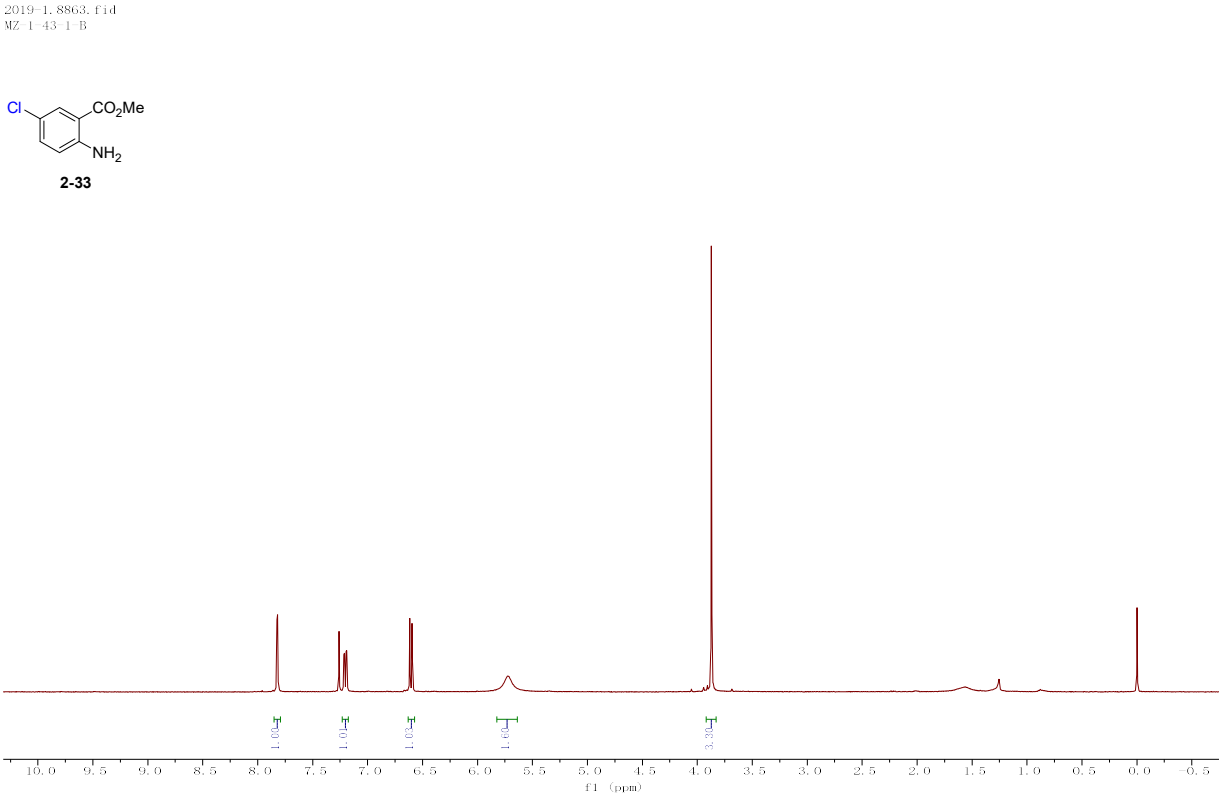

Figure S94. ^{1}H NMR of crude product **2-33**, related Table 3

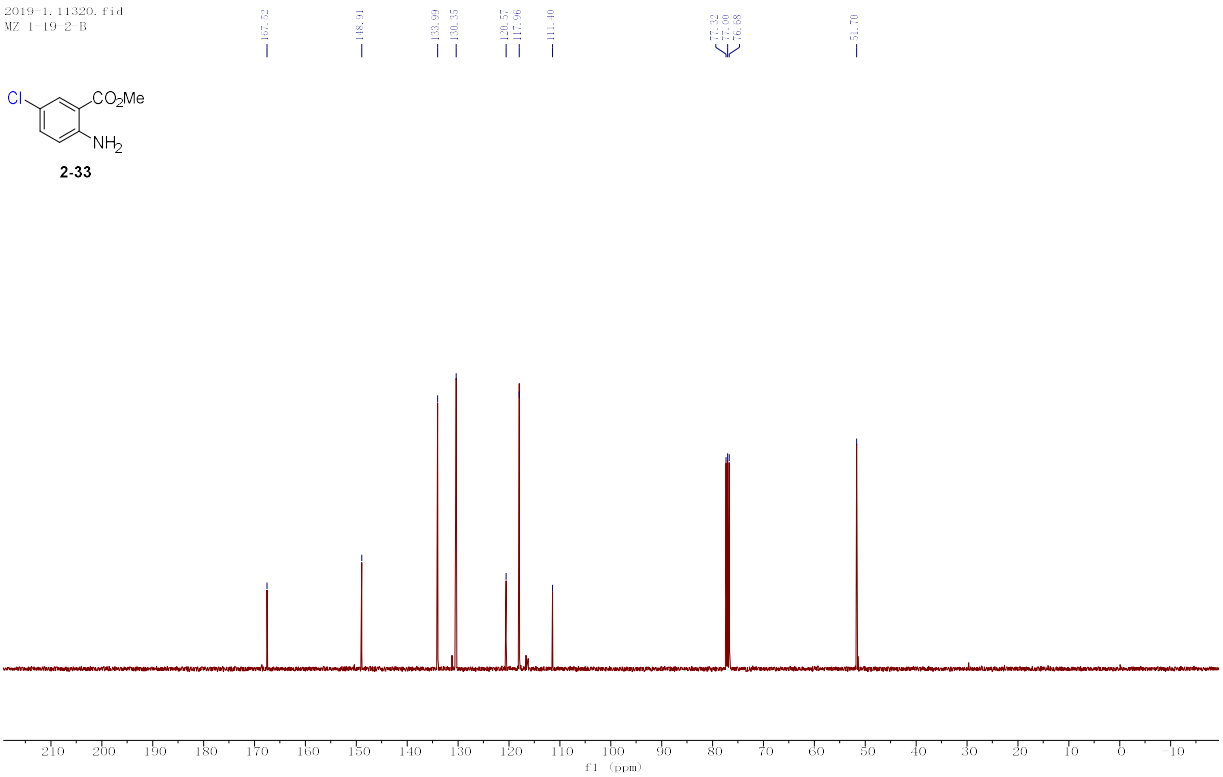

Figure S95. ^{13}C NMR of crude product **2-33**, related Table 3

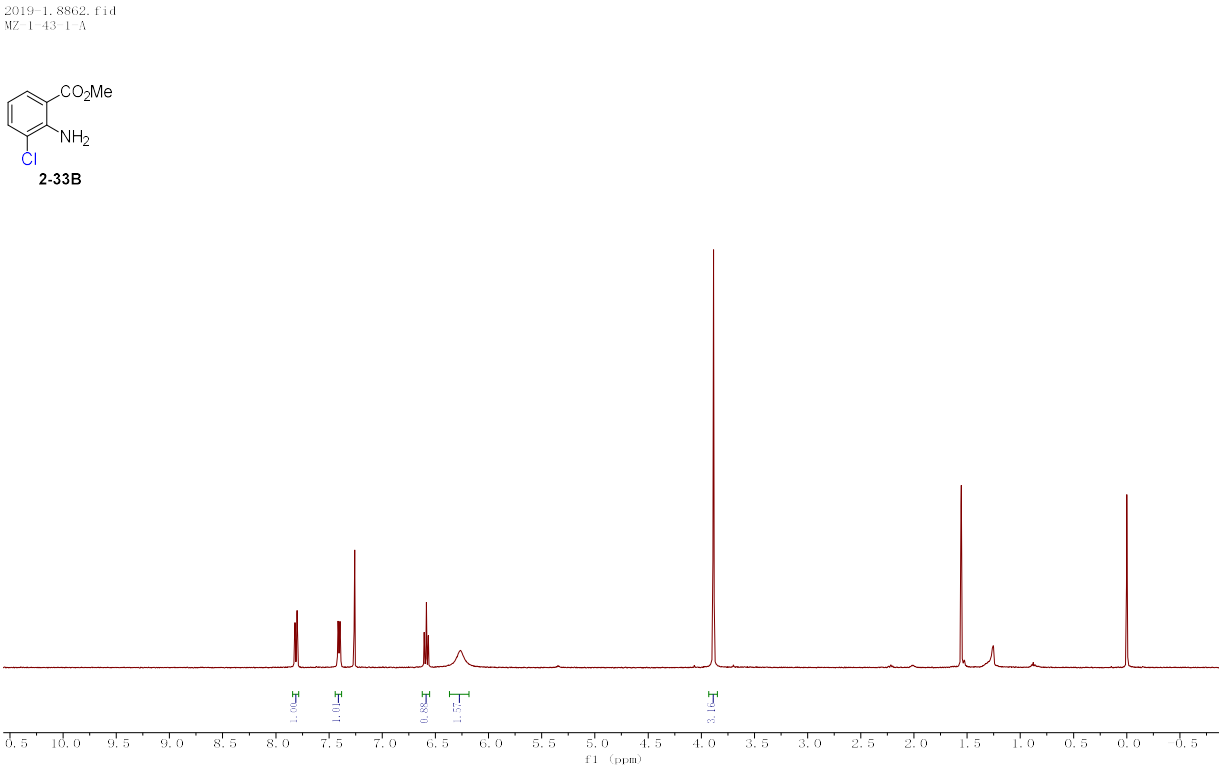

Figure S96. ^{1}H NMR of crude product **2-33B**, related Table 3

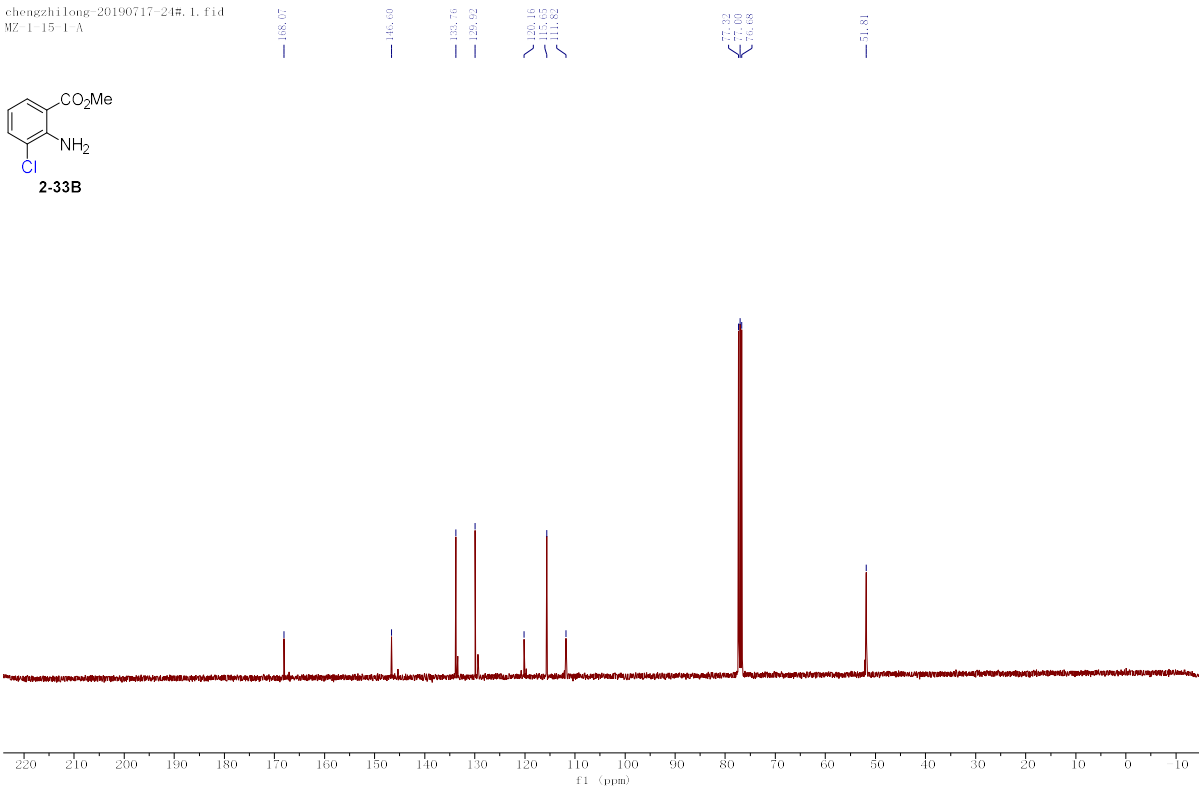

Figure S97. ^{13}C NMR of crude product **2-33B**, related Table 3

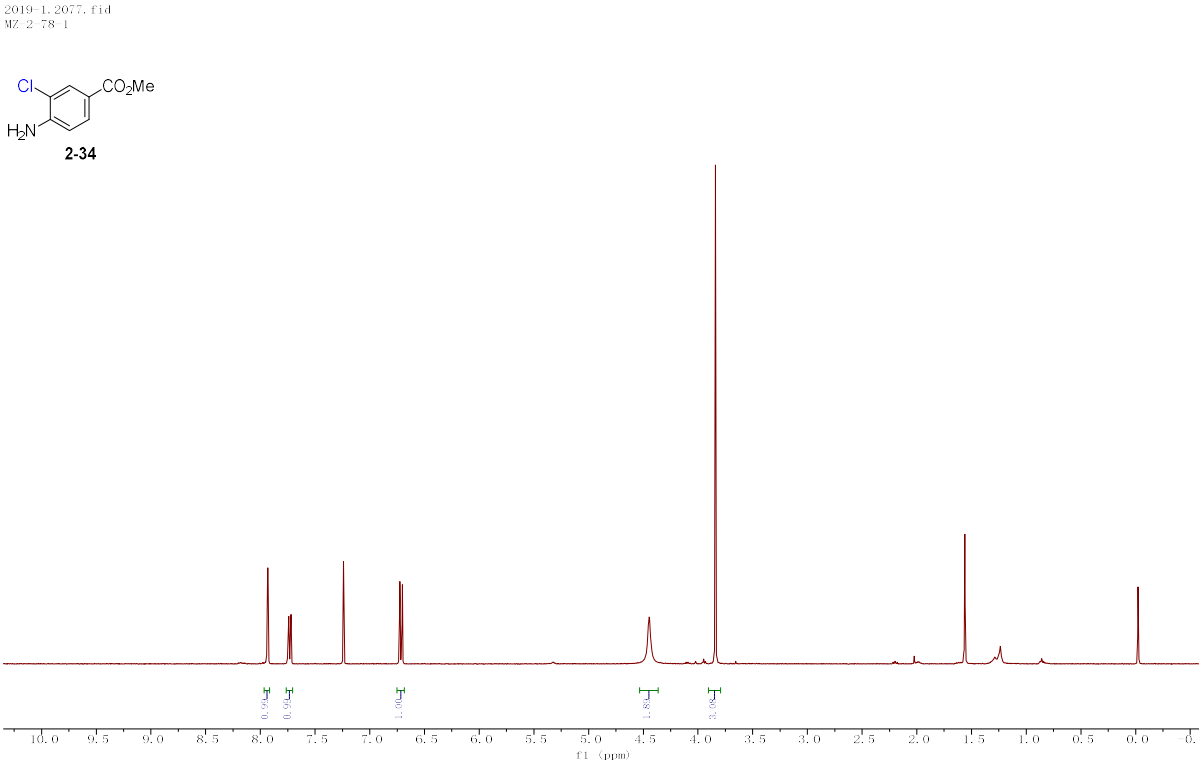

Figure S98. ^{1}H NMR of crude product **2-34**, related Table 3

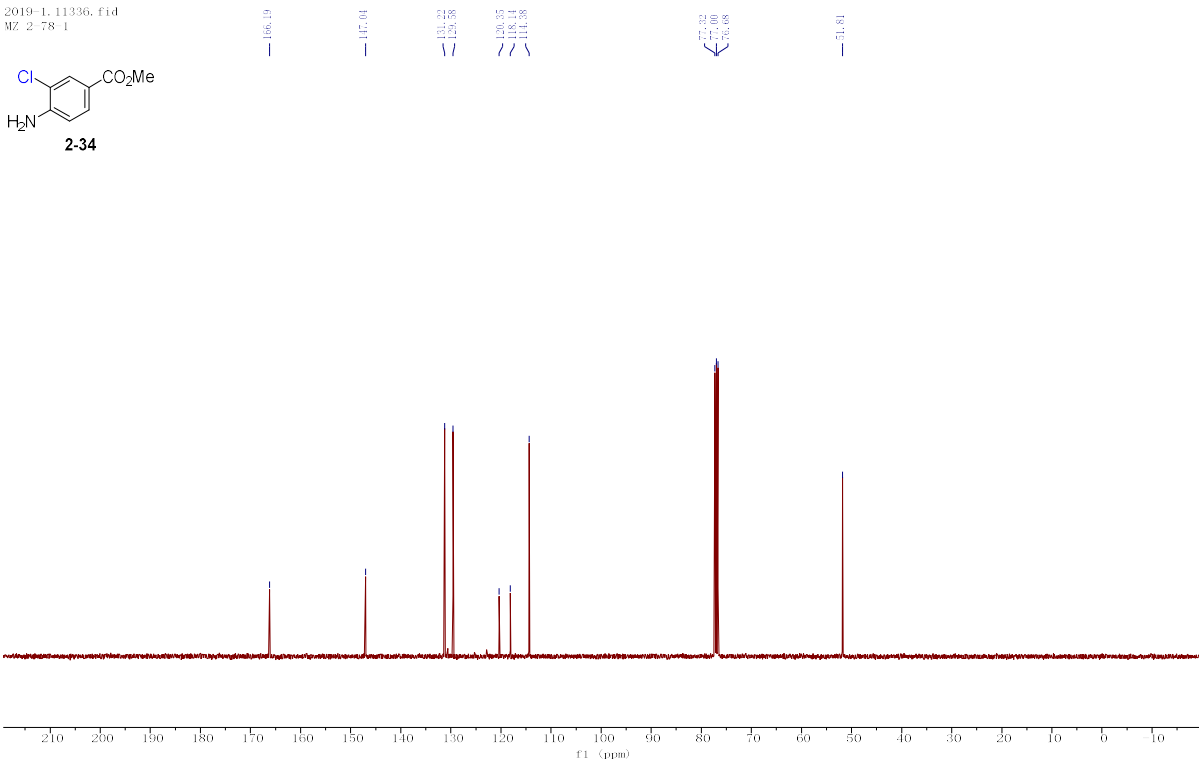

Figure S99. ^{13}C NMR of crude product **2-34**, related Table 3

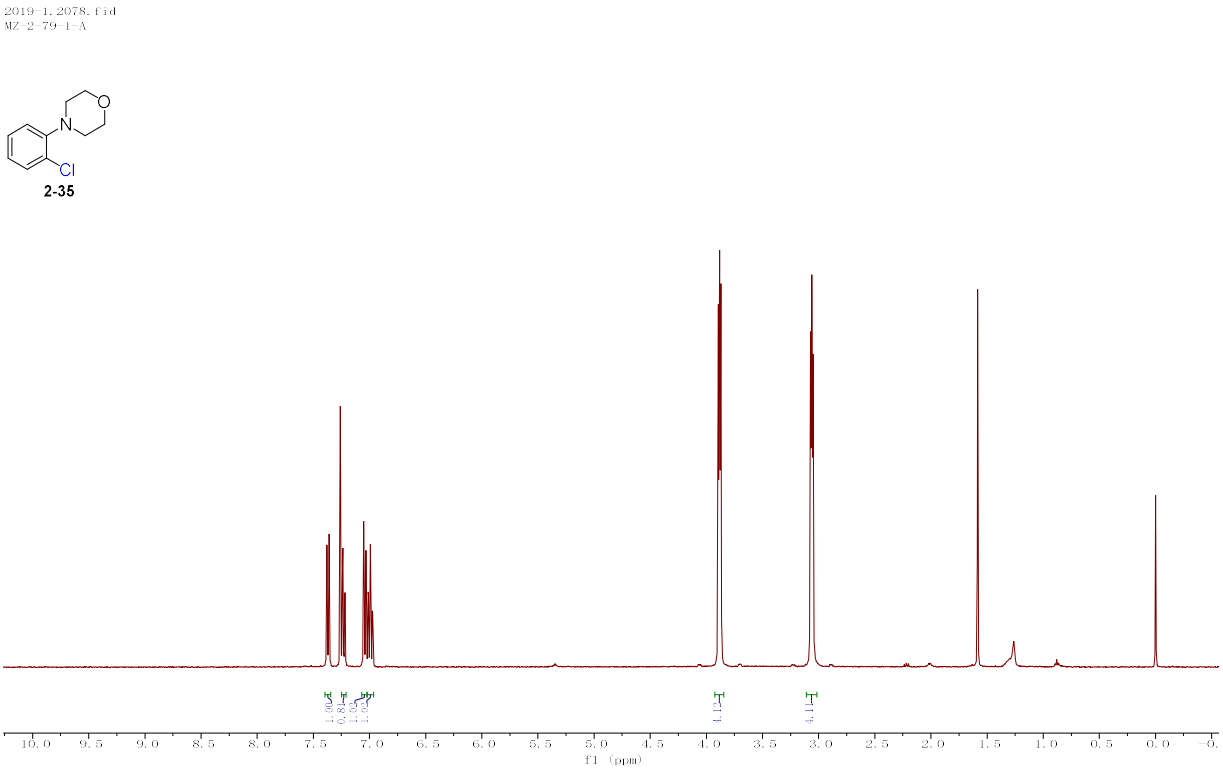

Figure S100. ^{1}H NMR of crude product **2-35**, related Table 3

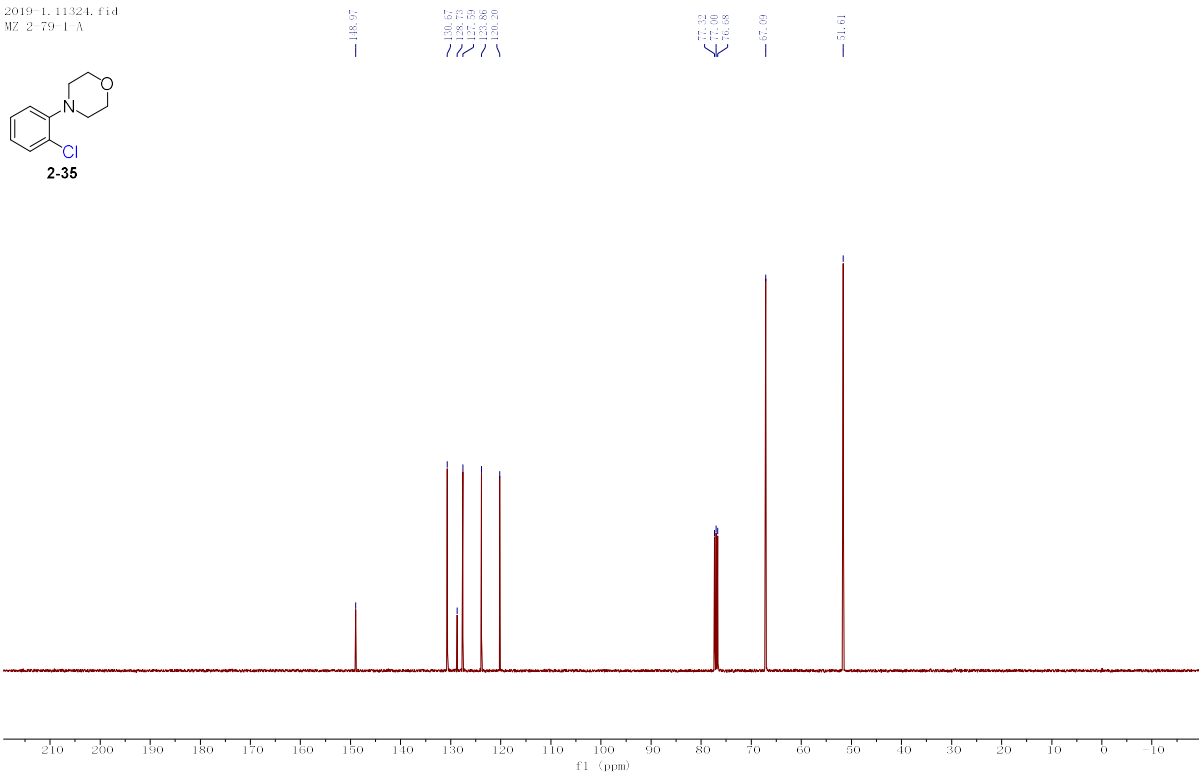

Figure S101. ^{13}C NMR of crude product **2-35**, related Table 3

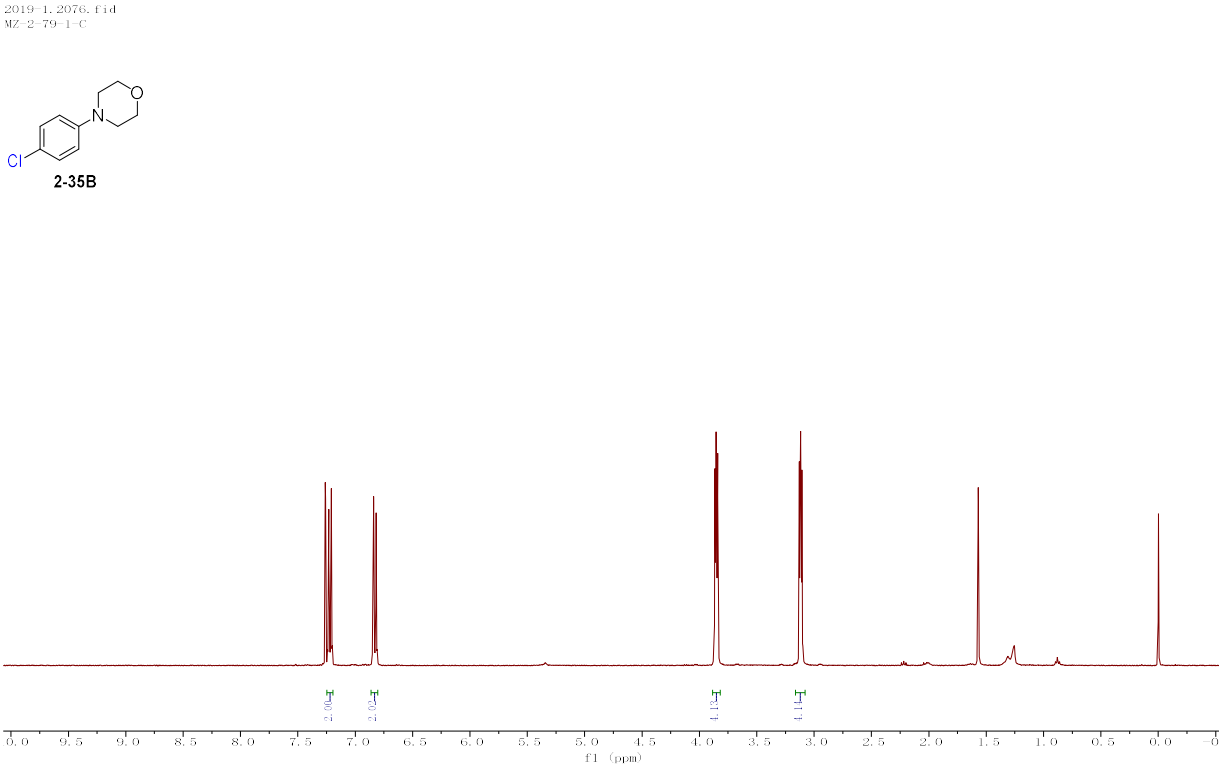

Figure S102. ^{1}H NMR of crude product **2-35B**, related Table 3

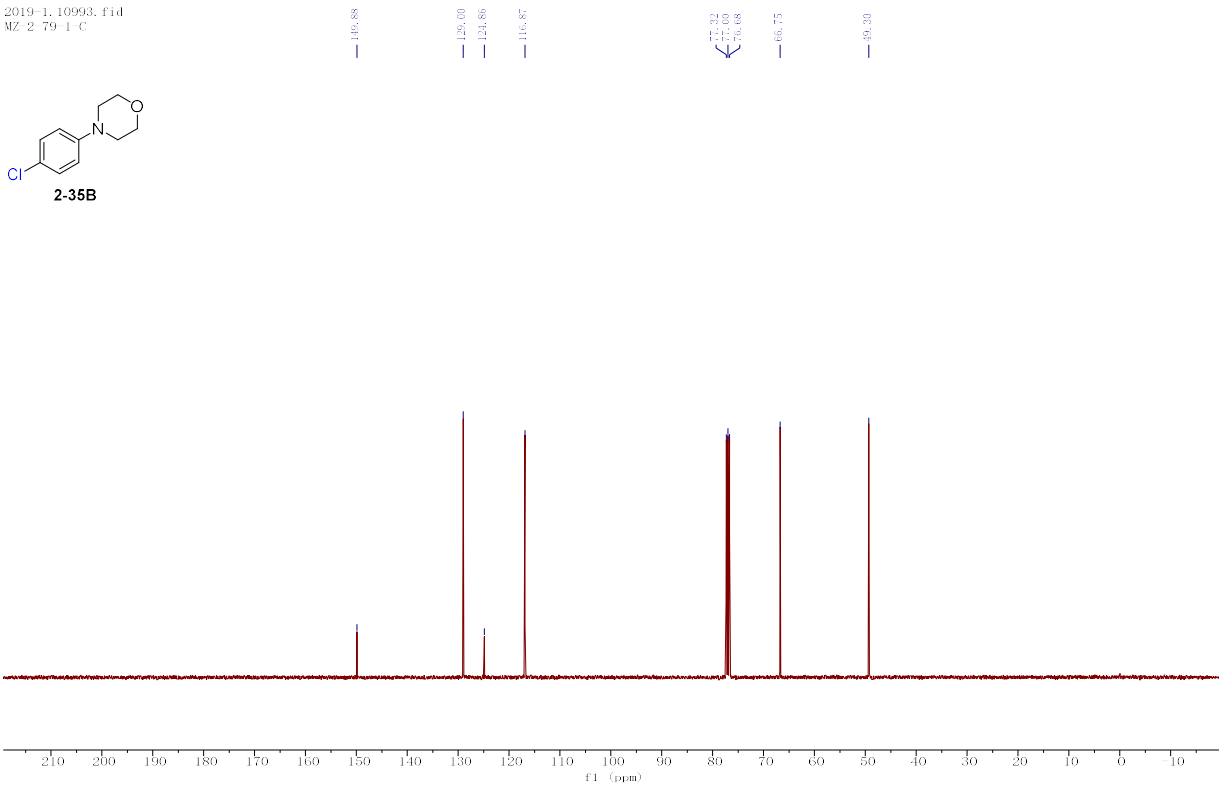

Figure S103. ^{13}C NMR of crude product **2-35B**, related Table 3

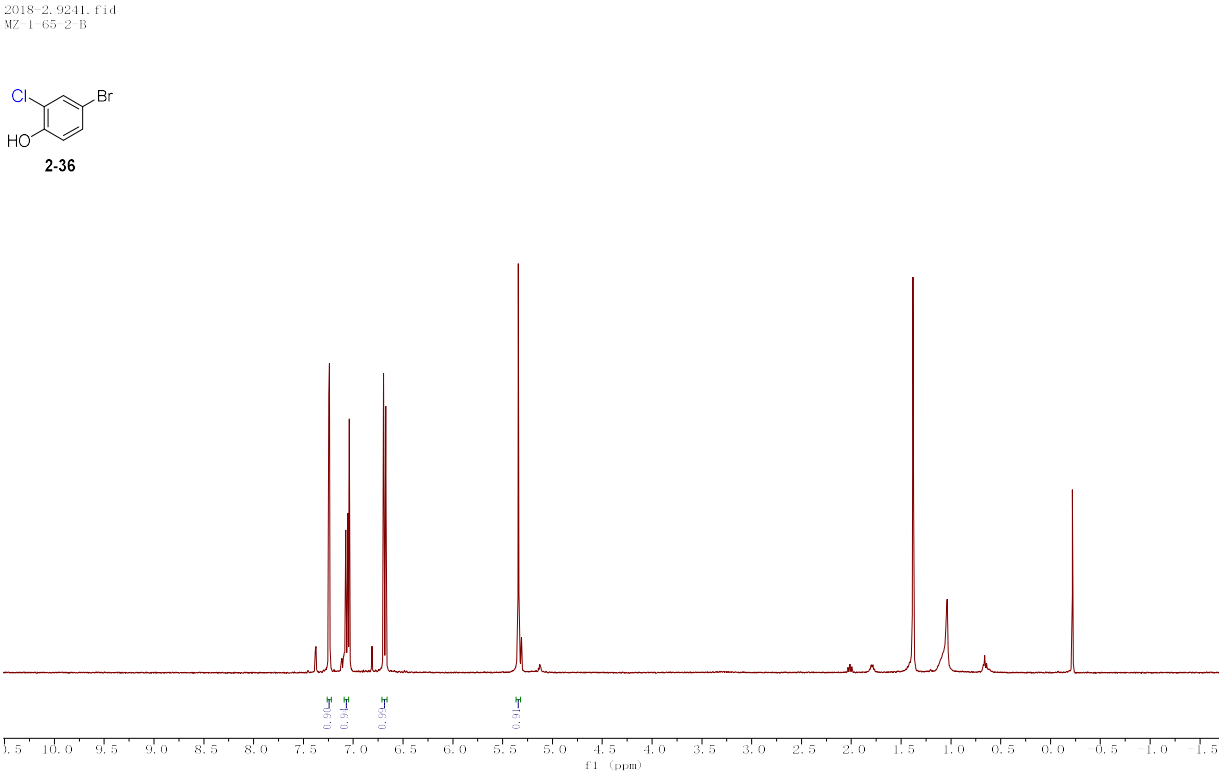

Figure S104. ^{1}H NMR of crude product **2-36**, related Table 3

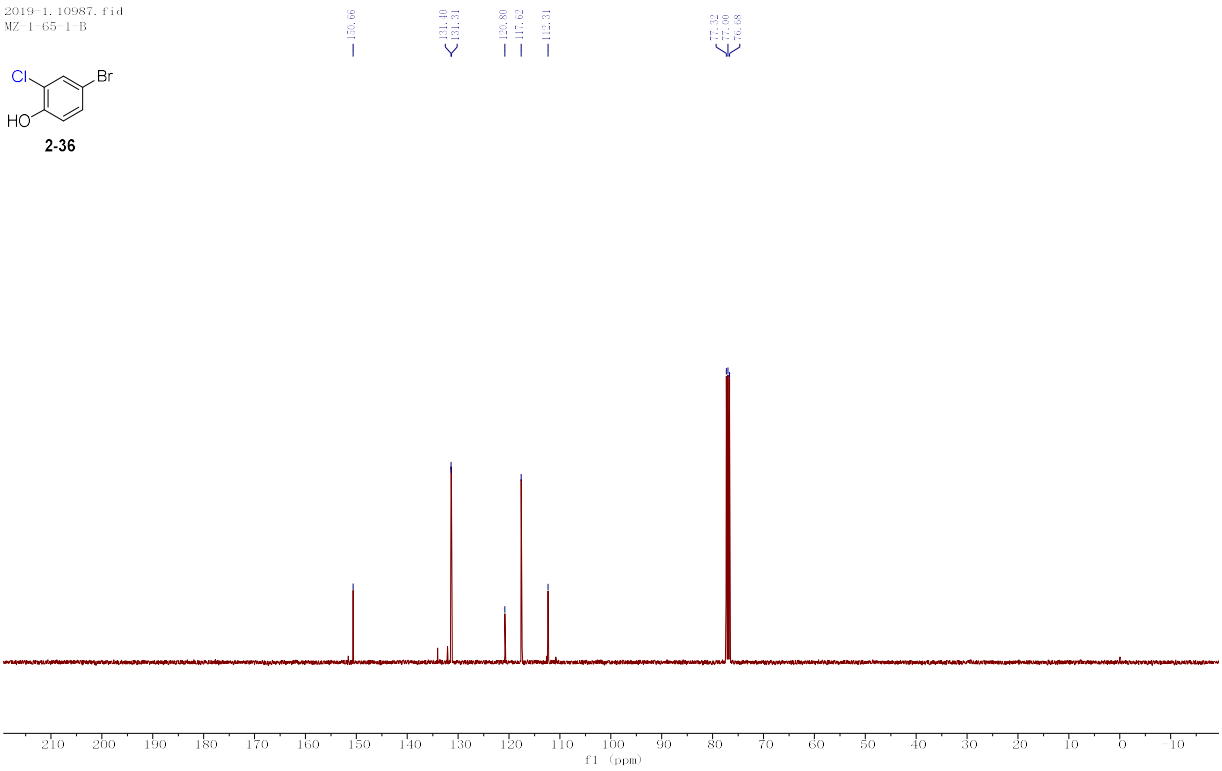

Figure S105. ^{13}C NMR of crude product **2-36**, related Table 3

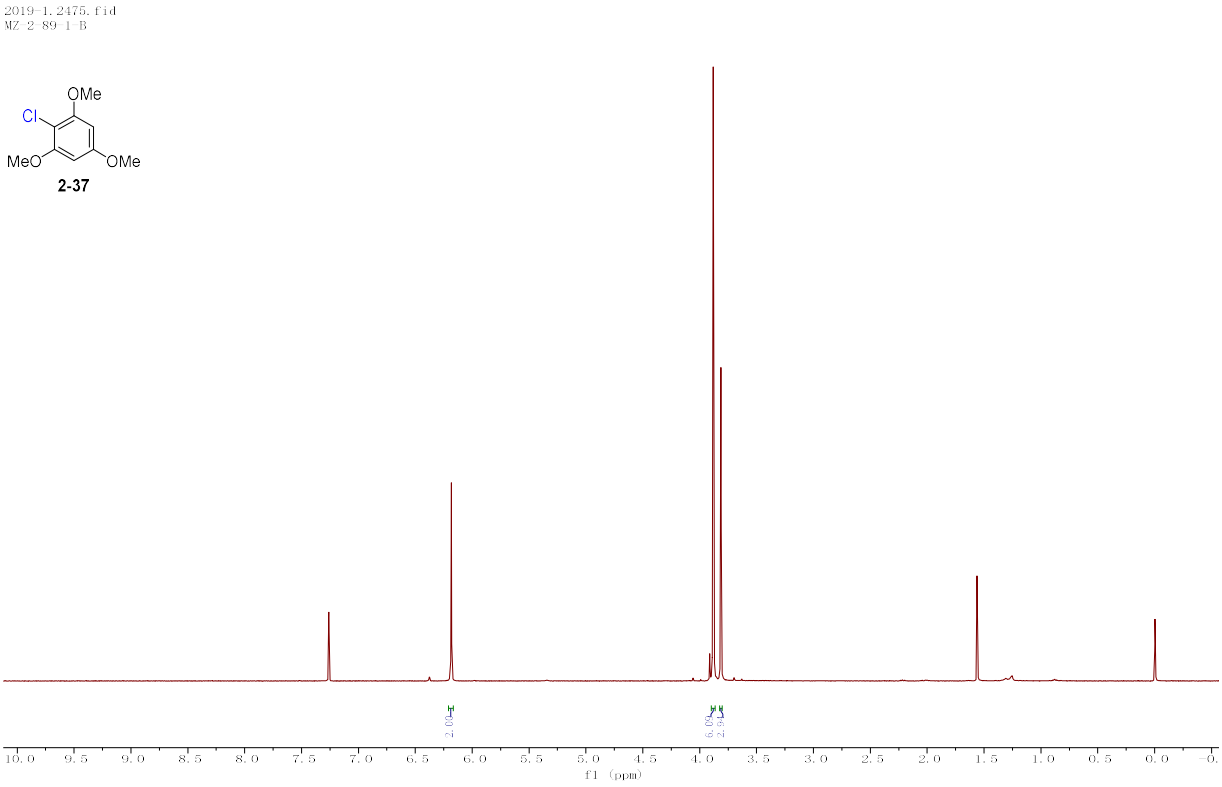

Figure S106. ^{1}H NMR of crude product **2-37**, related Table 3

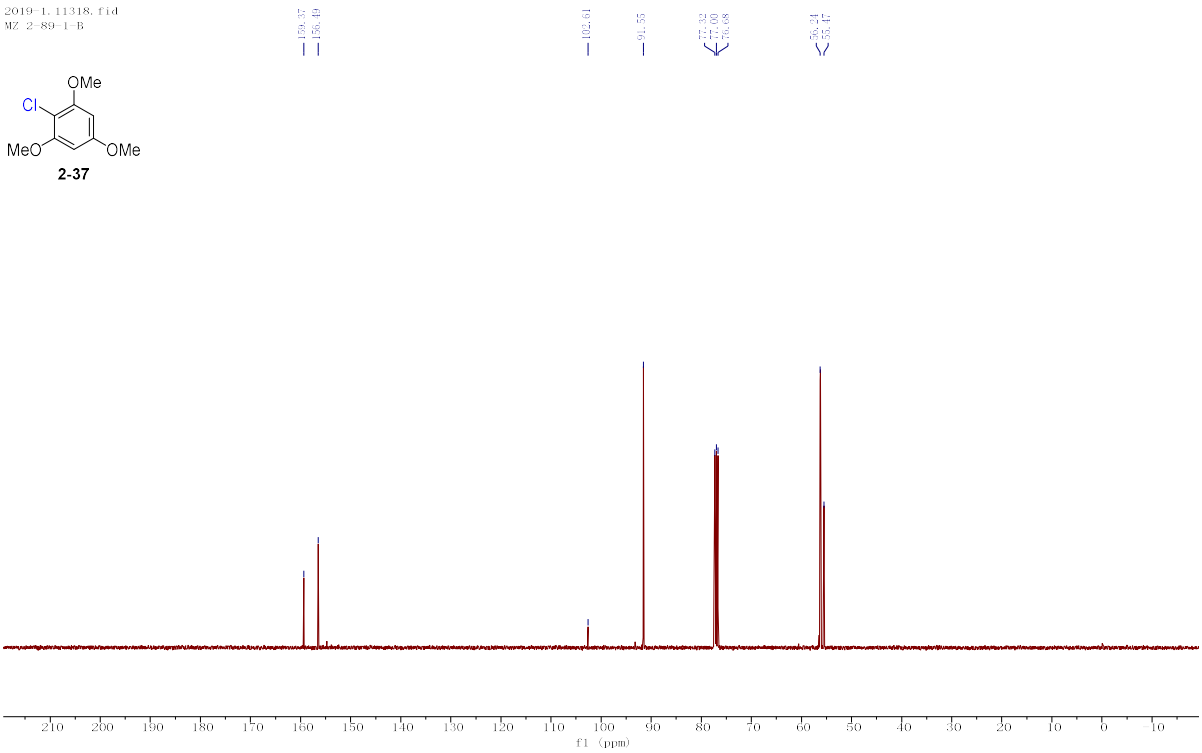

Figure S107. ^{13}C NMR of crude product **2-37**, related Table 3

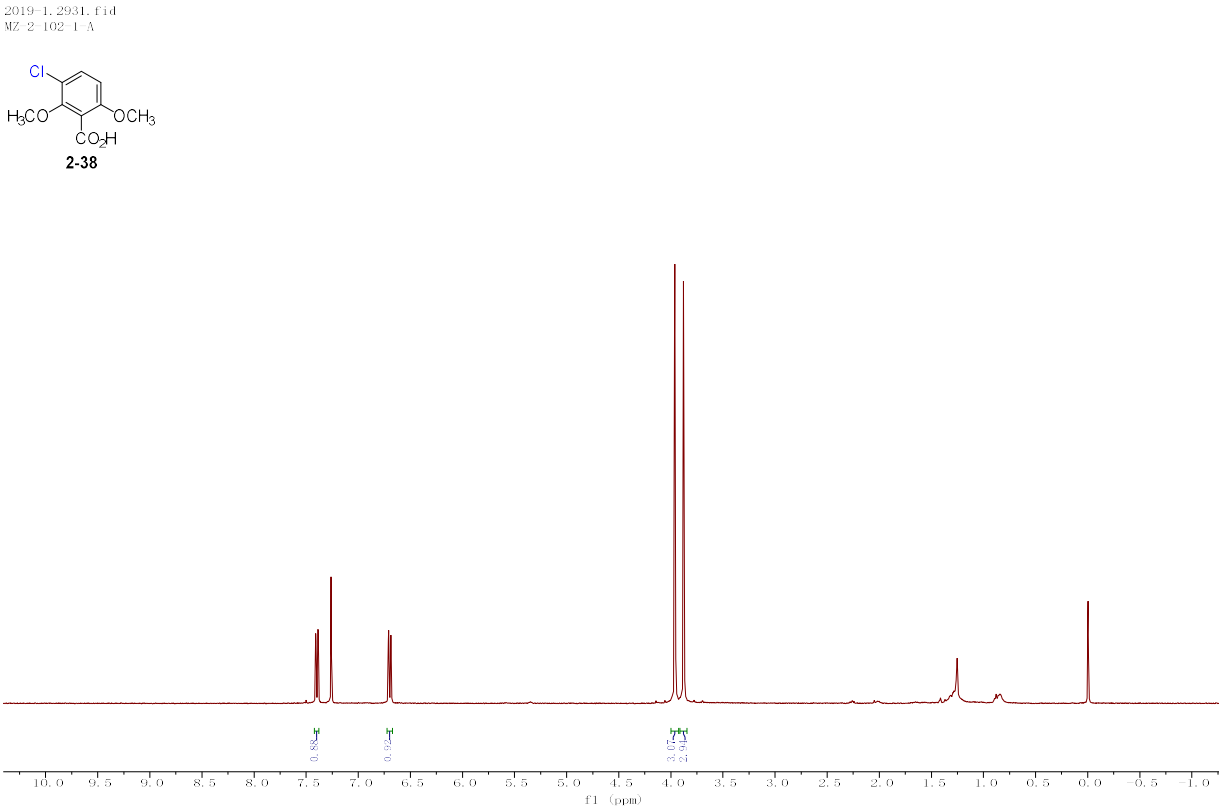

Figure S108. ^{1}H NMR of crude product **2-38**, related Table 3

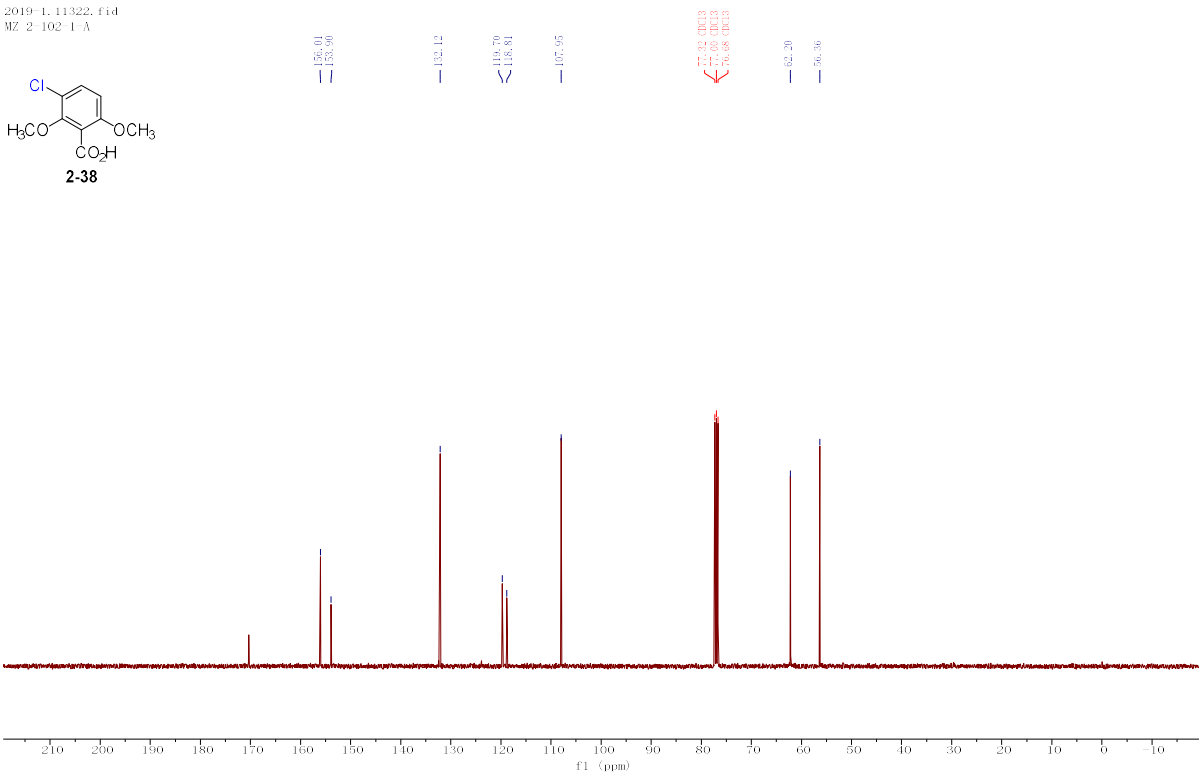

Figure S109. ^{13}C NMR of crude product **2-38**, related Table 3

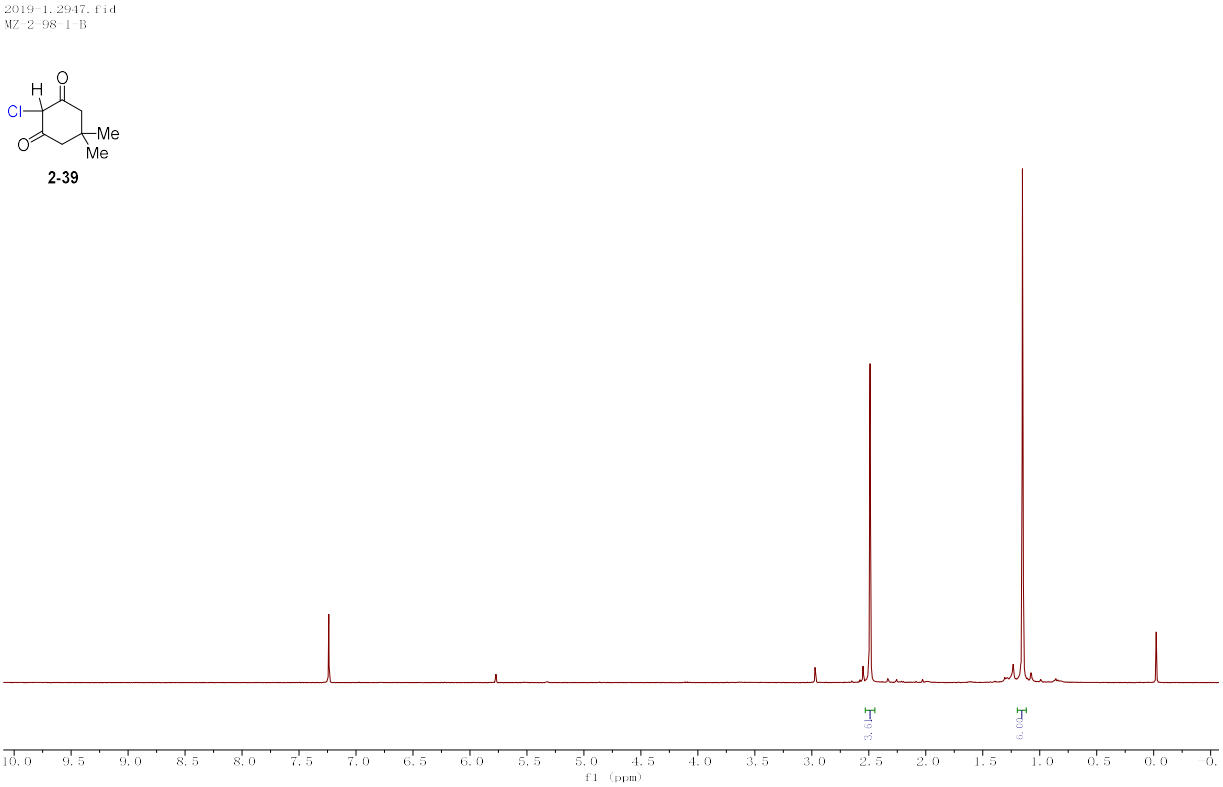

Figure S110. ^{1}H NMR of crude product **2-39**, related Table 3

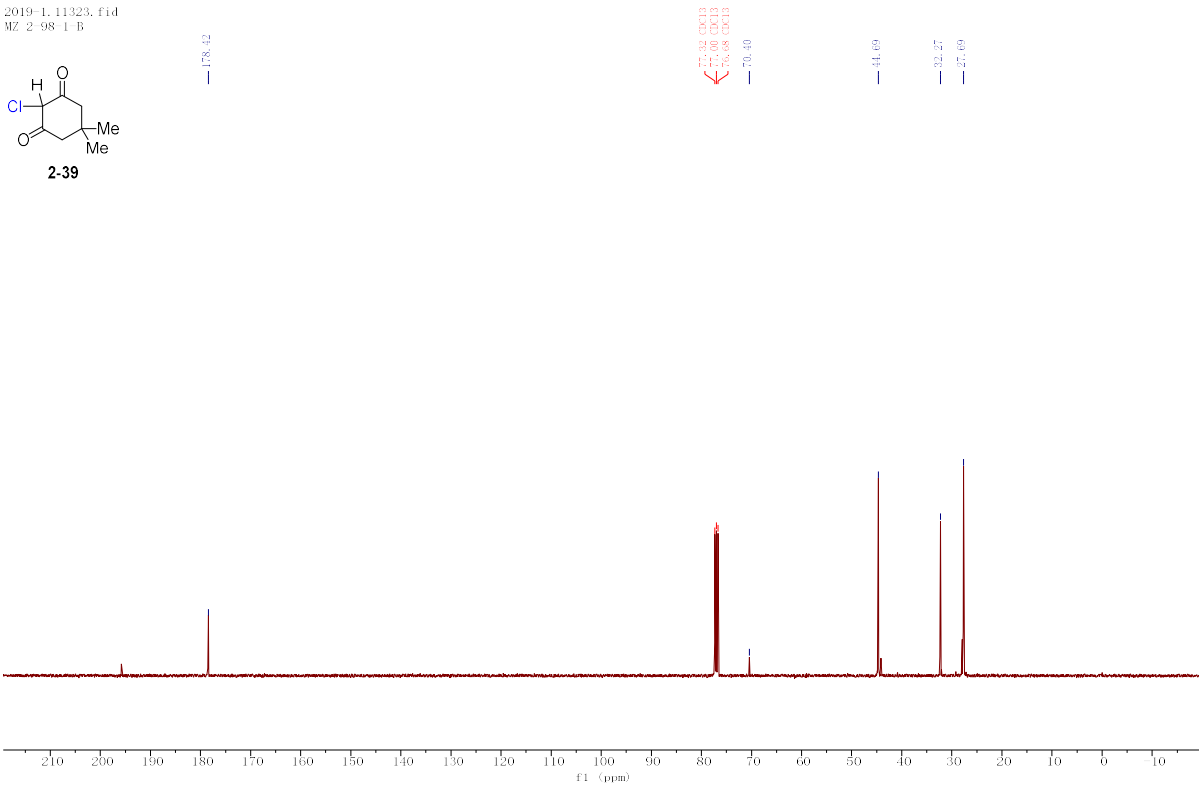

Figure S111. ^{13}C NMR of crude product **2-39**, related Table 3

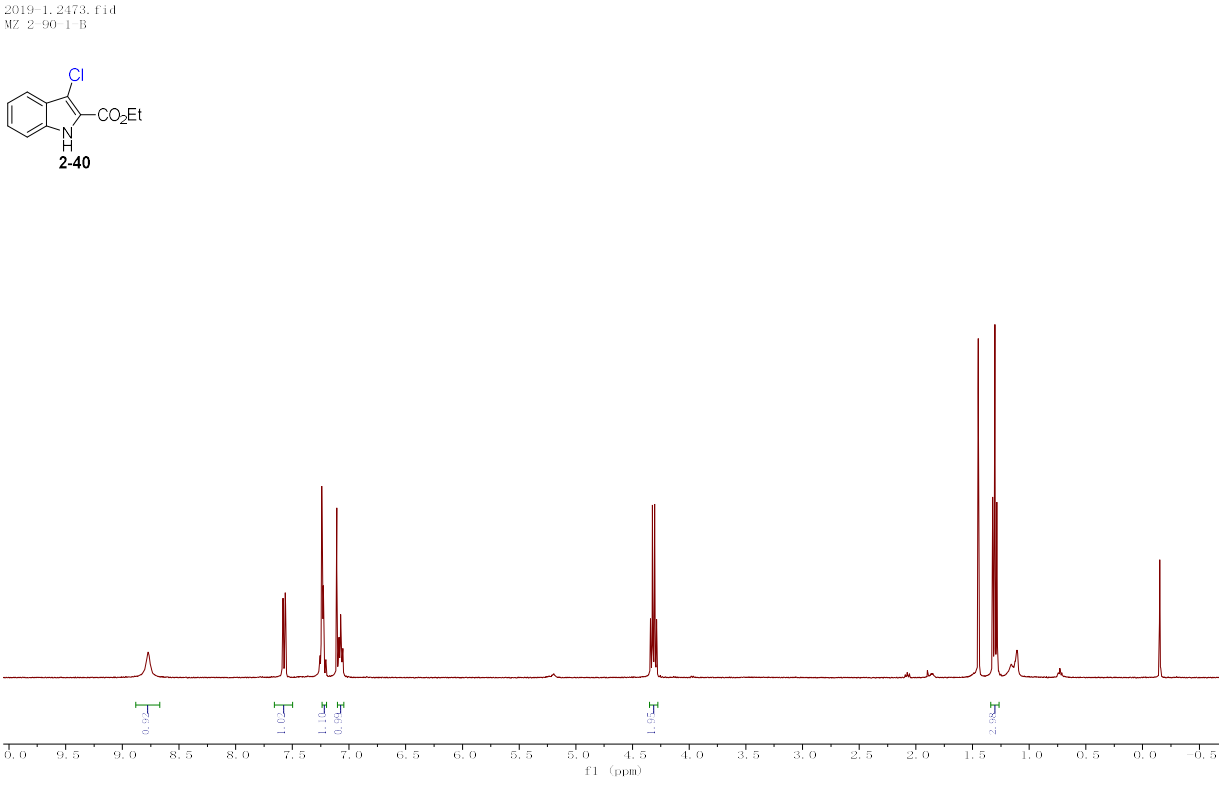

Figure S112. ^{1}H NMR of crude product **2-40**, related Table 3

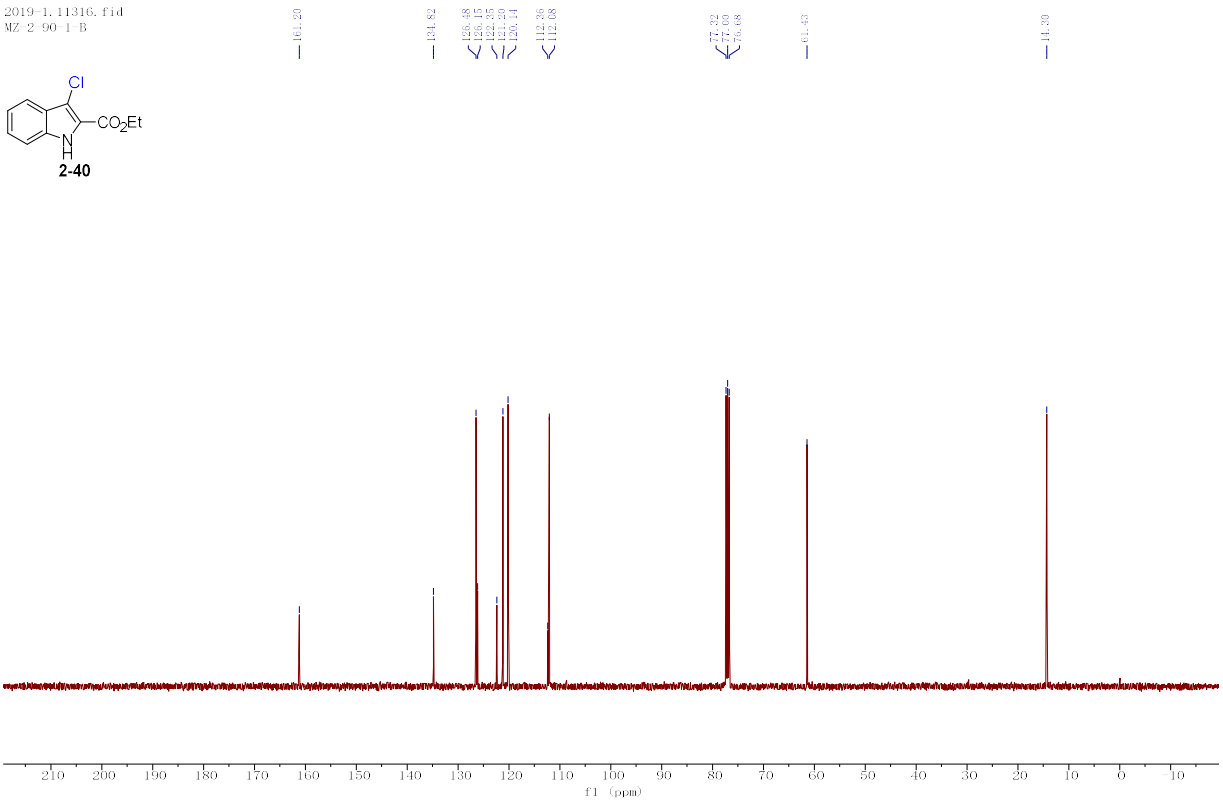

Figure S1113. ^{13}C NMR of crude product **2-40**, related Table 3

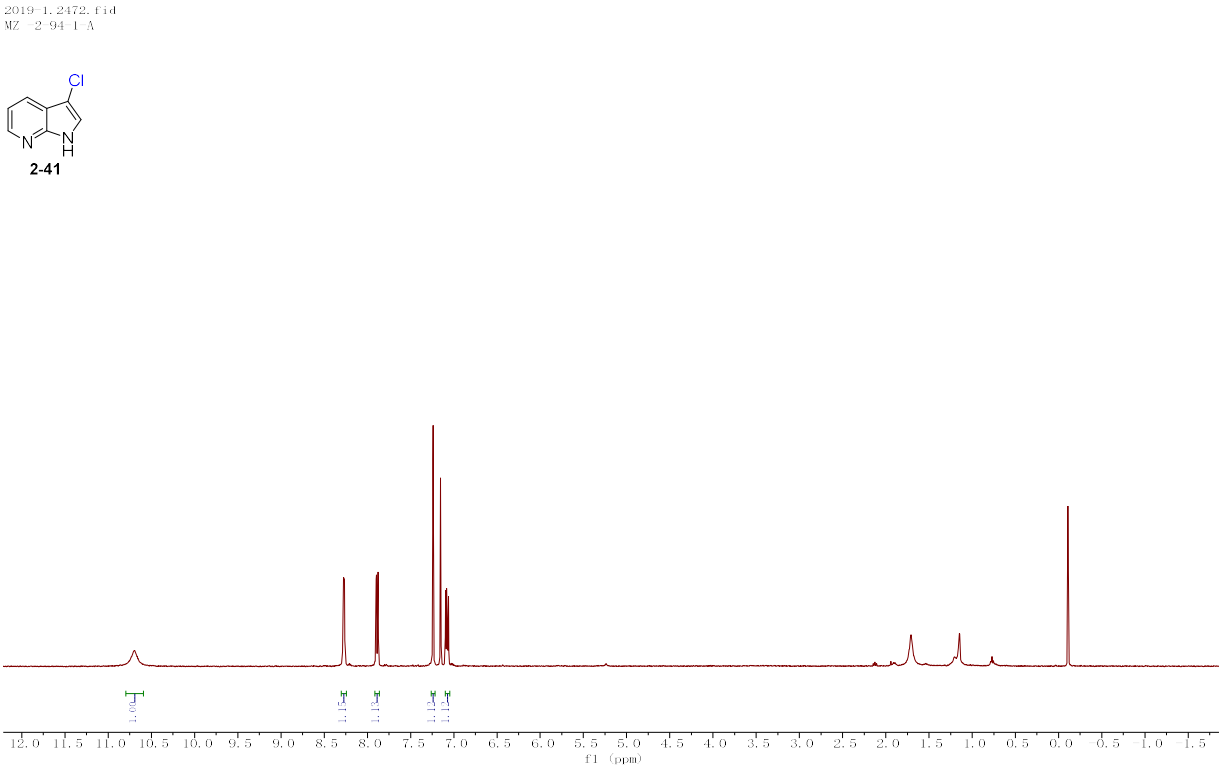

Figure S114. ^{1}H NMR of crude product **2-41**, related Table 3

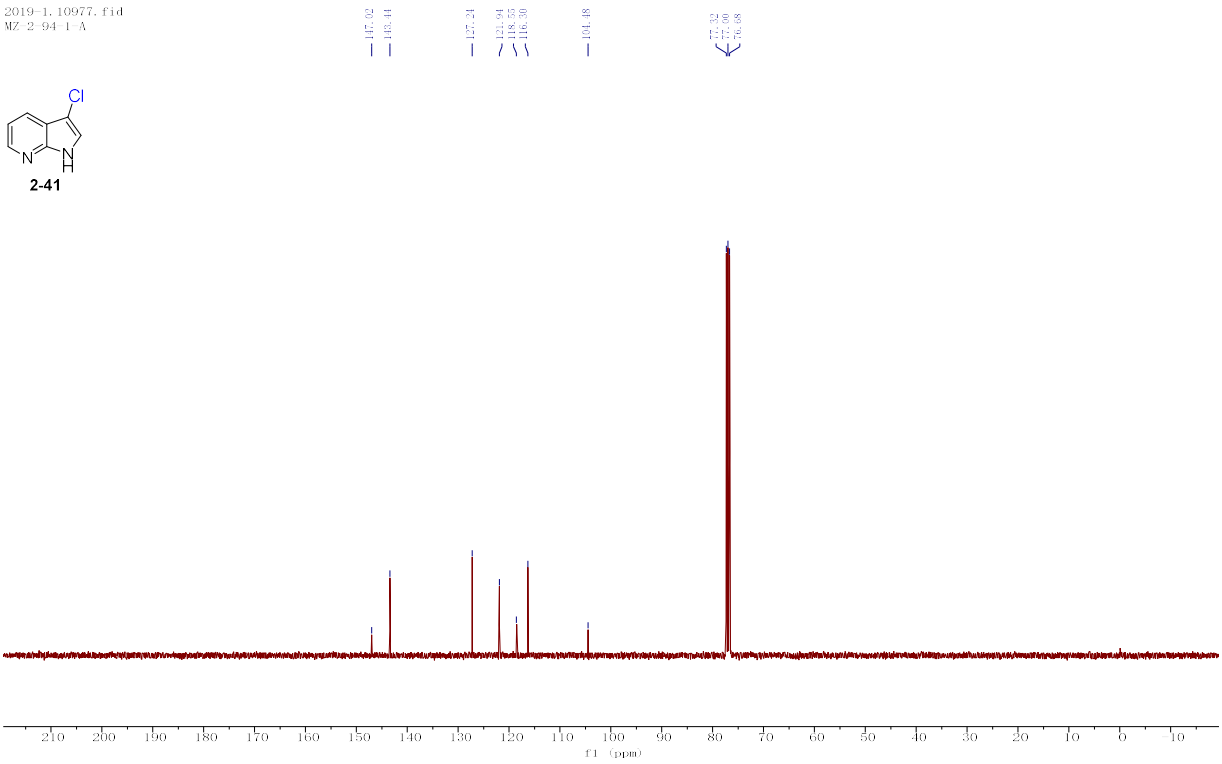

Figure S115. ^{13}C NMR of crude product **2-41**, related Table 3

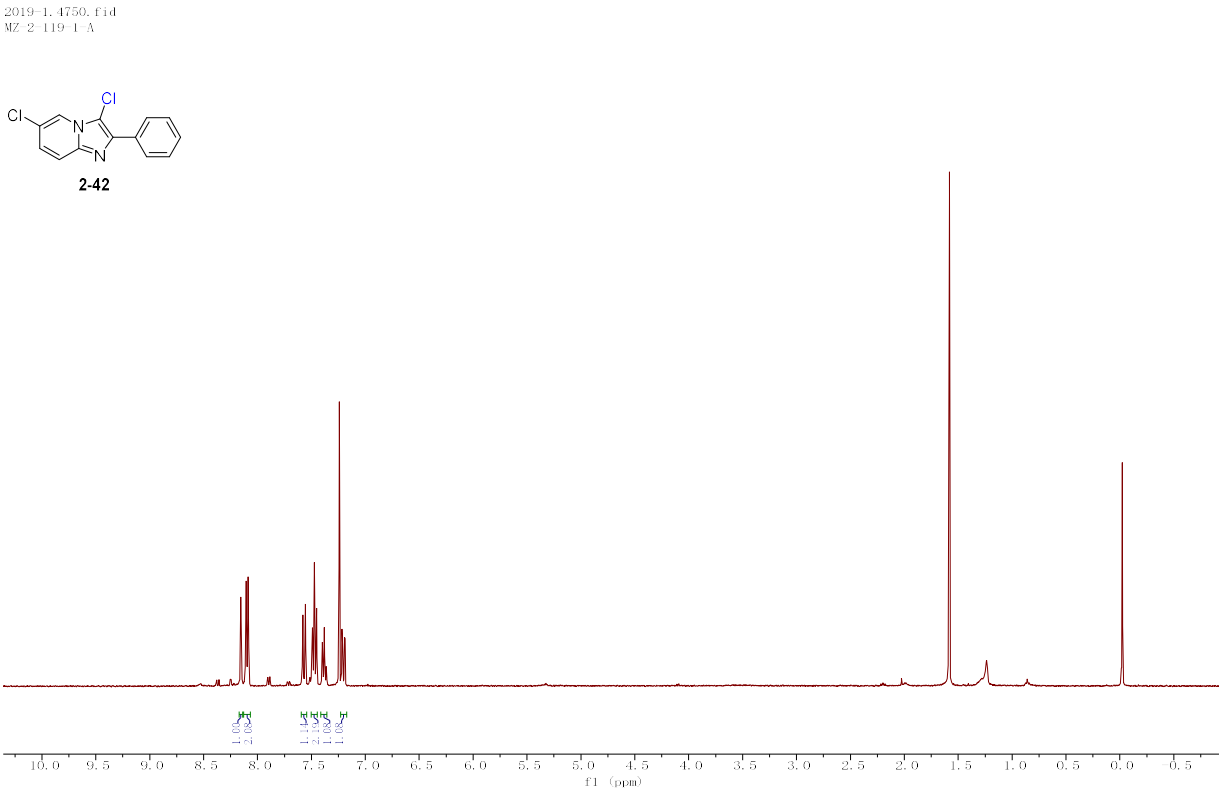

Figure S116. ^{1}H NMR of crude product **2-42**, related Table 3

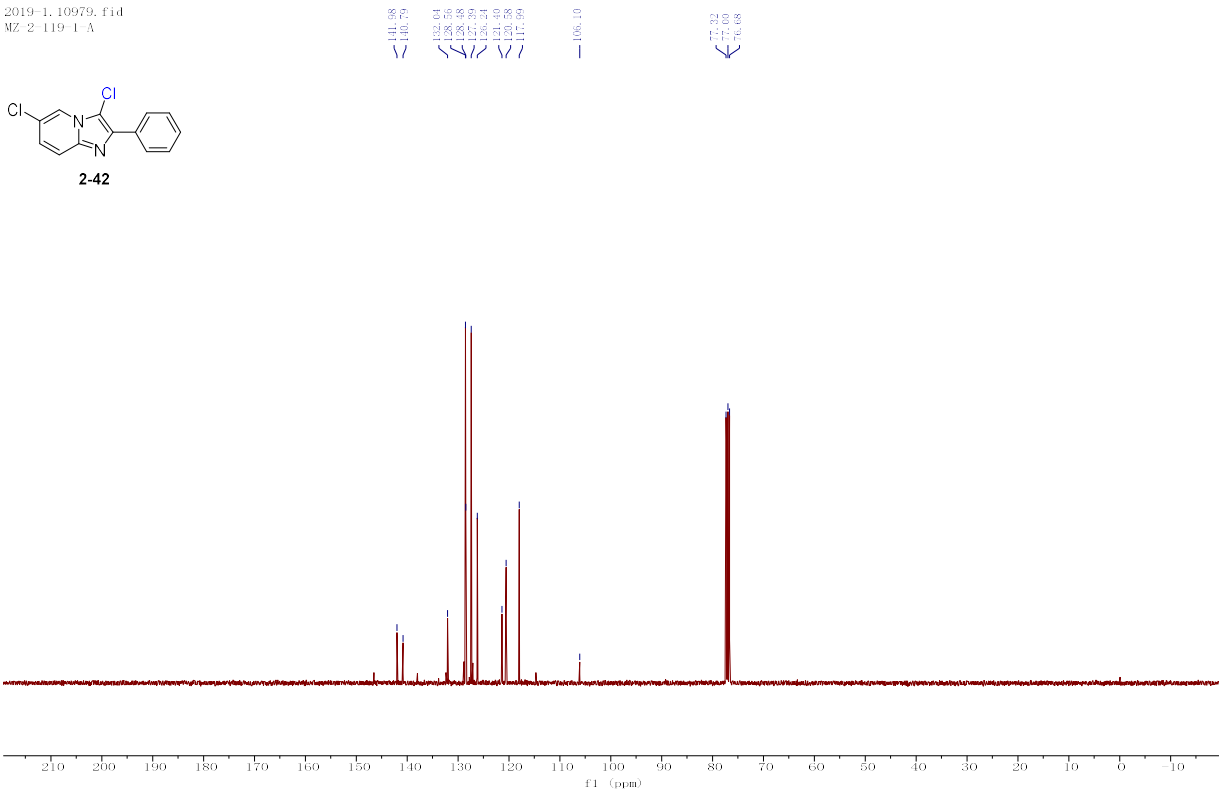

Figure S117. ^{13}C NMR of crude product **2-41**, related Table 3

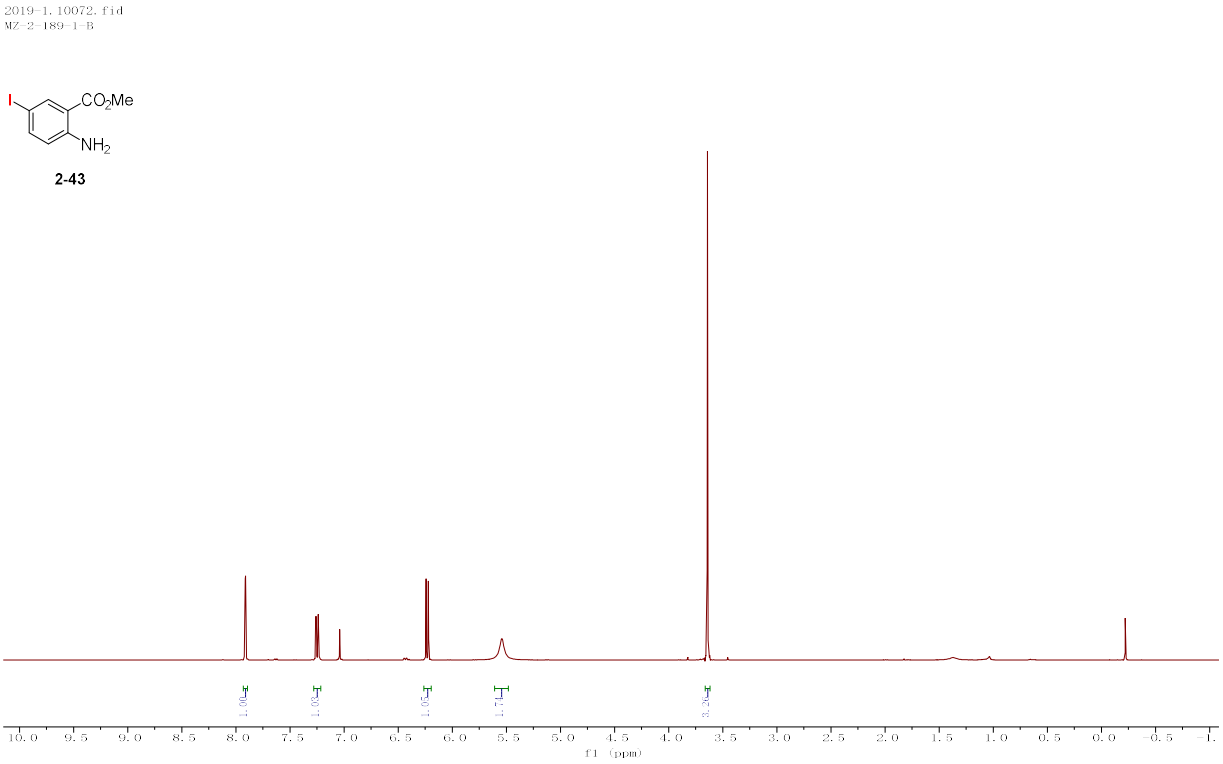

Figure S118. ^{1}H NMR of crude product **2-43**, related Table 3

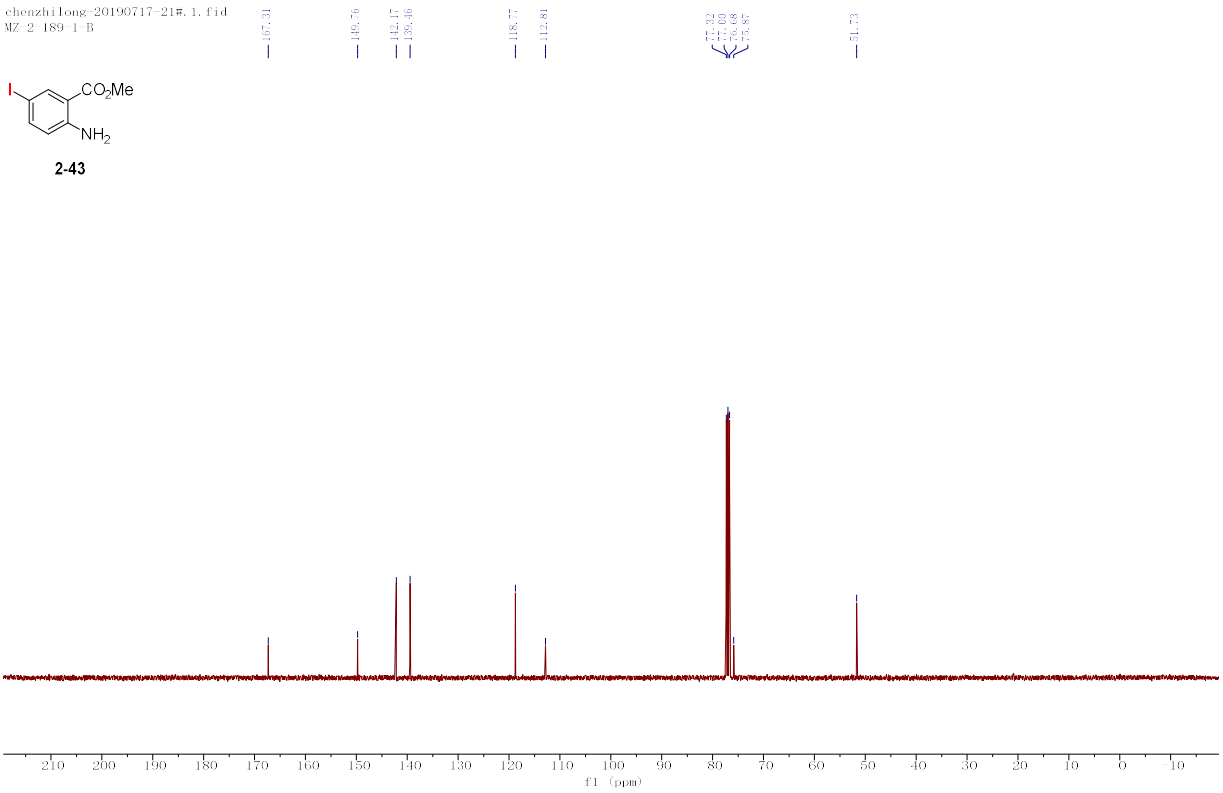

Figure S119. ^{13}C NMR of crude product **2-43**, related Table 3

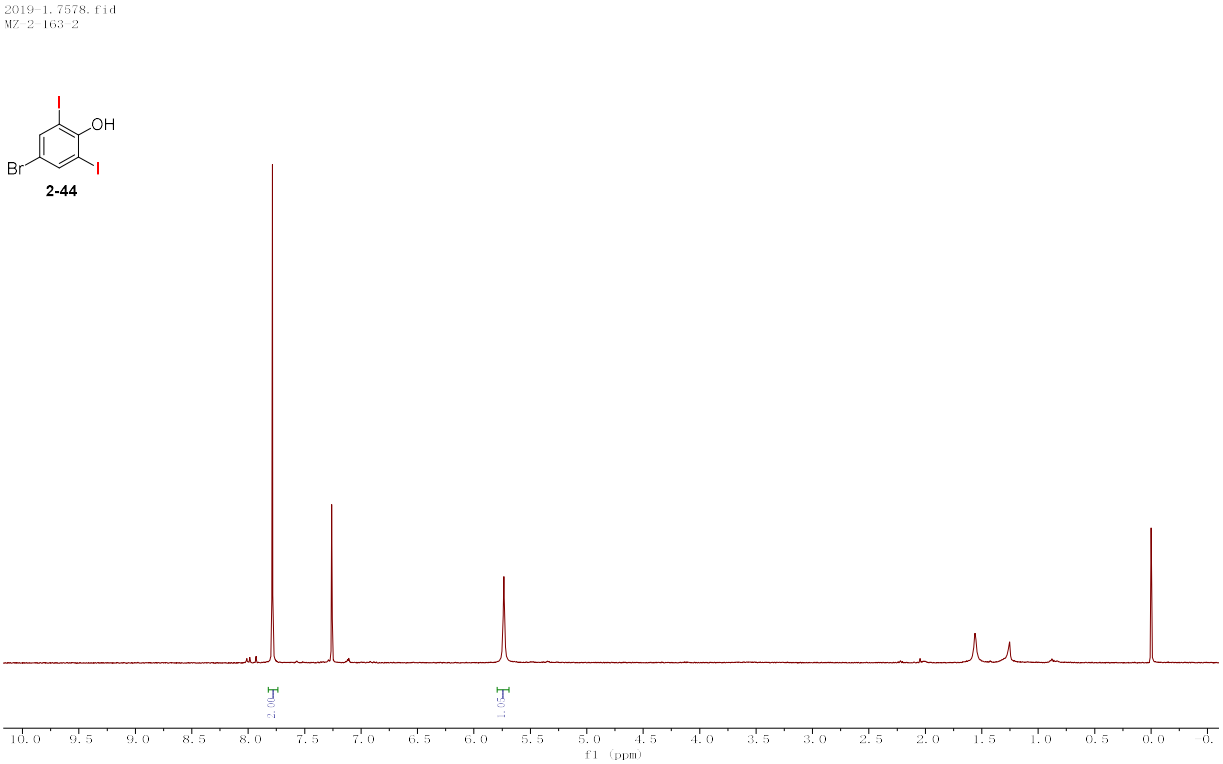

Figure S120. ^{1}H NMR of crude product **2-44**, related Table 3

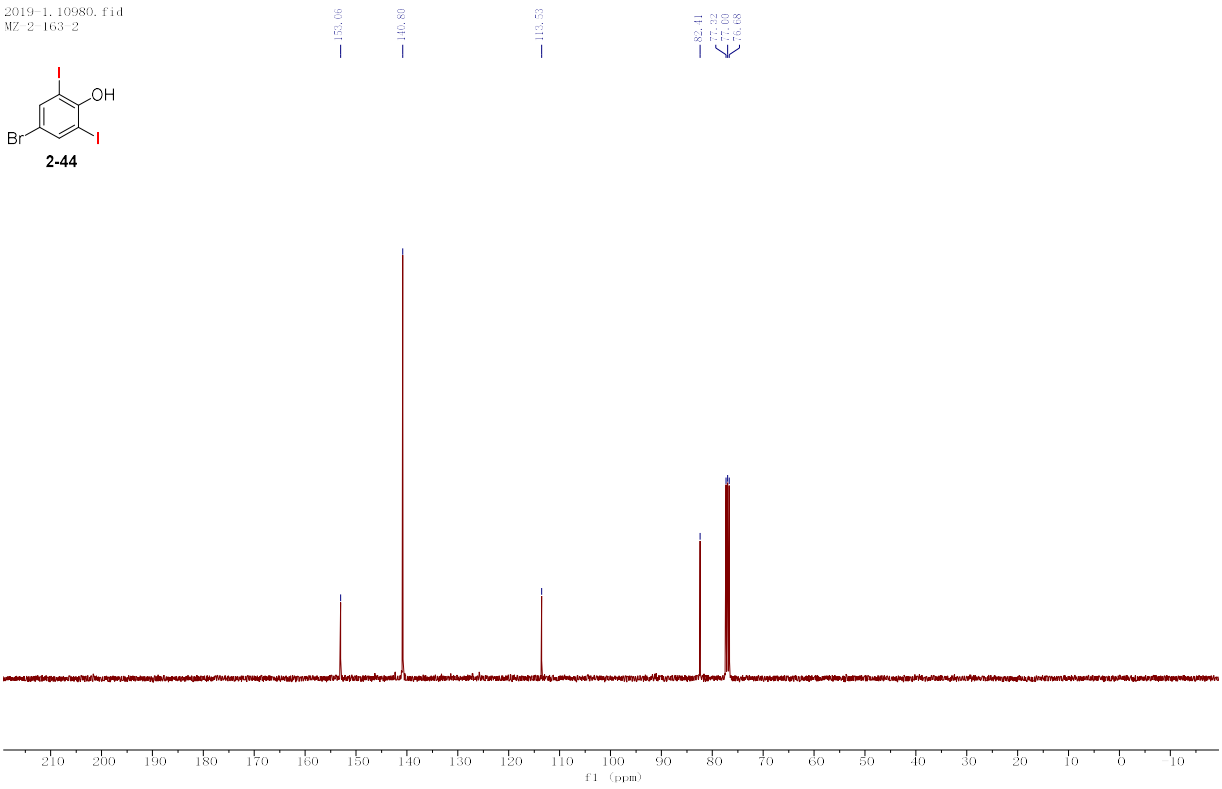

Figure S121. ^{13}C NMR of crude product **2-44**, related Table 3

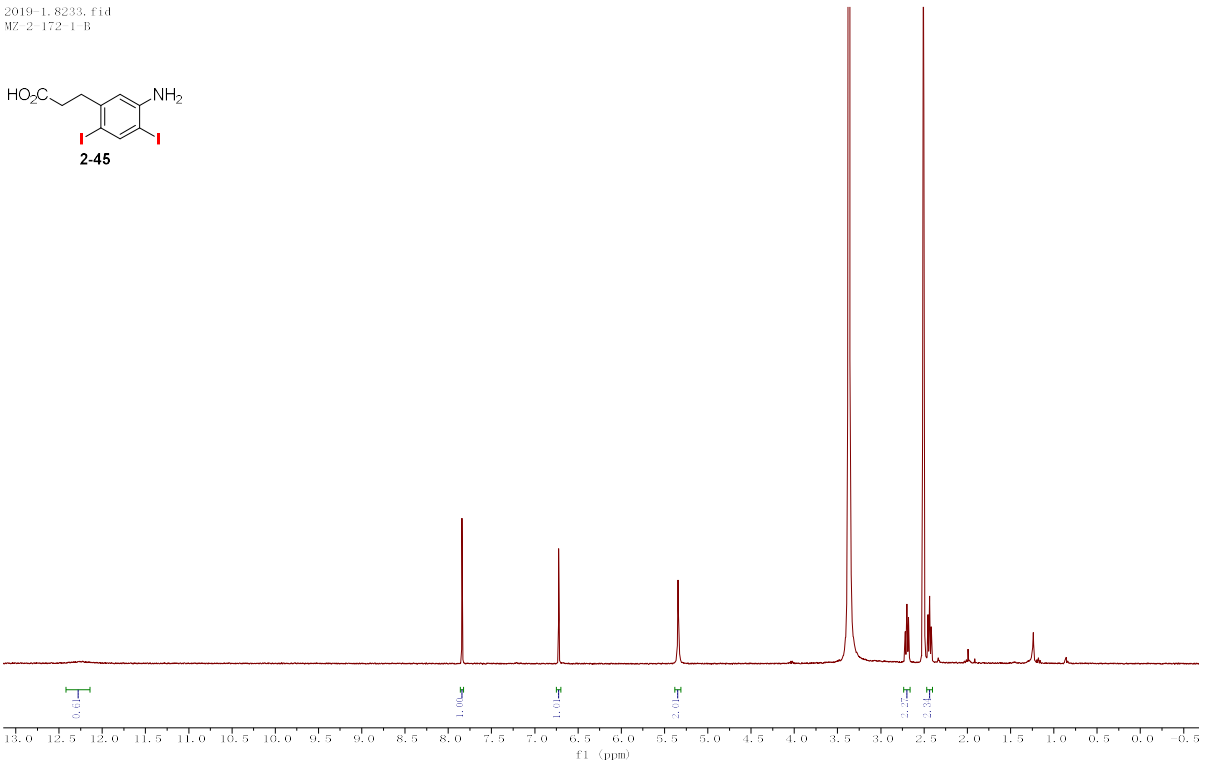

Figure S122. ^{1}H NMR of crude product **2-45**, related Table 3

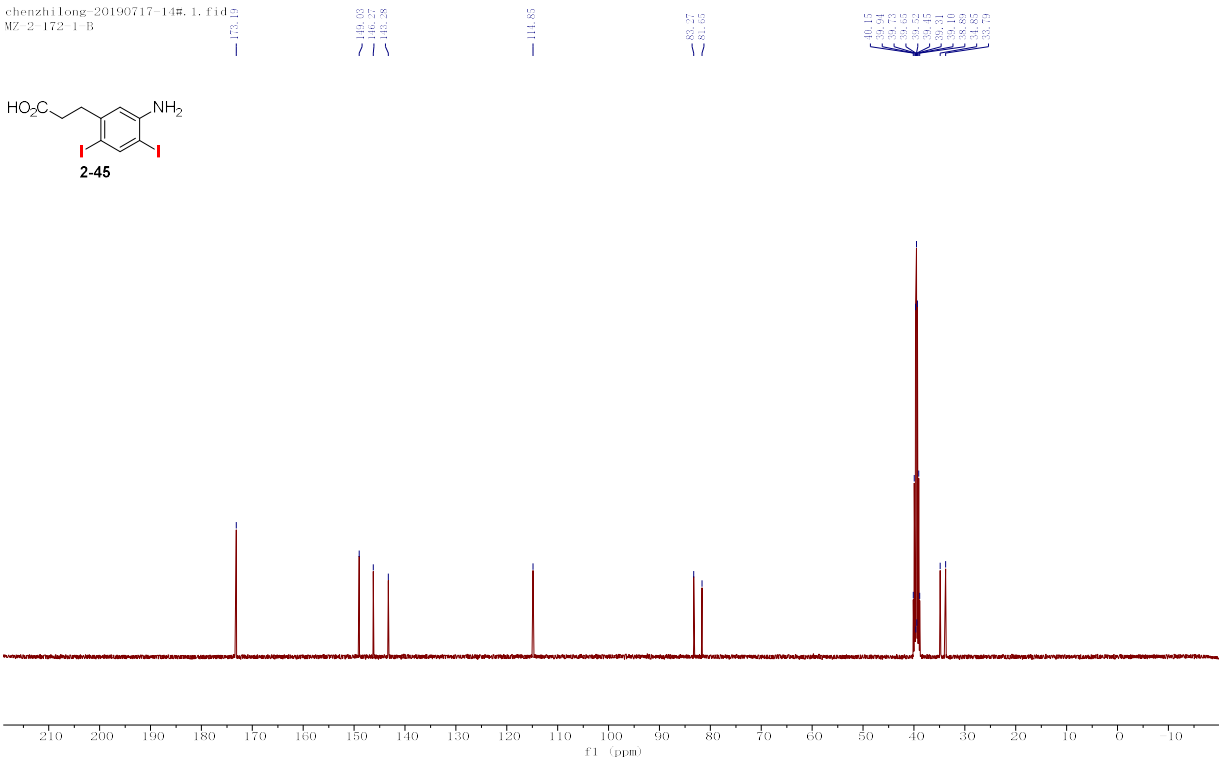

Figure S123. ^{13}C NMR of crude product **2-45**, related Table 3

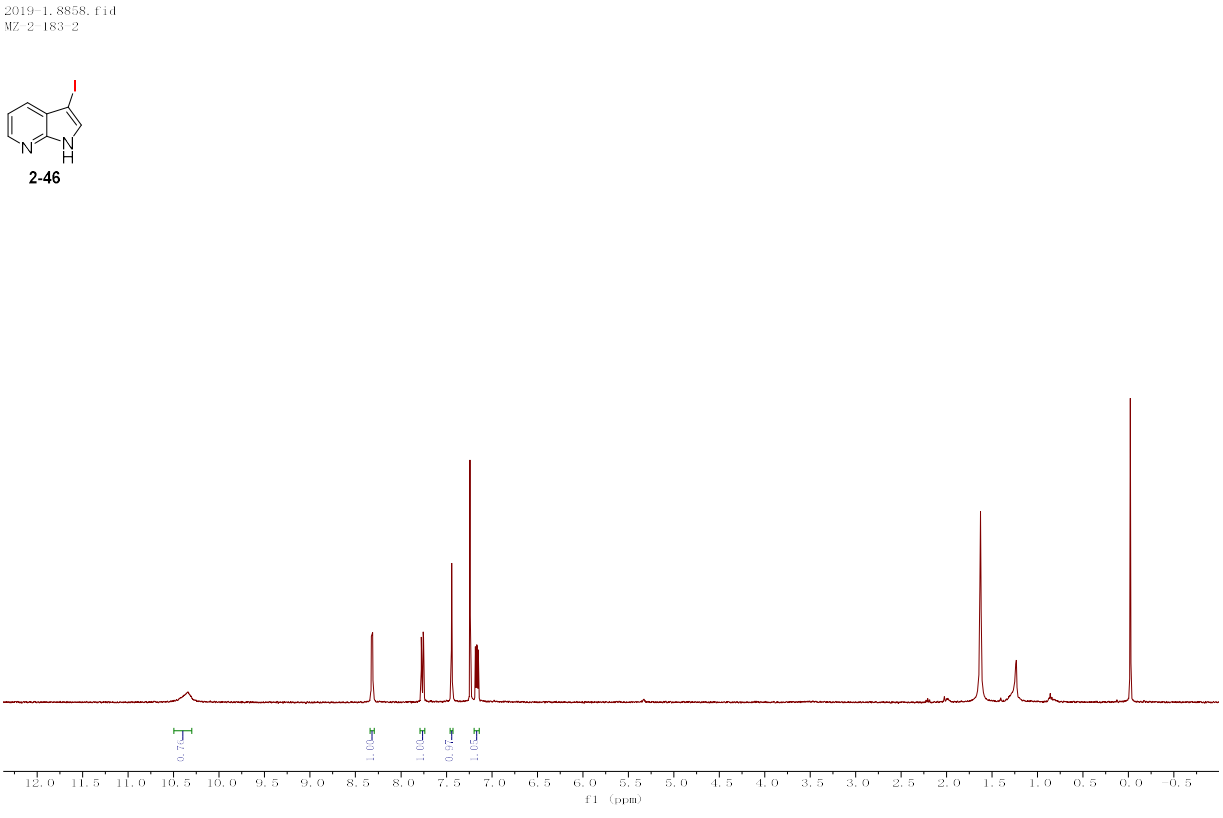

Figure S124. ^{1}H NMR of crude product **2-46**, related Table 3

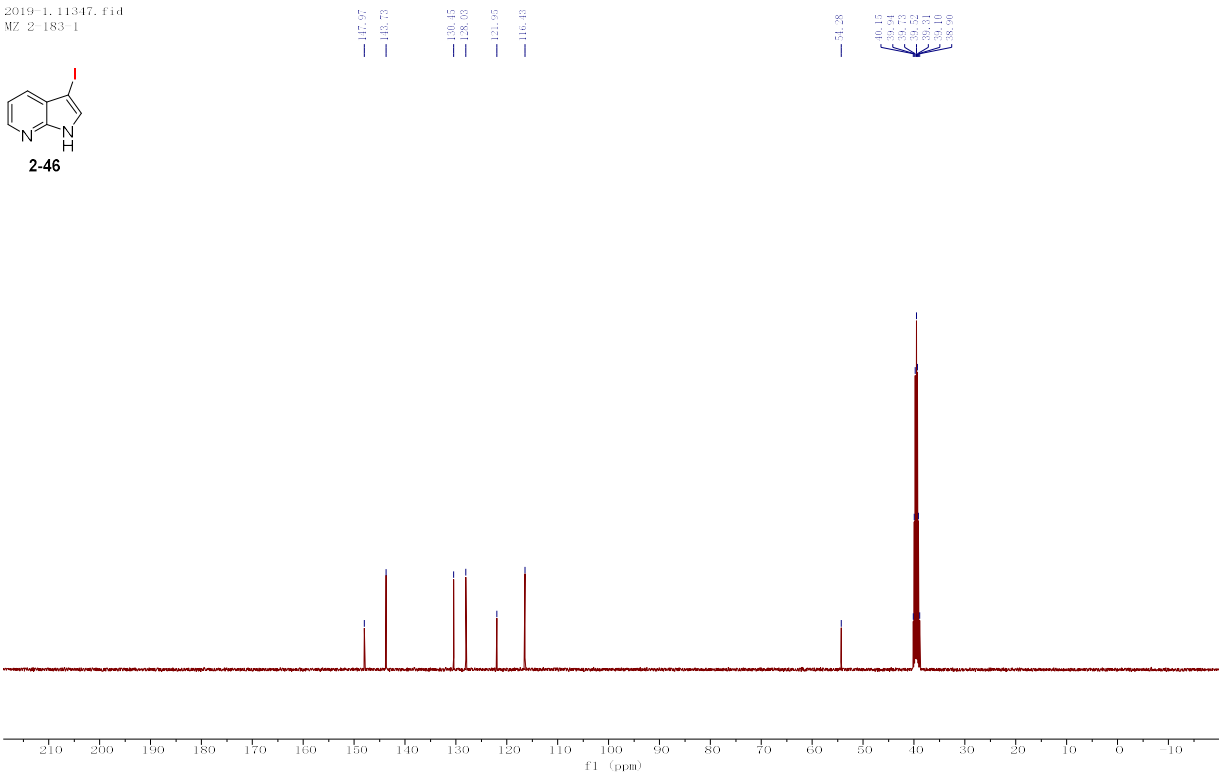

Figure S125. ^{13}C NMR of crude product **2-46**, related Table 3

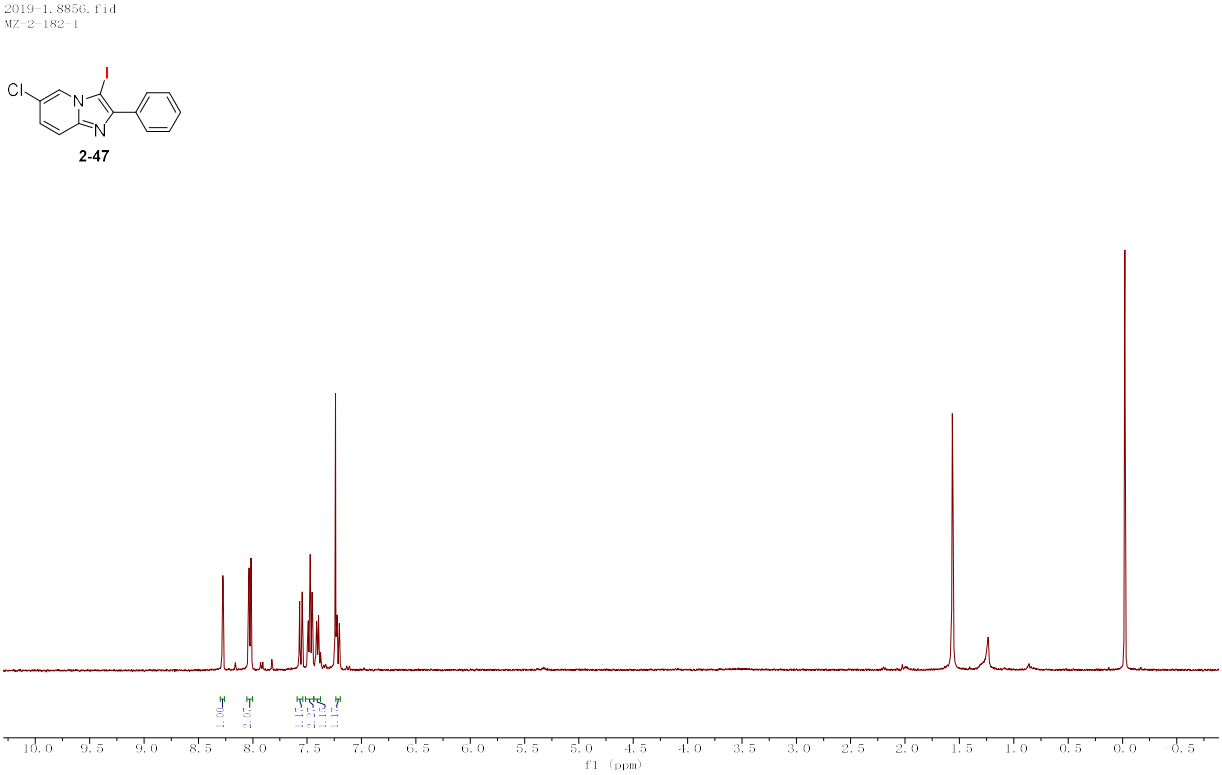

Figure S126. ^{1}H NMR of crude product **2-47**, related Table 3

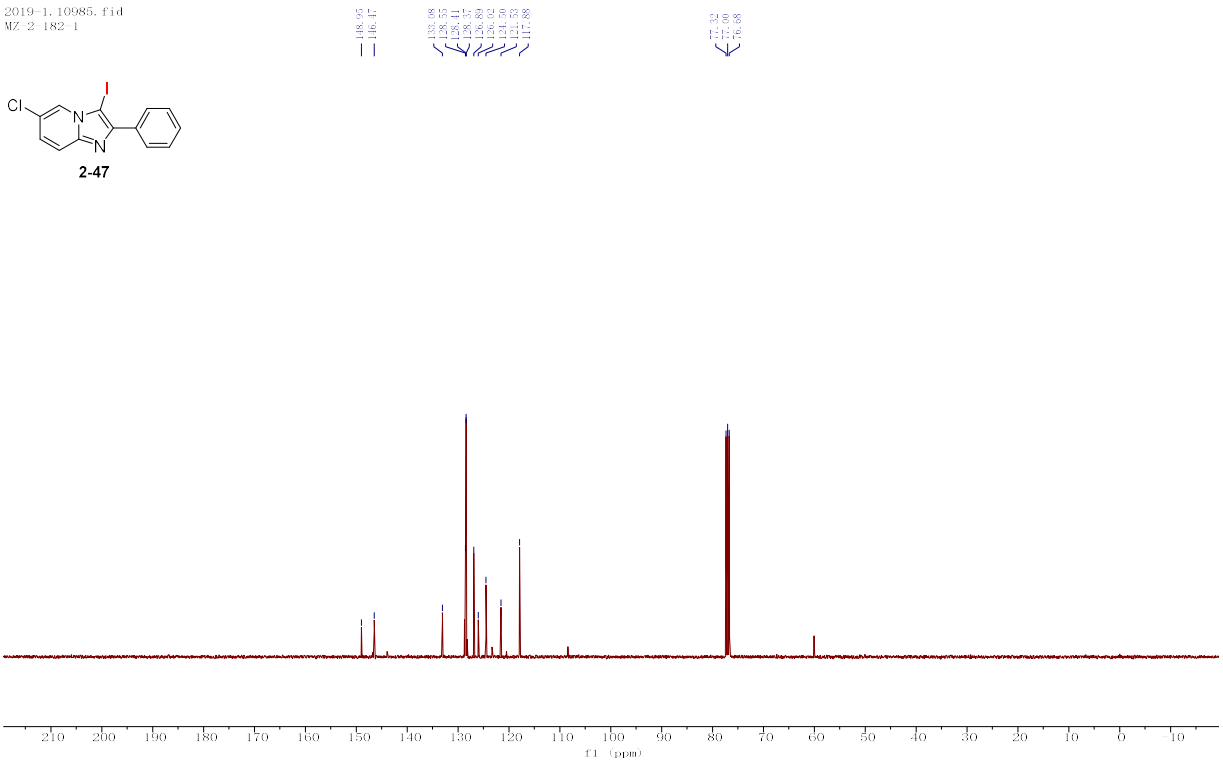

Figure S127. ^{13}C NMR of crude product **2-47**, related Table 3

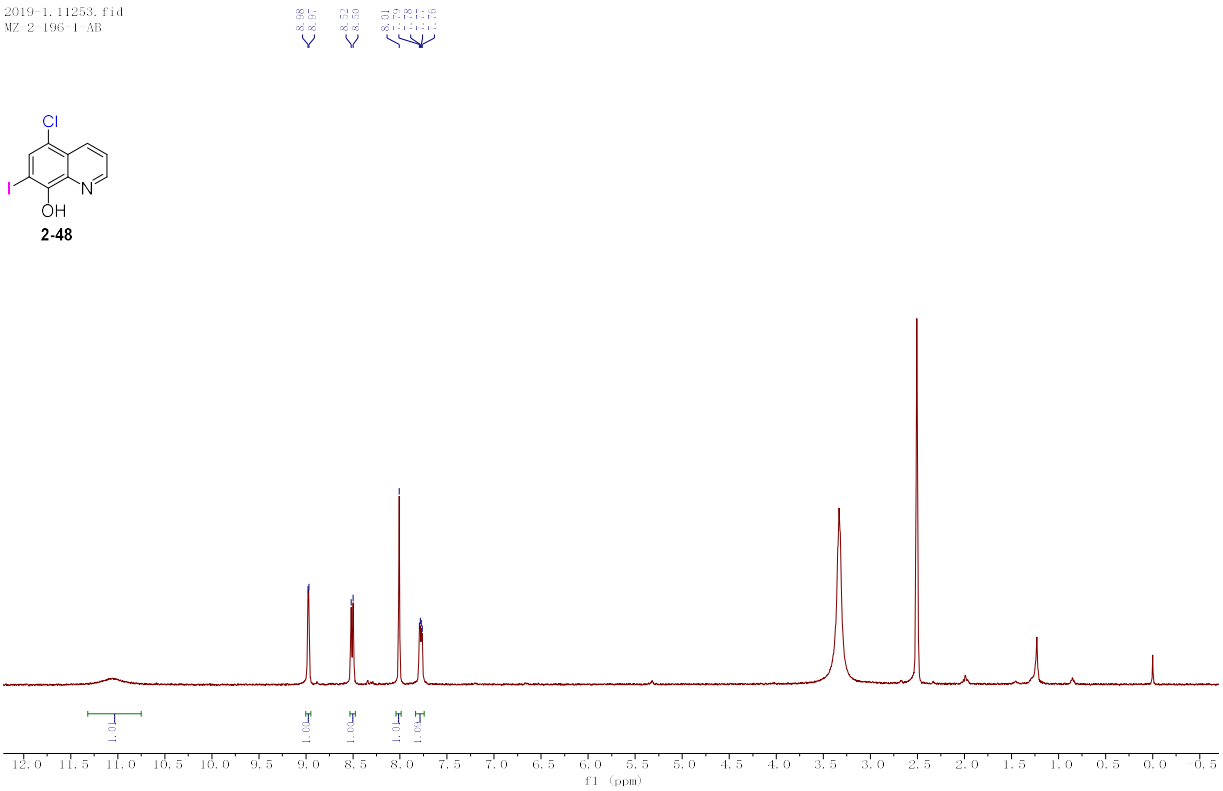

Figure S128. ^{1}H NMR of crude product **2-48**, related Figure 2

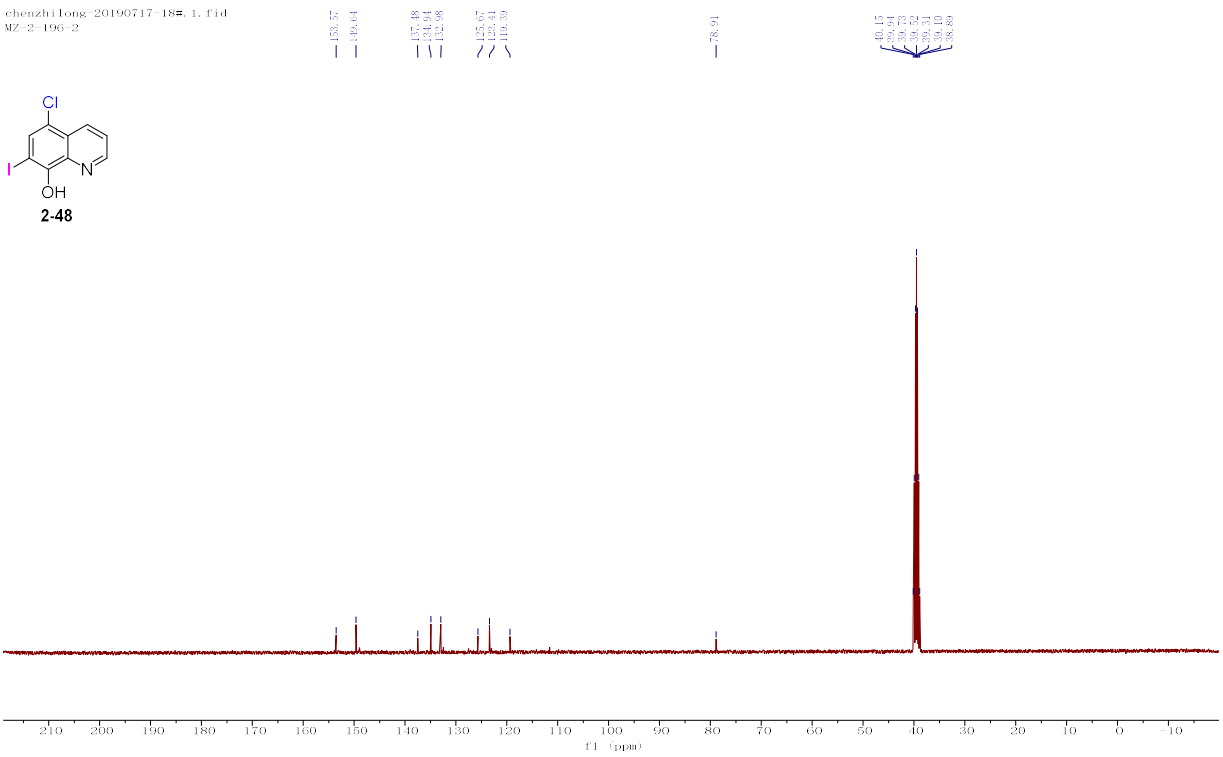

Figure S129. ^{13}C NMR of crude product **2-48**, related Figure 2

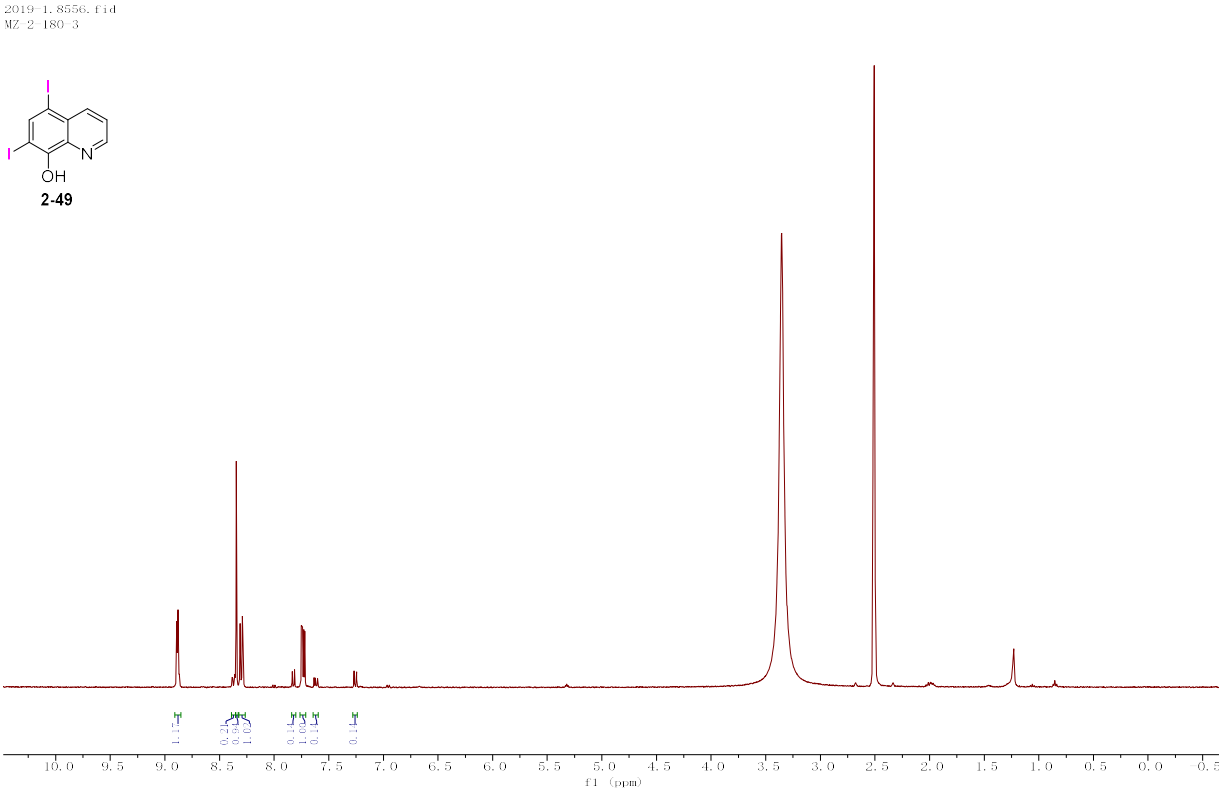

Figure S130. ^{1}H NMR of crude product **2-49**, related Figure 2

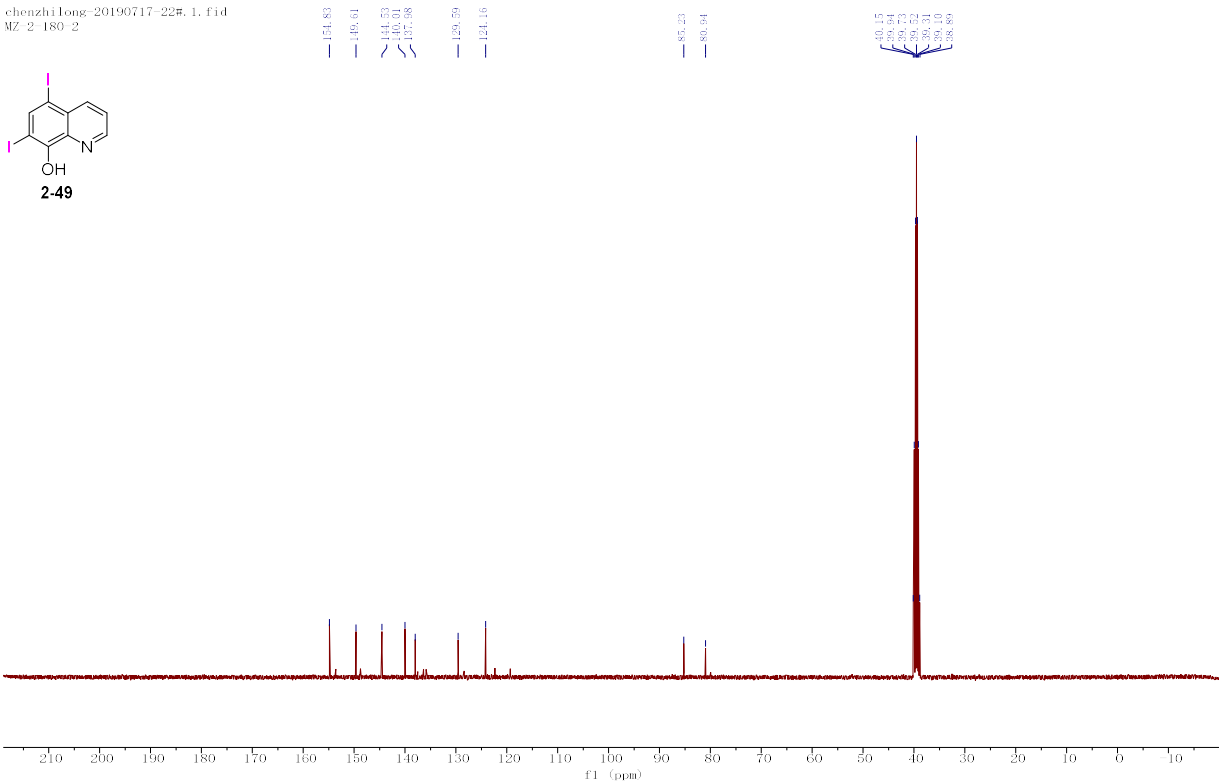

Figure S131. ^{13}C NMR of crude product **2-49**, related Figure 2

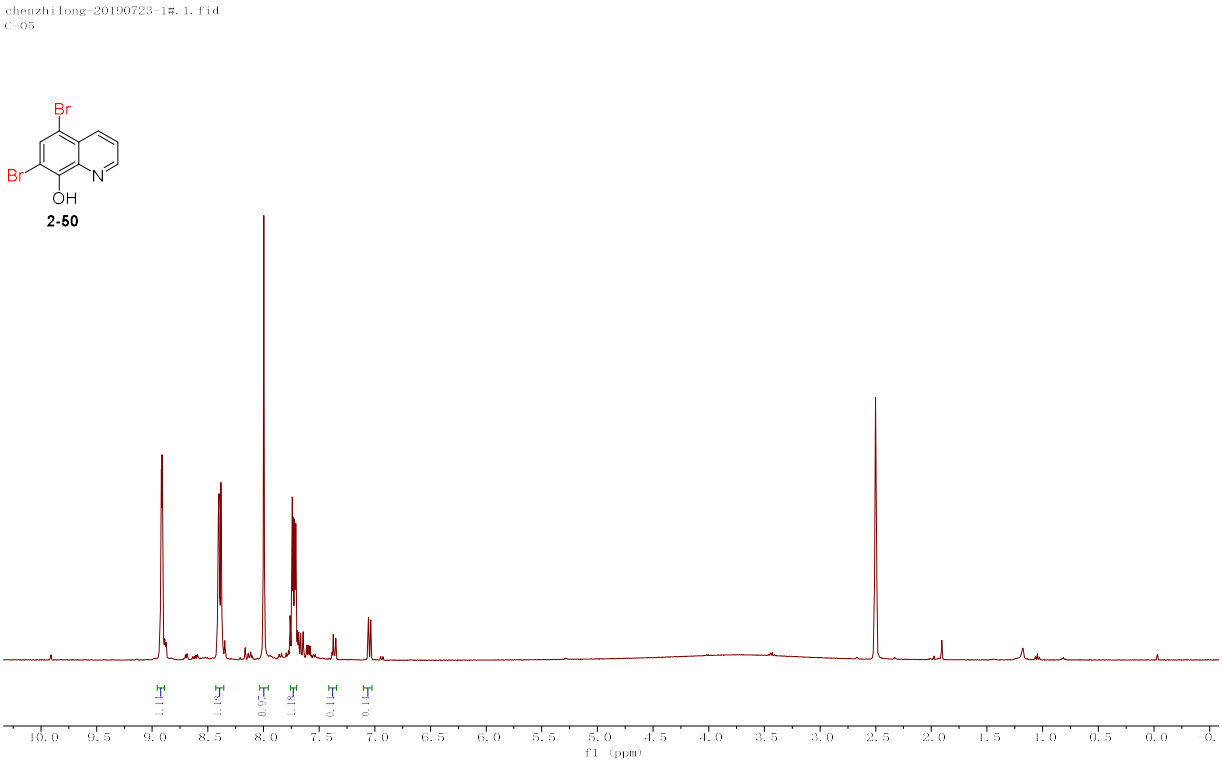

Figure S132. ^{1}H NMR of crude product **2-50**, related Figure 2

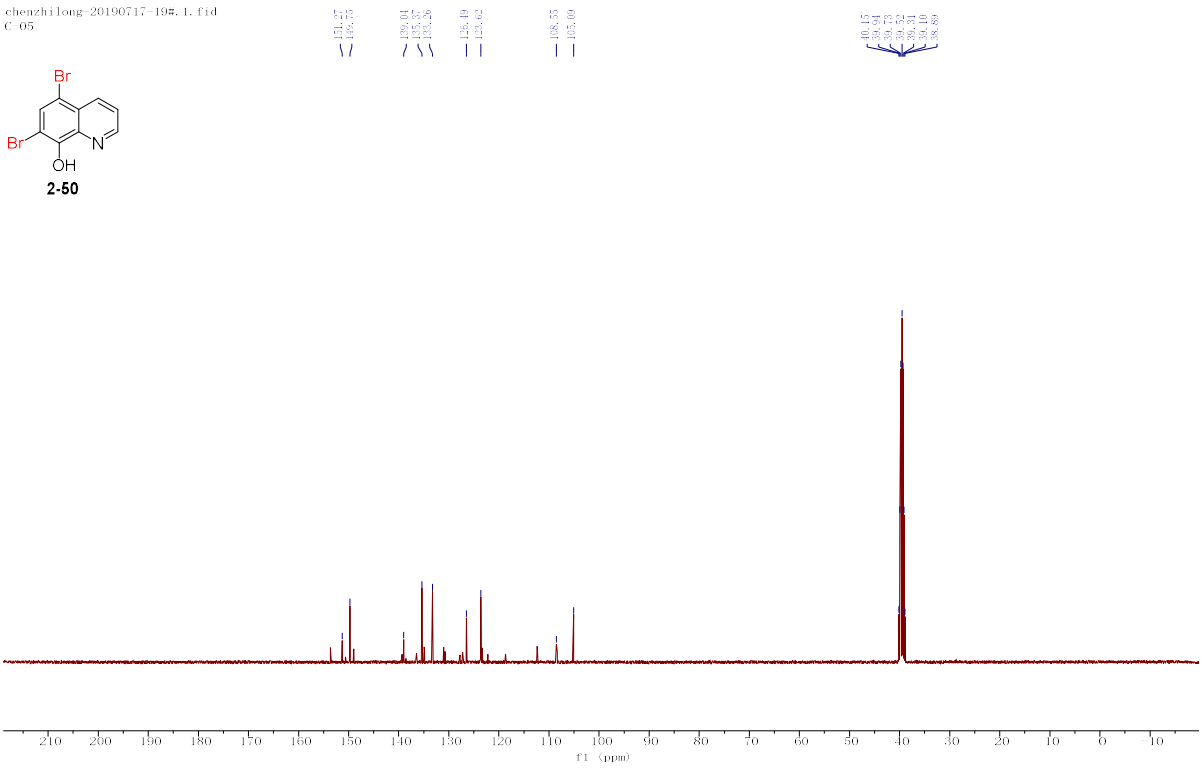

Figure S133. ^{13}C NMR of crude product **2-50**, related Figure 2

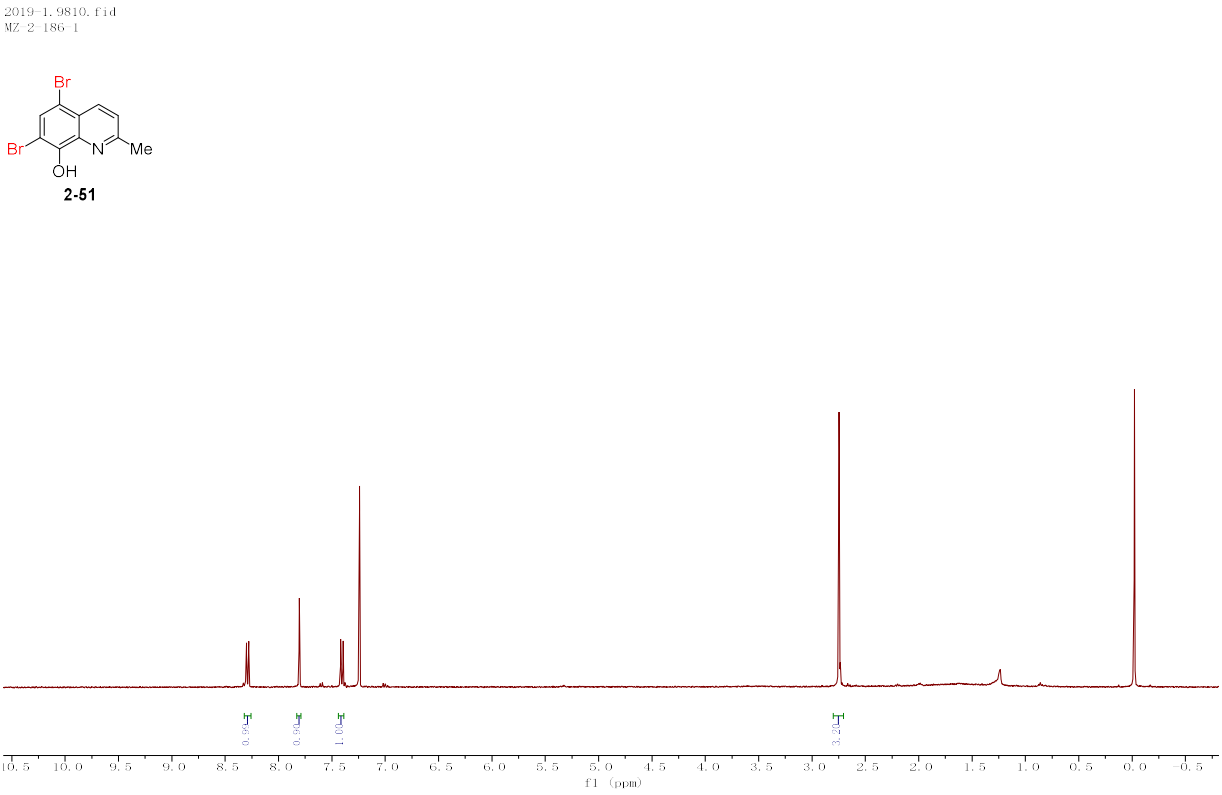

Figure S134. ^{1}H NMR of crude product **2-51**, related Figure 2

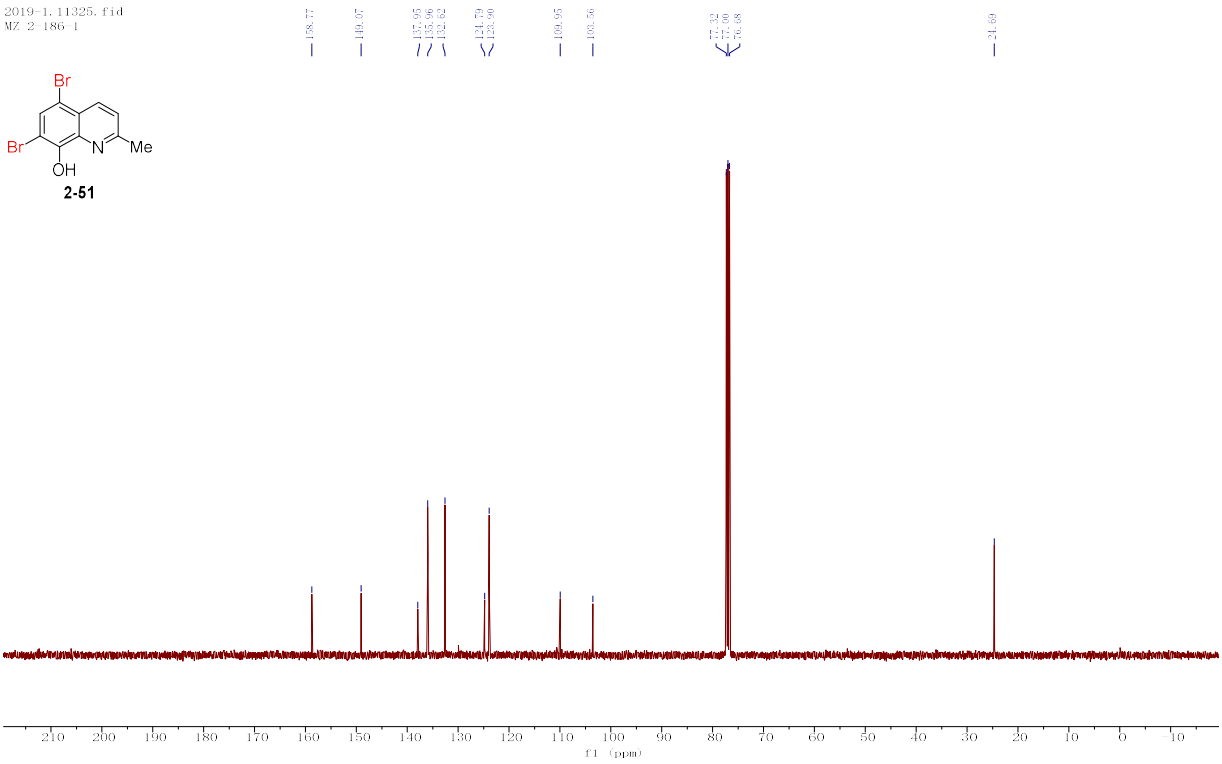

Figure S135. ^{13}C NMR of crude product **2-51**, related Figure 2

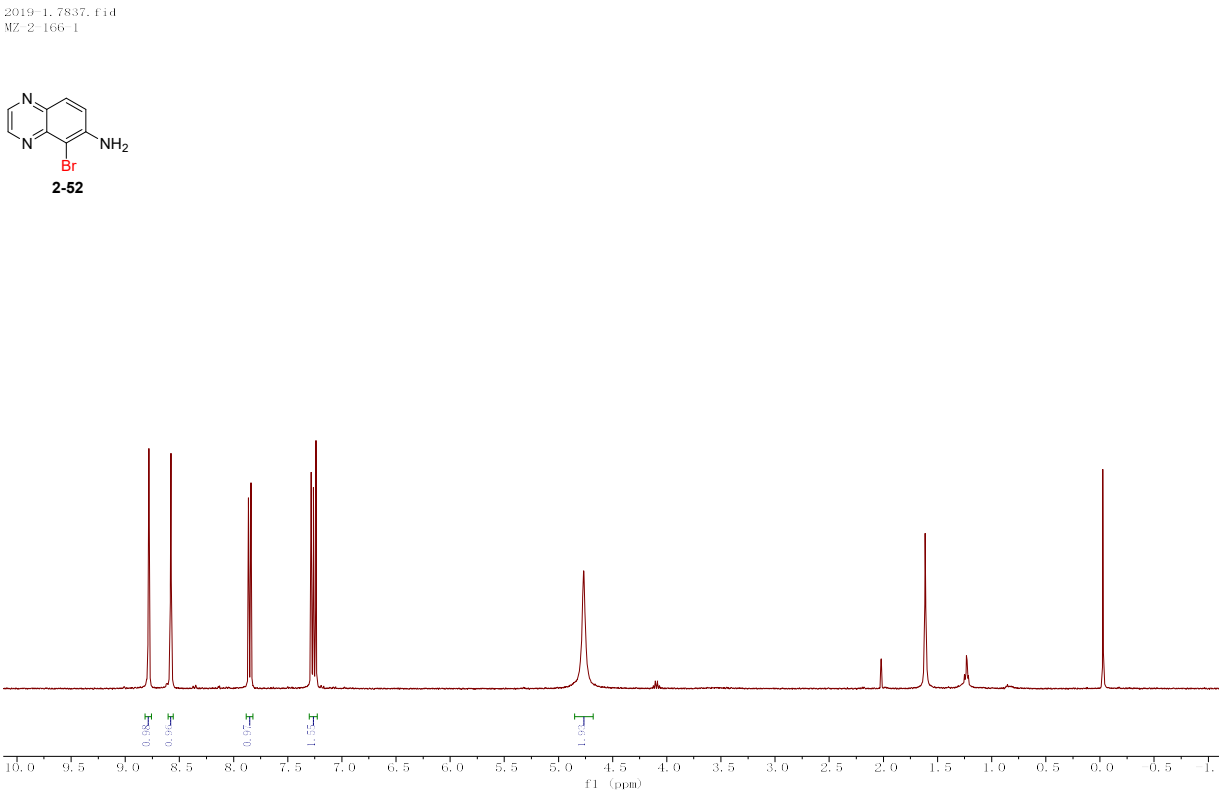

Figure S136. ^{1}H NMR of crude product **2-52**, related Figure 2

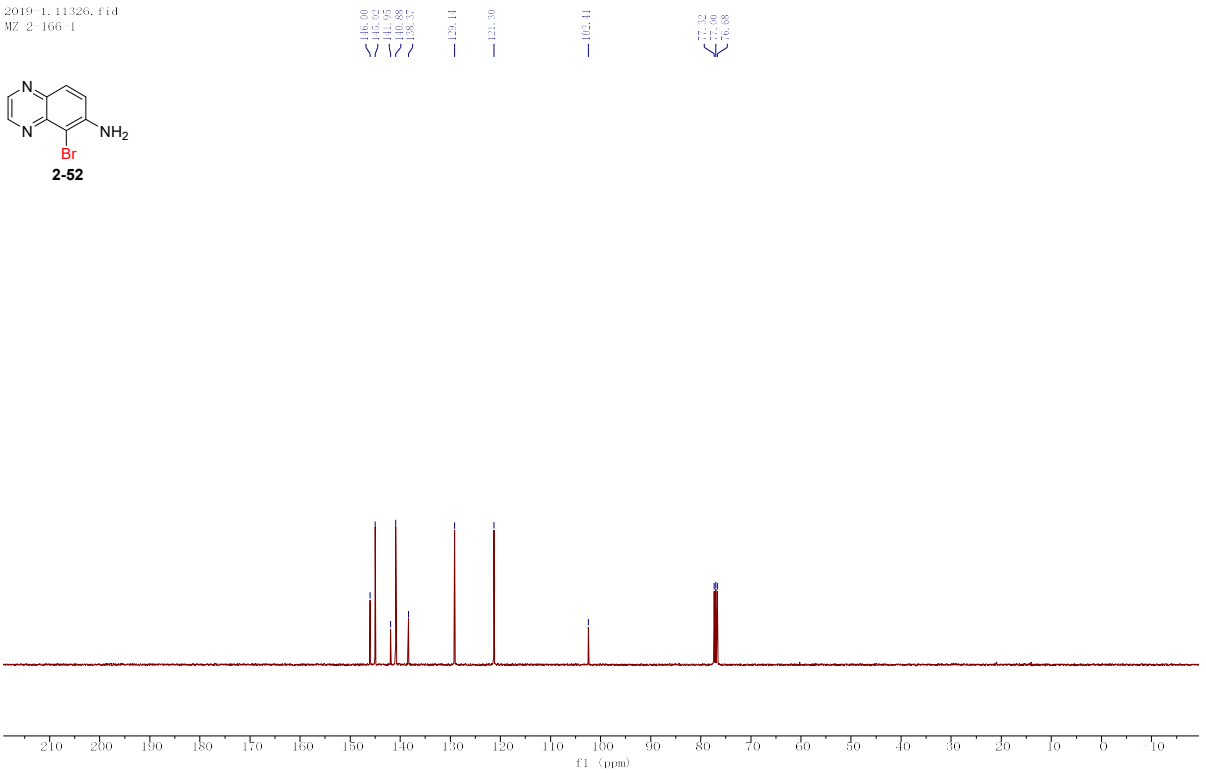

Figure S137. ^{13}C NMR of crude product **2-52**, related Figure 2

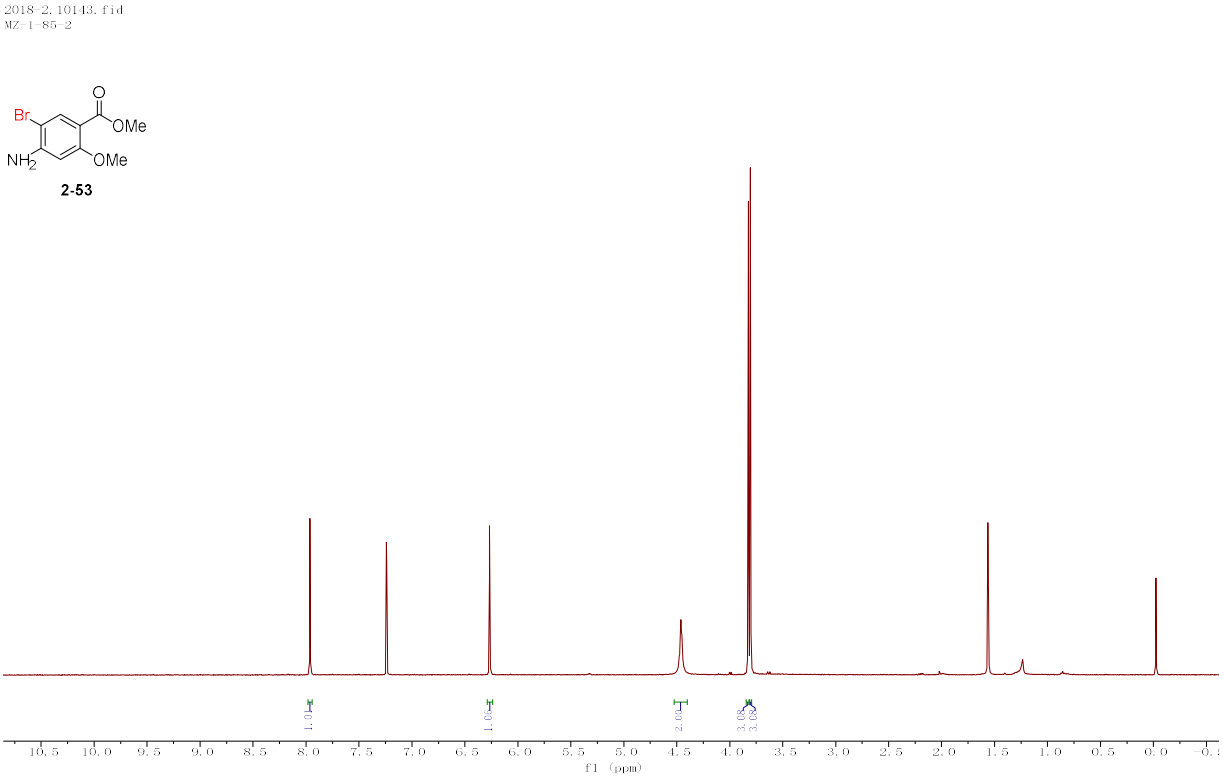

Figure S138. ^{1}H NMR of crude product **2-53**, related Figure 2

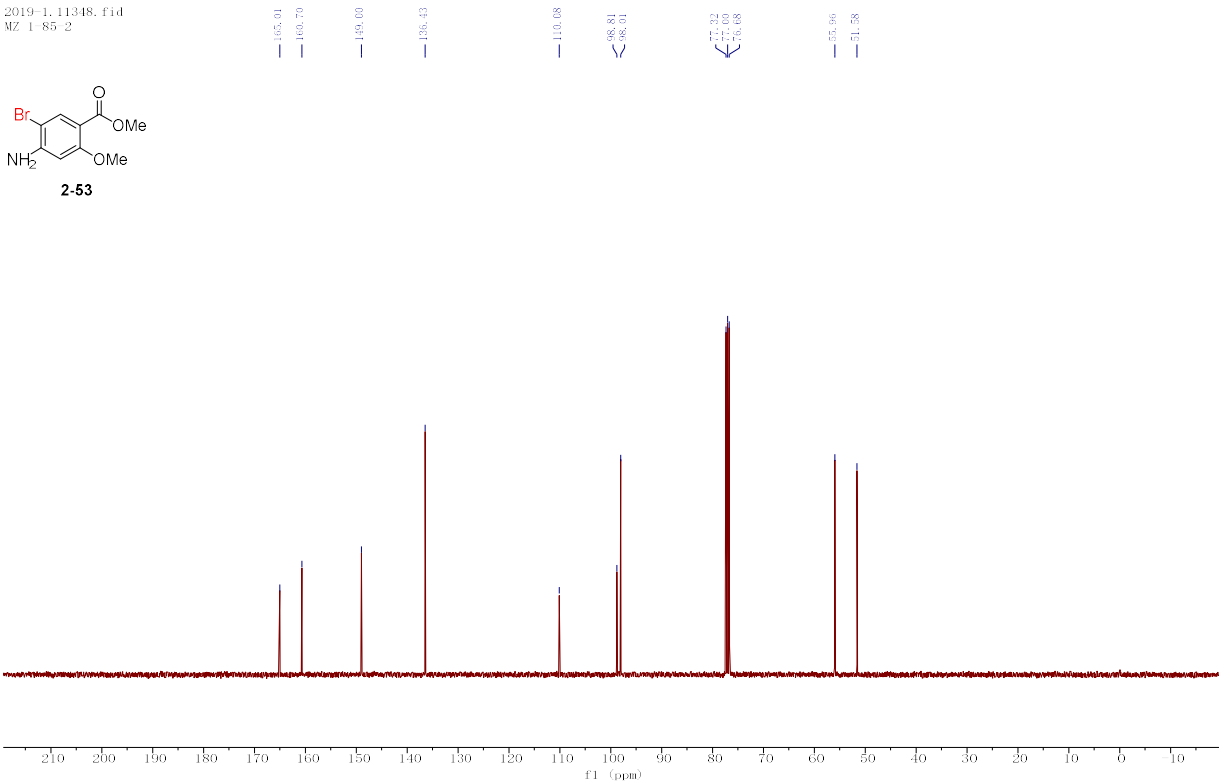

Figure S139. ^{13}C NMR of crude product **2-53**, related Figure 2

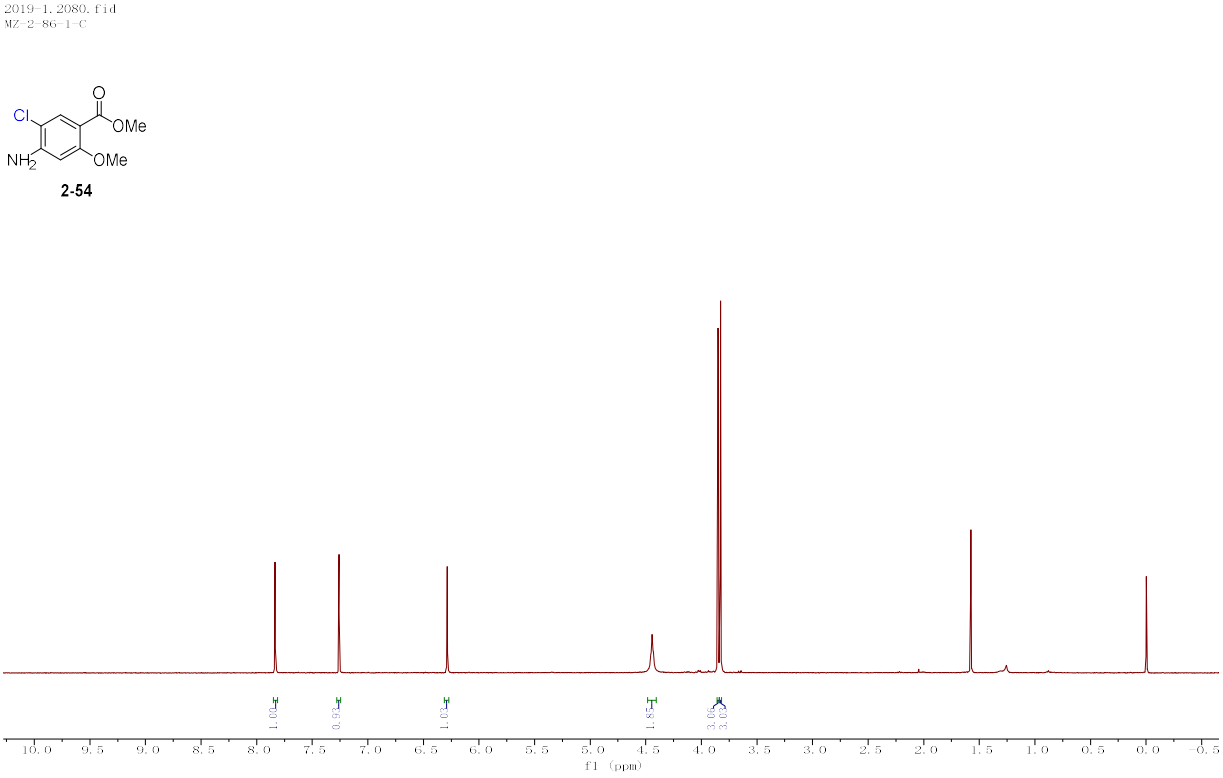

Figure S140. ^{1}H NMR of crude product **2-54**, related Figure 2

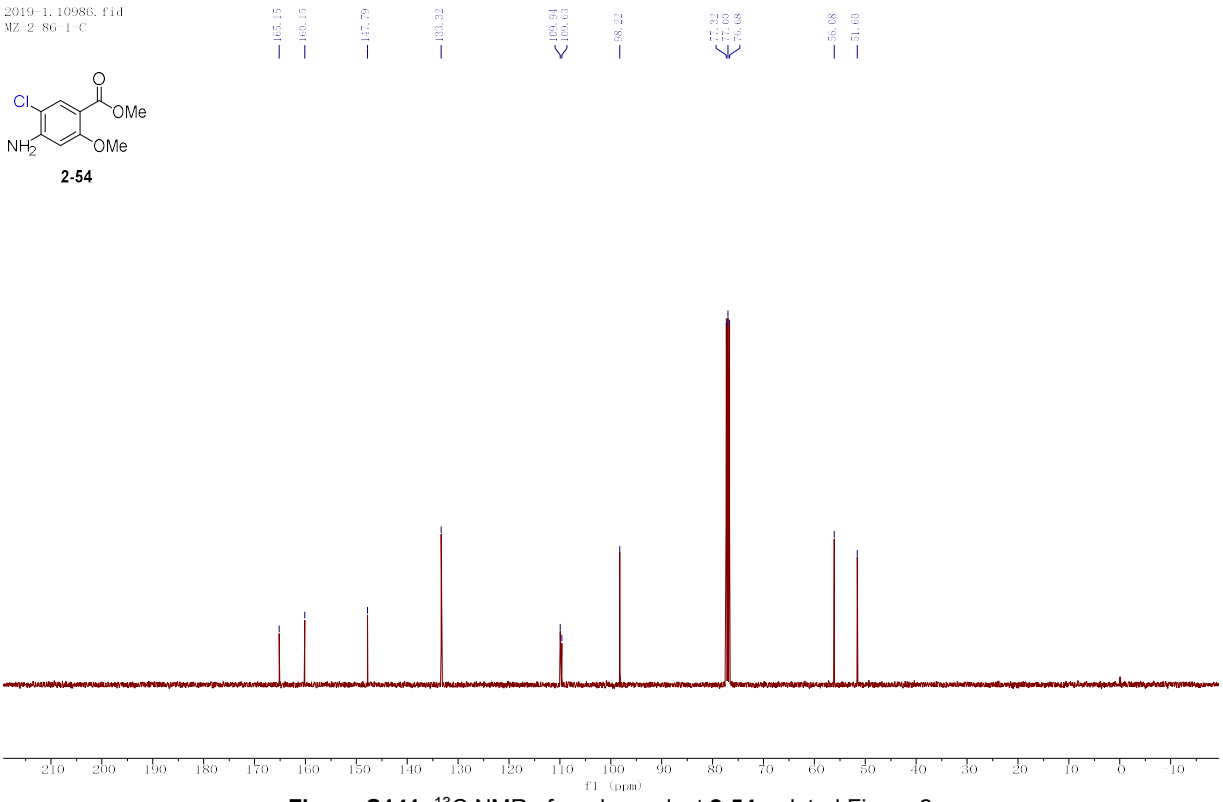

Figure S141. ^{13}C NMR of crude product **2-54**, related Figure 2

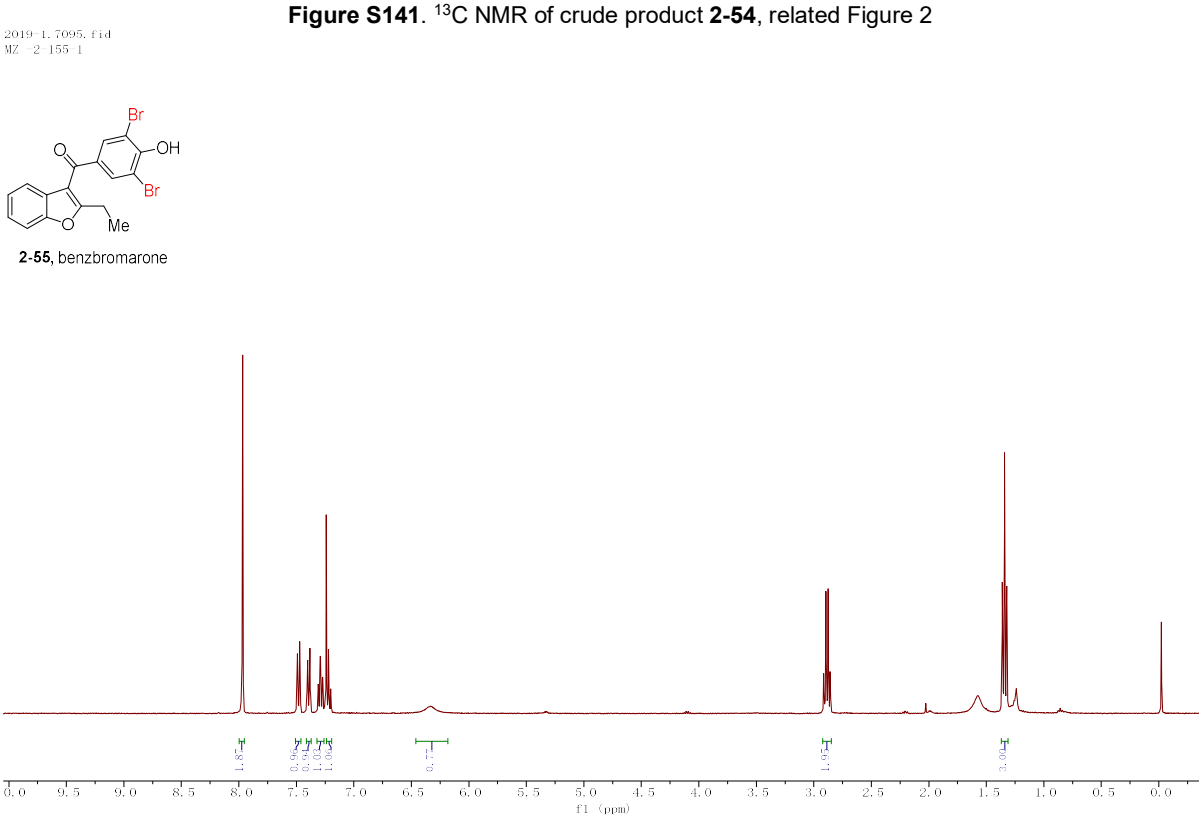

Figure S142. ^{1}H NMR of crude product **2-55**, related Figure 2

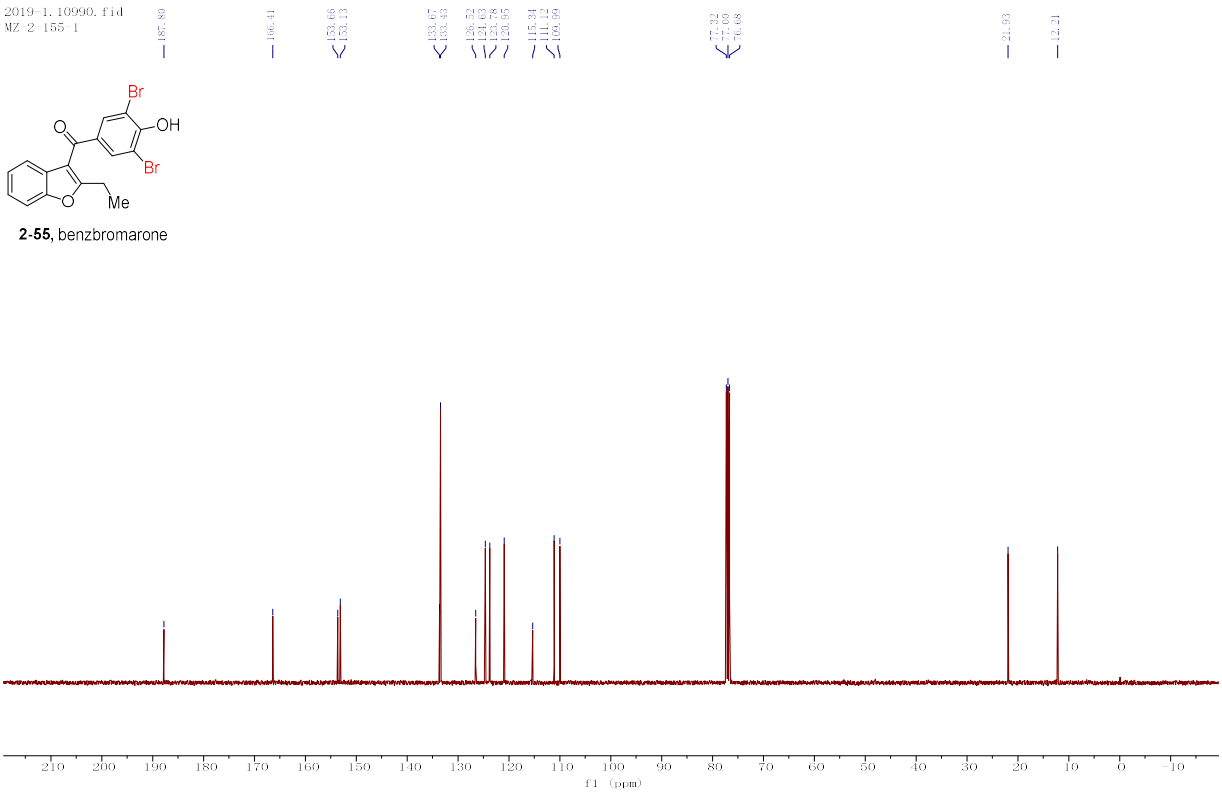

2-55, benzbromarone

Figure S143. ^{13}C NMR of crude product **2-55**, related Figure 2

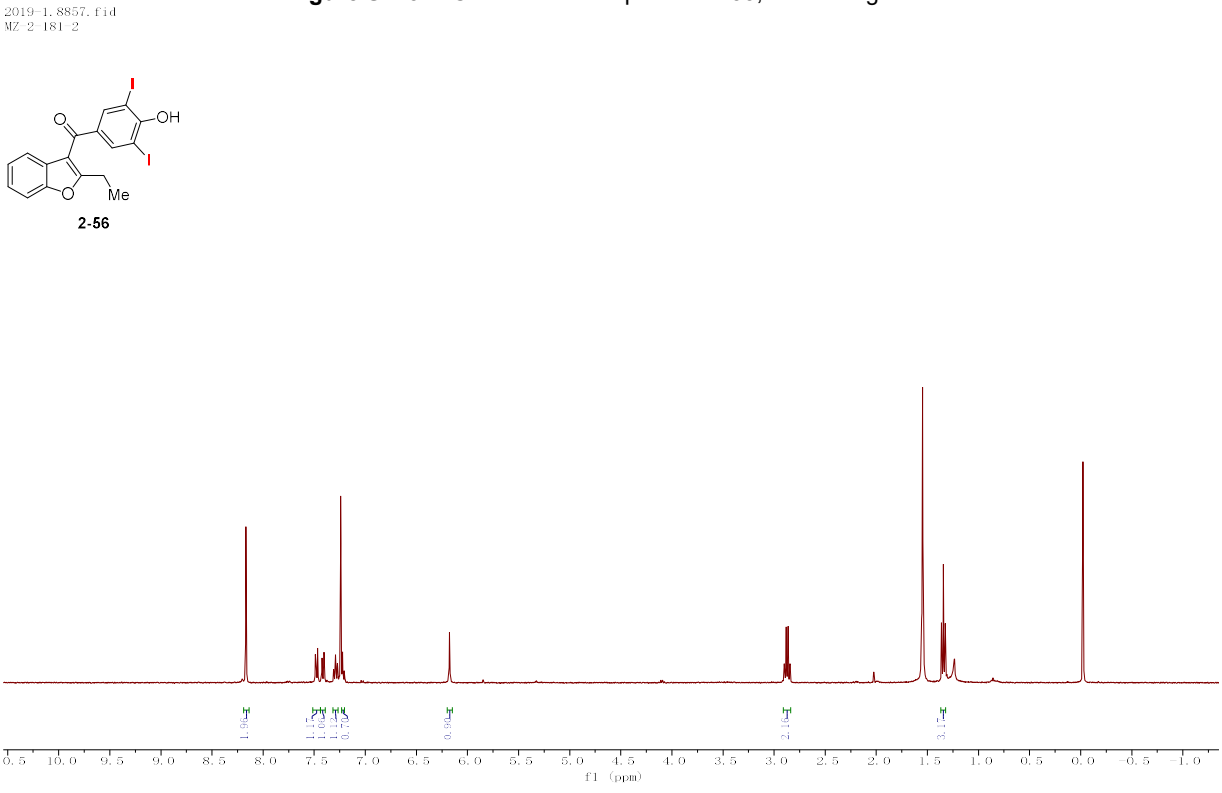

2-56

Figure S144. ^{1}H NMR of crude product **2-56**, related Figure 2

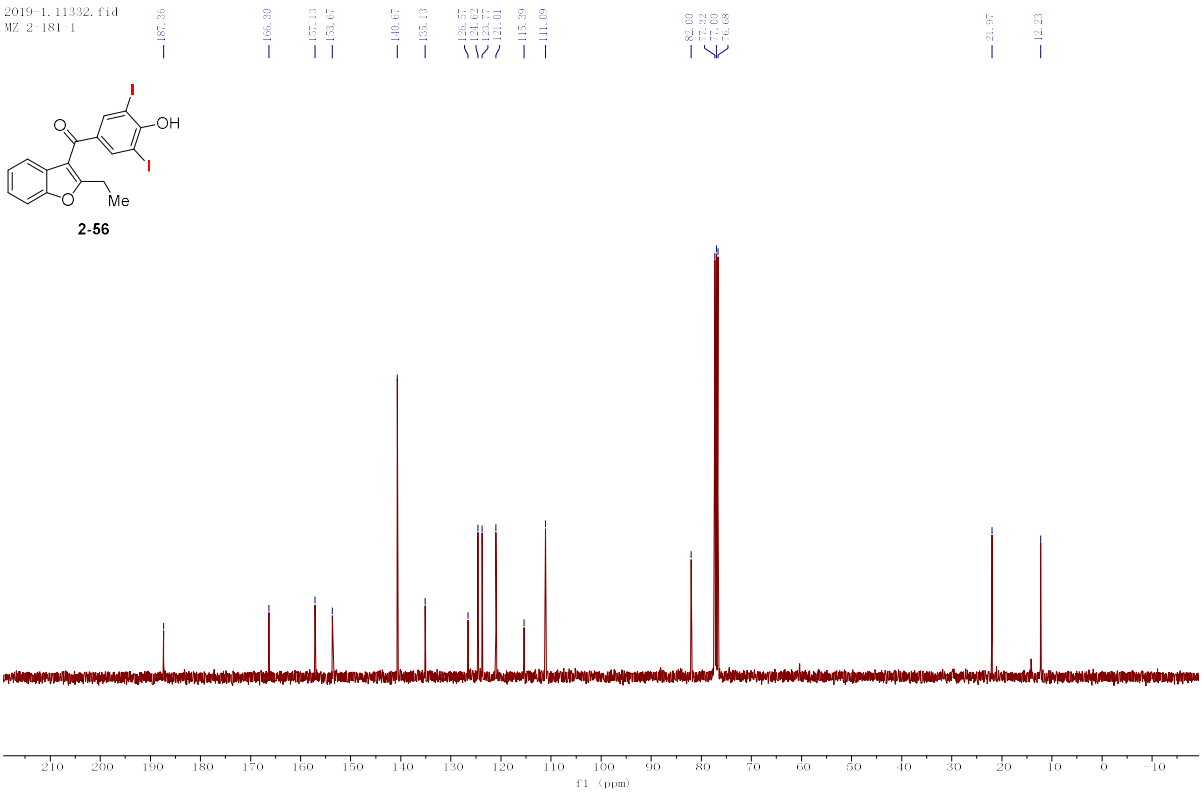

Figure S145. ^{13}C NMR of crude product **2-56**, related Figure 2

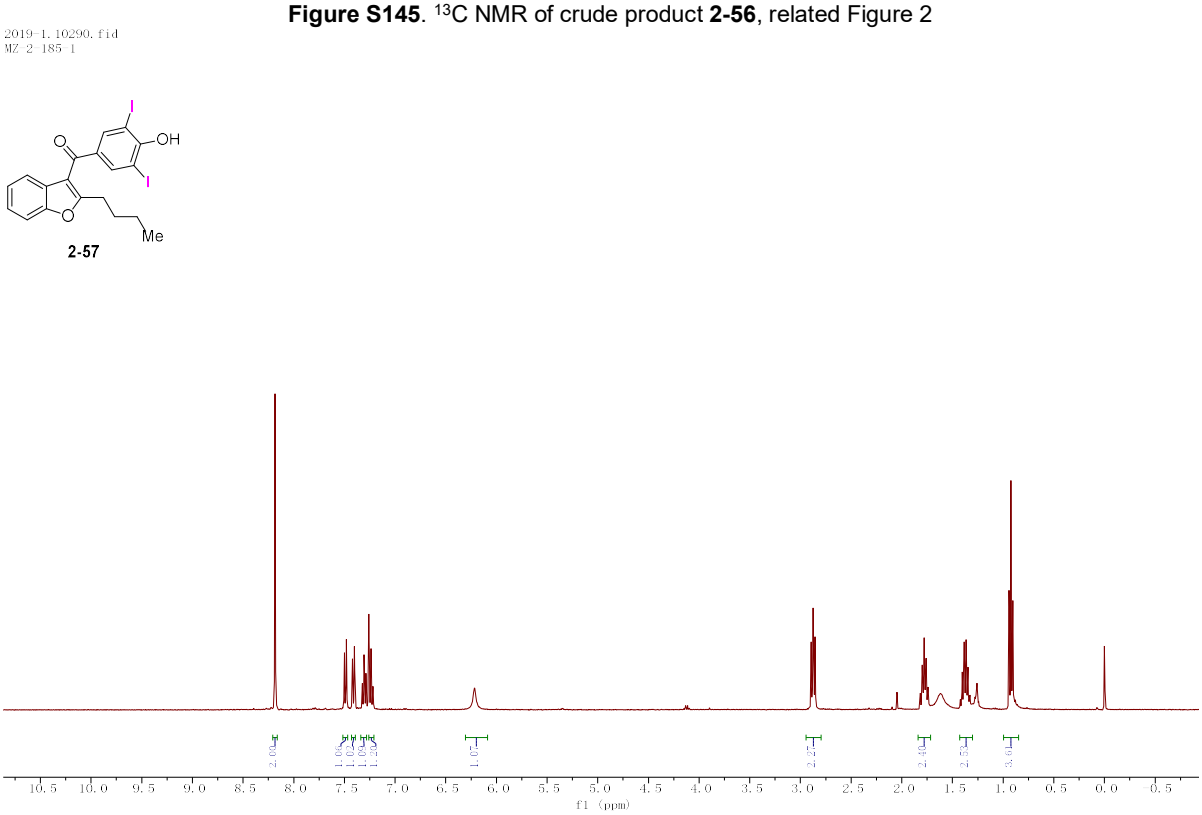

Figure S146. ^{1}H NMR of crude product **2-57**, related Figure 2

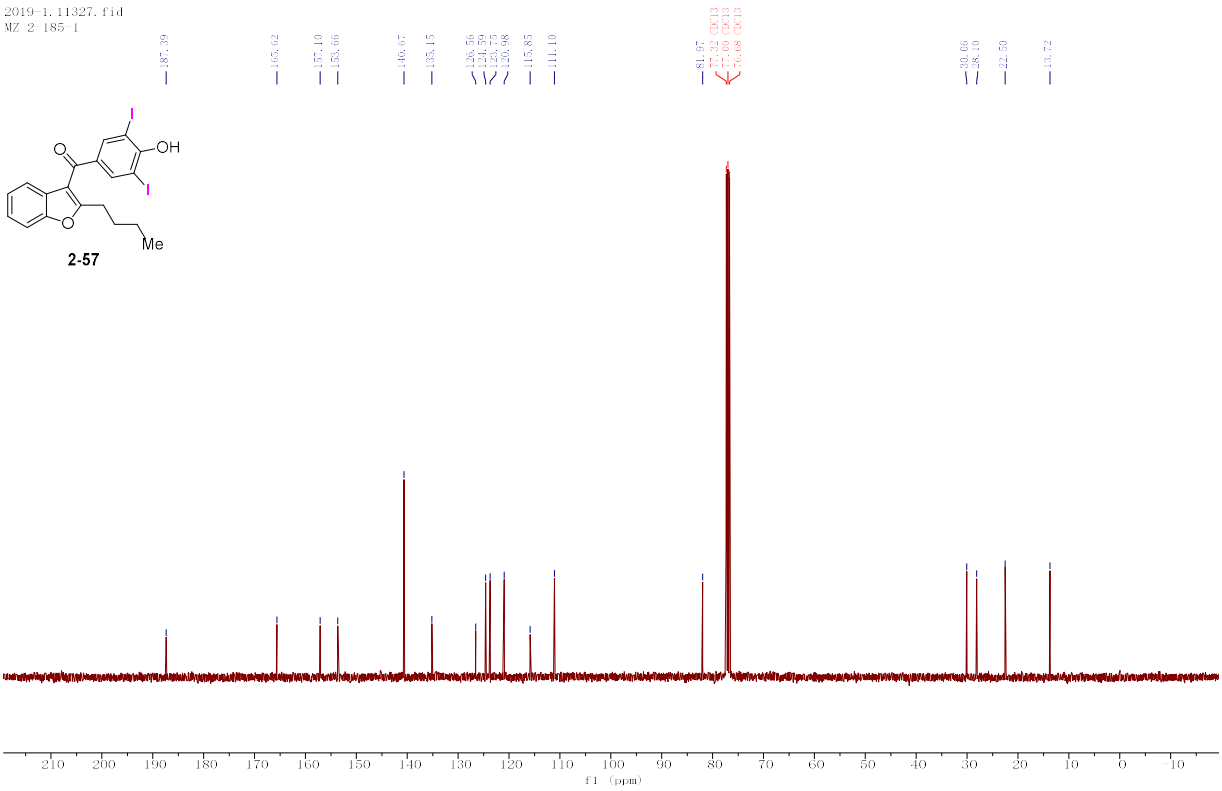

Figure S147. ^{13}C NMR of crude product **2-57**, related Figure 2

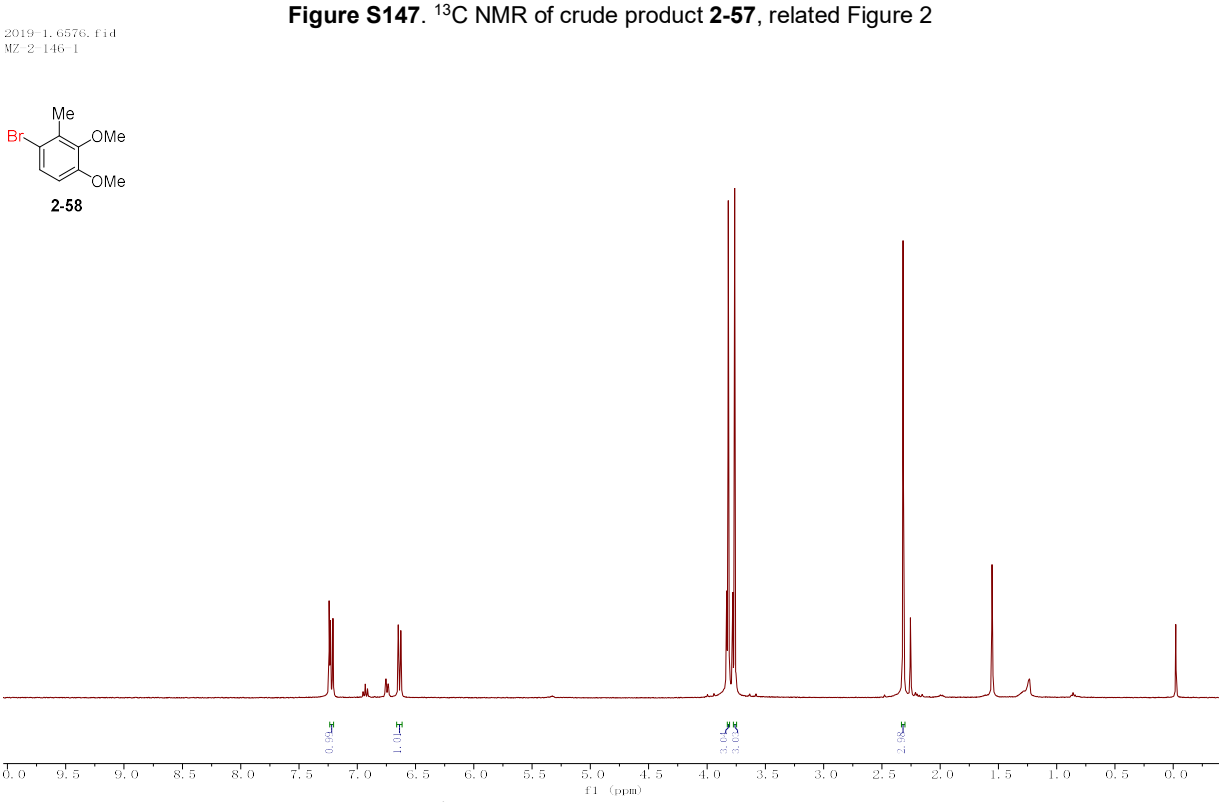

Figure S148. ^{1}H NMR of crude product **2-58**, related Figure 3

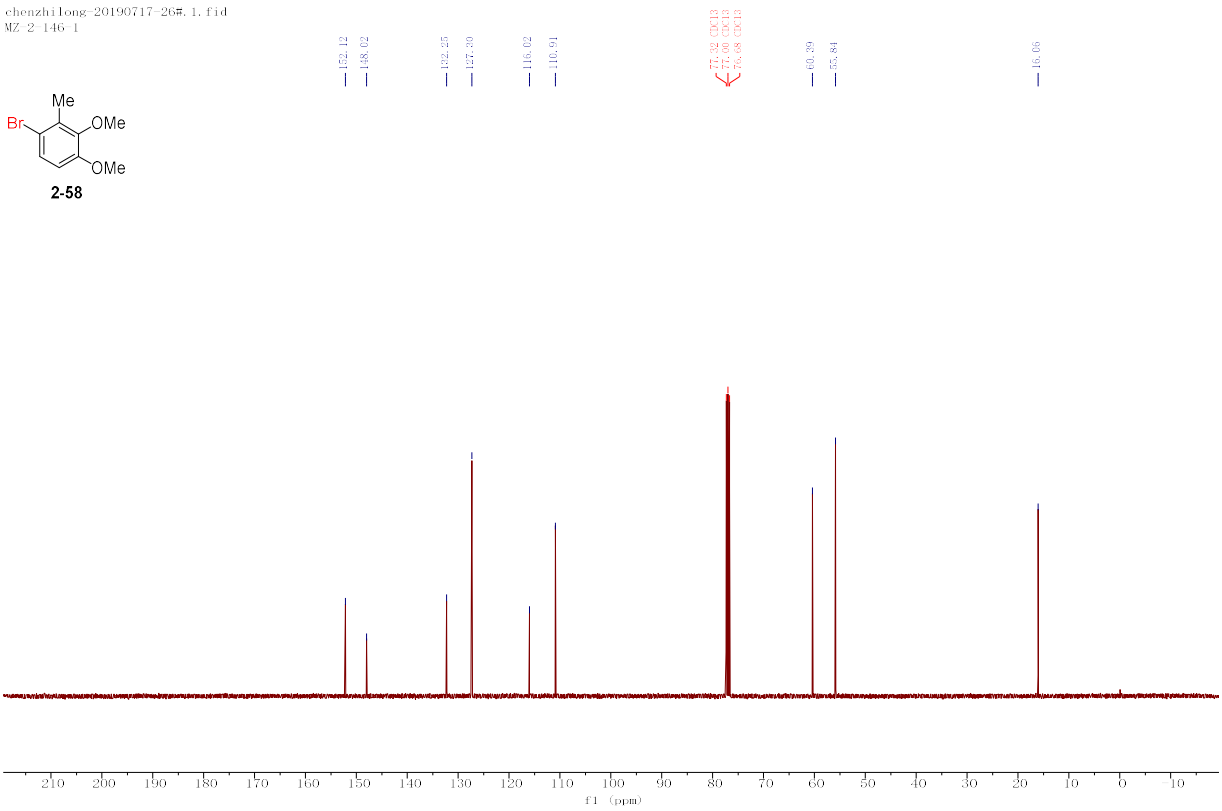

Figure S149. ^{13}C NMR of crude product **2-58**, related Figure 3

Data S1. Characterization of intermediates and products (related to Table 2, 3 and 4, Figure 2)

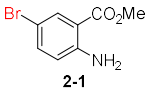

Methyl 2-amino-5-bromobenzoate (**2-1**) (Lehmann, 2007) was obtained as brown solid (192 mg, 91% yield) according to **General Procedure A** for 12h.

221g (93% yield) product **2-1** was isolated as a mixture with **2-1B** and **2-1C** when scaled up to 1.0 mol scale according to **General Procedure E**.

^{1}H NMR (400 MHz, Chloroform-*d*) δ 7.95 (d, *J* = 2.5 Hz, 1H), 7.30 (dd, *J* = 8.8, 2.3 Hz, 1H), 6.54 (d, *J* = 8.8 Hz, 1H), 5.73 (brs, 2H), 3.85 (s, 3H)

^{13}C NMR (101 MHz, Chloroform-*d*) δ 167.5, 149.3, 136.8, 133.4, 118.4, 112.1, 107.4, 51.8

Compounds **2-1B** and **2-1C** was obtained as mixture, (22 mg, **2-1B**: **2-1C** = 5:2 by ^{1}H NMR)

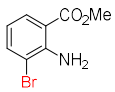

2-1B

Methyl 2-amino-3-bromobenzoate (**2-1B**) (Pierre et al., 2011)

^{1}H NMR (400 MHz, Chloroform-*d*) δ 7.85 (dd, *J* = 8.0, 1.5 Hz, 1H), 7.57 (dd, *J* = 7.8, 1.5 Hz, 1H), 6.53 (t, *J* = 8.0 Hz, 1H), 6.34 (brs, 2H), 3.88 (s, 3H)

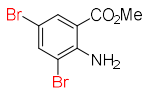

2-1C

Methyl 2-amino-3,5-dibromobenzoate (**2-1C**) (Zhou and Song, 2018)

^{1}H NMR (400 MHz, Chloroform-*d*) δ 7.97 (d, *J* = 2.3 Hz, 1H), 7.68 (d, *J* = 2.3 Hz, 1H), 6.34 (brs, 2H), 3.88 (s, 3H)

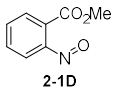

2-1D

Methyl 2-nitrosobenzoate (**2-1D**) (Leronimo et al., 2018) was obtained as a white solid as byproducts in condition screening.

^{1}H NMR (400 MHz, Chloroform-*d*) δ 7.92 (dd, *J* = 7.8, 1.5 Hz, 1H), 7.75 (dd, *J* = 7.4, 1.7 Hz, 1H), 7.68 (td, *J* = 7.4, 1.4 Hz, 1H), 7.63 (td, *J* = 7.6, 1.8 Hz, 1H), 3.93 (s, 3H)

^{13}C NMR (101 MHz, Chloroform-*d*) δ 165.8, 132.9, 131.7, 129.8, 127.5, 123.9, 53.2

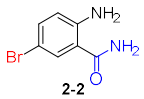

2-2

2-amino-5-bromobenzamide (**2-2**) (Latham et al., 2016) was obtained as yellow solid (112 mg, 52% yield) according to **General Procedure A** for 18.5h.

^{1}H NMR (400 MHz, DMSO-d_6) δ 7.89-7.77 (m, 1H), 7.69 (d, *J* = 2.4 Hz, 1H), 7.25 (dd, *J* = 8.8, 2.4 Hz, 1H), 7.18 (brs, 1H), 6.70 (brs, 2H), 6.65 (d, *J* = 8.8 Hz, 1H)

^{13}C NMR (101 MHz, DMSO-d_6) δ 170.0, 149.4, 134.4, 131.1, 118.5, 115.2, 104.7

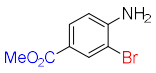

2-3

Methyl 4-amino-3-bromobenzoate (**2-3**) (Song et al., 2016) was obtained as yellow solid (194 mg, 85% yield) according to **General Procedure A** for 35h.

Product **2-3** was obtained in water (205 mg, 89% yield) according to **General Procedure B** for 24h.

100g-scale reaction afforded 107 g (94% yield, 0.5 mol scale) product **2-3** according to **General Procedure E**.

^{1}H NMR (400 MHz, Chloroform-*d*) δ 8.12 (d, *J* = 1.9 Hz, 1H), 7.79 (dd, *J* = 8.4, 1.9 Hz, 1H), 6.73 (d, *J* = 8.5 Hz, 1H), 4.51 (brs, 2H), 3.86 (s, 3H)

^{13}C NMR (101 MHz, Chloroform-*d*) δ 166.0, 148.1, 134.5, 130.2, 120.7, 114.2, 107.8, 51.8

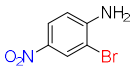

2-4

2-bromo-4-nitroaniline (**2-4**) (Kumar et al., 2011) was obtained as yellow solid (162 mg, 75% yield, 90% yield brsm; 23 mg starting material was recycled, 17% yield) according to **General Procedure A** for 24h.

^{1}H NMR (400 MHz, Chloroform-*d*) δ 8.38 (d, *J* = 2.5 Hz, 1H), 8.04 (dd, *J* = 9.0, 2.5 Hz, 1H), 6.74 (d, *J* = 8.9 Hz, 1H), 4.82 (brs, 2H)

^{13}C NMR (101 MHz, Chloroform-*d*) δ 149.9, 138.9, 129.2, 124.9, 113.4, 106.9

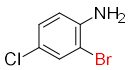

2-5

2-bromo-4-chloroaniline (**2-5**) (Gayakwad et al., 2019) was obtained as yellow solid (708 mg, 69% yield, 5.0 mmol scale) according to **General Procedure A** for 24h.

^{1}H NMR (400 MHz, Chloroform-*d*) δ 7.40 (d, *J* = 2.3 Hz, 1H), 7.06 (dd, *J* = 8.6, 2.4 Hz, 1H), 6.67 (d, *J* = 8.6 Hz, 1H), 4.02 (s, 2H)

^{13}C NMR (101 MHz, Chloroform-*d*) δ 146.6, 134.6, 133.9, 116.4, 114.9, 109.7

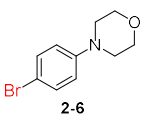

2-6

4-(4-bromophenyl) morpholine (**2-6**) (Song et al., 2015) was obtained as a white solid (139 mg, 57% yield) according to **General Procedure A** for 24h.

^{1}H NMR (400 MHz, Chloroform-*d*) δ 7.38-7.33 (m, 2H), 6.81-6.75 (m, 2H), 3.88-3.82 (m, 4H), 3.15-3.09 (m, 4H).

^{13}C NMR (101 MHz, Chloroform-*d*) δ 150.3, 131.9, 117.3, 112.1, 66.7, 49.1

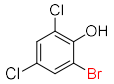

2-7

2-bromo-4,6-dichlorophenol (**2-7**) (Xiong and Yeung, 2018) was obtained as a white solid (157 mg, 65% yield) according to **General Procedure A** for 51h.

Product **2-7** was obtained in water (184 mg, 76% yield) according to **General Procedure B** for 24h.

^{1}H NMR (400 MHz, Chloroform-*d*) δ 7.40 (d, *J* = 2.4 Hz, 1H), 7.30 (d, *J* = 2.4 Hz, 1H), 5.85 (brs, 1H)

^{13}C NMR (101 MHz, Chloroform-*d*) δ 147.7, 130.9, 128.7, 125.8, 121.2, 110.4

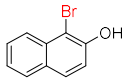

2-8

1-bromonaphthalen-2-ol (**2-8**) (Song et al., 2015) was obtained as a yellow solid (89 mg, 54% yield) according to **General Procedure A** for 15.5h.

^{1}H NMR (400 MHz, Chloroform-*d*) δ 8.10 (dt, *J* = 8.5, 0.9 Hz, 1H), 7.86-7.80 (m, 1H), 7.77 (d, *J* = 8.8 Hz, 1H), 7.63 (ddd, *J* = 8.4, 6.9, 1.3 Hz, 1H), 7.45 (ddd, *J* = 8.1, 6.9, 1.2 Hz, 1H), 7.34 (d, *J* = 8.8 Hz, 1H)

^{13}C NMR (101 MHz, Chloroform-*d*) δ 150.5, 132.3, 129.6, 129.3, 128.2, 127.8, 125.3, 124.1, 117.1, 106.1

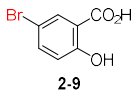

2-9

5-bromo-2-hydroxybenzoic acid (**2-9**) (Oberhauser, 1997) was obtained as white solid (193 mg, 70% yield) according to **General Procedure A** for 18h.

^{1}H NMR (400 MHz, Chloroform-*d*) δ 10.19 (brs, 1H), 9.46 (brs, 1H), δ 8.06 (d, *J* = 2.5 Hz, 1H), 7.63 (dd, *J* = 8.9, 2.5 Hz, 1H), 6.95 (d, *J* = 8.9 Hz, 1H)

^{13}C NMR (101 MHz, DMSO-d_6) δ 170.5, 160.1, 137.9, 132.1, 119.7, 115.1, 109.9

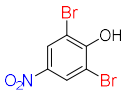

2-10

2,6-dibromo-4-nitrophenol (**2-10**) (Jiang and Yang, 2016) was obtained as a yellow solid (275 mg, 93% yield) according to **General Procedure A** with 2.2 equivalent of NaBr and HOAc for 22h.

^{1}H NMR (400 MHz, Chloroform-*d*) δ 8.39 (s, 2H)

^{13}C NMR (101 MHz, Chloroform-*d*) δ 155.0, 141.5, 127.9, 109.6

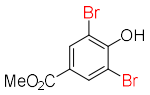

2-11

Methyl 3,5-dibromo-4-hydroxybenzoate (**2-11**) (Kansal et al., 2016) was obtained as a white solid (265 mg, 86% yield) according to **General Procedure A** with 2.2 equivalent of NaBr and HOAc for 60h.

136 g (88% yield) product **2-11** was isolated in 0.5 mol scale according to **General Procedure E**.

^{1}H NMR (400 MHz, Chloroform-*d*) δ 8.13 (s, 2H), 6.27 (s, 1H), 3.88 (s, 3H)

^{13}C NMR (101 MHz, Chloroform-*d*) δ 164.5, 153.2, 133.7, 124.8, 109.7, 52.5

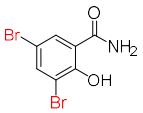

2-12

3,5-dibromo-2-hydroxybenzamide (**2-12**) (Capilato et al., 2017) was obtained as a yellow solid (243 mg, 83% yield) according to **General Procedure A** with 2.2 equivalent of NaBr and HOAc for 28h.

^{1}H NMR (400 MHz, DMSO-d_6) δ 14.29 (s, 1H), 8.72 (s, 1H), 8.33 (s, 1H), 8.15 (d, *J* = 2.3 Hz, 1H), 7.97 (d, *J* = 2.3 Hz, 1H)

^{13}C NMR (101 MHz, DMSO-d_6) δ 171.0, 157.8, 138.4, 129.6, 116.2, 112.1, 109.3

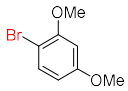

2-13

1-bromo-2,4-dimethoxybenzene (**2-13**) (Song et al., 2015) was obtained as a white solid (186 mg, 86% yield) according to **General Procedure A** for 24h.

^{1}H NMR (400 MHz, Chloroform-*d*) δ 7.39 (d, *J* = 8.7 Hz, 1H), 6.47 (d, *J* = 2.7 Hz, 1H), 6.38 (dd, *J* = 8.7, 2.7 Hz, 1H), 3.85 (s, 3H), 3.78 (s, 3H)

^{13}C NMR (101 MHz, Chloroform-*d*) δ 160.2, 156.5, 133.1, 105.8, 102.4, 99.9, 56.1, 55.5

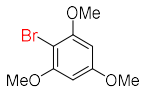

2-14

2-bromo-1,3,5-trimethoxybenzene (**2-14**) (Song et al., 2015) was obtained as a white solid (242 mg, 98% yield) according to **General Procedure A** for 24h.

Product **2-14** was also obtained in water (228 mg, 92% yield) according to **General Procedure B**.

123 g (99% yield) product **2-14** was isolated in 0.5 mol scale reaction according to **General Procedure E.**

^{1}H NMR (400 MHz, Chloroform-*d*) δ 6.15 (s, 2H), 3.86 (s, 6H), 3.80 (s, 3H)

^{13}C NMR (101 MHz, Chloroform-*d*) δ 160.4, 157.4, 92.0, 91.6, 56.3, 55.5

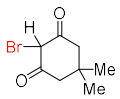

2-15

2,2-dibromo-5,5-dimethylcyclohexane-1,3-dione (**2-15**) (Podgoršek et al., 2017) was obtained as a brown solid (136 mg, 62% yield) according to **General Procedure A** for 24h.

^{1}H NMR (400 MHz, Chloroform-*d*) δ 2.49 (s, 4H), 1.15 (s, 6H)

^{13}C NMR (101 MHz, Chloroform-*d*) δ 178.4, 60.5, 44.7, 32.3, 27.8

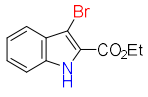

2-16

Ethyl 3-bromo-1*H*-indole-2-carboxylate (2-16) (Song et al., 2015) was obtained as a yellow solid (217 mg, 81% yield) according to **General Procedure A** for 16h.

^{1}H NMR (400 MHz, DMSO-d_6) δ 12.28 (brs, 1H), 7.57 (d, *J* = 1.2 Hz, 1H), 7.55 (d, *J* = 1.2 Hz, 1H), 7.36 (ddd, *J* = 8.0, 7.0, 1.2 Hz, 1H), 7.23-7.15 (ddd, *J* = 8.0, 7.0, 1.2 Hz, 1H), 4.39 (q, *J* = 7.1 Hz, 2H), 1.37 (t, *J* = 7.1 Hz, 3H).

2-17

3-bromo-1*H*-pyrrolo[2,3-b] pyridine (**2-17**) (Song et al., 2015) was obtained as a yellow solid (146 mg, 74% yield) according to **General Procedure A** for 40h.

^{1}H NMR (400 MHz, Chloroform-*d*) δ 10.96 (brs, 1H), 8.37 (dd, *J* = 4.8, 1.5 Hz, 1H), 7.93 (dd, *J* = 7.9, 1.6 Hz, 1H), 7.41 (s, 1H), 7.19 (dd, *J* = 7.9, 4.8 Hz, 1H)

^{13}C NMR (101 MHz, DMSO-d_6) δ 146.4, 143.2, 127.4, 126.0, 119.3, 116.5, 87.5

2-18

3-bromo-1*H*-pyrrolo[3,2-c] pyridine (**2-18**) (Gallou et al., 2007) was obtained as a brown solid (143 mg, 73% yield) according to **General Procedure A** for 18h.

^{1}H NMR (400 MHz, DMSO-d_6) δ 11.89 (brs, 1H), 8.70 (s, 1H), 8.25 (d, *J* = 5.8 Hz, 1H), 7.67 (s, 1H), 7.42 (dd, *J* = 5.8, 1.1Hz, 1H)

^{13}C NMR (101 MHz, DMSO-d_6) δ 141.7, 141.6, 139.5, 126.8, 123.7, 107.6, 88.2

2-19

5-bromo-7*H*-pyrrolo[2,3-d] pyrimidine (**2-19**) (Jonckers et al., 2016) was obtained as a brown solid (142 mg, 72% yield) according to **General Procedure A** for 48h.

^{1}H NMR (400 MHz, DMSO-d_6) δ 12.6 (s, 1H), 8.9 (d, *J* = 0.8 Hz, 1H), 8.8 (s, 1H), 7.8 (d, *J* = 2.5 Hz, 1H)

^{13}C NMR (101 MHz, DMSO-d_6) δ 151.9, 150.4, 147.8, 127.0, 117.4, 86.5

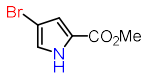

2-20

Methyl 4-bromo-1*H*-pyrrole-2-carboxylate (**2-20**) (Wischang et al., 2011) was obtained as a white solid (87 mg, 43% yield).

^{1}H NMR (400 MHz, Chloroform-*d*) δ 9.25 (brs, 1H), 6.93 (dd, *J* = 2.9, 1.6 Hz, 1H), 6.86 (dd, *J* = 2.7, 1.6 Hz, 1H), 3.84 (s, 3H)

^{13}C NMR (101 MHz, Chloroform-*d*) δ 160.9, 123.0, 122.8, 116.9, 97.8, 51.8

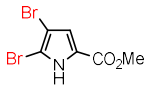

2-20B

Methyl 4,5-dibromo-1*H*-pyrrole-2-carboxylate (**2-20B**) (Wischang and Hartung, 2011) was obtained as a white solid (24 mg, 9% yield).

^{1}H NMR (400 MHz, Chloroform-*d*) δ 9.45 (s, 1H), 6.86 (d, *J* = 2.9 Hz, 1H), 3.85 (s, 3H)

^{13}C NMR (101 MHz, Chloroform-*d*) δ 160.4, 123.6, 118.0, 107.3, 100.6, 52.1

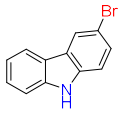

2-21

3-bromo-9*H*-carbazole (**2-21**) (Yang et al.,2018) was obtained as a white solid (90.5 mg, 38% yield; 79% yield based on starting material (brsm); starting material was recycled in 87 mg, 52% yield) according to **General Procedure A** for 22h.

^{1}H NMR (400 MHz, Chloroform-*d*) δ 8.17 (d, *J* = 1.9 Hz, 1H), 8.07 (brs, 1H), 8.02-7.98 (m, 1H), 7.48 (dd, *J* = 8.6, 1.9 Hz, 1H), 7.45-7.39 (m, 2H), 7.29 (d, *J* = 8.6 Hz, 1H), 7.26-7.20 (m, 1H)

^{13}C NMR (101 MHz, DMSO-d_6) δ 140.1, 138.4, 127.9, 126.4, 124.4, 122.8, 121.5, 120.7, 119.0, 112.9, 111.2, 110.6

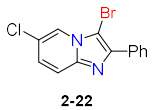

2-22

3-bromo-6-chloro-2-phenylimidazo[1,2-a] pyridine (**2-22**) (Yuan et al., 2019) was obtained as a yellow solid (283 mg, 92% yield) according to **General Procedure A** for 30h.

^{1}H NMR (400 MHz, Chloroform-*d*) δ 8.22 (d, *J* = 2.0 Hz, 1H), 8.09 (dd, *J* = 7.3, 1.8 Hz, 2H), 7.57 (d, *J* = 9.5 Hz, 1H), 7.47 (dd, *J* = 8.4, 6.8 Hz, 2H), 7.39 (t, *J* = 7.4 Hz, 1H), 7.22 (dd, *J* = 9.5, 2.0 Hz, 1H)

^{13}C NMR (101 MHz, Chloroform-*d*) δ 143.8, 143.6, 132.4, 128.5, 128.5, 127.8, 126.5, 121.9, 121.5, 117.9, 92.1

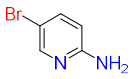

2-23

5-bromopyridin-2-amine (**2-23**) (Song et al., 2015) was obtained as a yellow solid (137 mg, 79% yield) according to **General Procedure A** for 24h.

146 g (85% yield) product **6-10** was isolated in 1.0 mol scale reaction according to **General Procedure E**.

^{1}H NMR (400 MHz, Chloroform-*d*) δ 8.08 (d, *J* = 2.4 Hz, 1H), 7.47 (dd, *J* = 8.7, 2.5 Hz, 1H), 6.42-6.37 (m, 1H), 4.44 (s, 2H).

^{13}C NMR (101 MHz, Chloroform-*d*) δ 157.0, 148.6, 140.1, 110.0, 108.2

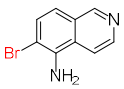

2-24

8-bromoisoquinolin-5-amine (**2-24**) (Gordon and Pearson, 1964) was obtained as a brown liquid (88 mg, 40% yield) according to **General Procedure A** for 21h.

^{1}H NMR (400 MHz, Chloroform-*d*) δ 9.53 (s, 1H), 8.56 (d, *J* = 5.9 Hz, 1H), 7.59 (d, *J* = 8.0 Hz, 1H), 7.53 (d, *J* = 6.0 Hz, 1H), 6.80 (d, *J* = 8.1 Hz, 1H), 4.23 (brs, 2H).

^{13}C NMR (101 MHz, DMSO-d_6) δ 150.6, 144.6, 141.8, 132.2, 126.7, 126.3, 115.5, 111.3, 104.5

HRMS (ESI): Calculated for [M+1] ($C_9H_8BrN_2^+$) 224.9845; found: 224.9845

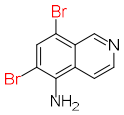

2-24B

6, 8-dibromoisoquinolin-5-amine (**2-24B**) (Gordon and Pearson, 1964) was obtained as a yellow solid (63 mg, 21% yield) according to **General Procedure A**.

^{1}H NMR (400 MHz, Chloroform-*d*) δ 9.50 (s, 1H), 8.60 (d, *J* = 6.0 Hz, 1H), 7.84 (s, 1H), 7.52 (d, *J* = 6.0 Hz, 1H), 4.71 (brs, 2H).

^{13}C NMR (101 MHz, DMSO-d_6) δ 150.6, 142.7, 141.5, 134.3, 126.7, 125.3, 115.8, 105.2, 104.1

HRMS (ESI): Calculated for [M+1] ($C_9H_7Br_2N_2^+$) 302.8950; found: 302.8949

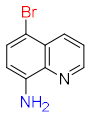

2-25

5-bromoquinolin-8-amine (**2-25**) (Chen et al., 2017) was obtained as a brown solid (74 mg, 33% yield) according to **General Procedure A** for 7h.

^{1}H NMR (400 MHz, Chloroform-*d*) δ 8.77 (dd, *J* = 4.3, 1.5 Hz, 1H), 8.41 (dd, *J* = 8.5, 1.6 Hz, 1H), 7.80 (s, 1H), 7.51 (dd, *J* = 8.5, 4.2 Hz, 1H), 5.47 (s, 2H)

^{13}C NMR (101 MHz, DMSO-d_6) δ 149.3, 143.5, 138.2, 135.5, 133.5, 126.6, 123.8, 105.0, 101.8

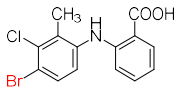

2-26

2-((4-bromo-3-chloro-2-methylphenyl) amino) benzoic acid (**2-26**) was obtained as a white solid (330 mg, 97% yield) according to **General Procedure A** for 40h.

^{1}H NMR (400 MHz, Chloroform-*d*) δ 7.57 (d, *J* = 2.4 Hz, 1H), 7.26 (dd, *J* = 8.5, 2.3 Hz, 1H), 6.99 (d, *J* = 8.6 Hz, 1H), 3.38 (t, *J* = 4.8 Hz, 4H), 3.29 (t, *J* = 4.8 Hz, 4H)

^{13}C NMR (101 MHz, DMSO-d_6) δ 168.8, 146.9, 139.0, 136.4, 134.0, 133.1, 130.6, 127.7, 125.6, 123.0, 115.8, 113.8, 107.5, 14.7

HMRS (ESI): Calculated [M-H] ($C_{14}H_{10}BrClNO_2^-$) 337.9589; found 337.9591

M.p. 176.1-177.0℃

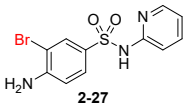

2-27

4-amino-3-bromo-N-(pyridin-2-yl) benzene sulfonamide (**2-27**) was obtained as a white solid (242 mg, 74% yield) according to **General Procedure A** for 24 h.

^{1}H NMR (400 MHz, DMSO-d_6) δ 8.10-8.02 (m, 1H), 7.80 (d, *J* = 2.2 Hz, 1H), 7.70 (ddd, *J* = 8.9, 7.3, 1.9 Hz, 1H), 7.53 (dd, *J* = 8.6, 2.2 Hz, 1H), 7.09 (d, *J* = 8.6 Hz, 1H), 6.91 (t, *J* = 6.3 Hz, 1H), 6.79 (d, *J* = 8.6 Hz, 1H), 6.13 (brs, 2H)

^{13}C NMR (101 MHz, DMSO-d_6) δ 152.5, 149.5, 145.1, 139.5, 131.4, 128.1, 127.6, 116.6, 114.0, 112.9, 105.5

HMRS (ESI): Calculated [M+1] ($C_{11}H_{11}BrN_3O_2S^+$): 327.9750; found 327.9751

M.p. 155.9-156.8℃

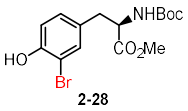

2-28

(*R*)-Methyl 3-(3-bromo-4-hydroxyphenyl)-2-((tert-butoxycarbonyl) amino) propanoate (**2-28**) (Georgiev et al., 2016) was obtained as a white solid (118 mg, 32 % yield, 98% yield brsm; starting material was recycled in 200 mg, 68 % yield) according to **General Procedure A** for 64h.

^{1}H NMR (400 MHz, Chloroform-*d*) δ 7.20 (s, 2H), 5.80 (s, 1H), 5.01 (d, *J* = 7.9 Hz, 1H), 4.49 (d, *J* = 7.3 Hz, 1H), 3.72 (s, 3H), 3.04 (dd, *J* = 13.9, 5.8 Hz, 1H), 2.90 (dd, *J* = 14.0, 6.1 Hz, 1H), 1.42 (s, 9H), 1.24 (s, 1H)

^{13}C NMR (101 MHz, Chloroform-*d*)) δ 171.8, 154.9, 148.5, 132.8 (two carbons), 130.8, 109.8, 80.2, 54.4, 52.4, 36.9, 28.3

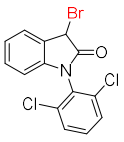

2-29

3-bromo-1-(2,6-dichlorophenyl) indolin-2-one (**2-29**) was obtained as a yellow solid (110 mg, 31% yield, 45% yield brsm; 85 mg starting material was recycled, 31% yield) according to **General Procedure A** for 64h.

^{1}H NMR (400 MHz, Chloroform-*d*) δ 7.5-7.47 (m, 3H), 7.39 (dd, *J* = 8.5, 7.7 Hz, 1H), 7.26 (d, *J* = 7.9 Hz, 1H), 7.15 (td, *J* = 7.6, 1.1 Hz, 1H), 6.39 (d, *J* = 7.8 Hz, 1H), 5.48 (s, 1H)

^{13}C NMR (101 MHz, Chloroform-*d*) δ 170.8, 142.1, 135.6, 135.5, 131.2, 130.4, 129.4, 129.2, 129.0, 126.5, 125.9, 124.0, 109.8, 38.2

HRMS (ESI): Calculated for [M+1] ($C_{14}H_9BrCl_2NO^+$) 357.9219; found 357.9222

M.p. 133.5-134.0℃

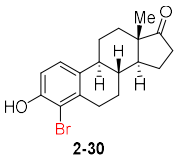

2-30

(8*R*, 9*S*, 13*S*, 14*S*)-4-bromo-3-hydroxy-13-methyl-6,7,8,9,11,12,13,14,15,16-decahydro-17*H*-cyclopenta[α]phenanthren-17-one (**2-30**) (Slaunwhite and Neely, 1962) was obtained as a yellow solid (153 mg, 44% yield, 51% brsm)

^{1}H NMR (400 MHz, Chloroform-*d*) δ 7.17 (d, *J* = 8.6 Hz, 1H), 6.85 (d, *J* = 8.5 Hz, 1H), 5.52 (s, 1H), 2.95 (dd, *J* = 17.8, 6.2 Hz, 1H), 2.77-2.65 (m, 1H), 2.50 (dd, *J* = 18.8, 8.7 Hz, 1H), 2.40-2.33 (m, 1H), 2.30- 2.22 (m, 1H), 2.21-2.13 (m, 1H), 2.08 (dd, *J* = 15.3, 7.3 Hz, 2H), 1.95 (s, 1H), 1.67-1.59 (m, 1H), 1.48 (dt, *J* = 9.7, 5.9 Hz, 5H), 0.88 (s, 1H)

^{13}C NMR (101 MHz, DMSO-D_6) 151.9, 136.4, 133.2, 125.0, 113.2, 112.5, 49.4, 47.2, 43.6, 37.0, 35.4, 31.3, 30.7, 26.2, 25.7, 21.7, 21.1, 13.5 (carbonyl missing)

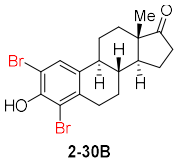

2-30B

(8*R*, 9*S*, 13*S*, 14*S*)-2,4-dibromo-3-hydroxy-13-methyl-6,7,8,9,11,12,13,14,15,16-decahydro-17H-cyclopenta[a]phenanthren-17-one (**2-30B**) (Slaunwhite and Neely, 1962) was obtained as a yellow solid (16 mg, 4% yield; 5% brsm).

^{1}H NMR (400 MHz, Chloroform-*d*) δ 7.39 (s, 1H), 5.83 (s, 1H), 2.92 (dd, *J* = 18.0, 6.2 Hz, 1H), 2.66 (ddd, *J* = 18.2, 11.9, 7.3 Hz, 1H), 2.50 (dd, *J* = 18.8, 8.8 Hz, 1H), 2.38-2.30 (m, 1H), 2.23 (d, *J* = 8.4 Hz, 1H), 2.19 – 2.11 (m, 1H), 2.10-2.02 (m, 2H), 1.97-1.92 (m, 1H), 1.67-1.58 (m, 1H), 1.46 (q, *J* = 10.6, 9.5 Hz, 5H), 0.88 (s, 3H)

^{13}C NMR (101 MHz, Chloroform-*d*) δ 147.3, 136.5, 135.0, 128.6, 113.2, 106.5, 50.2, 47.8, 43.9, 37.3, 35.8, 31.4, 30.9, 26.5, 26.1, 21.5, 13.8 (carbonyl missing)

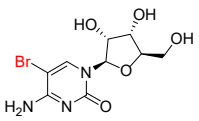

2-31 (crude)

4-amino-5-bromo-1-((2*R*,3*R*,4*R*,5*R*)-3,4-dihydroxy-5-(hydroxymethyl)-3-methyl-tetrahydrofuran-2-yl) pyrimidin-2(1*H*)-one (**2-31**) (Kumar et al., 2009)

^{1}H NMR (400 MHz, Methanol-d_4) δ 8.56 (s, 1H), 5.82 (d, *J* = 3.0 Hz, 1H), 4.17 – 4.10 (m, 2H), 4.05 – 4.01 (m, 1H), 3.93 (dd, *J* = 12.3, 2.5 Hz, 1H), 3.77 (dd, *J* = 12.3, 2.5 Hz, 1H), 1.91 (s, 3H).

^{13}C NMR (101 MHz, DMSO-d_6) δ 161.9, 154.0, 142.3, 89.6, 86.2, 84.1, 74.4, 68.7, 59.8

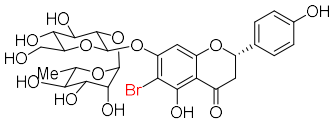

2-32

(*S*)-6-bromo-7-(((2*R*,3*S*,4*R*,5*R*,6*S*)-4,5-dihydroxy-6-(hydroxymethyl)-3-(((2*S*,3*R*,4*R*,5*R*,6*S*)-3,4,5-trihydroxy-6-methyltetrahydro-2*H*-pyran-2-yl)oxy)tetrahydro-2*H*-pyran-2-yl)oxy)-5-hydroxy-2-(4-hydroxyphenyl)chroman-4-one (**2-32**) was obtained as a white solid after HPLC purification (MeCN: H_2O = 25:75, 2 mL/min, 13.1 min) according to **General procedure A**.

^{1}H NMR (400 MHz, Methanol-d_4) δ 7.33 (t, *J* = 7.5 Hz, 2H), 6.86-6.78 (m, 2H), 6.38 (d, *J* = 3.7 Hz, 1H), 5.53-5.38 (m, 2H), 5.31 (dd, *J* = 7.7, 4.4 Hz, 1H), 3.94 (m, 1H), 3.91-3.81 (m, 2H), 3.76 (m, 1H), 3.72-3.59 (m, 3H), 3.45 (m, 2H), 3.36 (t, *J* = 9.5 Hz, 1H), 1.20 (m, 3H).

^{13}C NMR (101 MHz, Methanol-d_4) 198.3, 162.5, 159.0, 130.4, 129.2, 129.0, 116.4, 101.9, 101.7, 99.5, 97.2, 80.7, 79.1, 78.7, 78.6, 78.2, 74.1, 72.2, 72.0, 71.10, 71.05, 70.2, 62.2, 24.1, 18.5

HRMS (ESI): Calculated for [M+Na] ($C_{27}H_{31}BrNaO_{14}^{+}$) 681.0789; found 681.0783

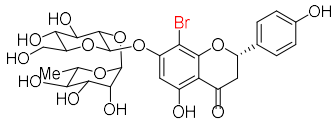

2-32B

(*S*)-8-bromo-7-(((2*R*,3*S*,4*R*,5*R*,6*S*)-4,5-dihydroxy-6-(hydroxymethyl)-3-(((2*S*,3*R*,4*R*,5*R*,6*S*)-3,4,5-trihydroxy-6-methyltetrahydro-2*H*-pyran-2-yl)oxy)tetrahydro-2*H*-pyran-2-yl)oxy)-5-hydroxy-2-(4-hydroxyphenyl)chroman-4-one (**2-32B**) was obtained as a pale-yellow solid by HPLC (MeCN:H_2O = 25:75, 2 mL/min, 16.3 min) according to **General procedure A**.

^{1}H NMR (400 MHz, Methanol-d_4) δ 7.33 (d, *J* = 7.9 Hz, 2H), 6.82 (dd, *J* = 8.6, 2.8 Hz, 2H), 6.40-6.30 (s, 1H), 5.54-5.36 (m, 2H), 5.36-5.22 (m, 1H), 3.94 (s, 1H), 3.85 (dd, *J* = 16.9, 8.5 Hz, 2H), 3.76 (t, *J* = 8.4 Hz, 1H), 3.63 (dt, *J* = 16.8, 9.0 Hz, 3H), 3.40 (dt, *J* = 29.8, 10.9 Hz, 3H), 1.90 (d, *J* = 2.4 Hz, 1H), 1.21 (d, *J* = 6.2 Hz, 3H).

^{13}C NMR (101 MHz, Methanol-d_4) 162.4, 159.2, 129.2, 129.0, 128.9, 116.4, 116.3, 101.9, 101.8, 99.4, 80.7, 79.1, 78.7, 78.19, 78.15, 74.0, 72.2, 72.0, 71.12, 71.06, 70.2, 62.2, 24.1, 18.5 (carbonyl not seen)

HRMS (ESI): Calculated for [M+Na] ($C_{27}H_{31}BrNaO_{14}^+$) 681.0789; found 681.0783

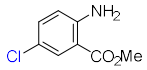

2-33

Methyl 2-amino-5-chlorobenzoate (**2-33**) (Zhou et al., 2017) was obtained as a yellow solid (104 mg, 56% yield).

^{1}H NMR (400 MHz, Chloroform-*d*) δ 7.80 (d, *J* = 2.5 Hz, 1H), 7.18 (dd, *J* = 8.8, 2.5 Hz, 1H), 6.59 (d, *J* = 8.8 Hz, 1H), 5.70 (brs, 2H), 3.85 (s, 3H)

^{13}C NMR (101 MHz, Chloroform-*d*) δ 167.5, 148.9, 134.0, 130.4, 120.6, 118.0, 111.4, 51.7

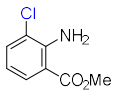

2-33B

Methyl 2-amino-3-chlorobenzoate (**2-33B**) (Cai et al., 2018) was obtained as yellowish oil (47 mg, 25% yield).

^{1}H NMR (400 MHz, Chloroform-*d*) δ 7.84-7.78 (m, 1H), 7.44-7.38 (m, 1H), 6.58 (t, *J* = 7.9 Hz, 1H), 6.27 (brs, 2H), 3.88 (d, *J* = 0.8 Hz, 3H)

^{13}C NMR (101 MHz, DMSO-d_6) δ 168.1, 146.6, 133.8, 129.9, 120.2, 115.7, 111.8, 51.8

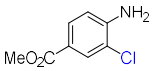

2-34

Methyl 4-amino-3-chlorobenzoate (**2-34**) (Yang et al., 2018) was obtained as a yellow solid (91 mg, 49% yield, 64 yield brsm; 35 mg starting materisl was recycled, 23% yield) according to **General Procedure C** for 27h.

^{1}H NMR (400 MHz, Methanol-d_4) δ 7.93 (d, *J* = 1.9 Hz, 1H), 7.73 (dd, *J* = 8.4, 1.9 Hz, 1H), 6.71 (d, *J* = 8.4 Hz, 1H), 4.45 (brs, 2H), 3.84 (s, 3H)

^{13}C NMR (101 MHz, Chloroform-*d*) δ 166.2, 147.0, 131.2, 129.6, 120.4, 118.2, 114.4, 51.8

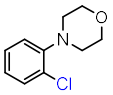

2-35

4-(2-chlorophenyl) morpholine (**2-35**) (Hendrick and Wang, 2015) was obtained as a pale-yellow liquid (89 mg, 45% yield)

^{1}H NMR (400 MHz, Chloroform-*d*) δ 7.35 (dd, *J* = 7.9, 1.5 Hz, 1H), 7.25-7.19 (m, 2H), 7.02 (dd, *J* = 8.1, 1.5 Hz, 1H), 6.97 (td, *J* = 7.7, 1.5 Hz, 1H), 3.89-3.84 (m, 4H), 3.07 – 3.02 (m, 4H)

^{13}C NMR (101 MHz, Chloroform-*d*) δ 149.0, 130.7, 128.7, 127.6, 123.9, 120.2, 67.1, 51.6

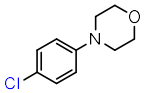

2-35B

4-(4-chlorophenyl) morpholine (**2-35B**) (Berman and Johnson, 2004) was obtained as a yellow solid (25 mg, 13% yield).

^{1}H NMR (400 MHz, Chloroform-*d*) δ 7.22 (d, *J* = 9.0 Hz, 2H), 6.83 (d, *J* = 8.9 Hz, 2H), 3.90-3.81 (m, 4H), 3.16-3.07 (m, 4H)

^{13}C NMR (101 MHz, Chloroform-*d*) δ 149.9, 129.0, 124.9, 116.9, 66.8, 49.3

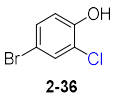

2-36

4-bromo-2-chlorophenol (**2-36**) (Oberhauser, 1997) was obtained as a yellow solid (169 mg, 82% yield) according to **General Procedure C** except using TFA instead of HOAc for 88h.

^{1}H NMR (400 MHz, Chloroform-*d*) δ 7.25 (s, 1H), 7.07 (dd, *J* = 8.7, 2.3 Hz, 1H), 6.68 (d, *J* = 8.7 Hz, 1H), 5.34 (s, 1H).

^{13}C NMR (101 MHz, Chloroform-*d*) δ 150.7, 131.4, 131.3, 120.8, 117.6, 112.3

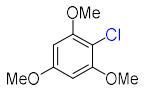

2-37

2-chloro-1,3,5-trimethoxybenzene (**2-37**) (Seel et al., 2018) was obtained as a white solid (103 mg, 51% yield, 74% yield brsm; 52 mg starting material was recycled, 31% yield) according to **General Procedure C** for 69h.

^{1}H NMR (400 MHz, Chloroform-*d*) δ 6.18 (s, 2H), 3.88 (s, 6H), 3.81 (s, 3H)

^{13}C NMR (101 MHz, Chloroform-*d*) δ 159.4, 156.5, 102.6, 91.6, 56.2, 55.5

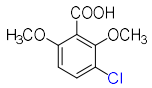

2-38

3-chloro-2,6-dimethoxybenzoic acid (**2-38**) (Florvall and Oegren, 1982) was obtained as a white solid (94 mg, 44% yield, 56% yield brsm; 38 mg starting material was recycled, 21% yield) according to **General Procedure C** for 46h.

^{1}H NMR (400 MHz, Chloroform-*d*) δ 7.40 (d, *J* = 8.9 Hz, 1H), 6.70 (d, *J* = 8.9 Hz, 1H), 3.96 (s, 3H), 3.88 (s, 3H)

^{13}C NMR (101 MHz, Chloroform-*d*) δ 156.0, 153.9, 132.1, 119.7, 118.8, 108.0, 62.0, 56.4

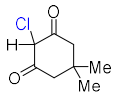

2-39

2,2-dichloro-5,5-dimethylcyclohexane-1,3-dione (2-39) (China et al., 2015) was obtained as a white solid (74 mg, 43% yield) according to **General procedure C** for 40h.

^{1}H NMR (400 MHz, Chloroform-*d*) δ 2.49 (s, 4H), 1.15 (s, 6H)

^{13}C NMR (101 MHz, Chloroform-*d*) δ 178.5, 70.4, 44.7, 32.3, 27.7

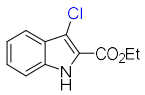

2-40

Ethyl 3-chloro-1H-indole-2-carboxylate (**2-40**) (Wang et al., 2016) was obtained as a white solid (155.5 mg, 70% yield, 91% yield brsm; 38 mg starting material was recycled, 23% yield) according to **General Procedure C** for 70h.

^{1}H NMR (400 MHz, Chloroform-*d*) δ 8.77 (brs, 1H), 7.57 (d, *J* = 8.2 Hz, 1H), 7.27-7.20 (m, 2H), 7.07 (ddd, *J* = 8.0, 5.6, 2.3 Hz, 1H), 4.31 (q, *J* = 7.1 Hz, 2H), 1.30 (t, *J* = 7.1 Hz, 3H)

^{13}C NMR (101 MHz, Chloroform-*d*) δ 161.2, 134.8, 126.5, 126.2, 122.4, 121.2, 120.1, 112.4, 112.1, 61.4, 14.3

2-41

3-chloro-1*H*-pyrrolo[2,3-b] pyridine (**2-41**) (Wang et al., 2016) was obtained as a yellow solid (85 mg, 56% yield, 62% yield brsm; 12 mg starting material was recycled, 10% yield) for 18h.

^{1}H NMR (400 MHz, Chloroform-*d*) δ 10.72 (brs, 1H), 8.29 (dd, *J* = 4.8, 1.5 Hz, 1H), 7.94-7.88 (m, 1H), 7.17 (s, 1H), 7.10 (dd, *J* = 7.9, 4.8 Hz, 1H).

^{13}C NMR (101 MHz, Chloroform-*d*) δ 147.0, 143.4, 127.2, 121.9, 118.6, 116.3, 104.4

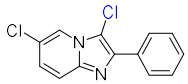

2-42

3, 6-dichloro-2-phenylimidazo[1,2-a] pyridin (**2-42**) (Xiao et al., 2015) was obtained as a white solid (92 mg, 35% yield, 78% yield brsm; 126 mg starting material was recycled, 55% yield) according to **General Procedure C** for 24h.

^{1}H NMR (400 MHz, Chloroform-*d*) δ 8.17 (d, *J* = 2.0 Hz, 1H), 8.15-8.09 (m, 2H), 7.59 (d, *J* = 9.5 Hz, 1H), 7.49 (dd, *J* = 8.5, 6.9 Hz, 2H), 7.40 (t, *J* = 7.3 Hz, 1H), 7.22 (dd, *J* = 9.5, 2.0 Hz, 1H).

^{13}C NMR (101 MHz, Chloroform-*d*) δ 142.0, 140.8, 132.0, 128.6, 128.5, 127.4, 126.2, 121.4, 120.6, 118.0, 106.1

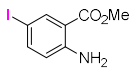

2-43

Methyl 2-amino-5-iodobenzoate (**2-43**) (Zhou and Song, 2018) was obtained as a brown solid (106 mg, 39% yield, 48% yield brsm; 28 mg starting material was recycled, 18% yield) according to **General Procedure D** for 17h.

^{1}H NMR (400 MHz, Chloroform-*d*) δ 7.91 (d, *J* = 2.2 Hz, 1H), 7.25 (dd, *J* = 8.7, 2.2 Hz, 1H), 6.23 (d, *J* = 8.7 Hz, 1H), 5.54 (brs, 2H), 3.64 (s, 3H).

^{13}C NMR (101 MHz, Chloroform-*d*) δ 167.3, 149.8, 142.2, 139.5, 118.8, 112.8, 75.9, 51.8

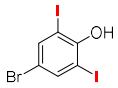

2-44

4-bromo-2,6-diiodophenol (**2-44**) (Satkar et al., 2019) was obtained as a brown solid (413 mg, 97% yield) according to **General Procedure D** for 13 h. Product **2-44** was also obtained (394 mg, 93% yield) in control experiment without catalyst for 17h.

^{1}H NMR (400 MHz, Chloroform-*d*) δ 7.79 (s, 2H), 5.73 (brs, 1H)

^{13}C NMR (101 MHz, Chloroform-*d*) δ 153.1, 140.8, 113.5, 82.4

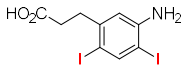

2-45

3-(5-amino-2,4-diiodophenyl) propanoic acid (**2-45**) was obtained as a brown solid (274 mg, 65% yield) according to **General Procedure D** for 40 min. Without catalyst, the reaction required 6 h to complete (279 mg, 66% yield).

^{1}H NMR (400 MHz, DMSO-d_6) δ 12.23 (brs, 1H), 7.83 (s, 1H), 6.72 (s, 1H), 5.34 (br, 2H), 2.69 (dd, *J* = 8.6, 7.0 Hz, 2H), 2.43 (dd, *J* = 8.6, 7.0 Hz, 2H)

^{13}C NMR (101 MHz, DMSO-d_6) δ 173.2, 149.0, 146.3, 143.3, 114.9, 83.3, 81.7, 34.4, 33.8

HRMS (ESI): Calculated for [M+1] ($C_9H_{10}I_2NO_2^+$): 417.8795; found 417.8797

M.p. 134.9-135.6℃

2-46

3-iodo-1H-pyrrolo[2,3-*b*] pyridine (**2-46**) (Iida et al., 2019) was obtained as a brown solid (217 mg, 89% yield) according to **General Procedure D** for 15 min. Product **2-44** was obtained (233.8 mg, 96% yield) in a control experiment without catalyst in 15 min.

^{1}H NMR (400 MHz, Chloroform-*d*) δ 10.35 (brs, 1H), 8.32 (dd, *J* = 4.7, 1.5 Hz, 1H), 7.76 (dd, *J* = 7.9, 1.5 Hz, 1H), 7.44 (s, 1H), 7.16 (dd, *J* = 7.9, 4.8 Hz, 1H).

^{13}C NMR (101 MHz, DMSO-d_6) δ 148.0, 143.7, 130.5, 128.0, 122.0, 116.4, 54.3

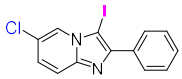

2-47

6-chloro-3-iodo-2-phenylimidazo[1,2-*a*] pyridine (**2-47**) (Zhou et al., 2019) was obtained as a yellow (172 mg, 97% yield) according to **General Procedure D** for 20 min. Product **2-47** was obtained (175 mg, 99% yield) without catalyst in a control experiment in 1h.

^{1}H NMR (400 MHz, Chloroform-*d*) δ 8.28 (t, *J* = 1.2 Hz, 1H), 8.03 (d, *J* = 7.6 Hz, 2H), 7.56 (d, *J* = 9.5 Hz, 1H), 7.47 (t, *J* = 7.6 Hz, 2H), 7.40 (d, *J* = 7.2 Hz, 1H), 7.21 (dd, *J* = 9.5, 1.9 Hz, 1H).

^{13}C NMR (101 MHz, Chloroform-*d*) δ 149.0, 146.5, 133.1, 128.6, 128.41, 128.37, 126.9, 126.0, 124.5, 121.1, 117.9

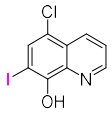

2-48

5-chloro-7-iodoquinolin-8-ol (**2-48**) (Deshmukh et al., 2015) was obtained as a brown solid (9 g, 89% yield for 50 mmol scale, isolated by filtration) according to **General Procedure E** for 1h.

^{1}H NMR (400 MHz, DMSO-d_6) δ 11.03 (s, 1H), 8.96 (d, *J* = 4.2 Hz, 1H), 8.49 (d, *J* = 8.0, 1H), 7.99 (s, 1H), 7.77 (dd, J_1 = 8.0 Hz, J_2 = 4.0 Hz, 1H)

^{13}C NMR (101 MHz, DMSO-d_6) δ 153.6, 149.6, 137.5, 134.9, 133.0, 125.7, 123.4, 119.4, 78.9

HRMS (ESI): Calculated for [M-H] ($C_9H_4ClINO^-$) 303.9032; found 303.9033

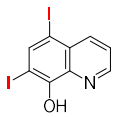

2-49

5, 7-diiodoquinolin-8-ol (**2-49**) (Swamy et al., 2016) was obtained as a brown solid (with catalyst, 3.8 g, mixture, diiodination product (di): monoiodination product (mo) = 5:1) by 1H-NMR, 83% yield) according to **General Procedure E** for 3h.

^{1}H NMR (400 MHz, DMSO-d_6) δ 8.88 (dd, *J* = 4.2, 1.5 Hz, 1H), 8.34 (s, 1H), 8.29 (dd, *J* = 8.5, 1.5 Hz, 1H), 7.73 (dd, *J* = 8.5, 4.2 Hz, 1H).

^{13}C NMR (101 MHz, DMSO-d_6) δ 154.8, 149.6, 144.5, 140.0, 138.0, 129.6, 124.2, 85.2, 80.9

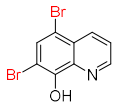

2-50

5, 7-dibromoquinolin-8-ol[xx] **(2-50)** was obtained as a yellow solid (19.3 g, 64% yield, 100 mmol scale) according to **General Procedure E** for 2h.

^{1}H NMR (400 MHz, DMSO-d_6) δ 8.94 (dt, *J* = 3.9, 1.9 Hz, 1H), 8.44 (dd, *J* = 8.6, 1.6 Hz, 1H), 8.04 (s, 1H), 7.76 (dd, *J* = 8.7, 4.2 Hz, 1H).

^{13}C NMR (101 MHz, DMSO-d_6) δ 151.3, 149.8, 139.0, 135.4, 133.3, 126.5, 123.6, 108.6, 105.1

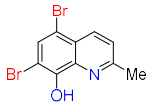

2-51

5,7-dibromo-2-methylquinolin-8-ol (**2-51**) (Bakewell et al., 2012) was obtained as a yellow solid (81.6 g, 52% yield) according to **General Procedure E** for 1.5h.

^{1}H NMR (400 MHz, Chloroform-*d*) δ 8.29 (d, *J* = 8.6 Hz, 1H), 7.80 (s, 1H), 7.41 (d, *J* = 8.6 Hz, 1H), 2.75 (s, 3H).

^{13}C NMR (101 MHz, Chloroform-*d*) δ 158.8, 149.1, 138.0, 136.0, 132.7, 124.8, 123.9, 110.0, 103.6, 24.7

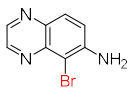

2-52

5-bromoquinoxalin-6-amine (**2-52**) (Munk et al., 1997) was obtained as a yellow solid (161 mg, 72% yield) according to **General Procedure A** for 5.5h.

^{1}H NMR (400 MHz, Chloroform-*d*) δ 8.80 (s, *J* = 2.0 Hz, 1H), 8.60 (d, *J* = 2.0 Hz, 1H), 7.87 (d, *J* = 9.0 Hz, 1H), 7.29 (d, *J* = 9.0 Hz, 1H), 4.79 (brs, 2H)

^{13}C NMR (101 MHz, Chloroform-*d*) δ 146.0, 145.0, 142.0, 140.9, 138.4, 129.2, 121.3, 102.4

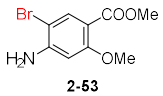

2-53

Methyl 4-amino-5-bromo-2-methoxybenzoate (**2-53**) (Lai et al., 2016) was obtained as a yellow solid (224 mg, 86% yield) according to **General Procedure A** for 5.5h.

Product **2-53** was obtained with water as solvent according to **General Procedure B** (195 mg, 75% yield; 2.5 mol% Na_2WO_4-$2H_2O$, 1.1 equivalent H_2O_2, 24h)

^{1}H NMR (400 MHz, Chloroform-*d*) δ 7.98 (s, 1H), 6.29 (s, 1H), 4.48 (brs, 2H), 3.84 (s, 3H), 3.83 (s, 3H)

^{13}C NMR (101 MHz, Chloroform-*d*) δ 165.0, 160.7, 149.0, 136.4, 110.1, 98.8, 98.0, 56.0, 51.6

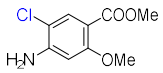

2-54

Methyl 4-amino-5-chloro-2-methoxybenzoate (**2-54**) (Selvakumar et al., 2016) was obtained as a yellow solid (91 mg, 42% yield) for 10h.

^{1}H NMR (400 MHz, Chloroform-*d*) δ 7.83 (s, 1H), 6.29 (s, 1H), 4.44 (brs, 2H), 3.85 (s, 3H), 3.83 (s, 3H)

^{13}C NMR (101 MHz, Chloroform-*d*) δ 165.2, 160.2, 147.8, 133.3, 109.9, 109.6, 98.2, 56.1, 51.6

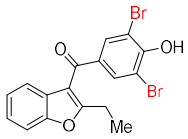

2-55

(3, 5-dibromo-4-hydroxyphenyl) (2-ethylbenzofuran-3-yl) methanone (**2-55**) (Huang et al., 2019) was obtained as a yellow solid (413 mg, 97% yield) according to **General Procedure A** by utilizing 2.2 equivalent of NaBr and HOAc for 48h.

^{1}H NMR (400 MHz, Chloroform-*d*) δ 7.99 (s, 2H), 7.50 (d, *J* = 8.2 Hz, 1H), 7.41 (d, *J* = 7.7 Hz, 1H), 7.31 (td, *J* = 8.2, 7.7, 1.4 Hz, 1H), 7.23 (d, *J* = 7.5 Hz, 1H), 6.37 (brs, 1H), 2.91 (q, *J* = 7.5 Hz, 2H), 1.36 (t, *J* = 7.5 Hz, 3H).

^{13}C NMR (101 MHz, Chloroform-*d*) δ 187.8, 166.4, 153.7, 153.1, 133.7, 133.4, 126.5, 124.6, 123.8, 121.00, 115.4, 111.1, 110.0, 21.9, 12.2

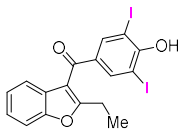

2-56

(2-ethylbenzofuran-3-yl) (4-hydroxy-3,5-diiodophenyl) methanone (**2-56**) (Huang et al., 2019) was obtained as a white solid (255 mg, 98% yield) according to **General Procedure D** for 40 min.

^{1}H NMR (400 MHz, Chloroform-*d*) δ 8.17 (s, 2H), 7.48 (d, *J* = 8.2 Hz, 1H), 7.41 (d, *J* = 7.8 Hz, 1H), 7.29 (t, *J* = 7.5 Hz, 1H), 7.21 (d, *J* = 7.4 Hz, 1H), 6.18 (s, 1H), 2.87 (q, *J* = 7.5 Hz, 2H), 1.34 (t, *J* = 7.5 Hz, 3H).

^{13}C NMR (101 MHz, Chloroform-*d*) δ 187.4, 166.3, 157.1, 153.7, 140.7, 135.1, 126.6, 124.6, 123.8, 121.0, 115.4, 111.1, 82.0, 22.0, 12.2

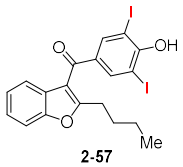

2-57

(2-butylbenzofuran-3-yl) (4-hydroxy-3,5-diiodophenyl) methanone (**2-57**) (Huang et al., 2019) was obtained as a brown solid (96 mg, 88% yield, 0.2 mmol scale) according to **General Procedure D** by utilizing 2.2 equivalent of KI and HOAc for 2h.

^{1}H NMR (400 MHz, Chloroform-*d*) δ 8.18 (s, 2H), 7.49 (d, *J* = 8.2 Hz, 1H), 7.41 (d, *J* = 7.7 Hz, 1H), 7.34 – 7.28 (m, 1H), 7.24 (t, *J* = 7.4 Hz, 1H), 6.22 (brs, 1H), 2.88 (t, *J* = 7.7 Hz, 2H), 1.78 (p, *J* = 7.7 Hz, 2H), 1.38 (h, *J* = 7.4 Hz, 3H), 0.92 (t, *J* = 7.3 Hz, 4H).

^{13}C NMR (101 MHz, Chloroform-*d*) δ 187.4, 165.6, 157.1, 153.7, 140.7, 135.2, 126.6, 124.6, 123.8, 121.0, 115.9, 111.1, 82.0, 30.1, 28.1, 22.5, 13.7

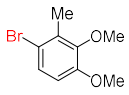

2-58

1-bromo-3,4-dimethoxy-2-methylbenzene (**2-58**) (Connolly et al., 2004) was obtained as a yellow liquid (145 mg, 63% yield) according to **General procedure A** for 82h.

^{1}H NMR (400 MHz, Chloroform-*d*) δ 7.24 (d, *J* = 8.8 Hz, 1H), 6.66 (d, *J* = 8.8 Hz, 1H), 3.84 (s, 3H), 3.78 (s, 3H), 2.34 (s, 3H)

^{13}C NMR (101 MHz, Chloroform-*d*) δ 152.1, 148.0, 132.3, 127.3, 116.0, 110.9, 60.4, 55.8, 16.1

Reference

Bakewell, C., Platel, R. H., Cary, S. K., Hubbard, S. M., Roaf, J. M., Levine, A. C., White, A. J. P., Long, N. J., Haaf, M. and Williams, C. K. (2012) Bis(8-quinolinolato)aluminum ethyl complexes: *iso*-selective initiators for *rac*-Lactide polymerization. Organometallics. *31*, 4729-4736.

Berman, A. M. and Johnson, J. S. (2004) Copper-catalyzed electrophilic amination of diorganozinc reagents, J. Am. Chem. Soc. *126*, 5680-5681.

Cai, Z., Li, S., Gao, Y., Fu, L. and Li, G. (2018) Weak, bidentate chelating group assisted cross-coupling of C(sp^3)–H bonds in aliphatic acid derivatives with aryltrifluoroborates. Chem. Commun. *54*, 12766-12769.

Capilato, J. N., Philippi, S. V., Reardon, T., McConnell, A., Oliver, D. C., Warren, A., Adams, J. S., Wu, C. and Perez, L. K. (2017) Development of a novel series of non-natural triaryl agonists and antagonists of the pseudomonas aeruginosa LasR quorum sensing receptor. Bio. Med. Chem. *25*, 153-165.

Chen, J., Wang, T., Liu, Y., Wang, T., Lin, A., Yao, H. and Xu, J. (2017) Metal-free C5-selective halogenation of quinolines under aqueous conditions. Org. Chem. Front. *4*, 622-626.

China, H., Okada, Y. and Dohi, T. (2015) The Multiple reactions in the monochlorodimedone assay: discovery of unique dehalolactonizations under mild conditions. Asian. J. Org. Chem. *4*, 1065-1074.

Connolly, T. J., Matchett, M., McGarry, P., Sukhtankar, S. and Zhu, J. A. (2004) Practical synthesis of 3,4-dimethoxy-*o*-toluic acid. Org. Pro. Res. Dev. *8*, 624-627.

Deshmukh, A., Gore, B., Thulasiram, H. V. and Swamy, V. P. (2015) Recyclable ionic liquid iodinating reagent for solvent free, regioselective iodination of activated aromatic and heteroaromatic amines. RSC Advances. *5*, 88311-88315.

Florvall, L. and Oegren, S. O. (1982) Potential neuroleptic agents. 2,6-dialkoxybenzamide derivatives with potential dopamine receptor blocking activities. J. Med. Chem. *25*, 1280-1286.

Gallou, F., Reeves, J. T., Tan, Z., Song, J. J., Yee, N. K., Harcken, C., Liu, P., Thomson, D. and Senanayake, C. H. (2007) Practical regioselective bromination of azaindoles and diazaindoles. Synlett. 211-214.

Gayakwad, E. M., Patel, K. P. and Shankarling, G. S. (2019) Sodium sulfate–hydrogen peroxide–sodium chloride adducts: selective protocol for the oxidative bromination, iodination and temperature dependent oxidation of sulfides to sulfoxides and sulfones. New J. Chem. *43*, 6001-6009.

Georgiev, D., Saes, W. B., Johnston, J. H., Boys, K. S., Healy, A. and Hulme, N. A. (2016) Selective and efficient generation of *ortho*-brominated *para*-substituted phenols in ACS-Grade methanol. Molecules. *21*, 88-96.

Gordon, M. and Pearson, D. E. (1964) The swamping catalyst effect. VI. The halogenation of isoquinoline and quinoline. J. Org. Chem. *29*, 329-332.

Hendrick, C. E. and Wang, Q. (2015) Synthesis of *ortho*-haloaminoarenes by aryne Insertion of nitrogen–halide bonds. J. Org. Chem. *80*, 1059-1069.

Huang, W., Xu, J., Liu, C., Chen, Z. and Gu, Y. (2019) Lewis acid-catalyzed synthesis of benzofurans and 4,5,6,7-tetrahydrobenzofurans from acrolein dimer and 1,3-dicarbonyl compounds. J. Org. Chem. *84*, 2941-2950.

Iida, K., Ishida, S., Watanabe, T. and Arai, T. (2019) Disulfide-catalyzed iodination of electron-rich aromatic compounds. J. Org. Chem. *84*, 7411-7417.

Jiang, P-P. and Yang, X-J. (2016) A quick, mild and efficient bromination using a CFBSA/KBr system. RSC. Adv. *6*, 90031-90034.

Jonckers, T. H. M., Mc, G., David, C., Raboisson, P. J.-M. B., Embrechts, W.C. J. and Guillemont, J. E. G. (2016) Heterocyclic indoles for use in influenza virus infection, WO 2016037953 A1 20160317.

Kansal, V. K., Mistry, D. N., Achanta, S., Ariyamuthu, S. Goswami, M. K. and Yazali, V. S. (2016) Improved processes for the preparation of sofosbuvir and intermediates thereof via coupling reaction of nucleosides with amino acid, WO 2016196735 A2 20161208

Kumar, L., Mahajan, T. and Agarwal, D. D. (2011) An instant and facile bromination of industrially-important aromatic compounds in water using recyclable $CaBr_2$–Br_2 system. Green. Chem. *13*, 2187-2196.

Kumar, V., Yap, J., Muroyama, A. and Malhotra, S. V. (2009) Highly efficient method for C-5 halogenation of pyrimidine-based nucleosides in Ionic liquids. Synthesis. 3957-3962.

Lai, J., Yu, A., Yang, L., Zhang, Y., Shah, B. P. and Lee, K. B. (2016) Development of photoactivated fluorescent *N*-hydroxyoxindoles and their application for cell-selective imaging. Chem. Eur. J. *22*, 6361-6367.

Latham, J., Henry, J-M., Sharif, H. H., Menon, B. R. K., Shepherd, S. A., Greaney, M. F. and Micklefield, J. (2016) Integrated catalysis opens new arylation pathways *via* regiodivergent enzymatic C–H activation. Nat. Commun. *7*, 11873-11881.

Lehmann, H. (2017) A scalable and safe continuous flow procedure for in-line generation of diazomethane and its precursor MNU. Green. Chem. *19*, 1449-1453.

Leronimo, G., Palmisano, G., Maspero, A., Marzorati, A., Scapinello, L., Masciocchi, N., Cravotto, G., Barge, A., Simonetti, M., Ameta, K. L., Nicholas, K. M. and Penoni, A. (2018) A novel synthesis of *N*-hydroxy-3-aroylindoles and 3-aroylindoles. Org. Bio. Chem. *16*, 6853-6859.

Munk, S. A., Harcourt, D. A., Arasasingham, P. N., Burke, J. A., Kharlamb, A. B., Manlapaz, C. A., Padillo, E. U., Roberts, D., Runde, E., Williams, L., Wheeler, L. A. and Garst, M. E. (1997) Synthesis and evaluation of 2-(arylamino)imidazoles as α_2-adrenergic agonists. J. Med. Chem. *40*, 18-23.

Oberhauser, T. (1997) A new bromination method for phenols and anisoles: NBS/$HBF_4 \cdot Et_2O$ in CH_3CN. J. Org. Chem. *62*, 4504-4506.

Pierre, F., Chua, P. C., O'Brien, S. E., Siddiqui-Jain, A., Bourbon, P., Haddach, M., Michaux, J., Nagasawa, J., Schwaebe, M. K., Stefan, E., Vialettes, A., Whitten, J. P., Chen, T. K., Darjania, L., Stansfield, R., Anderes, K., Bliesath, J., Drygin, D., Ho, C., Omori, M., Proffitt, C., Streiner, N., Trent, K., Rice, W. G. and Ryckman, D. M. (2011) Discovery and SAR of 5-(3-Chlorophenylamino)benzo[c][2,6]naphthyridine-8-carboxylic Acid (CX-4945), the First Clinical Stage Inhibitor of Protein Kinase CK2 for the Treatment of Cancer. J. Med. Chem. *54*, 635-654.

Podgoršek, A., Stavber, S., Zupan, M. and Iskra, J. (2007) Bromination of ketones with H_2O_2–HBr "on water". Green. Chem. *9*, 1212-1218.

Satkar, Y., Yera-Ledesma, L. F., Mali, N., Patil, D., Navarro-Santos, P., Segura-Quezada, L. A., Ramírez-Morales, P. I. and Solorio-Alvarado, C. R. (2019) Iodine(III)-mediated, controlled di- or monoiodination of phenols. J. Org. Chem. *84*, 4149-4164.

Seel, C. J., Králík, A., Hacker, M., Frank, A., König, B. and Gulder, T. (2018) Atom-economic electron donors for photobiocatalytic halogenations. Chem. Cat. Chem. *10*, 3960-3963.
Selvakumar, J., Grandhi, G. S., Sahoo, H. and Baidya, M. (2016) Copper-mediated etherification of arenes with alkoxysilanes directed by an (2-aminophenyl)pyrazole group. RSC Adv. *6*, 79361-79365.

Slaunwhite, J. R. W. R. and Neely, L. (1962) Bromination of phenolic steroids. I. substitution of estrone and 17β-estradiol in ring A. J. Org. Chem. *27*, 1749-1752

Song, S., Sun, X., Li, X., Yuan, Y. and Jiao, N. (2015) Efficient and practical oxidative bromination and iodination of arenes and heteroarenes with DMSO and hydrogen halide: a mild protocol for late-stage functionalization. Org. Lett. *17*, 2886-2889.

Swamy, V. P., Deshmukh, A. J., Gore, P. S. and Thulasiram, H. V. (2016) Novel recyclable iodinating agent and its applications; PCT Int. Appl., 2016113757

Wang, M., Zhang, Y., Wang, T., Wang, C., Xue, D. and Xiao, J. (2016) Story of an Age-Old Reagent: An Electrophilic Chlorination of Arenes and Heterocycles by 1-Chloro-1,2-benziodoxol-3-one. Org. Lett. *18*, 1976-1979.
Wischang, D. and Hartung, J. (2011) Parameters for bromination of pyrroles in bromoperoxidase-catalyzed oxidations. Tetrahedron. *67*, 4048-4054.

Wischang, D., Hartung, J., Hahn, T., Ulber, R., Stumpf, T. and Fecher-Trost, C. (2011) Vanadate(v)-dependent bromoperoxidase immobilized on magnetic beads as reusable catalyst for oxidative bromination. Green. Chem. *13*, 102-108.

Xiao, X., Xie, Y., Bai, S., Deng, Y., Jiang, H. and Zeng, W. (2015) Transition-metal-free tandem chlorocyclization of amines with carboxylic acids: access to chloroimidazo[1,2-α]pyridines. Org. Lett. *17*, 3998-4001.

Xiong, X. and Yeung, Y-Y. (2018) Ammonium salt-catalyzed highly practical *ortho*-selective monohalogenation and phenylselenation of phenols: scope and applications. ACS. Catal. *8*, 4033-4043.

Yang, L., Zhang, Y., Zou, X., Lu, H. and Li, G. (2018) Visible-light-promoted intramolecular C–H amination in aqueous solution: synthesis of carbazoles. Green Chem. *20*, 1362-1366.

Yang, X-Y., Zhao, H-Y., Mao, S. and Zhang, S-Q. (2018) Copper-mediated monochlorination of anilines and nitrogen-containing heterocycles. Syn. Commun. *48*, 2708-2714.

Yuan, Y., Yao, A., Zheng, Y., Gao, M., Zhou, Z., Qiao, J., Hu, J., Ye, B., Zhao, J., Wen, H. and Lei, A. (2019) Electrochemical oxidative clean halogenation using HX/NaX with hydrogen evolution. iScience. *12*, 293-303.

Zhou, B., Yuan, Y., Jin, H. and Liu, Y. (2019) I_2O_5-mediated iodocyclization cascade of *N*-(1-arylallyl)pyridine-2-amines with concomitant C=C bond cleavage: a synthesis of 3-iodoimidazo[1,2-a]pyridines. J. Org. Chem. *84*, 5773-5782
Zhou, Y. and Song, Q. (2018) Oxidative ring-opening of 3-aminoindazoles for the synthesis of 2-aminobenzoates. Org. Chem. Front. *5*, 3245-3249.

Zhou, Z., Ma, Z., Behnke, N. E., Gao, H. and Kürti, L. (2017) Non-deprotonative primary and secondary amination of (hetero)arylmetals. J. Am. Chem. Soc. *139*, 115-118.